1-1-2008

Environmental And Age-Related Deterioration Of Concrete Median Barriers

Kavitha. Madhu
Ryerson University

ENVIRONMENTAL AND AGE-RELATED DETERIORATION OF CONCRETE MEDIAN BARRIERS

By

Kavitha Madhu

Bachelor of Technology in Civil Engineering
University of Calicut, India, July, 1992

A thesis presented to Ryerson University

in the partial fulfillment of the
requirements for the degree of

Master of Applied Science
in the program of
Civil Engineering

Toronto, Ontario, Canada, 2008

ENVIRONMENTAL AND AGE-RELATED DETERIORATION OF CONCRETE MEDIAN BARRIERS

Master of Applied Science 2008

By

Kavitha Madhu
Department of Civil Engineering
Ryerson University, Toronto

ABSTRACT

The purpose of this research was to understand the time-dependent environmental and age-related deterioration mechanisms in the un-reinforced concrete barrier walls used in Ontario. The study concentrated mainly on the response of plain concrete barrier walls to time-dependent thermal loads and associated volume changes. The research involved temperature data collection, experimental study and numerical analysis. The temperature data was collected on an hourly basis from the temperature sensors installed in a live plain concrete barrier wall. In the experimental study, concrete samples were exposed to varying temperature and environmental conditions and tested to monitor the deviation of significant concrete parameters like compressive strength, tensile strength, modulus of elasticity etc. Based on the results from the experimental study and the temperature data collected from the sensors, a non-linear transient thermal and structural analysis was carried out on a three-dimensional model, developed using ANSYS program, for a time period of three years.

ACKNOWLEDGEMENTS

I would like to start by expressing my sincere gratitude and appreciation to my advisor Dr. Mohamed Lachemi for his numerous hours of guidance, advice, patience and mentoring throughout my graduate program. He gave me an opportunity to learn more and develop professionally with confidence. I am indebted to him. Without his support and encouragement, I would not have been able to stay through the course.

I would also like to thank Dr. Anwar Hossain for giving his valuable time and advice during my study at Ryerson. He was always there to help me with his smiling face and unfailing patience, whenever I faced difficulties during my thesis work.

This study was funded by the Ministry of Transportation Ontario (MTO) through the "Highway Infrastructure Innovation Funding Program". I would like to acknowledge Chris Wojcik, Senior Concrete/Materials Engineering Officer of MTO, for his support and effort throughout this research.

To Dr. Reza Khianoush and Dr. Lamya Amleh, thanks a lot for giving me the inspiration and courage to join Master of Science program at Ryerson. A special thanks to Dr. Medhat Shehata for his encouragement and support during the development of this thesis.

I want to give special recognition to Dr. Mustafa Sahmaran for his valuable support and advice with the experimental work. I am also very grateful to Amirreza Ghaemmaghami for providing me an excellent support and guidance in ANSYS.

Many thanks to Roger Smith, Mohamed Aldardari and Nidal Jalouk for providing technical assistance, during the experimental part of this thesis.

To my colleagues Sini, Gaurang and Nima, thank you for the memorable moments we shared together during our Masters program at Ryerson.

Finally, special gratitude goes to my family, in particular to my beloved son Hari. I am very grateful to them for their continuous support, concern, encouragement and sacrifice, without which my success would not have been possible.

TABLE OF CONTENTS

LIST OF TABLES

LIST OF FIGURES

Chapter 1

Introduction

Continous concrete barrier walls are large mass concrete members that can experience various types of short- and long-term deteriorations. It is hard to find concrete barrier walls, especially un-reinforced barriers, which have not been affected by cracking of some kind. Since Ontario is unique in the world in using un-reinforced concrete barriers, very few data on this topic is available from other jurisdictions and research institutions.

In un-reinforced barriers, concrete shrinkage and development of thermal stresses are the main concerns to be taken care of due to environmental deterioration. If proper curing is provided from the beginning, autogenous shrinkage can be ignored, however, drying shrinkage remains. For a wide range of concrete mixtures, about 75% of the twenty year drying shrinkage was realized in one year (Klieger and Lamond, 1994). The major effect of drying shrinkage on concrete barrier walls need to be considered only for the first year. Still cracks are seen developing in concrete barrier walls with time. Many plain concrete barriers of Ontario are facing crack failures, some within 4~5 years of service. The situation is very alarming, pointing out the urgent necessity of a research study.

Most of the distresses found in un-reinforced barrier walls built in the past have been attributed to ignoring the effect of temperature gradients, which set in due to seasonal changes. Now-a-days, the importance of the environmental loads due to temperature variations is being considered by structural engineers while designing barrier geometry

and position of joints. The use of slip-formed continuous span barrier walls being popular now-a-days, it is of utmost importance to analyse the structure for temperature effects.

1.1 Scope and Objectives

For Ministry of Transportation Ontario's "Highway Infrastructure Innovation Funding Program", a research study was instigated on environmental and age-related deterioration of concrete median barriers. The overall aim of this research program was to enhance our understanding of the environmental and age-related deterioration mechanisms in concrete barrier walls.

The following procedure was used to meet this goal. First, a study on thermal characteristics of concrete was conducted along with excerpts from literatures containing previous experimental and analytical procedures related to plain concrete components. Second, temperature and strain data were collected from site to get a clear picture of actual temperature variations from exposed concrete surface. For this, strain gauges and thermocouples were installed in a live barrier on Hwy 403 and temperature and strain data per hour was collected from the data acquisition unit. Third, ample concrete samples were tested in the laboratory under different temperature and humidity exposures and the variation of the important concrete parameters with respect to time was monitored. Fourth, using a commercial finite element analysis package ANSYS, an extensive analysis was performed to study the effect of some base parameters governing the performance of concrete barrier walls.

The desired outcome is to provide knowledge or tools, which could potentially enhance cost efficiency, resource optimization, crack minimization, and improvement of overall durability and long-term performance. This investigation was conducted to achieve a better knowledge of the response with time as well as the nature of the deterioration associated with thermal loads and volume changes in concrete.

1.2 Thesis Outline

Chapter 2 comprises of a detailed study on the behaviour of plain concrete barrier walls including various distresses found in barriers and a small note on the observations from a live barrier construction site visit, along with excerpts from available literature. Chapter 3 gives details about the experimental investigation which includes the lab work done on the mechanical properties of concrete mix and the field monitoring of barrier walls, including sensor installation. Chapter 4 explains about the steps and assumptions considered in the non linear transient thermal and structural analysis of barrier walls using ANSYS.

Chapter 5 gives the test results from experimental study conducted in Chapter 3. Chapter 6 describes the development of finite element model of barrier walls in ANSYS, crack evolutions with time and conclusions. Chapter 7 conducts a parametric study on the barrier wall analysis. The crack evolution patterns from the parametric study are shown in Appendix. Conclusions and future recommendations are outlined in Chapter 8.

Chapter 2

Behavior of Plain Concrete Barrier Walls

2.1 Introduction

The purpose of this chapter is to understand the relevance of characteristics and properties of concrete used in barrier walls, against its resistance towards environmental and age-related deteriorations. Environmental loadings, especially for a country like Canada, where there is a significant variation in daily ambient temperature, fluctuation of relative humidity, wind speed, freeze and thaw effects, exposure to chemically detrimental substances etc., can cause progressive deterioration of concrete structures. The long-term durability of concrete is to a large extent governed by the resistance of concrete against various environmental loadings. As the properties of concrete changes with respect to time and the environment to which it is exposed, an investigation on the effects of concrete aging is also important in performing durability evaluations. This has been studied extensively for several decades and now-a-days, durability based design governs the design of concrete structures, rather than strength based design. This chapter discusses the characteristics of concrete in relevance to its thermal properties and volumetric changes as well as a peek into the current prevalent practices and associated problems of barrier construction, along with excerpts from relevant literatures.

2.2 Thermal Properties of Concrete

It is very important to understand the thermal properties of concrete, especially in structures like barriers, which are exposed to varying environmental conditions throughout their service life.

Thermal properties of concrete necessary for the non-linear transient finite element analysis are thermal conductivity, specific heat and coefficient of linear thermal expansion.

2.2.1 Thermal Conductivity

Thermal conductivity measures the ability of the material to conduct heat. It can be defined as the ratio of the flux of heat to temperature gradient. Influencing factors on the thermal conductivity of concrete was investigated by Yang et al. (2003) using a conductivity tester developed in Japan known as QTM-D3. The factors considered in this experimental study were age, water-to-cement ratio (W/C), types of admixtures, aggregate volume fraction, fine aggregate fraction, and temperature and humidity condition of the specimen. According to the experimental results, aggregate volume fraction and moisture condition of specimen are revealed as the main affecting factors on the conductivity of concrete. Concrete age hardly affects its thermal conductivity, except for a very early age, i.e., about 2 days.

Density does not appreciably affect the thermal conductivity of ordinary concrete. However in the case of lightweight concrete, due to the low conductivity of air, the air acts as an insulator and reduces thermal conductivity. Since the thermal conductivity of liquid water is about 25 times greater than that of air, it is quite easy to understand how even small variations of the moisture content can have a significant impact on thermal performance. In the case of lightweight concrete, an increase in moisture content of 10% increases conductivity by about 50%. For low water content concrete mixes, conductivity will be higher since the conductivity of water is less than half that of hydrated cement paste.

The range of thermal conductivity of concrete is very wide, varying between 1.4 $J/m^2s^oC/m$ to 3.6 $J/m^2s^oC/m$ for normal saturated concrete (Neville, 1997). The value adopted in the finite element analysis is 2.4 $J/m^2s^oC/m$ and is assumed to be temperature independent during the analysis.

2.2.2 Specific Heat

Specific heat of concrete represents the heat capacity of concrete. It is the amount of heat needed to change temperature of 1gram of material by 1°C. The main factors that influence the specific heat of concrete are moisture and temperature. Specific heat increases with increase in moisture, increase in temperature and decrease in density of concrete. For ordinary concrete, specific heat range is between 840 J/kg/°C and 1170 J/kg/°C. The value adopted in the finite element analysis is 950 J/kg/°C.

2.2.3 Diffusivity

Diffusivity measures the rate with which temperature changes within a mass can take place. It is related to thermal conductivity, specific heat and density of concrete.

$$\text{Diffusivity} = \frac{\text{Thermal conductivity}}{(\text{Specific Heat x Density})}$$

The range of typical values of diffusivity of ordinary concrete is between $0.002m^2/h$ and $0.006m^2/h$.

2.2.4 Coefficient of Thermal Expansion

Coefficient of thermal expansion of concrete refers to the change in unit length per degree of temperature change and can be estimated from the volumetrically weighted average of the coefficients of the concrete components (Mehta and Monteiro, 1993). The thermal stress is a function of the temperature variation below the set temperature of the concrete, Young's modulus of concrete and the coefficient of thermal expansion of concrete material (Schoppel et al., 1994). Knowledge of thermal expansion of concrete is thus required in the design of expansion and contraction joints, in the design of statically indeterminate structures subject to temperature variation and in the assessment of thermal gradients in concrete.

The coefficient of thermal expansion of concrete is positive in normal temperature range, but relatively very low. Even then, if no provision is made for expansion, the repeated cycles of expansion and contraction can create cracks occurring in the parts of structure. A temperature differential exceeding 20°C between the concrete surface and the concrete core produces thermal shock that causes cracking in the concrete (Kristensen and Hansen, 1994). Hence it is necessary to understand the coefficient of thermal expansion of a concrete mix to evaluate its thermal properties.

The coefficient of thermal expansion of concrete materials is affected by aggregate type, aggregate volume fraction, admixture, age, temperature and relative humidity (Mindess and Young, 1981). Influencing factors on the thermal coefficient of concrete was also investigated by Yang et al. (2003). Factors considered in this experimental study were coarse aggregate, specimen shape and warming and cooling cycles. According to experimental results, specimen

shape is revealed as the main factor affecting the thermal coefficient of concrete. Prism concrete specimens produced almost same values of thermal coefficients under cycles of warming and cooling. However, cylinder specimens gave values of 1.8~2.6 x 10^{-6}/°C lower than the prism specimen. The type of coarse aggregate also influenced thermal coefficient of concrete specimen.

Volumetric changes of concrete as a result of temperature variations depend on a great number of factors among which Emanuel and Hulsey (1997) and Davis (1930) cite: the age of concrete, the type of aggregates, the water-to-cement ratio, the volume and type of cement, the moisture content, and the alternations of high and low temperature. Indeed, as has been pointed out by ACI Committee 517(1980) the coefficient of thermal expansion of fresh concrete is several times higher than the hardened concrete one. Thermal expansion coefficient of concrete is taken as a constant value of 11E-06/°C in the finite element study.

2.3 Type of Distress Observed

In order to have an understanding of the condition of plain concrete barriers constructed within the last ten years, a site survey was conducted with the Ministry of Transportation officials on the barriers placed at Hwy 401 and Hwy 403, to identify common distress states.

2.3.1 Vertical Cracking

Vertical cracks are the most common distress found in un-reinforced barrier walls. The number of vertical cracks in a barrier wall segment is proportional to its deterioration. Cracking forms on barriers primarily under restrained volume change. According to ACI 207(1995), fully base-

restrained un-reinforced concrete walls ultimately attain full-length vertical cracks, which are usually spaced between one to two times the heights of the wall.

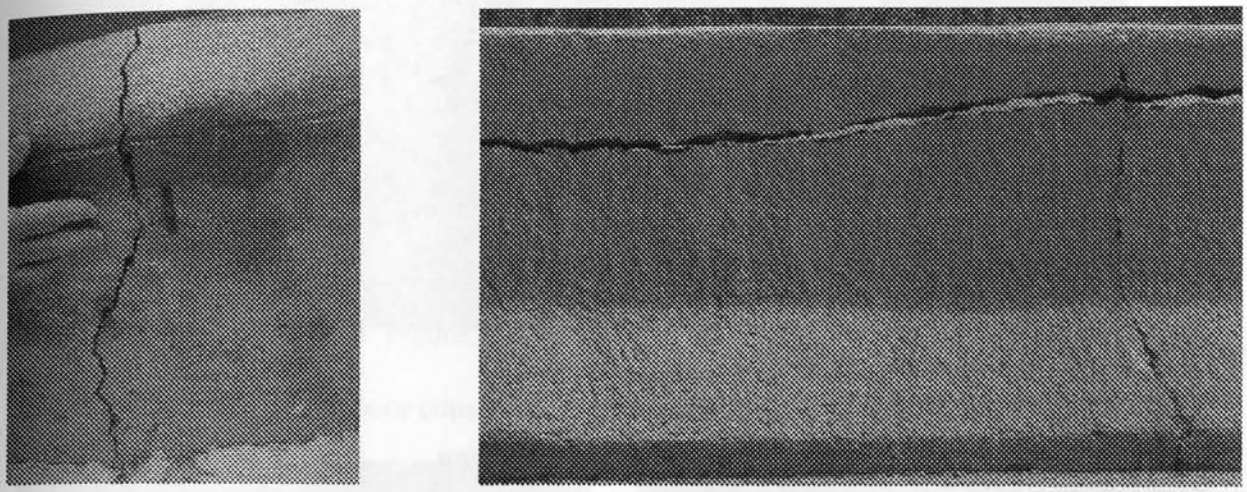

Figure 2.1: Vertical Cracking and Horizontal Cracking

2.3.2 Horizontal Cracking

Horizontal cracks are either local or continuous. They are mostly observed above the mid-level height of the barrier wall, through the vertical face. A significant section loss is often observed around the barrier top portion as shown in Figure 2.2. The most probable cause of cracking observed near the top of the barrier is perhaps due to the plastic settlement of insufficiently consolidated concrete. Vibration generated by the traffic adjacent to the newly cast barriers could contribute to the settlement of plastic concrete.

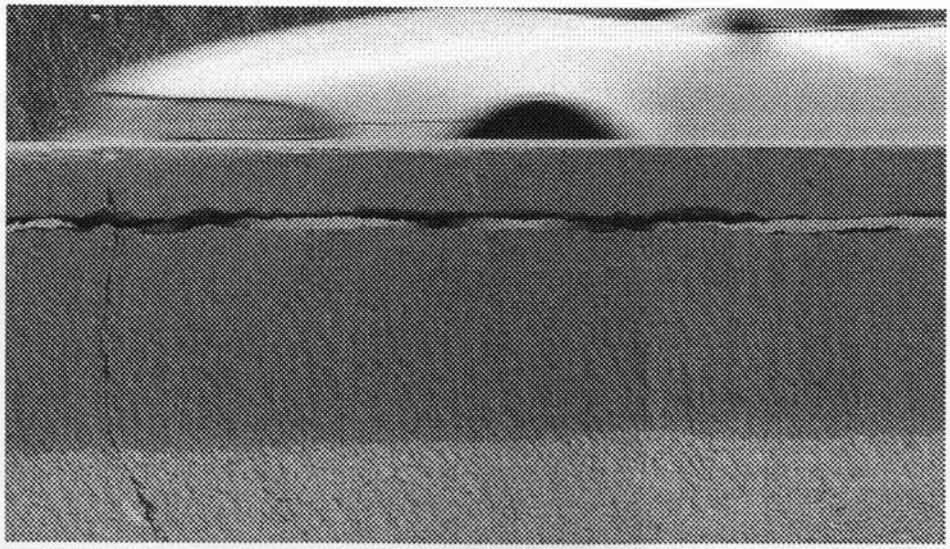

Figure 2.2: Horizontal Cracking

2.3.3 Spalling

When vertical or horizontal cracking is present in the barriers, it will assist the penetration of moisture inside the concrete. The effect of freeze and thaw cycles supplemented by the moisture presence increases the crack width, resulting in loss of sizable chunks of intact concrete called spalling (Figure 2.3).

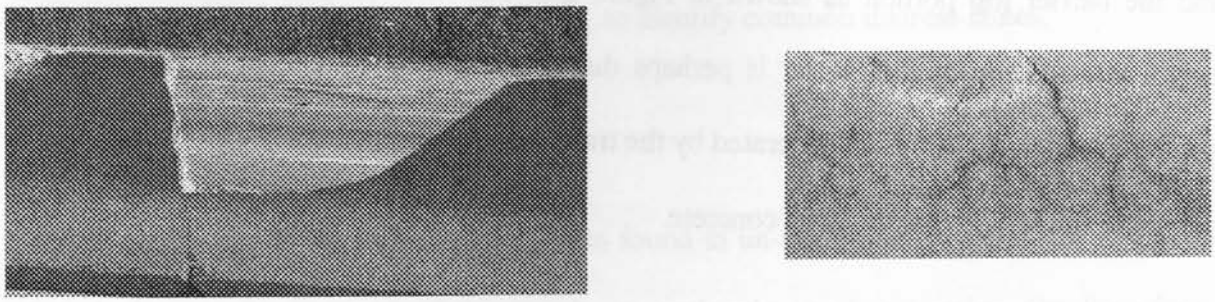

Figure 2.3: (a) Spalling (b) Map Cracking

2.3.4 Map Cracking

Map cracking of barriers is often related to the early thermal shrinkage cracking. The concrete external surface is subjected to water loss due to evaporation, thereby develops thermal stresses, causing map cracking on the surface. This is a common defect observed on the barrier surface and is dependent on the concrete material properties and construction practices.

2.3.5 Disintegration

Disintegration, as seen in Figure 2.4, is usually the loss of small particles and individual aggregate particles due to poor construction practices, freeze-thaw cycles or chemical attack

Figure 2.4: Disintegration due to (a) freeze and thaw effects and (b) poor construction practices

2.3.6 Delamination

Delamination is the separation of concrete layer along a plane parallel to the surface and it can happen due to many reasons. One of the causes most seen in the aged barrier walls is due to poor bond between two course placements, as explained here. Usually barriers near concrete bridge piers, lamp post foundations etc are cast-in-site manually and attached to piers or lamp post foundations with a 12 mm thick expansion joint placed between the two surfaces. The slip formed barrier wall that is adjacent to the cast-in-site barrier wall should have construction joint

between them. The absence of proper construction joints results in crushing with delamination of concrete as seen in Figure 2.5(b), due to the thermal expansion of slip form concrete wall at the free end. Vertical cracks are also seen developed near the junction. The resulting delaminations are generally thicker than those caused by improper finishing. If the delamination is not repaired, traffic may cause the area to pop out through pounding on the delaminated upper concrete layer.

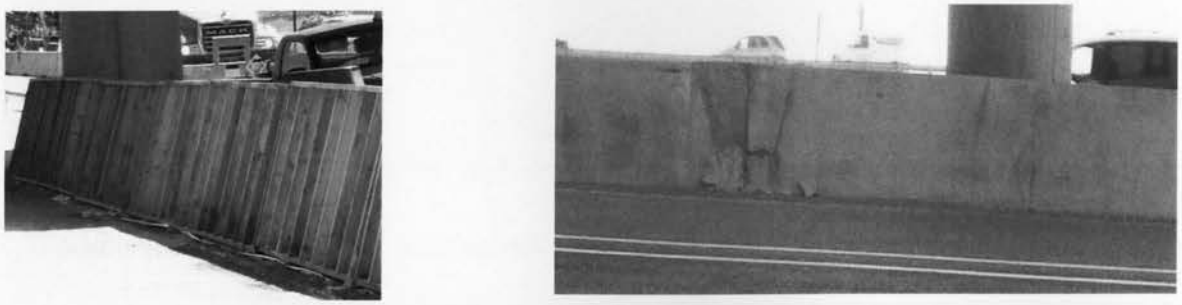

(a) Barrier construction near bridge pier (b) Crushing with delamination and vertical cracks

Figure 2.5: Delamination

2.4 Causes of Distress

Concrete properties are more complex than those of most materials because not only is concrete a composite material whose constituents have different properties, but its properties depend upon many factors like moisture, porosity etc. The resistance of concrete against physical and chemical deterioration processes extends the long-term durability of concrete.

Distress in plain concrete can be caused due to many reasons, such as shrinkage, creep, tension failure, compression failure, degree of external restraint, action of freezing and thawing cycles, development of thermal gradient between external surface and internal core, improper construction practices, chemical deterioration due to leaching of concrete constituents, alkali-aggregate reaction etc.

This study is mainly exploring the environmental and age related deterioration mechanisms in concrete.

2.4.1 Shrinkage, Thermal Loads and Restraint of Concrete

The causes of distress in analyzing the environmental and age related deterioration of concrete barriers is primarily due to environmental and structural effects, such as shrinkage, thermal loads and restraint of concrete. The environmental condition such as ambient temperature, relative humidity and wind velocity has a significant influence on the properties of fresh and hardened concrete. Shrinkage strain increases with increased ambient temperature and wind velocity and decreases with increased relative humidity. The temperature difference between the interior and exterior of the element causes restraint volume change and consequently stresses within the barrier section (ACI Committee 207, 1995)

Concrete shrinkage is a time-dependent decrease in the apparent volume of the concrete due to decrease in moisture content because of drying. Concrete shrinkage depends on material properties, ambient temperature, relative humidity, age and size of the structure. Non-uniform moisture distribution as well as non-uniform consolidation in concrete can cause differential shrinkage, which induces stress that may cause surface cracks (Kim and Lee, 1998). To reduce or prevent the occurrence of cracking during the hardening process, it is very important to understand how concrete shrinkage develops with time. To understand how concrete shrinkage evolves during hardening, it is necessary to learn the fundamentals of the parameters affecting this phenomenon.

Drying shrinkage is induced by the removal of water from the pore structure. As concrete dries, outer surface will dry quickly, while the inner core will remain nearly saturated. The true unrestrained drying shrinkage near the drying surface will be significantly higher than away from surface. For strain compatibility compression will develop in the most saturated regions with balancing regions of tension in the drier zones of the material. Larger pores tend to empty first, followed by progressively smaller pores. Once pores have been emptied to a diameter of about 50nm, concave capillary menisci begin to form (Mindess and Young, 1981). The formation of curved menisci disrupts the static equilibrium between the pore fluid pressure and the vapor pressure within the pores. As a result, a negative pressure develops within the pore fluid. This negative pore pressure can be described by the Laplace Equation (Eqn. 2.1) as

$$\sigma = \frac{2\gamma}{r} \qquad \text{.....(Eqn. 2.1)}$$

where σ is the negative pore fluid pressure, γ is the surface tension of water, and r is the average radius of meniscus curvature. As a reaction to the negative pressure ("tension") within the pore fluid, compression develops in the solid microstructure (Bissonnette et al., 2001). The response of the solid microstructure under compression results in shrinkage.

The important factors affecting drying shrinkage of concrete are the cement content, elastic modulus of aggregate, time and relative humidity of exposure. For a wide range of concrete mixtures, about 20~25% of the twenty year drying shrinkage was realized in two weeks, 50~60% in three months and about 75% in one year (Klieger and Lamond, 1994). Almost double drying shrinkage was obtained at 45% relative humidity as compared to 80% relative humidity exposure.

When an inspection was conducted in the newly reconstructed reinforced concrete barrier walls on Vachon Bridge near Montreal, just one day after concrete casting, it revealed intense closely spaced cracks running completely through the walls. The numerical analysis carried out by Cusson and Repette (2000) on these walls showed that the early-age damage mechanism was due to the combination of two phenomena:

- thermal stresses due to temperature gradients in the concrete during cement hydration and
- the development of autogenous shrinkage in the low water-to-cement ratio concrete used.

The strain development in concrete as a result of autogenous shrinkage is a direct consequence of the absolute volume contraction of the hydrated cement paste, known as chemical contraction, which always accompanies the release in heat due to cement hydration (Japanese Concrete Institute Technical Committee, 1998). The higher the W/C, the more the concrete has large capillaries and the smaller the interior tensile stresses created by the chemical contraction will be. For practical purposes, autogenous shrinkage can be ignored in uncured concrete that have W/C above 0.45, because autogenous shrinkage represents a small fraction of the final drying shrinkage (Davis, 1940). On the other hand, in uncured concrete with a low W/B, autogenous shrinkage can be equal to drying shrinkage, so that overall shrinkage can be doubled (Aïtcin et al., 1997). In the case of slip-form barriers, concrete with W/C less than 0.4 is used normally. Hence, the amount of shrinkage effect on these walls will be high. A good understanding of these volumetric changes coupled with proper curing and construction practices should minimize the often very harmful consequences of cracking, while enhancing the durability of concrete structures.

It is generally accepted that under thermal loading, concrete will never expand to its originally placed volume, and continues to shrink for years, after it is initially placed. Non-restrained concrete shrinks, but will not develop internal stress and hence will not develop cracks. But restrained concrete cracks, due to tensile stress induced by shrinkage while in use. Known as shrinkage cracks, this occurs when concrete members undergo restrained volumetric changes, i.e. shrinkage, due to either drying or thermal effects.

Experimental investigation conducted by Carlson and Reading (1988) has indicated that, for un-reinforced building walls, the shrinkage and the degree of restraint at the wall base were mainly responsible for the development of early-age cracks. Al Rawi and Kheder (1990) conducted tests on 100 mm thick, 500 mm high base-restrained un-reinforced walls, which were exposed to 40 days in summer and 40 days in winter. Vertical cracks were observed with a minimum spacing of 620 mm (1.24H), where H is the height of the concrete wall. According to ACI Committee 207 (1995), the degree of external restraint can greatly contribute to the development of damage in un-reinforced concrete walls.

A recent study conducted by the Michigan DOT Center of Excellence has pointed out that many of the New Jersey type reinforced concrete barriers used on Michigan bridges are deteriorating at a rate faster than expected (Michigan DOT Center of Excellence, 2004). The study was designed to further evaluate the field observations and to develop a comprehensive understanding of the barrier life span, from construction to repair or replacement. The study findings established that the deterioration of barriers is initiated by transverse cracking and accelerated by the presence of voids and cavities, reinforcement cover, and the overall soundness and quality of the concrete

barrier. The study concluded that the cracking of concrete is the result of stresses that form due to volume change under thermal and shrinkage loads by the restraint developed between the deck and the barrier base.

Free shrinkage has to be distinguished from restrained shrinkage. Free shrinkage is a property of the material. It depends only on how the concrete mixture is made, what type of cement is used, what the water/cement ratio is, etc. The effect of restrained shrinkage in structure is very dependent on the geometry of the structure, strength of concrete, modulus of elasticity and restraining material. The stresses in concrete increase due to restrained action. Cracks are formed in restrained concrete when stresses exceed tensile strength. They will continue to grow until stresses reach a magnitude that is insufficient to continue crack generation. In addition, cracks do not stop immediately when stresses are smaller than tensile stress of concrete. They usually continue to grow even at half of the stress field necessary to initiate crack. Stresses from internal restraint can result from the development of moisture gradients. Hence, restraint of shrinkage results in macro-scale tensile stresses that can cause cracking, even if it is either internal or external.

In the case of median barriers, external restraints can be light post foundations placed at usually 50 m intervals or bridge pier footings, base restraints or other boundary conditions. Internal restraint can happen due to differential drying shrinkage. When the tensile stress induced by shrinkage exceeds the tensile strength of concrete, crack develops. Therefore, in the case of plain concrete median barriers, the influential parameters for the development of shrinkage

cracks can bring down to two – the amount of shrinkage that occurs and the amount of restraint present.

When bulk expansion/shrinkage is restrained, coupled with physical and chemical deterioration processes, local stresses can be developed and accumulated in concrete. Also during its initial placement, concrete does not harden at its temperature of service and usually its cooling is not uniform, which leads to the development of tensile stresses. At the same time, the development of shrinkage tends to amplify tensile stresses during concrete hardening. These tensile stresses can result in the development of cracks if concrete tensile strength, at the age when these stresses are developed, is not high enough.

However, in most of the cases, cracks are visible on the concrete surface only after a lengthy time gap. To understand the reason why a concrete element may not crack at all or may crack but not soon after exposure to the environment, we have to consider how concrete would respond to sustained stress or to sustained strain.

The phenomenon of a gradual increase in strain with time under a given level of sustained stress is called creep. The phenomenon of gradual decrease in stress with time under a given level of sustained strain is called stress relaxation (Mehta and Monteiro, 1993). Both manifestations are typical of visco-elastic materials. When a concrete element is restrained, the visco-elasticity of concrete will manifest into a progressive decrease of stress with time, as shown in Figure 2.6. Thus with restraining conditions present in concrete, the interplay between elastic tensile stresses

induced by shrinkage strains and stress relief due to visco-elastic behavior, influences the deformation and cracking in concrete structure (Mehta and Monteiro, 1993).

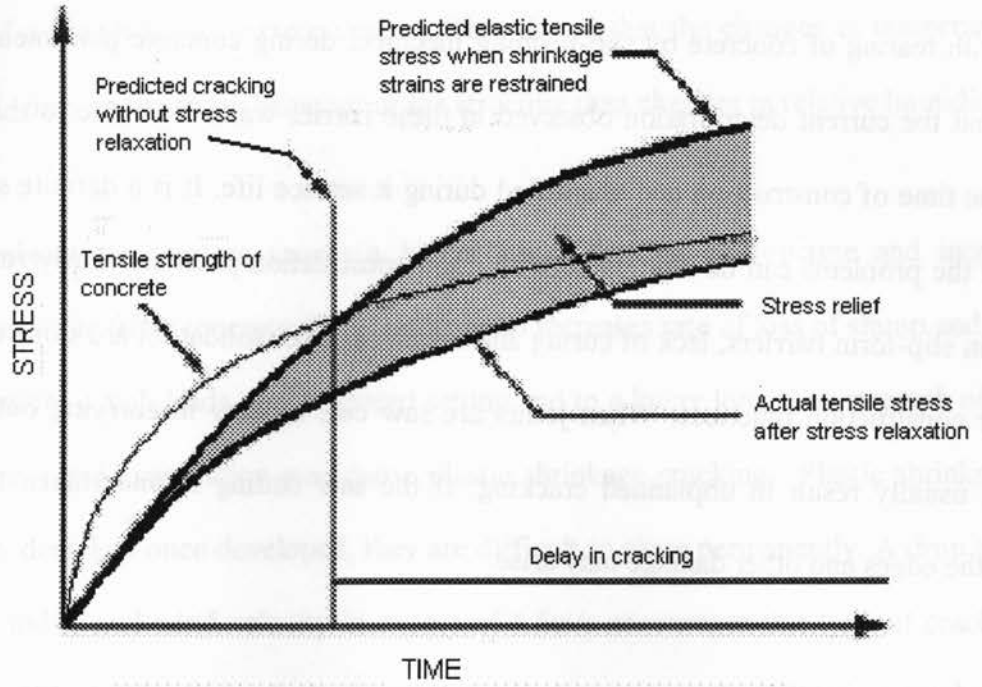

Figure 2.6: Stress-Time curve (Mehta and Monteiro, 1993)

With low tensile strength materials such as concrete, it is the shrinkage strain from cooling that is more important, when compared to the expansion from heat generated by cement hydration. This is because, depending on the elastic modulus, for a fully restrained concrete with no provision for stress relaxation, the resulting tensile stresses can be large enough to cause cracking.

2.4.2 Improper Construction Practices

In 2006, MTO conducted examination of cores taken from slip-formed tall wall median barrier on Highway 401- Trenton area, which showed significant deterioration within 10 years of its service life (Saucier et al., 1997). Upon examination, no durability issues were found in cores,

like distresses related to freezing and thawing action or due to reactivity of aggregates. However, the cores showed distress related to poor construction practices, like poor consolidation, inadequate mixing of concrete and development of cracks in the early stages, especially in consistent with tearing of concrete by slip-forming machine, during concrete placement. It was very clear that the current deterioration observed in these barrier walls were due to the defects created at the time of construction and magnified during it service life. It is a definite statement that most of the problems can be eliminated with good construction practices. Early removal of formworks in slip-form barriers, lack of curing and insufficient consolidation are some examples of improper construction practices. When joints are saw cut, a delay in carrying out the saw cutting will usually result in unplanned cracking. If the saw cutting is undertaken too early, raveling of the edges and other damage may arise.

2.4.3 Climatic Impacts

Climatic conditions can contribute to damage over the lifetime of the barrier, long after the effect of heat of hydration has dissipated. An exposed concrete barrier wall is continuously gaining and losing heat due to solar radiation, radiation to or from the sky or surrounding objects and by convection to or from the surrounding atmosphere. Temperature variation due to these sources depends upon location and orientation of the structure, geometrical and material properties of the structure and environmental conditions.

The exposure of mature concrete to alternating freezing and thawing cycles due to seasonal temperature variations are always there in nature, especially in colder regions like Canada. As the temperature of the saturated exposed concrete is reduced, the water held in the capillary pores

freezes and expansion of concrete takes place. So when freezing follows subsequent thawing, further expansion takes place. Repeated cycles of freezing and thawing have a cumulative effect. Howells et al. (2005) conducted a study on the influence of environmental effects on the behavior of a pre-stresses concrete viaduct. They found that the changes in temperature had a greater influence on the strain behavior of the structure than changes in relative humidity.

A high ambient temperature causes a higher water demand of concrete and increases the temperature of the fresh concrete. This results in an increases rate of loss of slump and in a more rapid hydration, which leads to accelerated setting and to a lower long-term strength of concrete. Furthermore, rapid evaporation may cause plastic shrinkage cracking. Plastic shrinkage cracks can be very deep and once developed, they are difficult to close permanently. A drop in ambient relative humidity and wind velocity in excess of 4.5m/s encourages this type of cracking (ACI Committee 305, 1992). Risk of plastic cracking is the same at the following combinations of temperature and relative humidity:

- 41°C and 90% RH
- 35°C and 70% RH
- 24°C and 30% RH

Hence the impact of climatic conditions, mainly the temperature variations during seasonal changes need to be analyzed seriously. For this purpose, it is better to have an idea about the thermal properties of concrete.

2.5 Observations from a Slip-formed Barrier Construction Site

Barriers were cast in a continuous slip form process. Low slump concrete is used in slip form barrier construction. The loss of slump in stiff mixes is less influenced by temperature because such mixes are less affected by changes in water content (Neville, 1997). Therefore, even in hot days, there need not be any concern regarding the workability of stiff concrete mix, as the ambient temperature does not affect it.

Immediately prior to concrete placement, the compacted granular fill was dampened. According to Ontario Provincial Standard Specifications, contractor should wet down the sub-grade by means of a uniform spray of water sufficient to wet the sub-grade thoroughly, without leaving standing water. Water was sprayed on the compacted granular fill, however no control measures were seen executed inorder to ensure that the sub-grade was dampened enough. It is not advisable to rely on the experience factor of the workers, in this case.

As the form moved, numerous defects were visible on the concrete surface (Figure. 2.7). A portion of the concrete from the top surface collapsed. Rock pockets and cavities were visible on the barrier surface. Concrete plastic flow was observed. All these explain that the vibration was not sufficient in intensity to uniformly consolidate the low slump concrete, prior to placing. After placing, vibration generated by the traffic adjacent to these barrier walls, contributed to the settlement of plastic concrete. The fresh concrete surface was fairly rough and required extensive floating. Final surface finishing was performed with wooden floats.

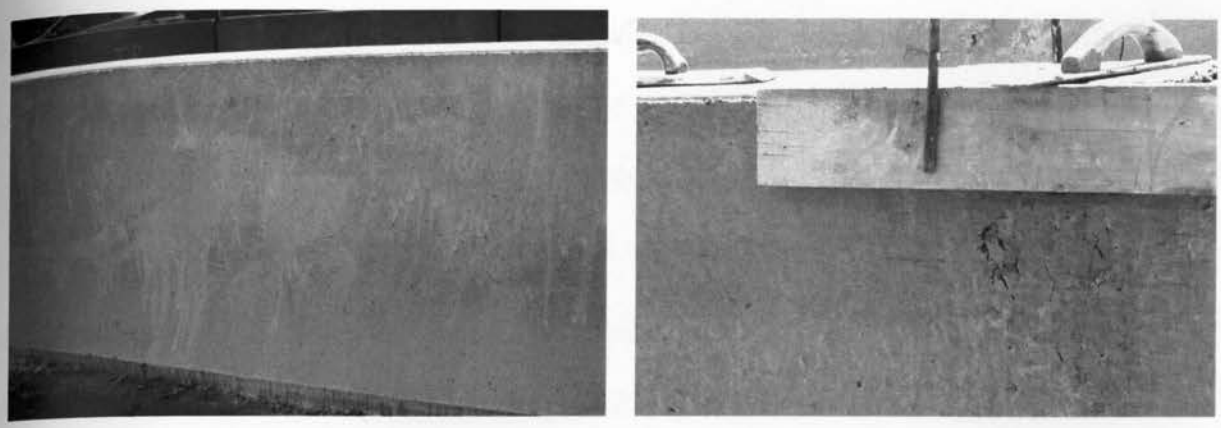

Figure 2.7: (a) Uneven application of curing compound (b) Surface finishing using wooden floats; Honey combing can be seen

Though curing compound was sprayed, it did not form a uniform layer over the barrier surface. Drip marks were also observed. Because of the absence of uniform impervious membrane, the barrier is exposed to ambient air at very early ages. Concrete exposure to the environment at early ages affects the gain in compressive strength and tensile strength of concrete (RILEM-42-CEA, 1981). Uneven application of curing compound and slip forming promotes rapid loss of mix water, thereby generating a high temperature gradient between the interior and exterior surface of concrete. Additionally, thermal and drying shrinkage strains are amplified. These effects, combined with restraint effects may result in cracking and other distresses.

Control joints were hand-cut while the concrete is in a plastic state. In this project, control joint depth of 45mm is made every 4m interval. Control joints are planned breaks in concrete that allow it to move and prevent random cracking. Control joints are made after concrete has been placed and compacted. This is to allow the inevitable cracks to occur at these particular points, where they can be managed and out of sight. Wet formed joints are inserted with the use of a grooving tool, to create a plane of weakness, which conceals where the shrinkage crack will

occur. Control joints may also be sawn, but timing of sawing is very important. If the saw cut is too early, then it can ravel the concrete settings. If the saw cut is too late, the concrete might have already cracked randomly due to shrinkage plus restraint action.

The position and number of control joints must be carefully planned. In slip formed plain concrete barriers found in Ontario, control joints are placed at every 4 m to 9 m interval, with a depth of 20mm to 25 mm, within 12 hours of placing the concrete. According to the standard specifications of New Brunswick Department of Transportation, contraction joints shall be cut neatly in a vertical plane to a minimum depth of 50 mm and at a uniform spacing not exceeding 6 m. To be effective, the joint must be tooled to a minimum depth of quarter to one-third depth of the concrete (Concrete Basics, CCAA, 2004). For example, joint depth for a 100 mm thick concrete should be a minimum of 25 mm to 35 mm.

Figure 2.8: Construction Joint

Construction joint was done at the beginning of the slip formed barrier wall, as shown in Figure 2.8. Construction joint means the surface where two successive placements of concrete meet or where new concrete is placed against old concrete. As per Ontario Provincial Standard Specifications, for tall wall concrete barrier, five epoxy coated 25 mm diameter reinforcing bars of 1m long should be placed, with 500 mm on each side of the joint. The location of the bars should be in such a way that all bars should be placed in centerline, with the first bar placed at 150 mm from top, and the remaining equally spaced at 150 mm below it. However, in the site as seen in Figure 2.8, the first reinforcement bar is not placed as per specification. Based on the following observations, it is recommended to improve the construction practices while performing slip forming operations, with main emphasis on consolidation and curing practices.

Chapter 3

Experimental Investigation

3.1 Introduction

The aim of this study was to get a clear understanding of the effect of temperature on concrete properties. To get the correct information of actual temperature variations occurring on an exposed concrete surface, strain gauges and thermocouples were installed on a live concrete barrier wall located on Hwy 403. Temperature and strain data were stored in a data acquisition unit every hour and the data was collected every month.

At the same time, lab work was also conducted to monitor the variation of some important concrete parameters with time under different temperature exposures. This study involved a testing program of large number of concrete samples for quality control. Concrete samples were tested at room temperature and with exposure to temperature extremes from -50°C to +50°C in different humidity conditions, to evaluate basic properties such as modulus of elasticity, Poisson's ratio, coefficient of thermal expansion, compressive strength and tensile strength. The obtained information, that is the temperature data from the sensors and the concrete properties from lab experiments, was then incorporated into the numerical study of the behavior of concrete in long term.

3.2 Field Monitoring

The concrete barrier wall that was selected for this study is located on southbound Highway 403, near Highway 401. The barrier walls were cast slip-form on May 12, 2004. For slip-form casting,

a very low slump concrete is placed as a steel form was slowly moved, generating an extruded concrete profile. Very little vibrating was performed in order to retain the limited workability of concrete. The score joints or control joints were placed at 4 m intervals. They were planned breaks in concrete to prevent random cracking. The selected barrier length was in good shape at the time of site inspection and sensor installation during summer 2007. Only map cracks were visible on barrier surface, possibly due to plastic shrinkage and no symptoms of alkali aggregate reaction was found. Upon inspection, covering the entire barrier walls spanning almost 50 m in length, two vertical cracks were found, spaced almost 20 meters apart, might be happened due to concrete shrinkage. The cracks were less than 2 mm wide. Hairline vertical cracks were seen through almost every score joint.

Four strain gauges and two temperature sensors were installed on the surface of the barrier wall. Two temperature sensors were placed inside the concrete wall in order to measure the temperature inside the concrete core. Strain gauge units were placed at key locations in the barrier wall to measure strain in the concrete structure, as shown in the Figure 3.1. The installation of logging equipment allowed strain and temperature readings to be taken at regular intervals. Both data loggers were protected from dust and condensation.

All sensor wires were properly protected and attached to concrete surface. The wires are carried out into junction boxes located on the back face of the barrier wall. The sensors were then connected to the data acquisition unit in an enclosure with added interior insulation to reduce temperature extremes. The data acquisition unit was selected for its capability to support various types of sensors, high accuracy, on-line data manipulation and statistical functions. This

instrument used defined instructions to read data from the different sensors to which it was connected, and stored the data onto a memory card, until it was transformed to a personal computer. The data logger was programmed to take hourly readings from the sensors. The data was collected on a monthly basis.

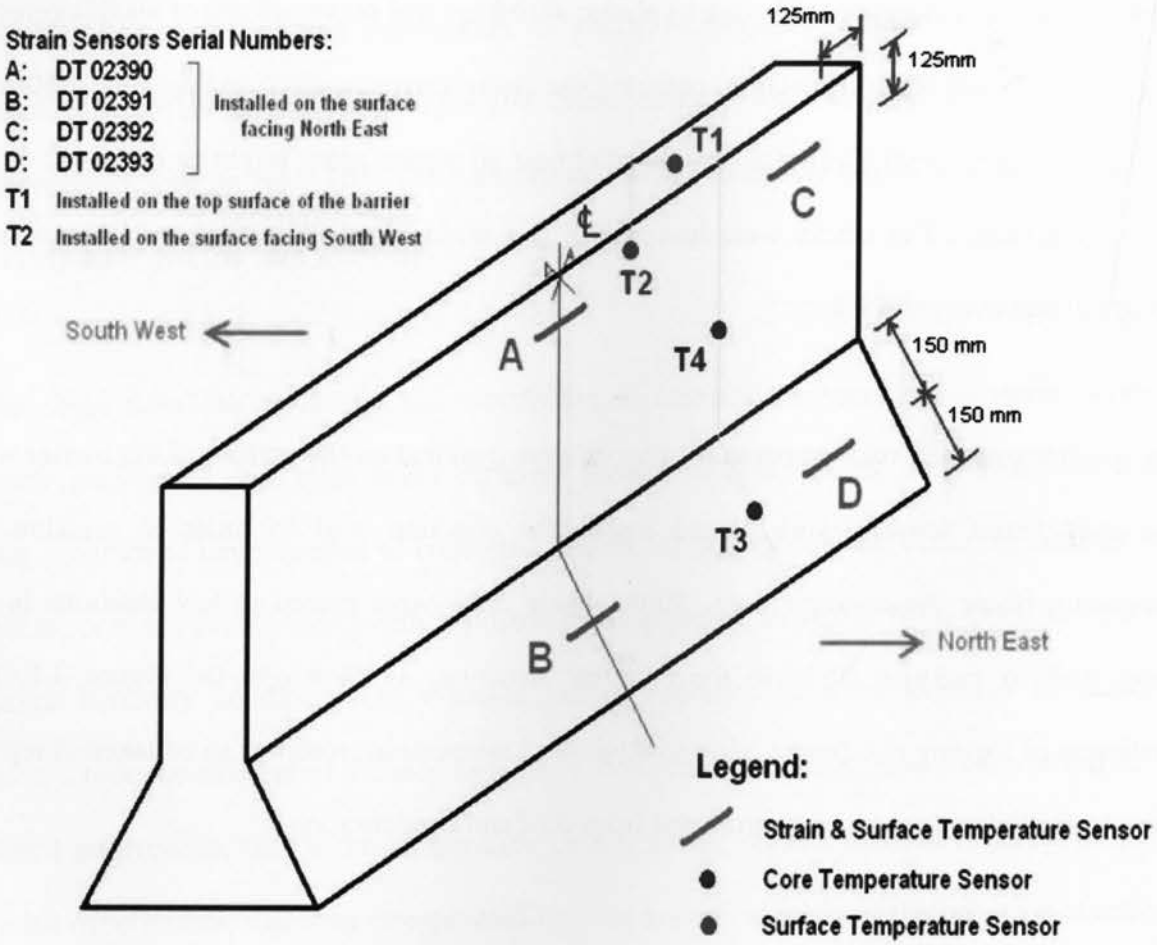

Figure 3.1: Sensor Locations on the Barrier wall

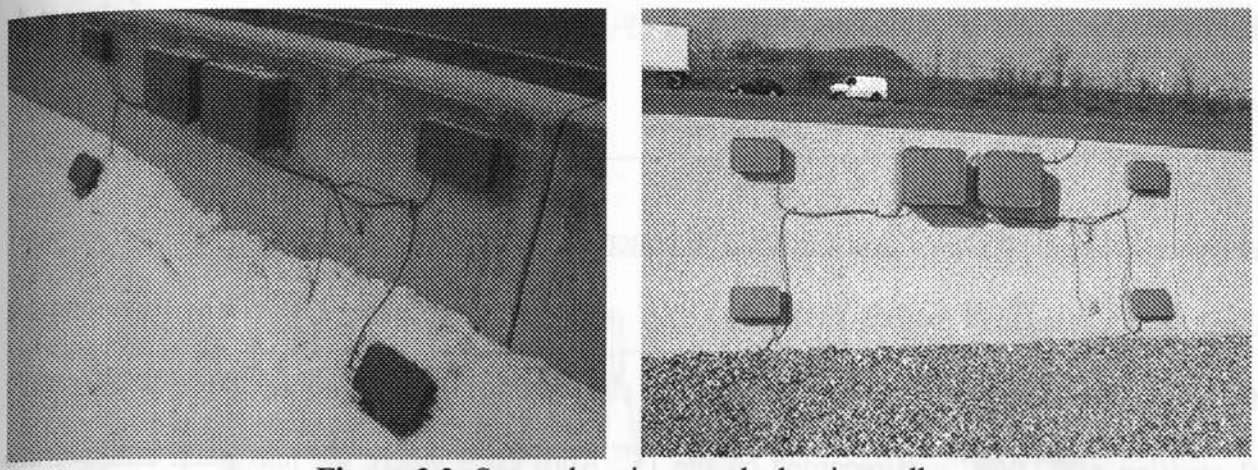

Figure 3.2: Sensor locations on the barrier wall.

Photo taken (a) during winter (b) during summer

During winter 2007-2008, freeze and thaw effect on barrier walls was very prominently seen. As seen in the Figure 3.2(a), snow shoveled out from road was thrown onto the rear side of the barrier walls, which kept the walls saturated almost throughout the wintertime. When saturated concrete is subjected to freezing and thawing cycles, external and internal damage can occur. External damage can be identified from the weathering of thin outer mortar layers and aggregate. This was pretty visible in the barrier walls under study. Internal damage can cause microscopic cracks in the cement paste, leading to change in mechanical parameters of the concrete.

Ultrasonic pulse velocity (UPV) test was performed on the top section of the barrier wall segment under study, in compliance with ASTM C 597. In this test, the pulse velocity of stress waves propagating through the concrete barrier wall was used to determine the homogeneity of concrete, the presence of voids, cracks or other imperfections, changes in the concrete which may occur with time through the frost or chemical attack and the quality of the concrete, which generally refer to its strength. The test gave an average pulse velocity of 4578m/s, which proved

that the concrete quality in the barrier segment wall selected for study, even at an age of almost 4 years, was still good.

Between August 2007 and April 2008, the concrete temperature measured in the barrier wall displayed a seasonal pattern between –13°C and +35°C (Figure 3.3). Daily temperature fluctuations of up to 27°C were recorded in the barrier wall. Maximum daily temperature fluctuation of 27.96°C was recorded on the 15th April 2008 where the maximum temperature observed was 26.744°C on the top surface of the barrier wall at 4.00PM and the minimum temperature observed was -1.213°C at the south west side of the barrier wall at 5.00AM.

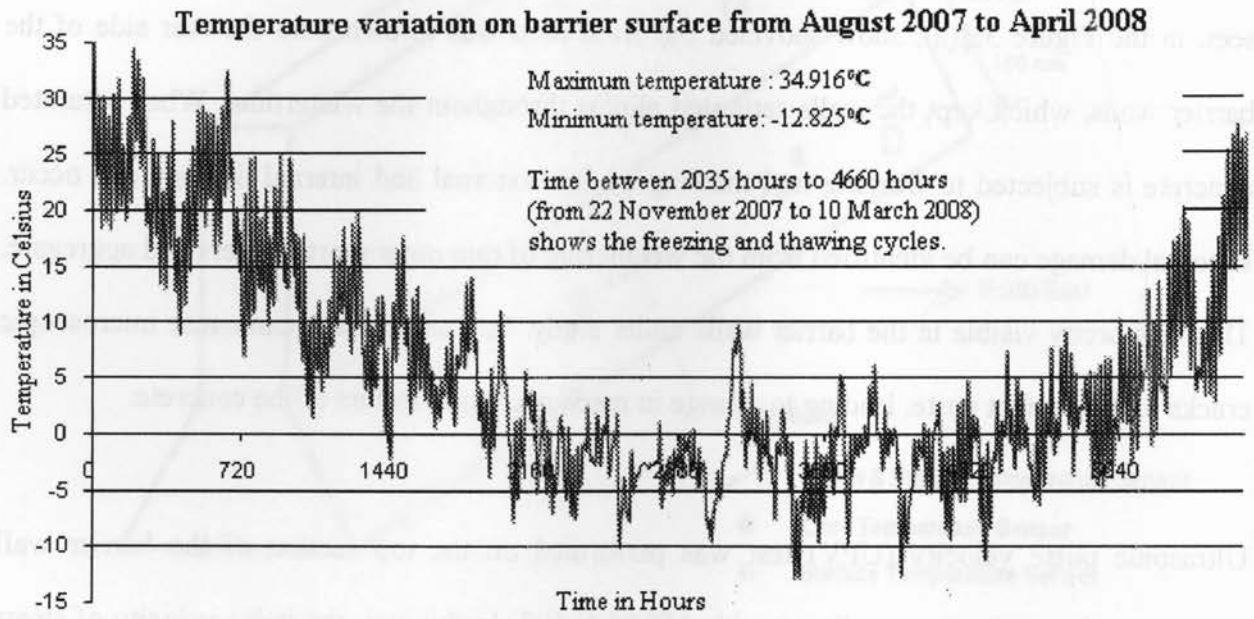

Figure 3.3: Temperature measured from sensors installed on barrier surface from August 2007 to April 2008

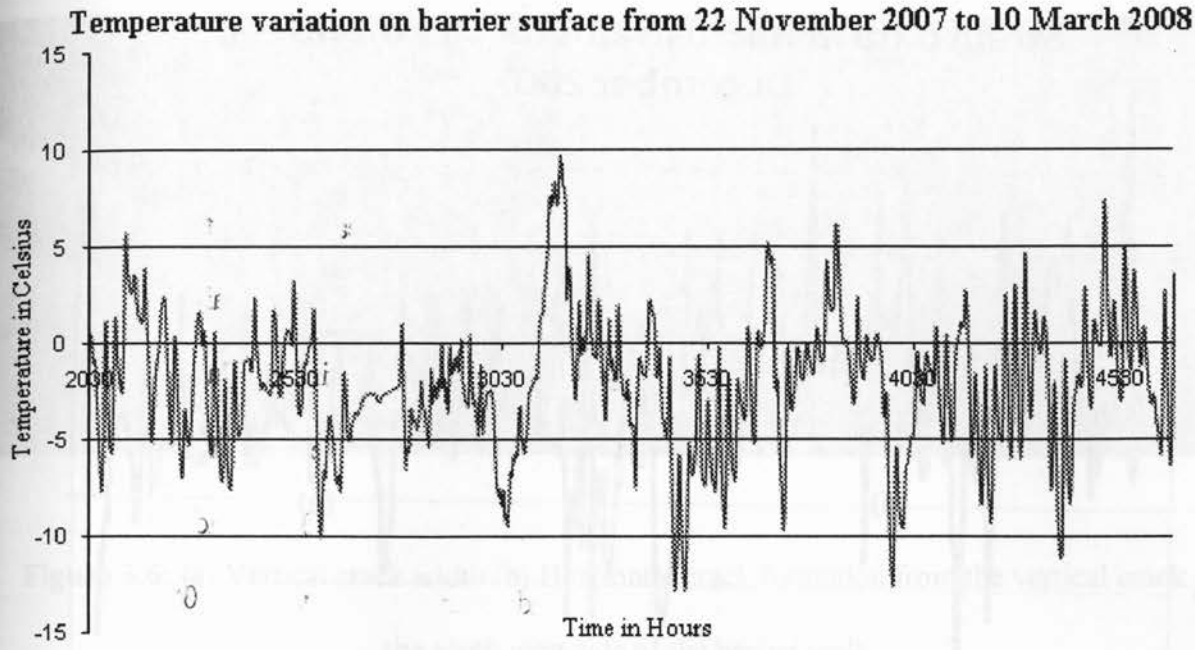

Figure 3.4: Freeze and Thaw cycles occurred in winter of 2007

The concrete temperature data were also used to estimate the number of freezing and thawing cycles that occurred in the concrete barrier wall. Assuming that capillary water in conventional concrete freezes at approximately –5°C and thaws at 0°C as suggested by Neville (1995), it was estimated that 21 freezing and thawing cycles occurred annually in the barrier wall during the last winter period (Figure 3.4). Figure 3.5 represents the hourly record of the total longitudinal strain along the length of the wall and the surface temperature, taken during the month of December 2007. The total strain measured clearly displayed a pattern similar to that of the surface temperature measurement. The trends of strains in concrete surface are dominated by the change in the surface temperature. This means that environmental conditions produce a far more significant response on the behavior of concrete barriers.

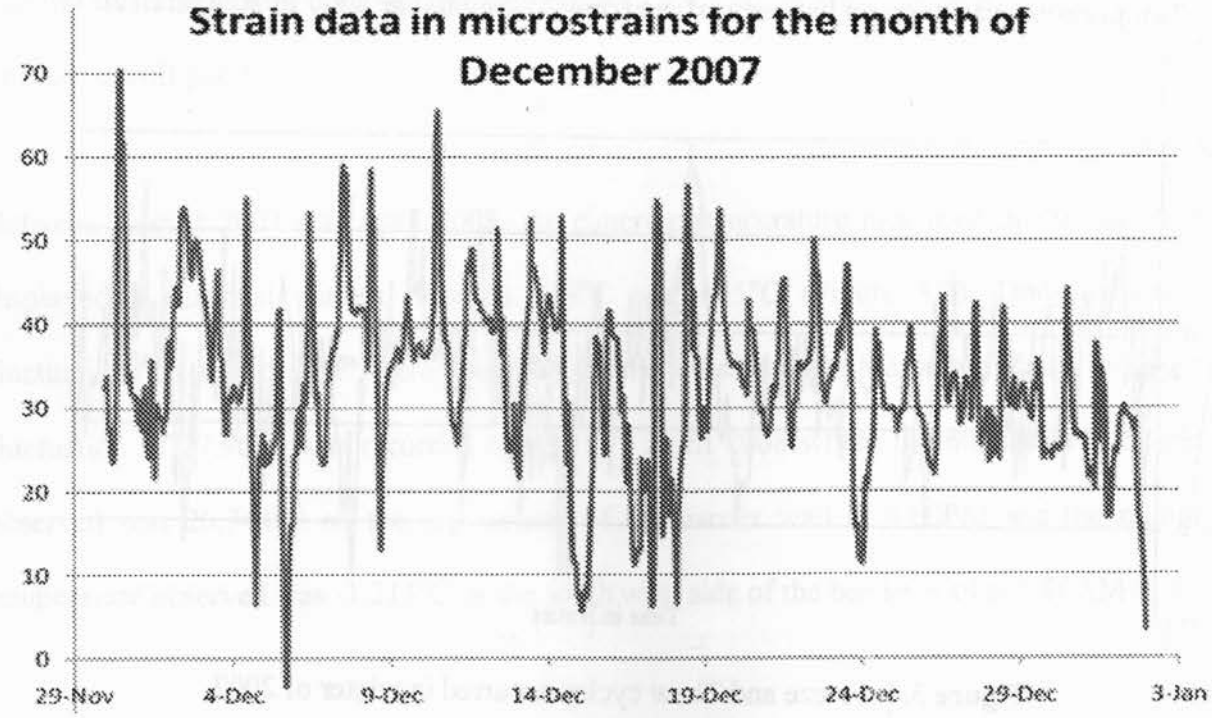

353

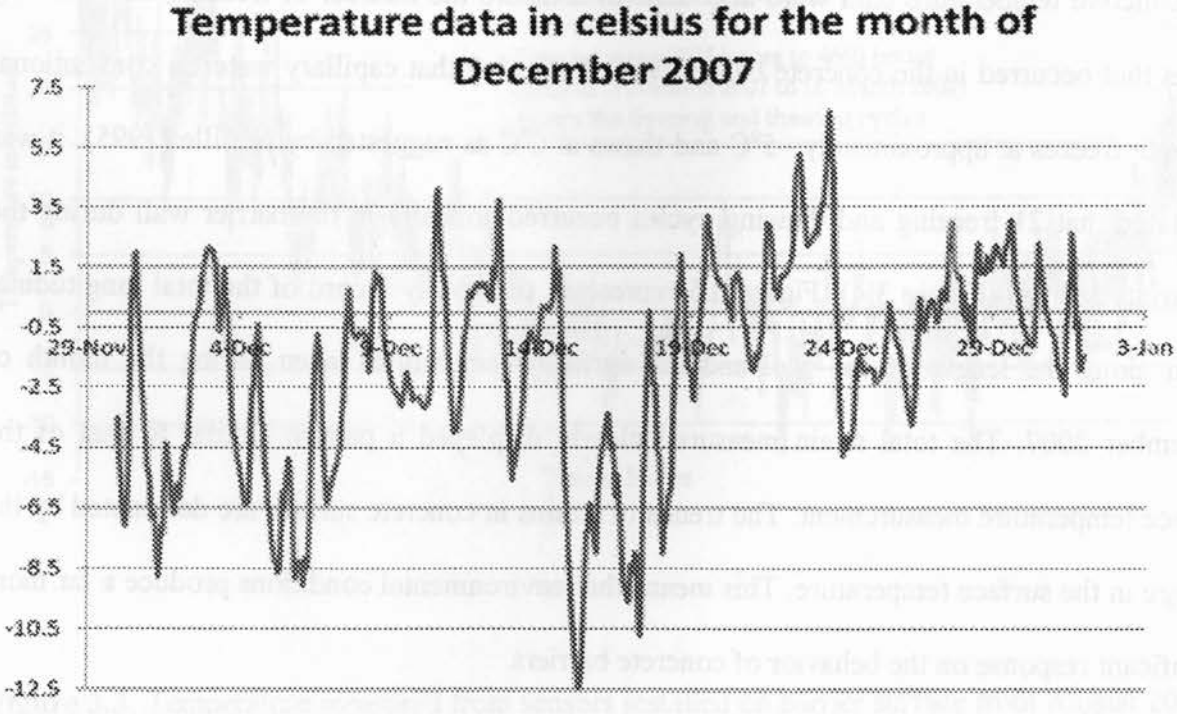

Figure 3.5: Total Longitudinal Strain and Temperature readings taken from Barrier surface

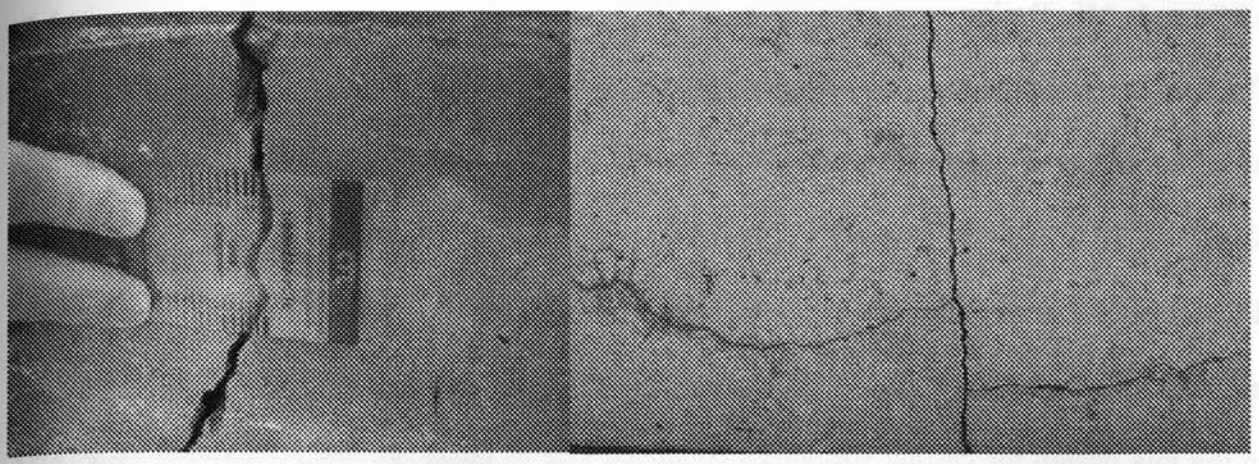

(a) (b)

Figure 3.6: (a) Vertical crack width (b) Horizontal crack formation from the vertical crack on the south west side of the barrier wall

The width of two full cut vertical cracks found within the entire span of barrier wall, was found increasing during winter (Figure 3.6 (a)). However, on a site visit during June 2008, the crack width decreased, indicating a possible expansion of concrete due to temperature increase. Also, another important fact to notice was that, horizontal cracks started forming on the south west side of the barrier wall, starting from the vertical crack, as shown in Figure 3.6 (b). No horizontal crack was seen on the north east face of the barrier wall, even though the vertical crack was full cut through the width of the barrier wall. From the temperature data obtained from the installed sensors, the temperature on the south west face of barrier wall is higher than the temperature on the north east face, on an average basis. Therefore, in this case, the formation of horizontal cracks only on the south west face of the barrier wall can be due to the influence of this temperature variation. However, in the case of horizontal cracking as seen in Figure 2.2, the cause is due to the improper construction practices.

3.3 Sample Mix Design

The field investigation was also complemented by the lab work, to monitor the variation of some important concrete parameters with time under different temperature exposures.

The selection of materials and concrete mix design was finalized in consultation with MTO engineers. Table 3.1 shows the mix design adopted for the experimental work. The concrete used in the mix design for casting specimens contained slag as pozzolan, had a maximum aggregate size of 19 mm and design strength of 35 MPa. Since low slump concrete was used in slip-forming works, to increase workability, water reducer/retarder was used in real construction practices. Also to reduce freeze and thaw actions, air-entraining agent is widely used. Hence, in the sample mix design, Daratard HC was the chemical admixture used as the water reducer/ retarder and Ever Air Plus was used as the air-entraining agent.

Material used	**Quantity**
Cement, Type 10	289 kg/m^3
Slag Cement	96 kg/m^3
Coarse Aggregate, maximum size of 19mm	1070 kg/m^3
Fine Aggregate	737 kg/m^3
Water Content	140 l/m^3
Chemical admixture	400 ml/kg of cement

Table 3.1. Sample Mix Design Adopted

3.4 Concrete Properties

Mechanical and other physical properties related to concrete durability were obtained through several standard tests. Mechanical properties of concrete were obtained from compressive strength and elastic modulus tests in accordance with ASTM C 39 and ASTM C 469 respectively. Mechanical vibration was applied to all specimens and samples were kept in the moist curing room. All samples were de-molded on the next day. The program outline for testing the specimens was as follows:

- ✓ X samples were cured for 28 days and stored in temperature controlled room at 21 ± 2°C and 50 ± 4% RH.

Figure 3.7: Samples in Environmental Chamber

- ✓ Y samples were cured for 28 days and exposed to temperature variation from -50°C to +50°C in "Wet" condition. Samples after 28 days of curing were immersed in a pail of water and kept in an environmental chamber. Chamber controlled the temperature cyclically, completing one cycle from -50°C → +50°C → -50°C linearly.

- ✓ Z samples were cured for 28 days and exposed to temperature variation from -50°C to +50°C in "Dry" condition. Samples after 28 days of curing were kept in an environmental chamber with humidity control disabled, so as to keep the samples in dry condition. Chamber controlled the temperature cyclically, completing one cycle from -50°C → +50°C → -50°C linearly.

3.4.1 Slump Test

Slump Test was performed for each batch prepared, using specifications as per ASTM C 143-90a.

3.4.2 Air Content Test

Air content test on fresh concrete was carried out on each batch mix as per ASTM C 231 specification.

3.4.3 Compressive Strength Test

Durability properties of concrete can be strongly related to its compressive strength. The strength test was performed on standard cylinder specimens of 100 x 200mm as per specification ASTM C 39. A total of twenty four cylinders were tested as per the following outline:

- X = 3 + 3 + 3 + 3= 12 samples for determining 7, 28, 56 and 112 day compressive strength.
- Y = 3 + 3= 6 samples for determining 56 and 112 day compressive strength.
- Z = 3 + 3= 6 samples are used for determining 56 and 112 day compressive strength.

3.4.4 Splitting Tensile Strength Test

Splitting tensile test was performed on twenty one 100 x 200 mm cylinder specimens according to the specification ASTM C 496-96. The samples were tested as per the following outline:

- X = 3 + 3 + 3 = 9 samples for determining 28, 56 and 112 day tensile strength.
- Y = 3 + 3 = 6 samples for determining 56 and 112 day tensile strength.
- Z = 3 + 3 = 6 samples for determining 56 and 112 day tensile strength.

3.4.5 Modulus of Elasticity Test

The knowledge of elastic modulus is very important from a design point of view when the deformations of a structure have to be calculated (Oluokun et al., 1991). After cracking, the elastic modulus of the concrete element is reduced to zero, only in the direction parallel to the principal tensile stress direction. However when crushing of concrete occurs due to compressive stresses, the elastic modulus is reduced to zero in all three principal directions, and thus the structural integrity is completely lost.

As per the specification ASTM C 469, test was conducted on eighteen 100 x 200 mm cylinder specimens to determine Young's modulus of Elasticity. The samples were tested as per the following outline:

- X = 3 + 3 = 6 samples for determining 56 and 112 day modulus
- Y = 3 + 3 = 6 samples for determining 56 and 112 day modulus.
- Z = 3 + 3 = 6 samples for determining 56 and 112 day modulus.

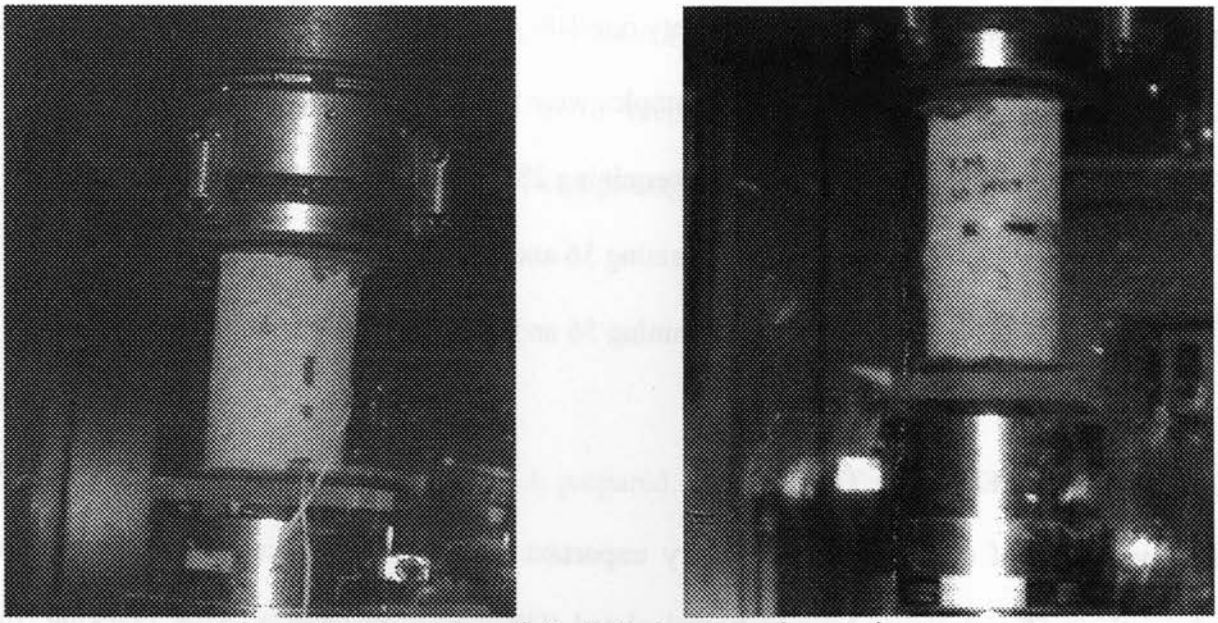

Figure 3.8: Modulus of elasticity testing using strain gauges

3.4.6 Length Change in Hardened Concrete

ASTM C 490 – 00a procedure was used to determine the change in length in hardened concrete due to causes other than any applied load. Three prisms of size 75 x 75 x 285 mm having gage length of 250 mm were used for this test. The prisms were moist cured for 14 days and were monitored on the 14^{th} day. The prisms were placed at room temperature of 23°C and 50% humidity. The dial indicator system was initially calibrated and reset using the invar rod. The prismatic shrinkage specimens were located in the comparator system using the inserts at the ends of the specimen. Comparator readings were taken in seven day interval time for five months. At each monitoring time, the length change of the specimen was measured and recorded three times. The average of these three readings was used for calculation purposes.

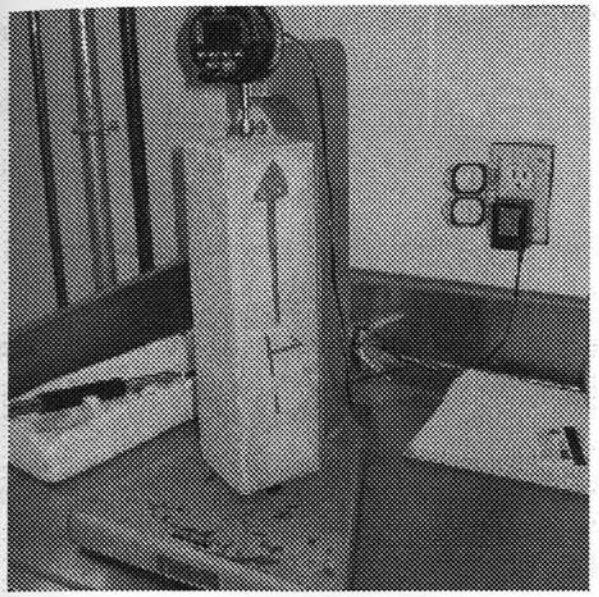

Figure 3.9: Comparator for Shrinkage tests

3.4.7 Ultrasonic Pulse Velocity Test

Ultrasonic pulse velocity (UPV) test was performed in compliance with ASTM C 597. The UPV test measures the velocity of stress waves propagating through the concrete specimen. The pulse velocity of stress waves in concrete is related to its elastic properties and density. This test method is often used to evaluate the uniformity and relative quality of concrete and to indicate the presence of voids and cracks. It may also be used as evidence to the changes in concrete properties. This test was performed on specimens at laboratory on 28^{th}, 56^{th} and 112^{th} day of casting. This test was also performed on the barrier wall selected for field study.

Chapter 4

Numerical Analysis of Concrete Barrier Wall

4.1 Introduction

Experimental based testing method produces real life response, but it is extremely time consuming. Also, the use of materials and time consuming can be quite costly. Many empirical models have been proposed to quantify the degradation effects of various deterioration processes. However each empirical model usually characterizes a single deterioration process, without considering the interactions with other deterioration processes. Many empirical models are limited to individual observation or environments, and thus it is difficult to apply practical condition on it. Because in reality, fully exposed concrete structures like barrier walls, with arbitrary geometries and dimensions, are subjected to randomly varying environmental loadings. To account the highly interactive and non-linear nature of the coupled deterioration processes in exposed concrete structures, finite element analysis may be more efficient and easy to apply.

Finite element method gives mathematical solution to complex differential equations of an engineering problem, approximated algebrically. The geometry of the problem is described by discrete elements of finite dimensions, analyzed through the application of engineering mechanics principles. Results of the finite element analyses are aggregated to approximate the exact mathematical solution. Unfortunately, early attempts to accomplish this were also time consuming and infeasible. However, in the recent years, the use of finite element analysis to study concrete elements has increased due to progressing knowledge and capabilities of

computer software and hardware. It has now become the choice method to analyze concrete structural components, since it is extremely cost effective and less time consuming.

In spite of the traditional way of designing and analyzing concrete, the development of finite element method has a significant implication on concrete structural analysis in a practical way. The simulation of concrete properties was never been an easy task, due to the complexity of the concrete and uncertainty of its material properties. Concrete is a quasi-brittle material and behaves differently in tension and compression state. Un-reinforced concrete structures are the most fracture sensitive. Fracture being the most important mode of deformation and damage in concrete structures; it is often necessary to use finite element analysis to accurately predict its behavior. The two dominant techniques used in the finite element modeling of fracture are (a) the discrete crack approach, where the cracks are modeled discretely and (b) the smeared crack approach, where cracks are distributed and so the damage.

4.2 ANSYS

There are a number of computer programs available in the market for concrete structural analysis. In this thesis, finite element software ANSYS is used to conduct the thermal and structural analysis and to understand the response and effects of temperature variations on the un-reinforced concrete barrier walls. ANSYS uses smeared crack approach, which is the most widely used approach in practice. This is because the procedure is computationally convenient. Usually, a crack in concrete is not straight, but highly tortuous and such a crack can be adequately represented by a smeared crack band.

4.2.1 Transient Analysis

The response of plain concrete barrier walls to environmental thermal actions is a complex transient phenomenon as these structures are subjected to daily repeated cycles of solar heating and cooling. It is subjected to ambient temperatures that vary with time due to diurnal and seasonal changes in climatic/atmospheric conditions. The temperature distributions in exposed barrier walls depend upon environmental, meteorological, structural geometry and material parameters. Due to poor thermal conductivity of concrete, there is an hourly change of temperature from the concrete surface to the interior point of the structure, resulting in non-linear temperature distribution across the cross section. Consequently, self-equilibrating thermal stresses are produced in these structures. Base and end restraint conditions have an add-on effect on these stresses. A comprehensive non-linear transient thermal and structural analysis should be performed to study the effect of some base parameters governing the behavior with time of un-reinforced concrete barrier walls. In this research concrete barrier wall was analyzed for structural boundary conditions along with the temperature-induced stresses from the thermal analysis.

4.2.1.1 Elements used in Transient Analysis

In the present study, finite element model was developed using graphical user interface (GUI) in ANSYS. A two-step solution was employed in order to enable the model to predict the field conditions in a better way. The simulation of hourly temperature variation and the associated thermal stress was performed first using the transient thermal analysis procedure in ANSYS. The analysis was three-dimensional and the element type used is SOLID70. It was an eight noded three-dimensional thermal element with degree of freedom as temperature at each node. The

geometry, node locations and coordinate system of SOLID70 element are shown in Figure 4.1. The temperature readings taken every hour at various sensor locations on barrier wall were entered in the model as input.

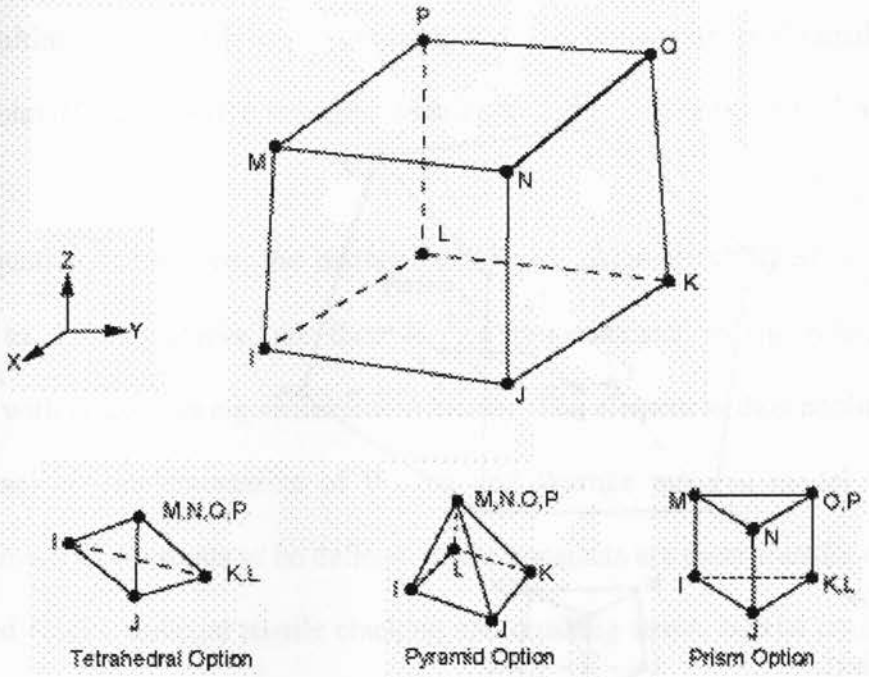

Figure 4.1: SOLID70 Element (ANSYS 9.0)

The thermal analysis was followed by non-linear structural analysis. To simulate the effect of concrete, ANSYS uses element SOLID65. It is a 3-D solid isoperimetric element with eight nodes and three translation degrees of freedom at each node. . The geometry, node locations and coordinate system of SOLID65 element are shown in Figure 4.2. It is used to model the nonlinear behavior, and can predict the failure mode of brittle materials like concrete. The element is capable of cracking (in three orthogonal directions), crushing, plastic deformation and creep. The element includes a smeared crack analogy for cracking in tension zones and a plasticity algorithm to account for the possibility of concrete crushing in compression zones.

Each element has eight integration points at which cracking and crushing checks are performed. The solution output consists of nodal displacements, normal, shear and principal components of stresses and strains in x, y and z directions. The element's stress directions are parallel to the element's coordinate system.

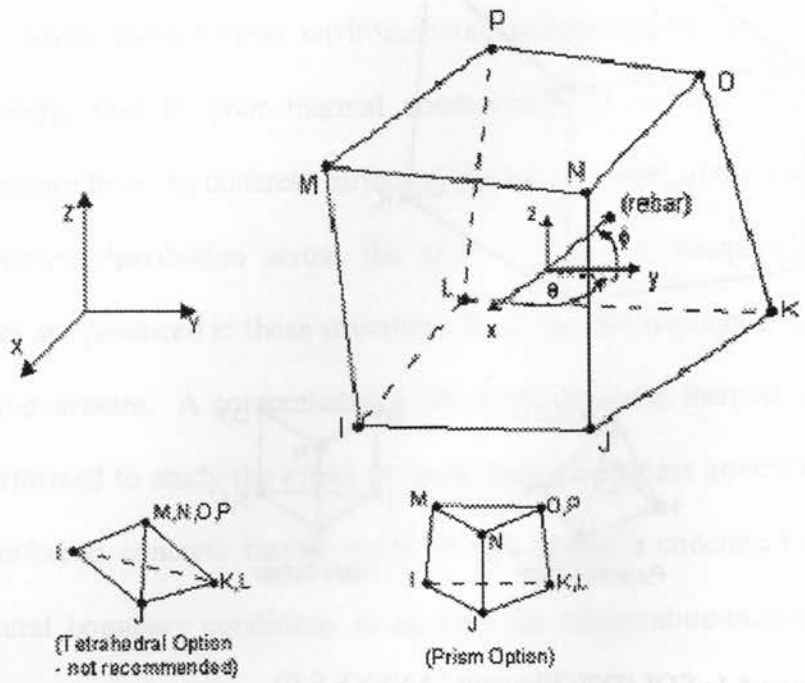

Figure 4.2: SOLID65 Element (ANSYS 9.0)

The element behaves in a linear elastic manner until either of the specified tensile or compressive strengths is exceeded. Cracking or crushing of an element is initiated once one of the element principal stresses, at an element integration point, exceeds the tensile or compressive strength of the concrete. ANSYS uses the following equation calculated by Willam and Warnke (1975) as the criterion for failure of concrete due to a multi-axial stress state, which is expressed as

$$F/f'c - S \geq 0 \quad \text{.....(4.1)}$$

where,

F is a function of the principal stress state (σ_{xp}, σ_{yp}, σ_{zp})

S is the failure surface expressed in terms of principal stresses and five parameters f_t, f'_c, f_{cb}, f_1 and f_2.

f'_c is the ultimate uniaxial crushing strength; f_t is the ultimate uniaxial tensile strength; f_{cb} is the ultimate biaxial compressive strength, defaults to 1.2 f'_c ; f_1 defaults to 1.45 f'_c ; f_2 defaults to 1.725 f'_c

If this equation is satisfied, the material will crack or crush. Cracked or crushed regions, as opposed to discrete cracks, are then formed perpendicular to the relevant principal stress direction with stresses being redistributed locally. The element is thus nonlinear and requires an iterative solver. Implementation of Willam and Warnke material model in ANSYS requires different material constants to be defined. These constants are shear transfer coefficients for open and closed cracks, uniaxial tensile cracking and crushing stress, biaxial crushing stress, ambient hydrostatic stress state, biaxial crushing stress under ambient hydrostatic stress, uniaxial crushing stress under ambient hydrostatic stress state and stiffness multiplier for cracked tensile condition.

4.2.1.2 Material Properties and Element Constants

The material properties were provided in the model to match with those obtained from the experimental tests done of a selected mix design concrete samples, mostly used in barrier construction as per MTO specifications. The SOLID65 element requires linear isotropic and multi-linear isotropic material properties to properly model concrete. Concrete is a quasi-brittle material and has different behavior in compression and tension.

In compression, the stress-strain curve for concrete is linearly elastic up to about 30% of the maximum compressive strength (Figure 4.3). After this the stress increases gradually up to the maximum compressive strength. Once it reaches the maximum compressive strength σ_c, the curve descends into a softening region and eventually crushing failure occurs at an ultimate strain ε_c

In tension, the stress-strain curve for concrete is approximately linearly elastic up to the maximum tensile strength. After this point, the concrete cracks and the strength decreases gradually to zero.

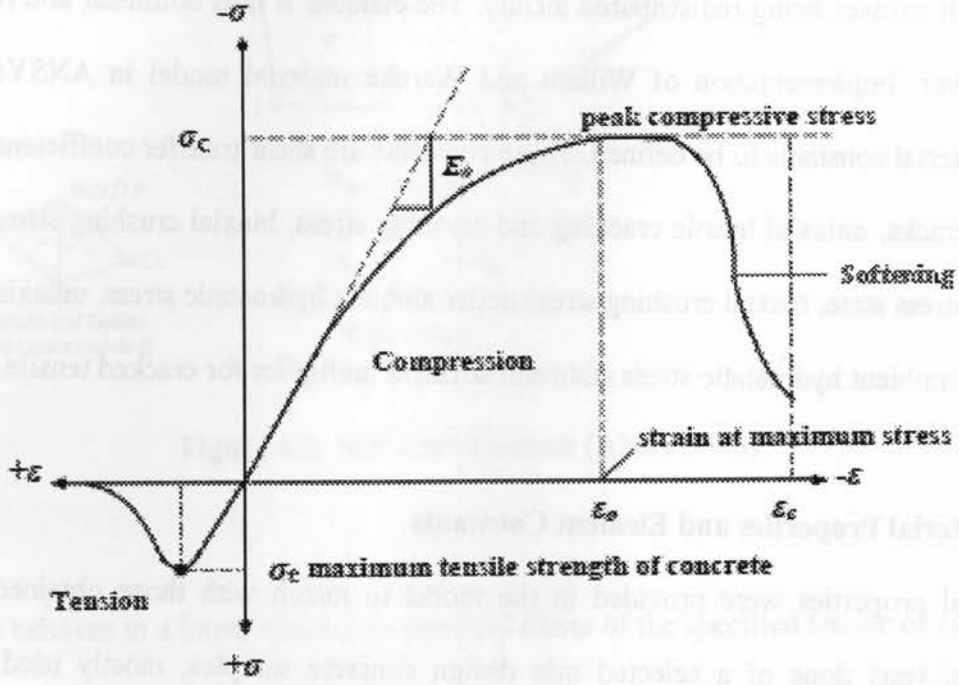

Figure 4.3: Typical uniaxial compressive and tensile stress-strain curve for concrete (Kachlakev, 2001)

For linear isotropic model, elastic modulus (E) and Poisson's ratio were entered. For multilinear isotropic model, ANSYS program requires the uniaxial stress-strain relationship for concrete in

compression. The multilinear curve is used to help with convergence of the nonlinear solution algorithm. The uniaxial stress-strain relationship of concrete was entered with several points, which were calculated using the following equations proposed by Popovics (1973) to compute the stress-strain distribution of concrete for compressive strengths from 14MPa to 70MPa.

$$f_c = f'_c \frac{\epsilon_c}{\epsilon_o} \{ n / [(n-1)+(\epsilon_c/\epsilon_0)^n] \} \quad \text{.....(4.2)}$$

$$n = 0.4 \times 10^{-3} f'_c + 1$$

$$\epsilon_0 = 2.74 \times 10^{-4} \sqrt[4]{f'c}$$

where

f_c is the stress at any strain ϵ_c, in psi (MPa)

ϵ_0 is the strain at the ultimate compressive strength f'_c

n is the coefficient for concrete behavior that can be expressed as an approximate function of the compressive strength of normal weight concrete.

The expression for secant modulus of elasticity E in GPa and f'_c in MPa, recommended by ACI 318-89 (1996) for structural calculations, applicable to normal weight concrete, is

$$E = 4.73(f'_c)^{0.5} \quad \text{.....(4.3)}$$

The concrete elastic modulus obtained from experiments is 42.3Gpa. From equation 4.3, f'_c can be calculated as 80MPa. The stress-strain points are calculated using equation 4.2 and given in Table 4.1.

Element Type	Value Adopted			
SOLID65	Thermal Conductivity		2.4W/m-K	
	Density		2350kg/m3	
	Linear Isotropic			
	EX	42.3GPa		
	PRXY	0.2		
	Multilinear Isotropic			
	Points	Strain	Stress	
	Point 1	0.0003	10.41	MPa
	Point 2	0.0006	20.82	MPa
	Point 3	0.0009	31.21	MPa
	Point 4	0.0012	41.56	MPa
	Point 5	0.0015	51.71	MPa
	Point 6	0.0018	61.36	MPa
	Point 7	0.0021	69.90	MPa
	Point 8	0.0024	76.39	MPa
	Point 9	0.0027	79.74	MPa
	Point 10	0.003	79.05	MPa
	Concrete Material Data			
	Shear Coeff-Open Cracks		0.3	
	Shear Coeff-Closed Cracks		0.9	
	Uniaxial Tensile Stress		4.5MPa	
	Uniaxial Compressive Stress		-1	
	Stiffness multiplier		0.6	
SOLID70	Thermal expansion Coeff		1.1e-05/^{0}K	
	Specific Heat		950J/kg-K	
	Density		2350kg/m3	

Table 4.1 Material Properties adopted for the Analysis

The values adopted in the finite element analysis are provided in Table 4.1. However, these default values are valid only for stress states where the hydrostatic stress $|\sigma h| \leq \sqrt{3}$ f'c is satisfied, where $\sigma h = \frac{1}{3}(\sigma_{xp} + \sigma_{yp} + \sigma_{zp})$.

4.2.1.3 Analysis Assumptions

1. The computational time for the non-linear coupled transient thermal/structural analysis was too long when conducted on a per hour basis for a period of 3 years. Hence the time frame of analysis was restricted to 3 years.
2. Temperature input for the transient analysis was taken from the temperature sensors installed on the barrier wall, which started from August 29, 2007, recording temperature measurements on an hourly basis. The temperature recorded till April 22, 2008 was taken in the analysis. Rest of the temperature points to complete one year was calculated manually, taking into consideration the atmospheric temperature measurements given at Environmental Canada website. The temperature points were thus set for duration of one year. The one year points were repeated for the next two year intervals to analyze the model for three year duration. The reference temperature was taken as 21°C, i.e. 294°K.
3. In the numerical routines, the formation of a crack was achieved by the modification of the stress-strain relationships of the element to introduce a plane of weakness in the requisite principal stress direction. After cracking, the tension stress of the concrete element was set to zero in the direction normal to the crack plane. The amount of shear transfer across a crack could be varied between full shear transfer represented by one and no shear transfer represented by zero at a cracked section. In the analysis here, shear transfer coefficient for open crack was taken as 0.3 and for closed crack as 0.9. The higher values of shear transfer coefficient were used to avoid convergence problems during iteration. Kachlakev et al. (2001) and Wolanski (2004) used 0.3 for open crack constant in modeling normal strength concrete. Wolanski (2004) reported that

convergence problems repeatedly occurred when the shear transfer coefficient for an open crack dropped below 0.2.

4. For uniaxial crushing stress f'_c, experimental value of concrete compressive strength was available. However, this constant was set to a value of -1 in ANSYS material data, which turns off the crushing capability of Solid65 element. When the crushing capability was turned on, the solution did not converge. A pure compression failure of barrier wall is unlikely to happen due to environmental or age effects. Many past researchers like Kachlakev (2001), Wolanski (2004) and Zhenhua (2006) had suggested to turn off the crushing capability to avoid non convergence problem. Therefore, in this study, the failure of the finite element model was controlled by the cracking of concrete.
5. The crushing algorithm was similar to plasticity law that once a section had crushed, any further application of load in that direction developed increasing strains at constant stress. Subsequent to the formation of an initial crack, stresses tangential to the crack face might cause a second or third crack, to develop at an integration point. Stress relaxation after cracking was included in the material constants. Relaxation of concrete in tension can be beneficial because it may reduce tensile stress caused by internal and external restraints (Saucier et al 1997).
6. No settlement occured in the granular foundation.
7. Thermal expansion coefficient of concrete was taken as a constant value of 11E-06/°C.
8. Stiffness multiplier constant for cracked tensile condition was assumed as 0.6. This constant was used to define the effect of tension stiffening as shown in Figure 4.3. In this figure, f_t is the uniaxial tensile strength of the concrete. Upon cracking, the tensile stress drops abruptly to a fraction of it, $T_c f_t$, where T_c is a multiplier for the amount of tensile

stress relaxation (ANSYS 9.0). Thereafter, the tensile stress of concrete approaches to zero at a strain 6 times the cracking. T_c has a value between zero and one. An input of zero stands for a complete loss of tensile stress at cracking; and a value of one means no sudden loss of tensile stress at cracking. System default value of 0.6 was adopted in this study.

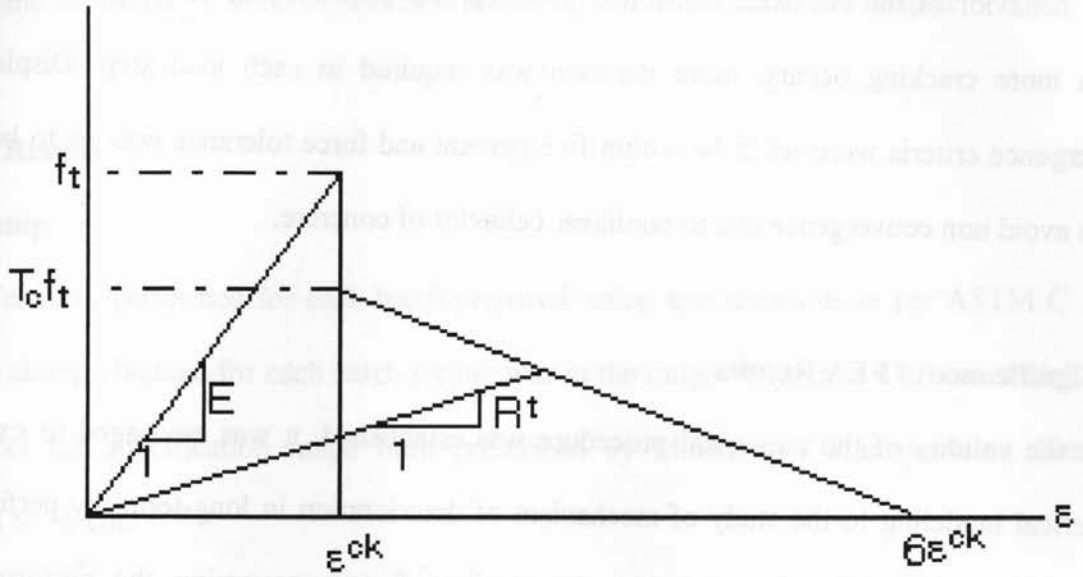

Figure 4.4: Tensile Strength of Cracked Concrete (ANSYS)

4.2.1.4 Analysis Type and Solution Controls

For running non-linear analysis, the "Solution Controls" option needed to be set for an appropriate iteration process and output of the program. The "Solution Controls" contained a set of related parameters, as follows: Basic, Transient, Solution Options, Non-linearity and Advanced Non-linearity. Under "Basic" controls, Small Displacement Transient Analysis was selected to perform a linear transient analysis, in which large deformation effects were ignored. "Number of substeps" provided a measure of rate of loading. Here, single substep was given for

each load step and hence, the automatic control was turned off. For structural analysis, line search option was turned on.

In non-linear controls, criteria for convergence were based on force and displacement. To obtain accurate predictions, Newton-Raphson equilibrium iteration was used to resolve for the non-linear behavior of the concrete, controlled by force and displacement convergence tolerances. When more cracking occurs, more iteration was required in each load step. Displacement convergence criteria were set to be within five percent and force tolerance was set to be within 10, to avoid non convergence due to nonlinear behavior of concrete.

4.3 Significance of FEA Results

Once the validity of the numerical procedure was established, it was envisaged to extend the numerical modeling to the study of mechanism of deterioration in long-term, by performing a parametric study, taking into consideration various factors governing the performance of concrete barrier walls. The ultimate objective of this task was to model age-related phenomena on these types of structures in order to provide designers with a working tool that allowed the conception of crack-free and durable concrete barrier systems. The results obtained will relate to the performance of the whole structure subjected simultaneously to a number of rapidly alternating environmental and in-service conditions.

Chapter 5

Experimental Test Results

5.1 Introduction

The results of the experimental program conducted in the laboratory for the concrete mix design selected and approved by MTO engineers is presented and discussed in this chapter.

5.2 Test Results

5.2.1 Slump

Slump Test was performed for each batch prepared, using specifications as per ASTM C 143-90a. The slump obtained for each batch testing was in the range of 12cm to 14.5 cm, which was well under the specification range limit prescribed by Ministry of Transportation Ontario. ie, 10 cm to 15 cm.

5.2.2 Air Content

Air content test on fresh concrete was carried out on each batch mix as per ASTM C 231 specification. The percentage air content obtained for each batch testing was between 6% and 8%.

5.2.3 Compressive Strength

The strength test was performed on standard cylinder specimens of 100mm x 200 mm as per specification ASTM C 39. A total of twenty four cylinders were tested. Table 5.1 and Fig. 5.1 show the result of compressive strength of cylindrical specimens measured at 7, 28, 56 and 112

days. The samples showed a 28-day compressive strength of more than 40 MPa, which can be treated as a high strength concrete that requires special placement and curing procedures. The mix design used in the samples was approved by MTO, and has been used in the real barrier construction.

The strength decrease of wet and dry samples with time due to repeated action of freezing and thawing is very prominent, especially in the case of wet samples. In the real life situation, concrete barriers experience these situations, especially during winter season. If the barrier is on the road side, there is no doubt that half of the barrier portion will be fully immersed in snow during heavy winters, since the snow ploughs throw the snow from road to the rear side of the barriers. In such cases, the rate of strength increase in an exposed concrete with time will be less than that predicted.

Age of the Specimen (day)	Compressive Strength in MPa		
	Moist	Wet	Dry
7	32.63	32.63	32.63
28	41.03	41.03	41.03
56	51.11	48.79	50.52
84	55.88	51.52	54.14
112	56.32	50.72	53.07

Table 5.1: Compressive strength of concrete tested under dry, moist and wet conditions.

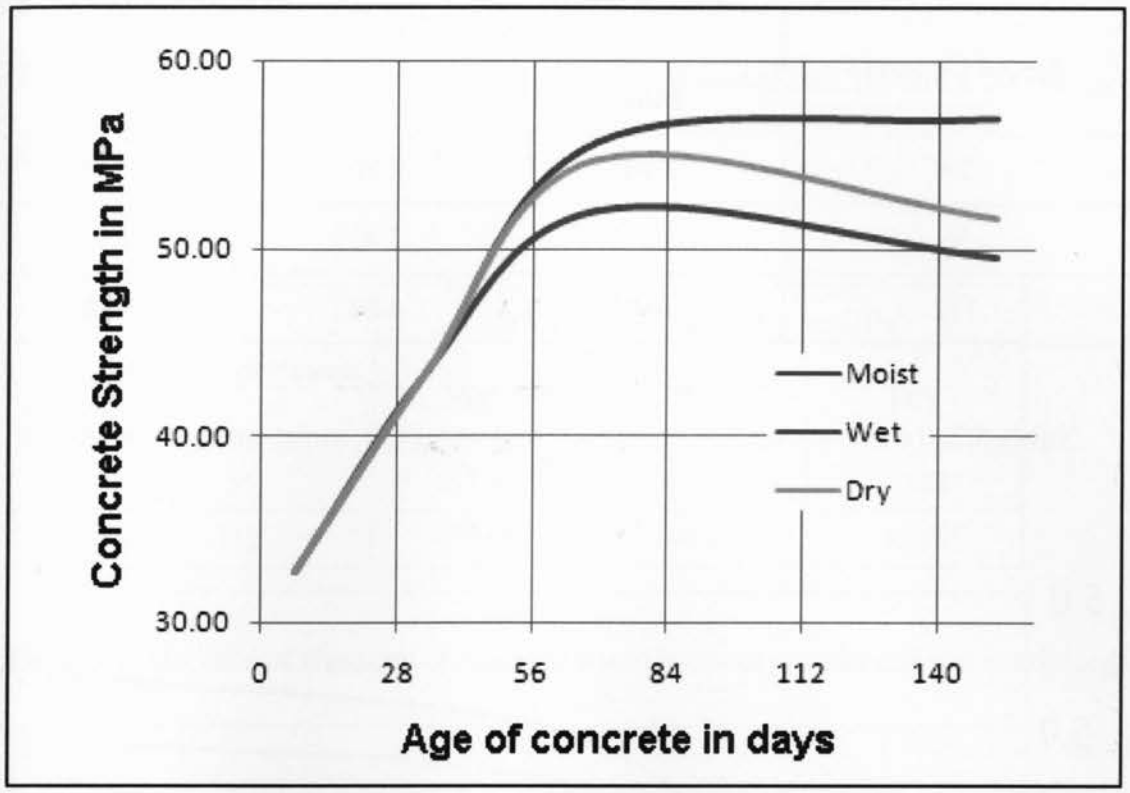

Figure 5.1: Compressive strength of concrete tested under dry, moist and wet conditions.

5.2.4 Splitting Tensile Strength

Splitting tensile test was performed on twenty one 100mm x 200mm cylinder specimens according to the specification ASTM C 496-96. Table 5.2 and Fig 5.2 show the result of tensile strength of cylindrical specimens measured at 28, 56 and 112 days. Dry specimens exhibited higher tensile strength values in due course of time, whereas wet specimens showed the least. The cracking initiates when concrete fails in tension. Thermal cracks, shrinkage cracks and flexural cracks are all tensile failures. Since the tensile strength of concrete is lowest when it is exposed to wet condition, precautions should be taken for the complete removal of snow around the barrier wall during winter.

Age of Concrete	Tensile Strength in MPa		
	Moist	Wet	Dry
28	2.707	2.707	2.707
56	3.954	3.432	4.196
112	4.76	4.293	5.189

Table 5.2: Tensile strength of concrete tested under dry, moist and wet conditions.

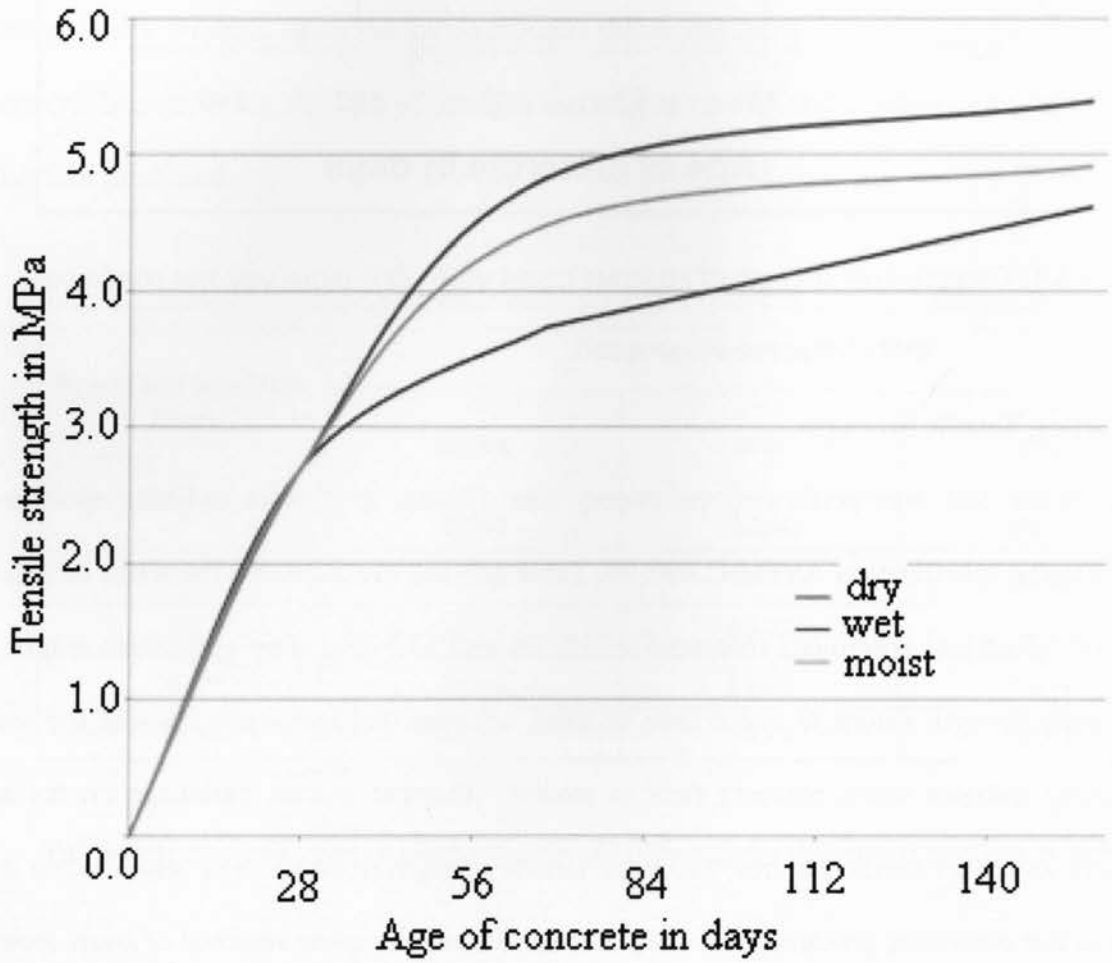

Figure 5.2: Tensile strength of concrete tested under dry, moist and wet conditions.

5.2.5 Modulus of Elasticity Test

As per the specification ASTM C 469, test was conducted on eighteen 100mm x 200mm cylinder specimens to determine Young's modulus of Elasticity.

Age of Specimens	Modulus of Elasticity in GPa		
	Moist	Wet	Dry
56	35.34	42.81	40.82
112	36.65	46.10	42.99

Table 5.3: Modulus of elasticity of concrete tested under dry, moist and wet conditions.

Test results show higher values of modulus of elasticity for wet specimens compared to dry and moist specimens, indicating good resistance to deformation (Table 5.3). However based on the compressive / tensile strength test results, wet specimens performed poorly than dry specimens. Mehta and Monteiro (1993) explained about this paradoxical results. In a saturated cement paste, the adsorbed water in the C-S-H is load bearing, therefore its presence contributes to the elastic modulus. On the other hand, the disjoining pressure in the C-S-H tends to reduce the van der Waals force of attraction, thus lowering the strength. That is why the wet specimens have high elastic modulus and low compressive strength compared to dry specimens.

5.2.6 Length Change in Hardened Concrete

ASTM C 490 – 00a procedure was used to determine the change in length in hardened concrete under dry conditions, due to causes other than any applied load. Three prisms of size

75x75x285mm having gage length of 250mm were used for this test. In about 160 days, percentage change in length was about 0.1% for the concrete prisms (Fig. 5.3).

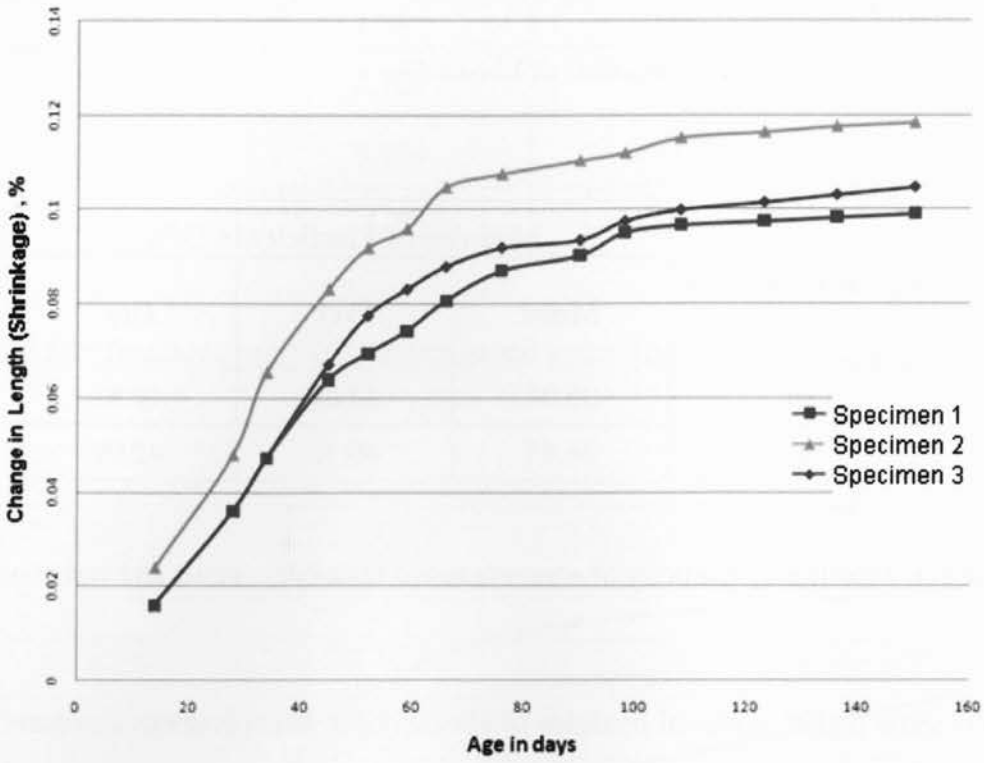

Figure 5.3: Percentage of change in length of samples tested under dry condition

5.2.7 Ultrasonic Pulse Velocity

Ultrasonic pulse velocity (UPV) test was performed in compliance with ASTM C 597. This test was performed on specimens at laboratory on 28^{th}, 56^{th} and 112^{th} day of casting. The results are given in Table 5.4. This test was also performed on the barrier wall selected for field study, and gave the UPV value of 4985m/sec. The value proves that the quality of concrete in the barrier wall is in a very good condition after four years, with fewer voids.

Specimen	UPV Speed (m/sec)			
	28days	56days	84days	112days
1	4950	4980	5005	5005
2	4950	4970	4995	5005
3	4960	4980	5000	5005

Table 5.4: UPV results on concrete samples tested under dry conditions

Chapter 6

Development of Finite Element Model of Barrier Wall

6.1 Introduction

Concrete is a composite material whose constituents have different properties. As the properties of concrete changes with respect to time and the environment to which it is exposed, a numerical analytical study was essential. Once the validity of the numerical procedure was established, the study of mechanism of deterioration in long-term was extended by performing a parametric study, taking into consideration of the response of unreinforced concrete barrier walls with time. The basics of finite element modeling with material and other modeling parameters including assumptions are explained in Chapter 4.

6.2 Model Mesh Geometry

The element mesh of the model geometry is as shown in the Figure 6.1. In this analysis study, no change in mesh size was adopted since more finer the mesh, the solution had non-convergence issues. In this three dimensional model, Z represents the longitudinal direction, X is the transverse direction and Y is the direction of the height. The orientation of the model is as shown in Figure 6.1, resembling to that of site barrier wall selected in the study. The NE face of the wall model will be called as "front face" and SW face of the wall will be called as "back face" in this study. Model has 4m length, 0.625m base bottom width, 0.1m base bottom height, 0.175m wall width at stem top and

1m overall height. The length of the model was chosen 4m since most of the unreinforced concrete barrier walls in Ontario have crack arrester joints at 4 to 8 meter intervals.

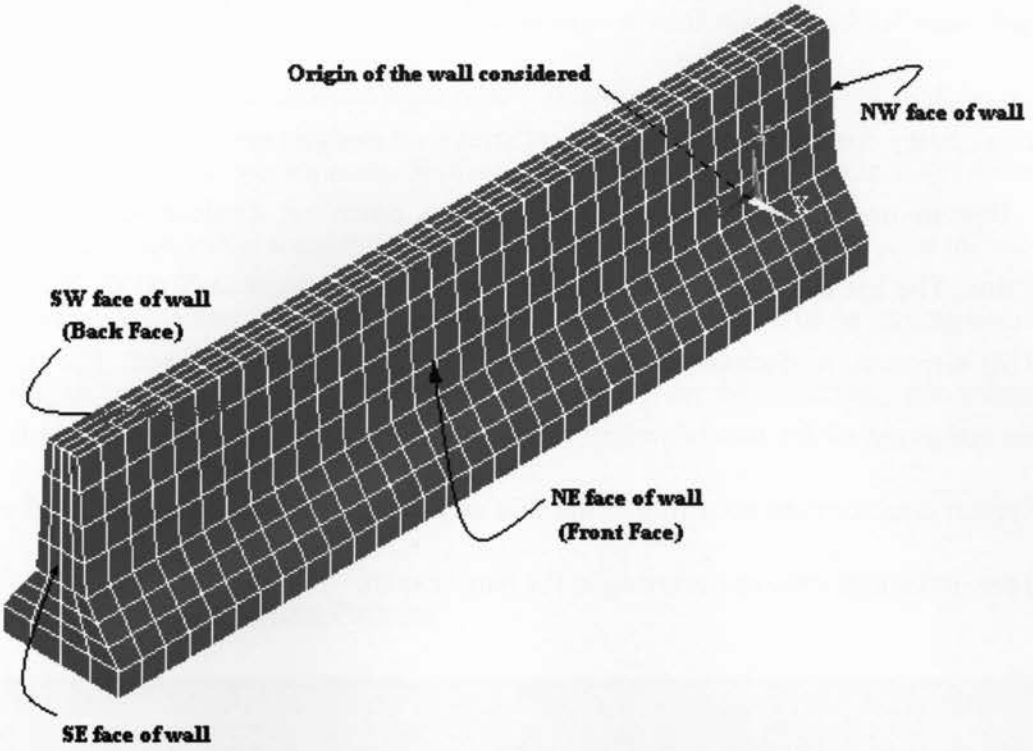

Figure 6.1: Element Mesh Geometry of the model

6.3 Boundary Conditions

Boundary conditions in transient thermal analysis are thermal boundary conditions. Per hour reading of temperatures taken from sensors are applied to the element nodes. For proper unit consideration, time is taken in seconds. Therefore, one time step is one hour, i.e., 3600 seconds. In three years, there are 26350 time steps. Even though the bottom of the model is not exposed, the temperature of the granular fill below the barrier wall is considered maintaining the ambient temperature conditions. It is assumed in this study that being the width of the barrier wall is comparatively smaller; there will not be much significant variation in temperature between the base exterior surface nodes and base

interior surface nodes of the barrier wall. Thus during the thermal analysis, ambient temperature is applied to the nodes at the bottom surface of the barrier wall, on an hourly basis.

Two boundary conditions used in transient structural analysis are as shown in the Figure 6.2. Bottom nodes are restrained against going down i.e displacement in Y (UY) direction. The left end nodes are restrained against displacement in X (UX), Y (UY) and Z (UZ) direction, to demonstrate the rigidity by making that end fixed. The right end nodes are analyzed for two boundary conditions. First case (a), as free end, to find the maximum displacement occurring at the free end nodes, second case (b) as fixed end, to find the maximum stresses occurring in the barrier span.

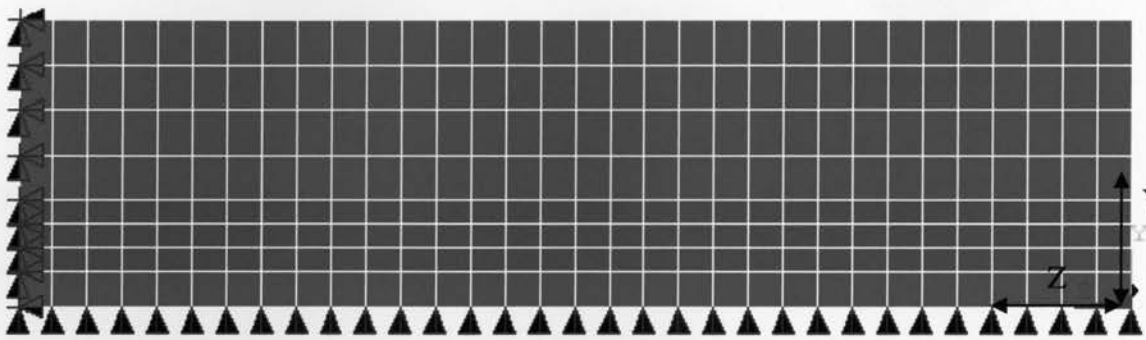

(a) fixed-free

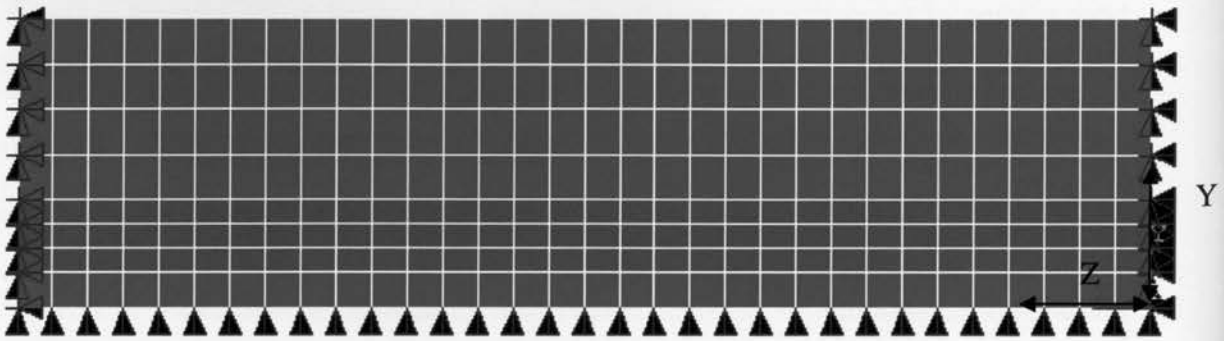

(b) fixed-fixed

Figure 6.2: Boundary conditions for structural analysis

The boundary conditions are selected in such a way as to resemble the actual boundary conditions in the field. Plain concrete barrier walls are usually constructed using slip-forming method, where the concrete wall can have a total span length of more than 30 meters. Mostly spanning between light pole foundations, the barrier wall will be having fixed end condition at two supports. With age, cracks develop in concrete walls since it is exposed and subjected to temperature and environmental loading. Because of the vertical crack formations penetrating full depth of the wall, barrier wall will be having boundary condition of one end free and other end fixed. Hence, these two boundary conditions are used in the finite element analysis.

6.4 Crack Identification and Pattern

In ANSYS, outputs are calculated at integration points of the concrete solid elements used in the models. Figure 6.3 shows integration points in a concrete solid element. In ANSYS, a crack is shown as a circle outline in the plane of the crack. Open crack shows open circles and closed cracks have cross lines inside the circle.

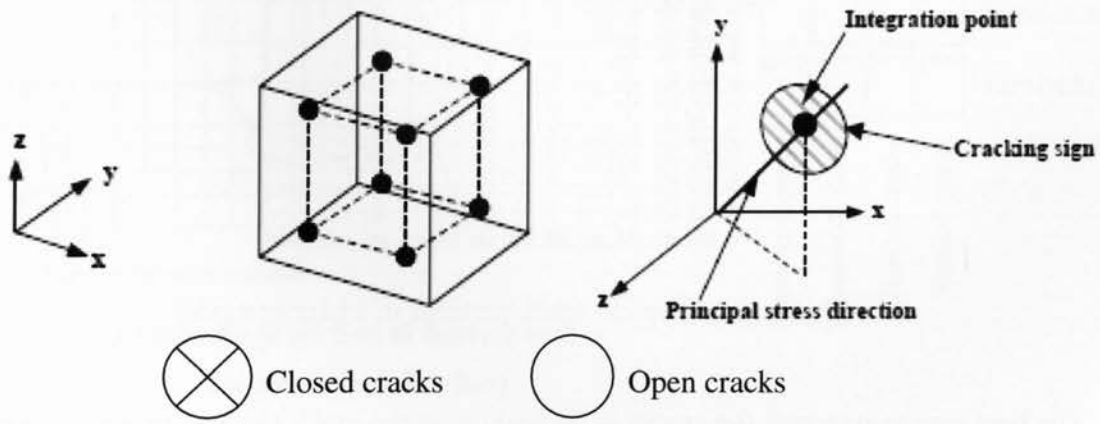

Figure 6.3: Integration points and crack sign in concrete solid element (ANSYS)

The first cracking sign appears when principal tensile stress exceeds the ultimate tensile strength of the concrete. No more than three cracks can be predicted in each Solid65 element and they are color coded to make it easily identifiable. These cracks are developed at same gauss points but at different orientation. A sample of the color coding is shown in Figure 6.4. The first cracks are shown in red color, the second cracks are shown in green color and the third cracks are shown in blue color.

Second and third crack occur at the same integration point of the first crack, but with a different principal stress direction. Therefore, the amount of cracks seen in the solution is affected by the size of the mesh. Using a finer mesh results in more cracks and using a coarser mesh results in less cracks. In this study a finer mesh size is used to achieve more accurate results and to have better crack distribution. Hence it is understood that the amount of cracks shown in the ANSYS solution (due to smeared cracking approach) will be much more than what is observed in the real barriers. ANSYS Solid65 element output does not include prediction of crack widths.

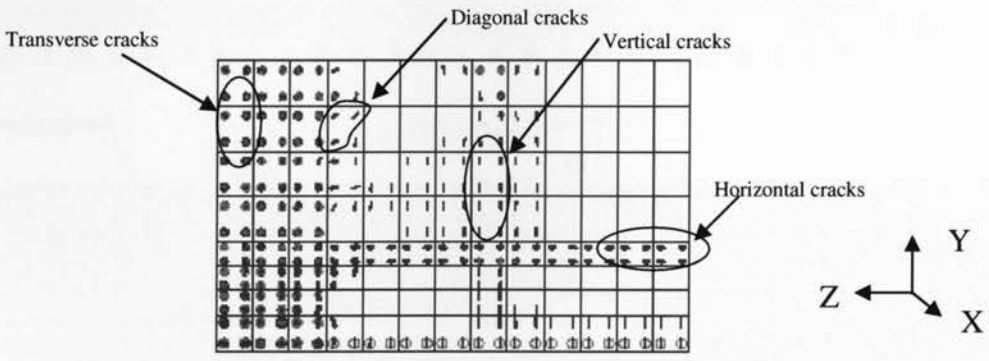

Figure 6.4: Typical crack patterns in a barrier model

The best way to interpret the cracks is by looking at the crack patterns in the longitudinal view of the barrier wall (Figure 6.4). The cracks that form vertically up are termed in this

study as vertical cracks. Vertical cracks occur when the principal tensile stresses in the *Z* direction exceed the ultimate tensile strength of the concrete. The cracks that appear as horizontal straight lines are termed in this study as horizontal cracks. Here, the principal tensile stresses in the *Y* direction exceed the ultimate tensile strength of the concrete and thereby the cracks appear perpendicular to the principal stresses in the *Y* direction, i.e. parallel to *XZ* lane. The cracks shown in circles occur when the principal tensile stresses in the *X* direction exceed the ultimate tensile strength of the concrete. These cracks are called in this study as transverse cracks. Where the directions of tensile principal stresses are inclined from the horizontal, diagonal tension cracks are formed (Figure 6.4).

6.5 Evolution of Crack Patterns in 4 m Barrier Walls

ANSYS records a crack pattern at each applied load step. In order to describe the crack evolution patterns in a more simplified way, some terms have been introduced in the following study as illustrated in Figure 6.5.

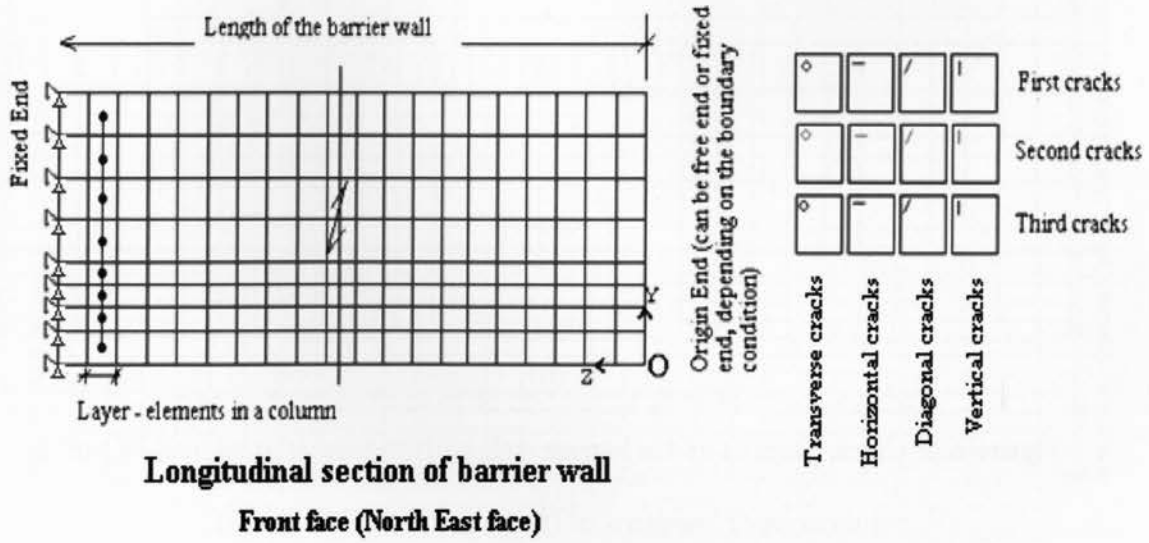

Figure 6.5: Definition of terms considered in the crack pattern study

Looking at the front face (north east face) of the barrier wall, the left wall end is termed as fixed end and the right end is termed as origin, since it can be either free end or fixed end depending on the boundary condition. The length of the barrier wall is measured from the origin end. Element mesh considered in this analysis can be treated as elements arranged in rows and columns. A column layer and row layer are terms for elements coming under a column and row respectively.

6.5.1 Case 1: Barrier Wall with both ends Fixed

Figure 6.6 to Figure 6.13 show the evolution of crack patterns for a 4 m barrier wall with both ends restrained in X, Y and Z directions.

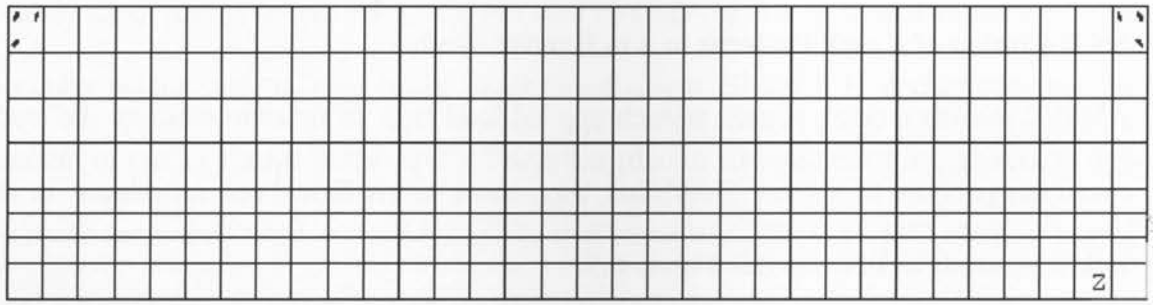

(a)

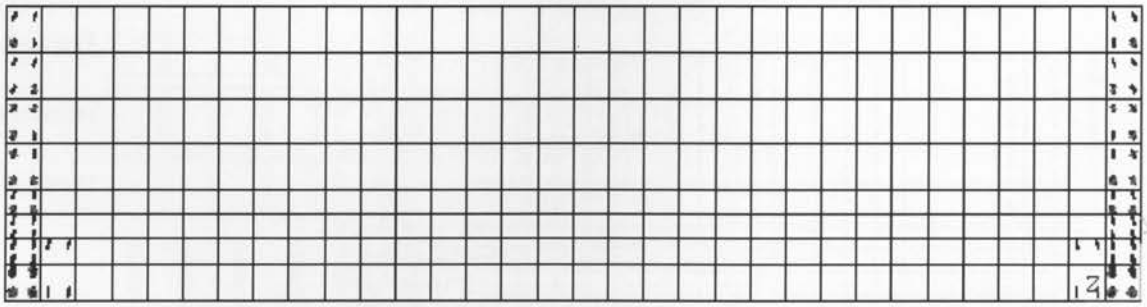

(b)

Figure 6.6: Crack patterns of 4m barrier wall with ends restrained in X, Y and Z directions (Time steps of (a) 10 hours (b) 100 hours).

From Figure 6.6(a), at time step of 10 hours, diagonal cracks started appearing at the top corners of the fixed ends. When viewed the crack pattern at the time step of 100 hours (Figure 6.6(b)), the cracks propagated vertically down through the elements, changing slowly from diagonal cracks to vertical cracks. Vertical cracks were also started to propagate away from the fixed end as can be observed from the developed vertical cracks appeared at the bottom on the next immediate column layer from the fixed ends. Second crack formations had also started appearing at the fixed ends. On the bottom of the fixed ends, they appeared as transverse cracks, however on the thinner wall section, the second cracks formed were diagonal cracks.

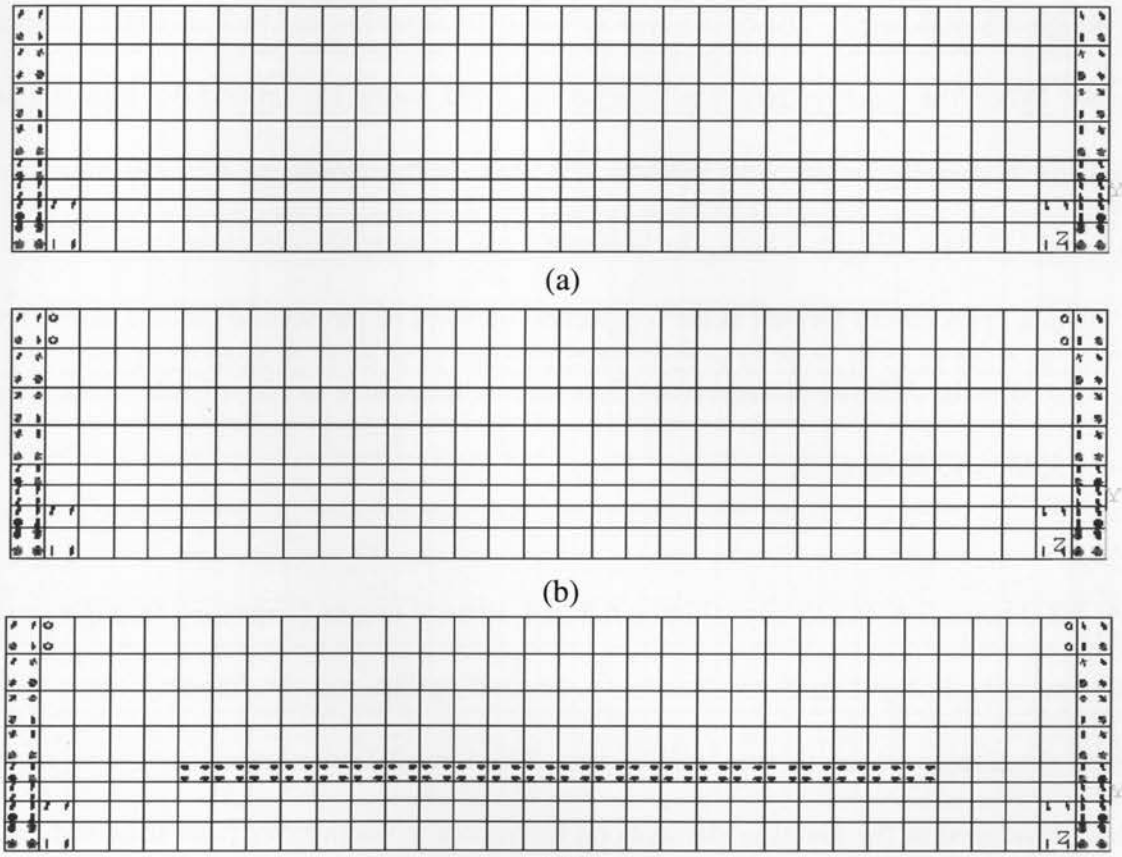

(a)

(b)

(c)

Figure 6.7: Crack patterns of 4m barrier wall with ends restrained in X, Y and Z directions (Time steps of (a) 250 hours (b) 300 hours, i.e12.5 days (c) 500 hours).

After the second crack formation at the fixed ends as seen at time step 100 hours, when studied the time step at 250 hours as seen in Figure 6.7(a), the third crack formation had started. When studied the time step at 300 hours, i.e. 12.5 days (Figure 6.7(b)), transverse cracks started forming at the top element at the next immediate column layer from the fixed ends. When checked at 500 hours,, i.e. around 21 days (Figure 6.7(c)), horizontal cracks are seen forming along the wall on the back face (south west surface), at the junction where the barrier wall widens. The cracks appear to be closed.

From Figure 6.8(a), at 1000 hours, i.e. around 42 days, horizontal cracks propagated fully through the wall length. The cracks still appear to be closed as can be seen in the close up view. When the crack pattern was checked at 2000 hours, i.e. around 84 days (Figure 6.8(b)), horizontal cracks were opened as shown in the close up. At 2750 hours, i.e. around 115 days (Figure 6.8(c)), the horizontal cracks were seen in closed position. New diagonal cracks were formed at the top second element of the second column layer from the fixed ends. Additional third crack formations, transverse cracks of blue color, were seen at the two fixed ends.

At 3000 hours, i.e. at 125 days (Figure 6.8 (d)), vertical cracks progressed throughout the second column layer from the fixed end. Second cracks, mostly diagonal cracks were seen developing in the thinner wall section. Third crack formation of transverse cracks had developed at the junction elements on the second column layer from the fixed ends. Horizontal cracks in the junction were now seen in open position. Horizontal cracks were also seen forming from the top element of the third column layer from the fixed ends.

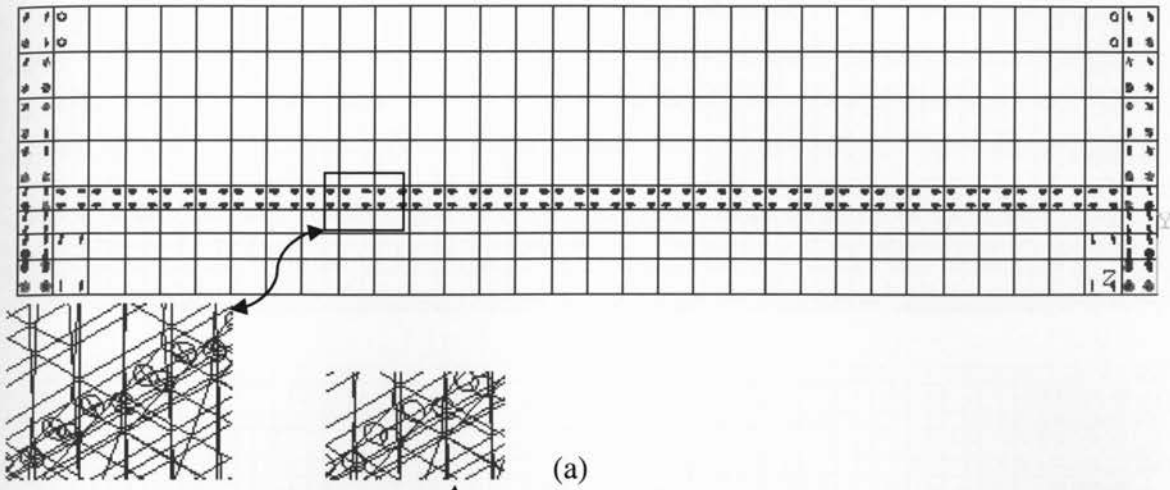

(a)

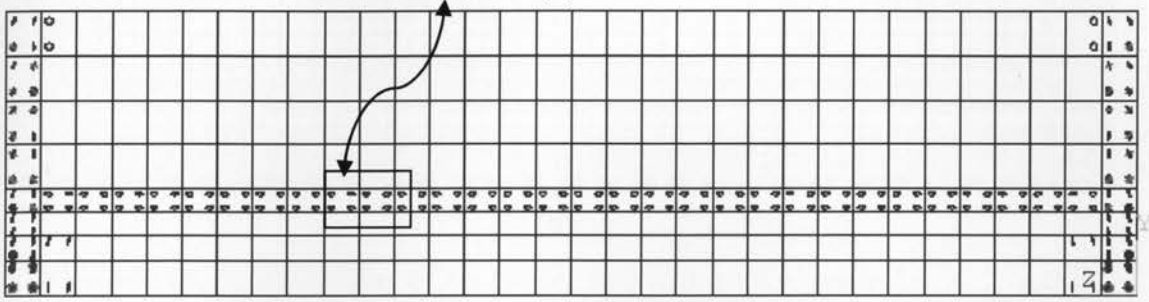

(b)

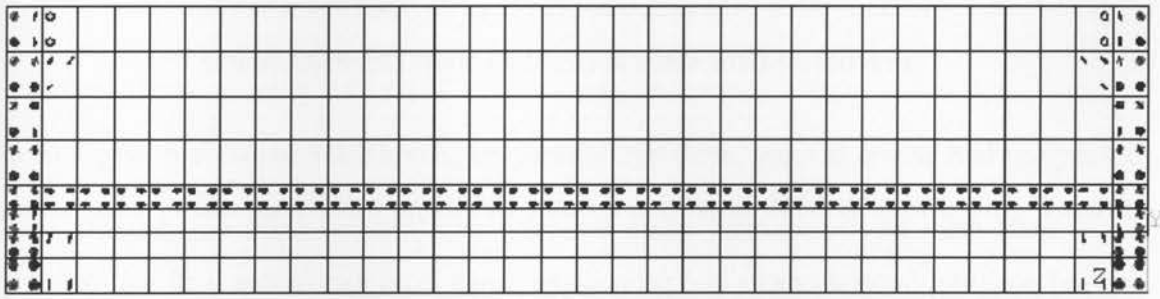

(c)

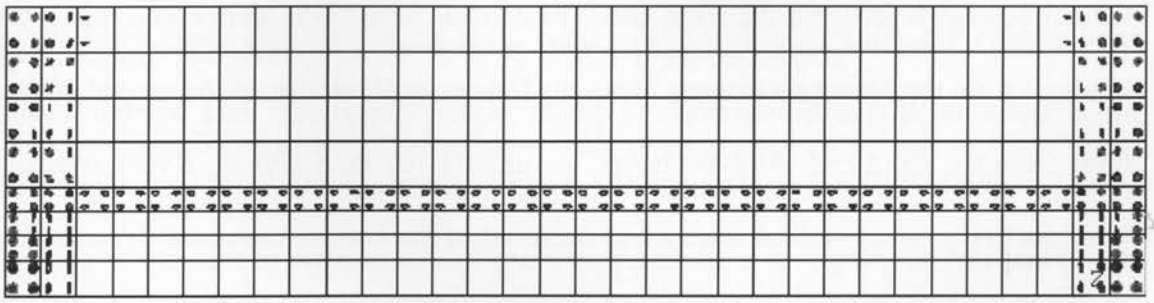

(d)

Figure 6.8: Crack patterns of 4m barrier wall with ends restrained in X, Y and Z directions (Time steps at (a) 1000 hours (b) 2000 hours (c) 2750 hours (d) 3000 hours).

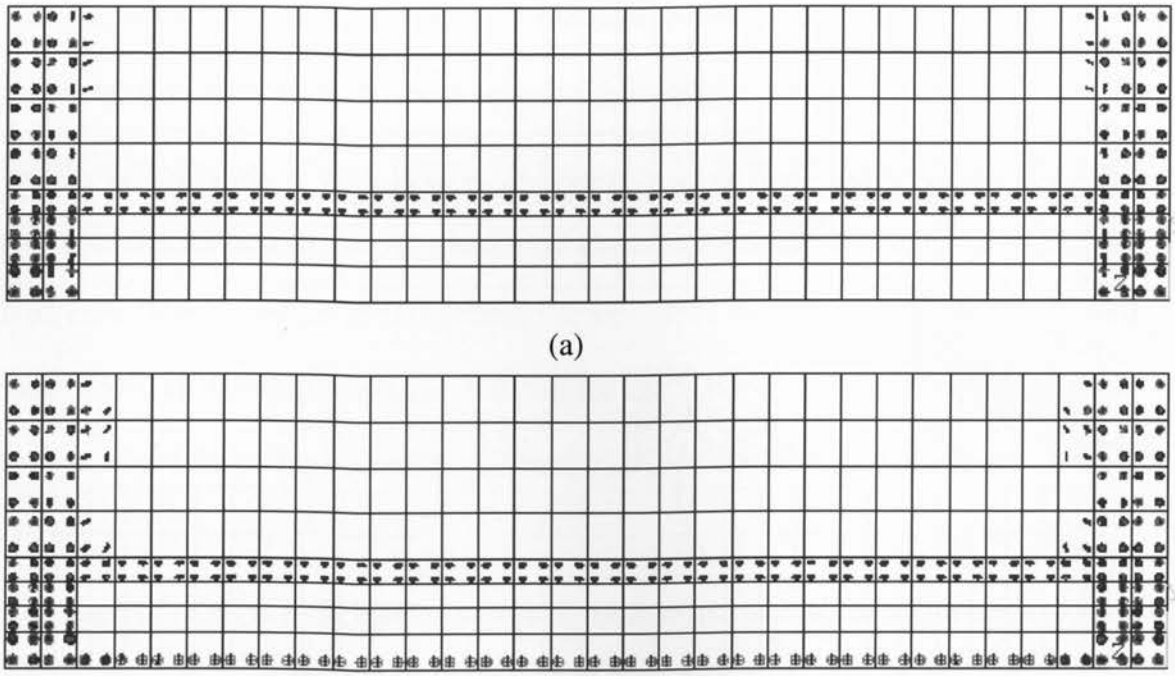

Figure 6.9: Crack patterns of 4m barrier wall with ends restrained in X, Y and Z directions (Time steps at (a) 3500 hours (b) 4000 hours).

From Figure 6.9(a), at 3500 hours i.e. around 146 days, horizontal cracks were seen in closed position. Second cracks had propagated down from the thinner wall section, at the second column layer from the fixed end. Third crack formations were seen propagating upwards from the junction elements along the thinner wall section, in the second column layer from the fixed end. At 4000 hours, i.e. around 167 days (Figure 6.9(b), red color (denotes first cracks) vertical cracks had occurred in the bottom elements. Second crack formations of transverse cracks were also seen in the central bottom elements, but in closed position. Diagonal cracks were seen progressing in the third column layer elements, from the fixed end. Horizontal cracks at the junction elements were still in the closed position, however, near the fixed ends these cracks were seen in open position.

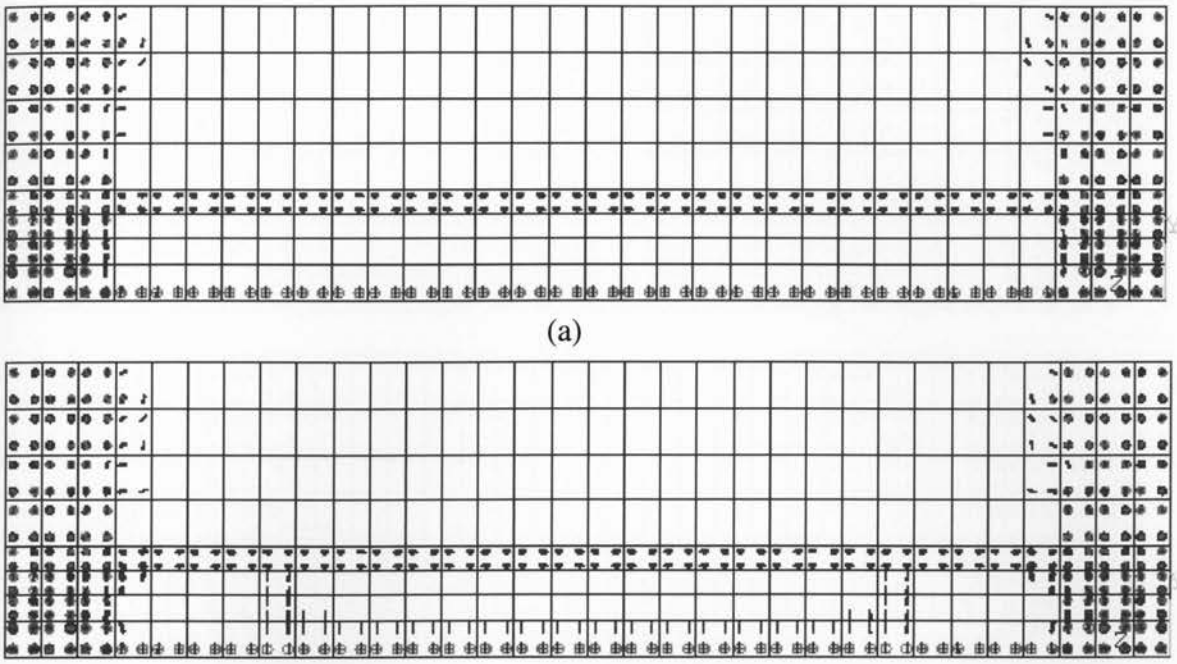

(a)

(b)

Figure 6.10: Crack patterns of 4m barrier wall with ends restrained in X, Y and Z directions (Time steps at (a) 5000 hours (b) 6500 hours).

From Figure 6.10(a), at 5000 hours, i.e. around 209 days, vertical cracks had progressed down through the third column layer. Second crack formations and even third crack formations were seen developing in the thinner wall section elements of the third column layer. Cracks were also developing at the thinner wall section in the fourth column layer from the fixed ends. Horizontal cracks at the junction elements still remained in the closed position. At 6500 hours, i.e. around 271 days (Figure 6.10(b)), cracks started forming at the thicker wall section of the fourth column layer elements. Vertical cracks were seen forming at the central portion of the bottom middle region. Horizontal cracks at the junction elements still remained in the closed position.

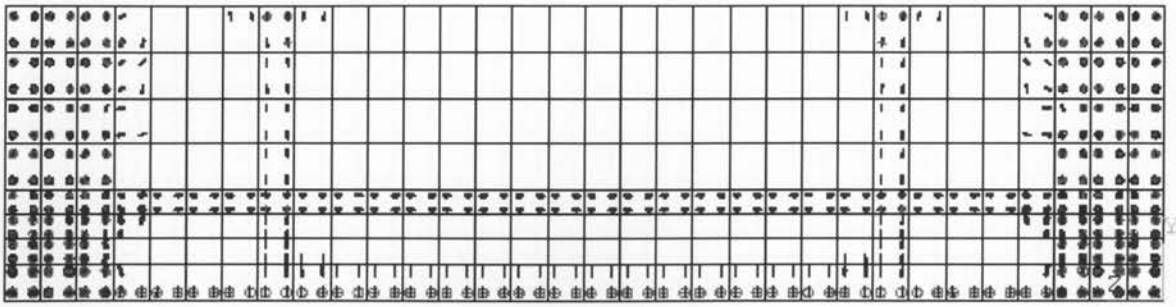

(a)

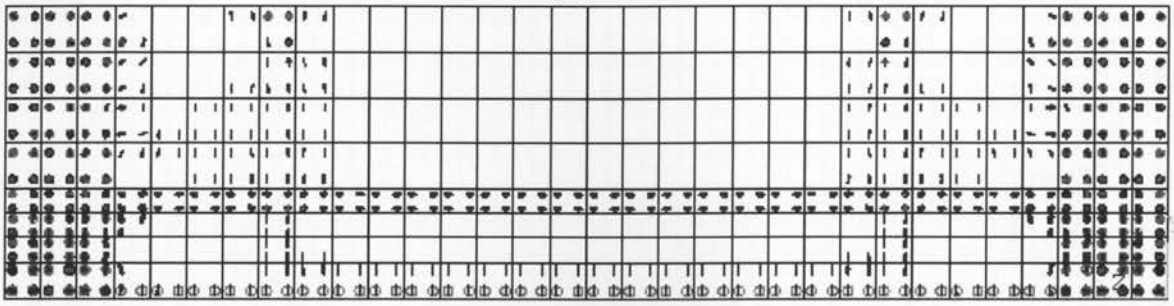

(b)

Figure 6.11: Crack patterns of 4m barrier wall with ends restrained in X, Y and Z directions. (Time steps at (a) 7500 hours (b) 10000 hours)

From Figure 6.11(a), at 7500 hours, i.e. 312.5 days, full length vertical cracks were seen at a distance of 1m from the end section. Second crack formation also started from the top element at 1m from fixed ends. At 10000 hours, i.e. around 417 days (Figure 6.11(b)), vertical cracks were seen developing in the thinner wall section, in between 1m from the fixed ends. Horizontal cracks at the junction elements were still remaining in the closed position. Full length vertical cracks were seen developing in the immediate column layer elements after 1m.Third crack formation also began at the top element at 1m from fixed ends.

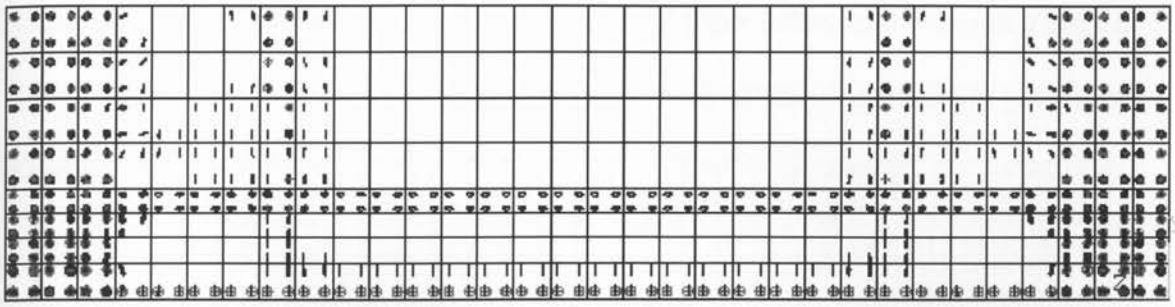

(a)

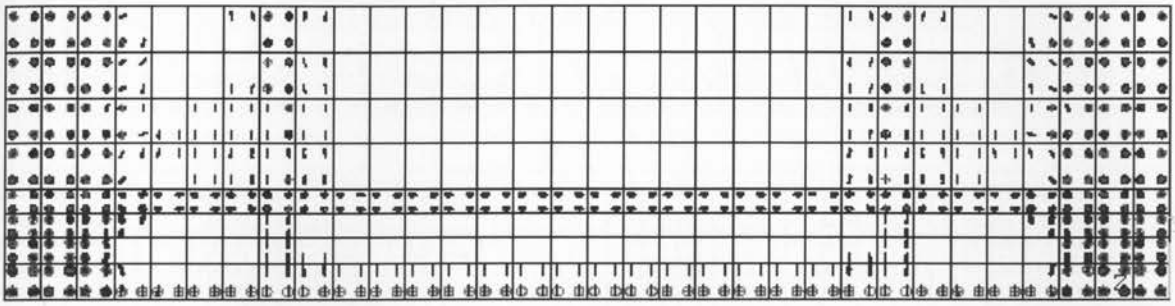

(b)

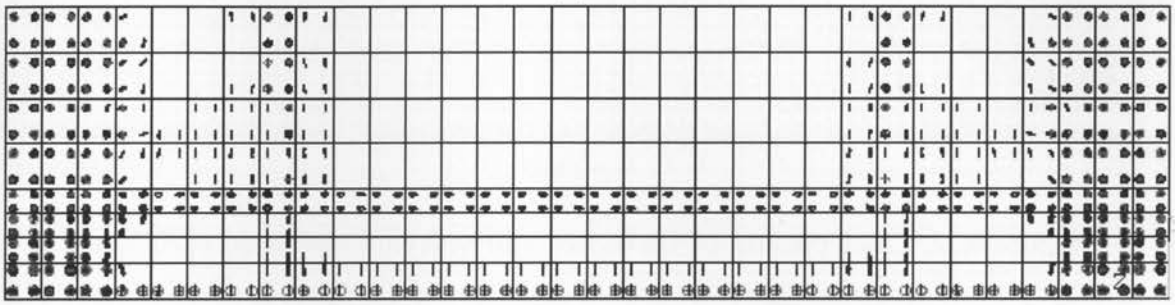

(c)

Figure 6.12: Crack patterns of 4m barrier wall with ends restrained in X, Y and Z directions. (Time steps at (a) 15000 hours (b) 21000 hours (c) 22000 hours)

From Figure 6.12(a), at 15000 hours, i.e., at 625 days, horizontal cracks at the junction elements were seen in open position. Second crack formations propagated down from the top elements, along the elements at 1m from fixed ends. At 21000 hours, i.e. at 875 days (Figure 6.12(b)), horizontal cracks at the junction elements were seen in closed position. Third crack formations propagated down from the top elements, along the column layer elements at 1m from the fixed ends. At 22000 hours, i.e. around 917 days (Figure

6.12(c)), horizontal cracks at the junction elements that lie in the middle range were still remaining in closed position; however those near the ends were in open position.

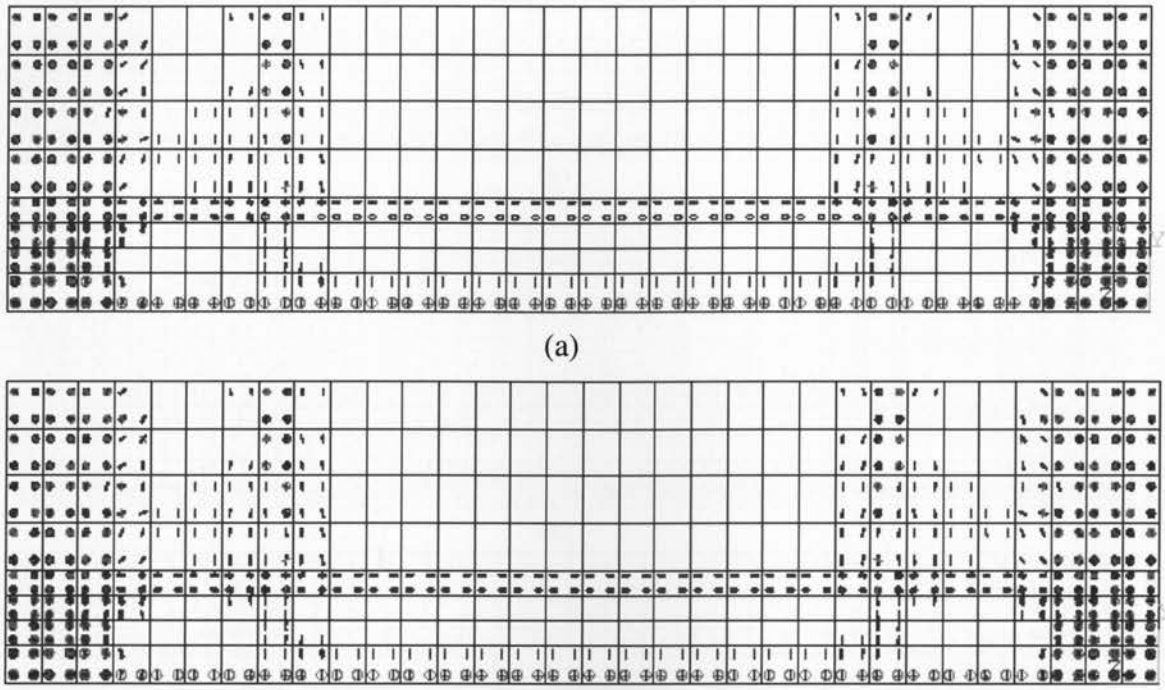

(a)

(b)

Figure 6.13: Crack patterns of 4m barrier wall with ends restrained in X, Y and Z directions (Time steps at (a) 25000 hours (b) 26350 hours).

From Figure 6.13(a), at 25000 hours, i.e. around 1042 days, horizontal cracks at the junction elements in the central region were also changed from closed to open position. Transverse cracks of second crack formation that had developed already at the bottom nodes during the time step of 4000 hours were still remaining in the closed position, however, those near the vertical crack line at 1m distance from the fixed ends were open. At the end of 3 years, i.e. at 26350 hours, i.e. around 1098 days (Figure 6.13(b)), most of these transverse cracks formed at the bottom elements were in open position. However, horizontal cracks at the junction elements were seen in closed position.

6.5.2 Case 2: Barrier Wall with one end Fixed and the other end Free

Figure 6.14 to Figure 6.24 show the evolution of crack patterns for a 4m barrier wall with the origin end free and the other end restrained in X, Y and Z directions.

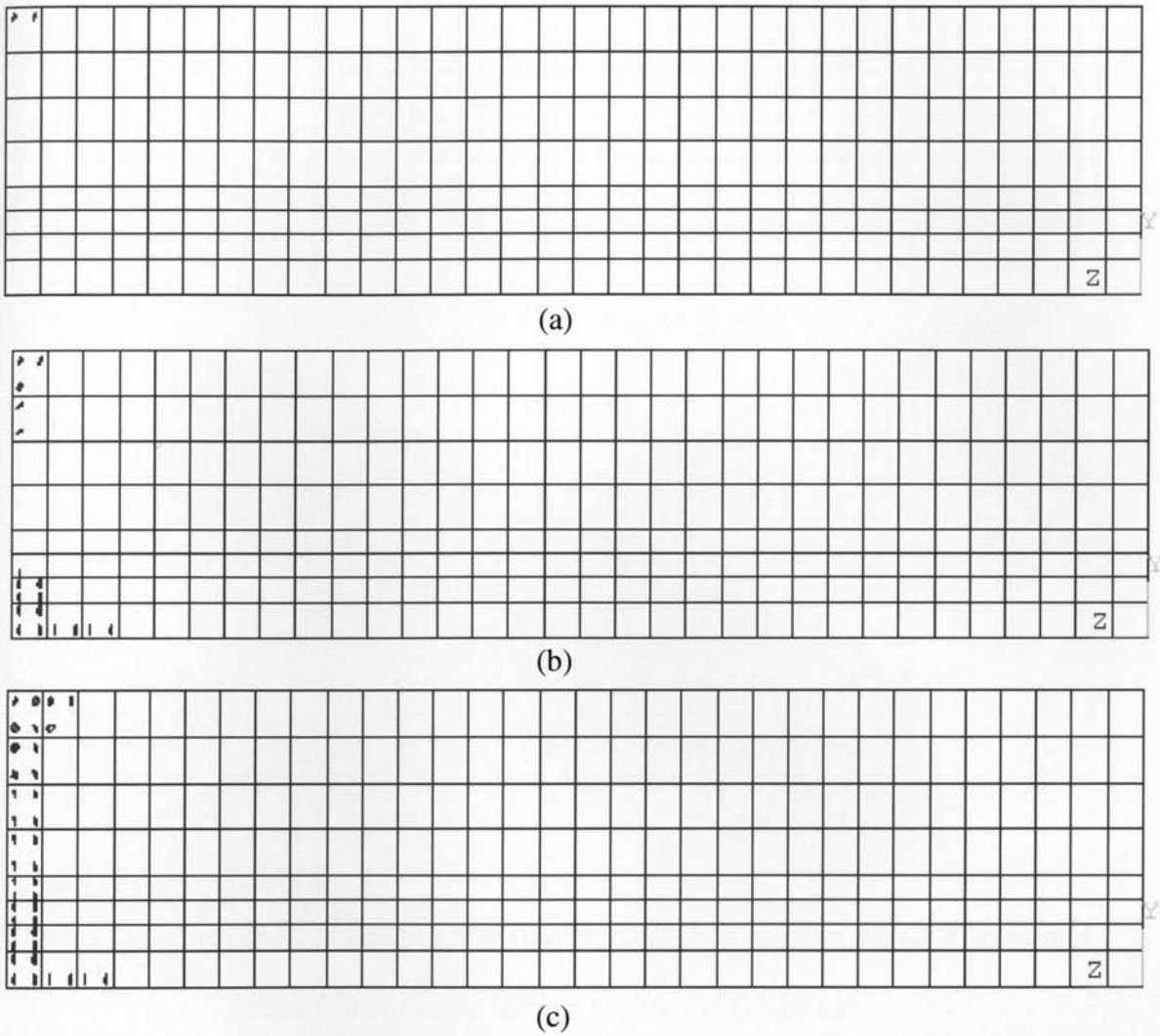

Figure 6.14: Crack patterns of 4m barrier wall with left end fixed and right end free (Time steps at (a) 10 hours (b) 50 hours (c) 100 hours).

From Figure 6.14(a), at 10 hours, diagonal cracks started appearing at the top corner elements of the fixed end. At 50 hours (Figure 6.14(b)), vertical cracks appeared at the bottom corner elements of the fixed end and progressed upward. At 100 hours (Figure

6.14(c)), the fixed end elements were filled with cracks and vertical cracks started appearing at the top second layer from the fixed end.

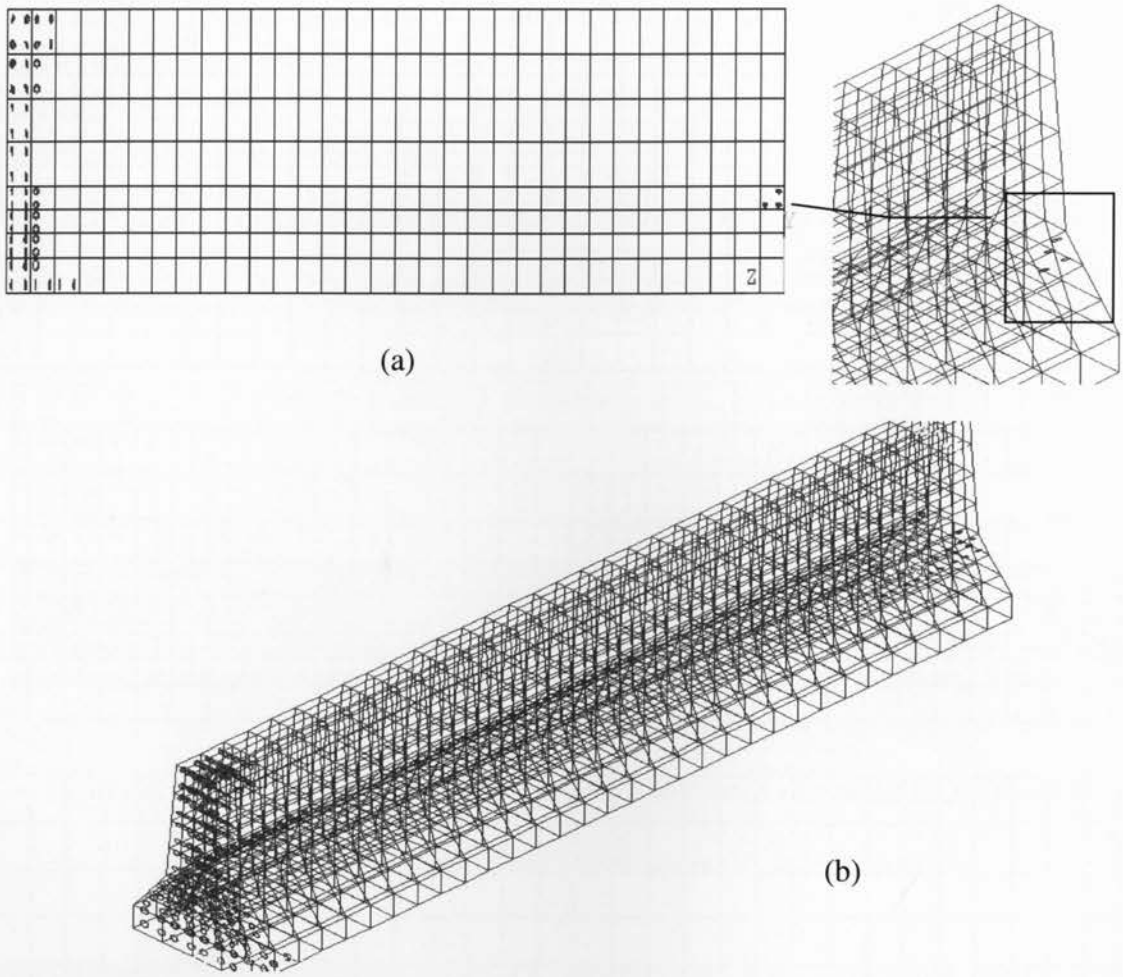

Figure 6.15: Crack patterns of 4m barrier wall with left end in fixed condition and right end free (Time step at (a) 300 hours (b) 350 hours)

By the time frame of 300 hours, i.e. at 12.5 days (Figure 6.15(a)), more transverse cracks from bottom developed in the second column layer elements from the fixed end. Also horizontal cracks started forming at the north east corner of the free end, near the junction where the barrier wall widens. A close up picture of the cracks is shown in Figure 6.15(a). At 350 hours, horizontal cracks started appearing at the south west side of the

wall near the junction area where the barrier wall widens as shown in Figure 6.15(b). The cracks first appeared at the mid section and then propagated towards the both sides. Also the horizontal cracks at the north east corner were spreading out.

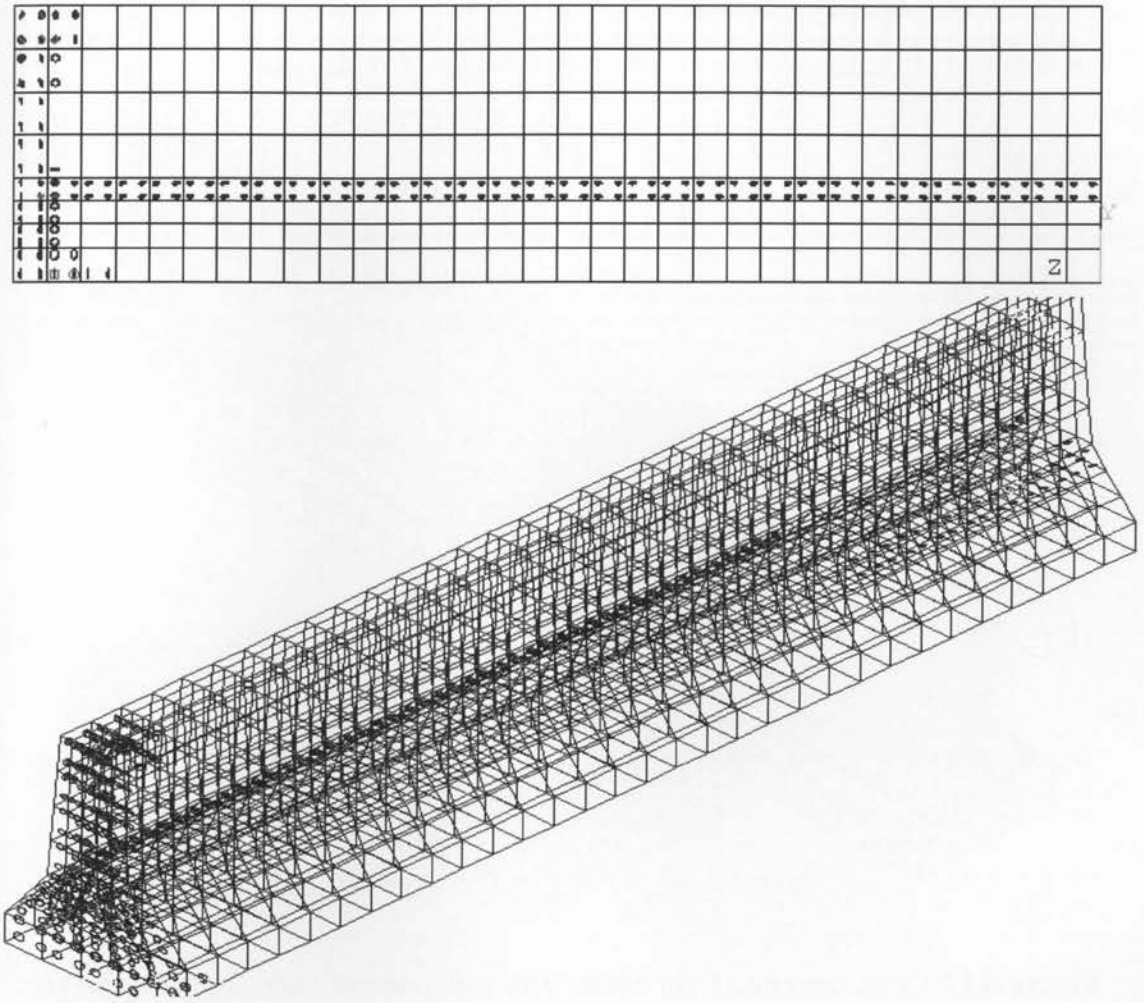

Figure 6.16: Crack patterns of 4m barrier wall with one end fixed and other end free (Time step at 400 hours).

At 400 hours, i.e. around 17 days, horizontal cracks propagated at the north east side cracks towards the fixed end and at the south west side cracks towards the free end (Figure 6.16).

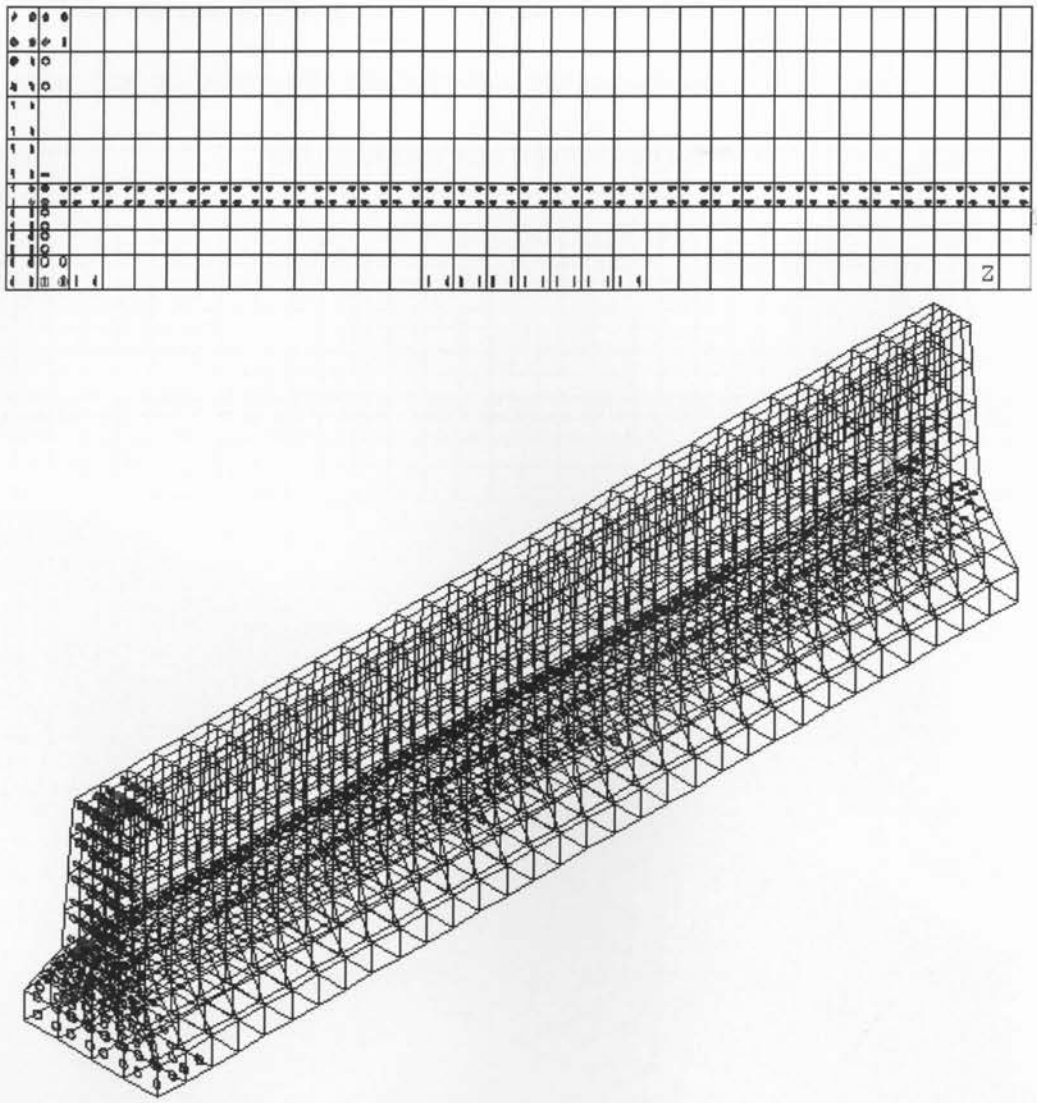

Figure 6.17: Crack patterns of 4m barrier wall with one end fixed and other end free (Time steps at 500 hours).

At 500 hours, i.e. around 21 days, open cracks are appearing at the bottom elements, on the south west face as shown in the Figure 6.17. This is due to the resistance against the bottom restraint due to change in curvature of curling action of barrier wall.

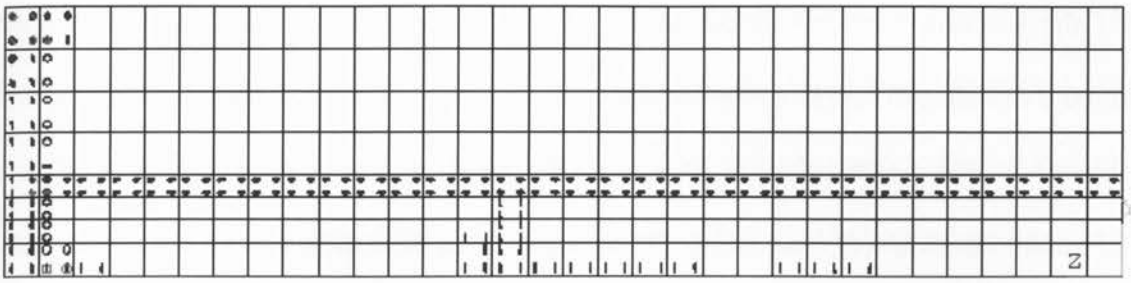

(a)

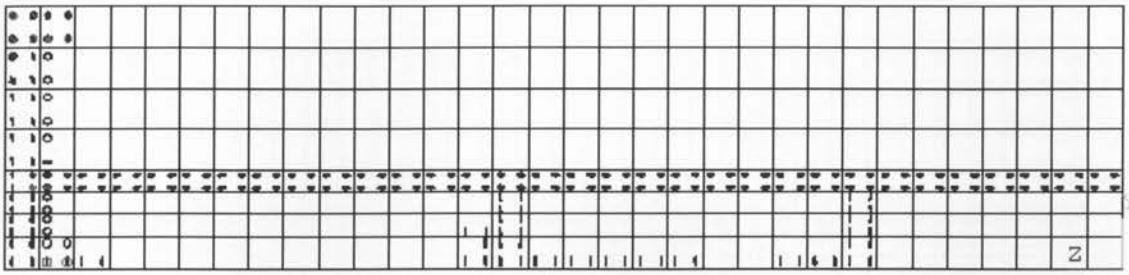

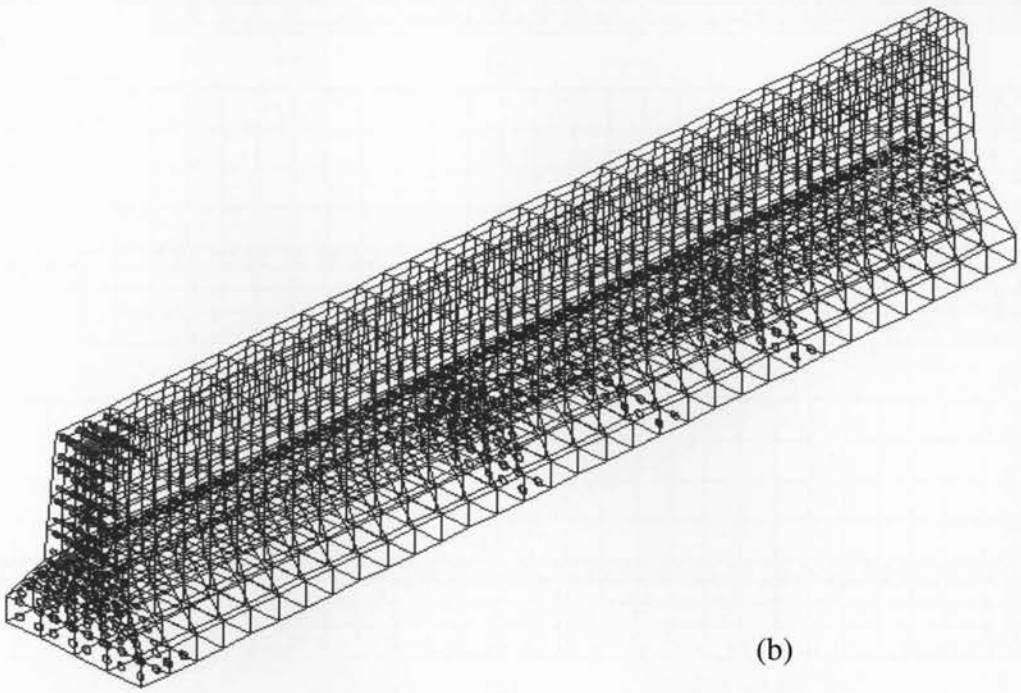

(b)

Figure 6.18: Crack patterns of 4m barrier wall with one end fixed and other end free (Time steps at (a) 900 hours (b) 1200 hours).

At 900 hours, i.e. at 37.5 days, we can observe more vertical cracks appearing at the bottom in the vertical direction. Vertical cracks at 1.875 m from the fixed end had extended upward to the middle height level as seen in Figure 6.18(a). Horizontal cracks

on the junction elements at the south west side of the barrier wall, had propagated throughout the full length of the barrier wall. At 1200 hours, the bottom cracks spreaded throughout the width of the wall as seen in the isometric view in Figure 6.18(b). In addition to the vertical cracks at 1.875 m, another set of vertical cracks had developed at 3.125 m from the fixed end and extended upwards till the middle height.

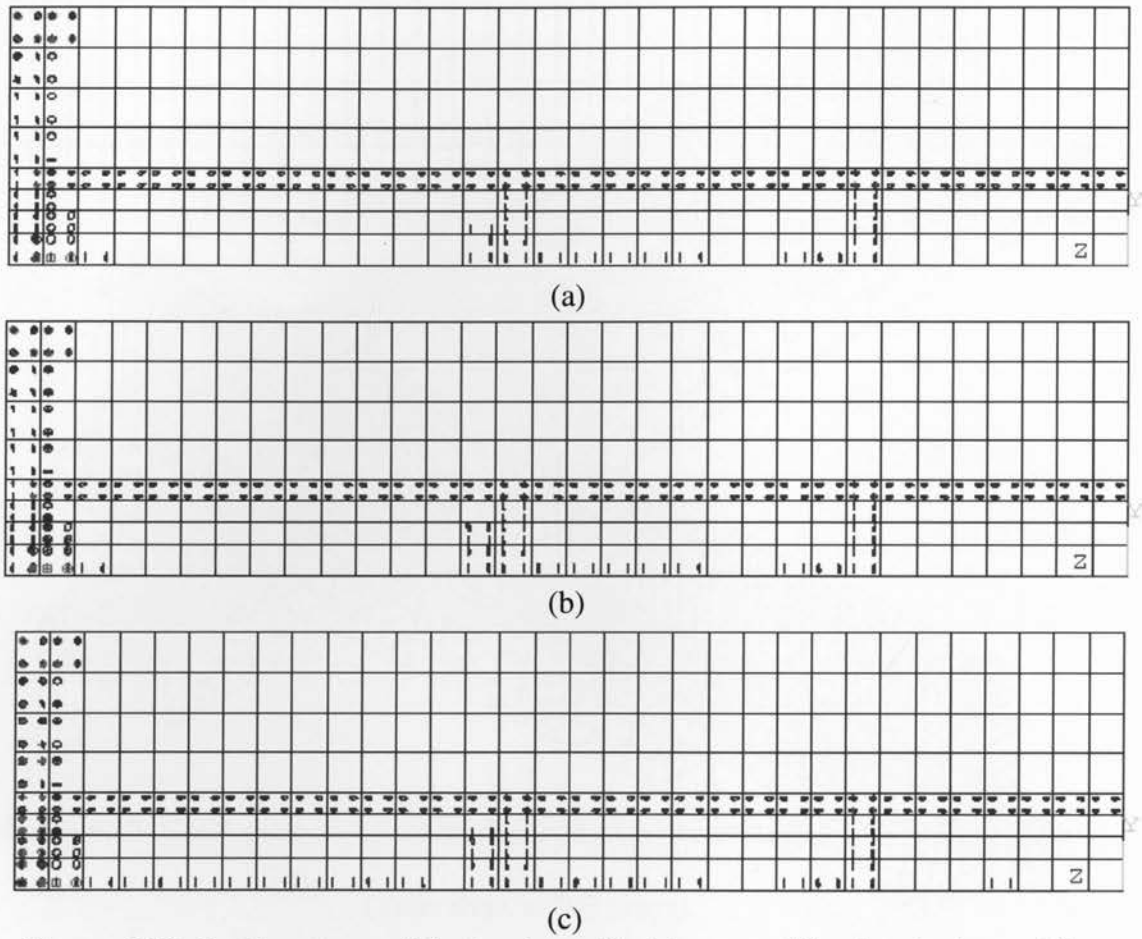

(a)

(b)

(c)

Figure 6.19: Crack patterns of 4m barrier wall with one end fixed and other end free (Time steps at (a) 2000 hours (b) 2500 hours (c) 3000 hours).

From Figure 6.19(a), at 2000 hours, i.e around 84 days, the horizontal cracks at the junction elements were seen in open position. The transverse cracks seen in the second column layer from the fixed end remained in the open state. However, at 2500 hours, i.e.

around 105 days (Figure 6.19(b)), these transverse cracks were found in closed state. The horizontal cracks at the junction elements also appeared in closed state. At 3000 hours, ie.e at 125 days (Figure 6.19(c)), many vertical cracks had appeared at the bottom row layer elements. Even some of the closed transverse cracks on the second column layer from the fixed end were found open.

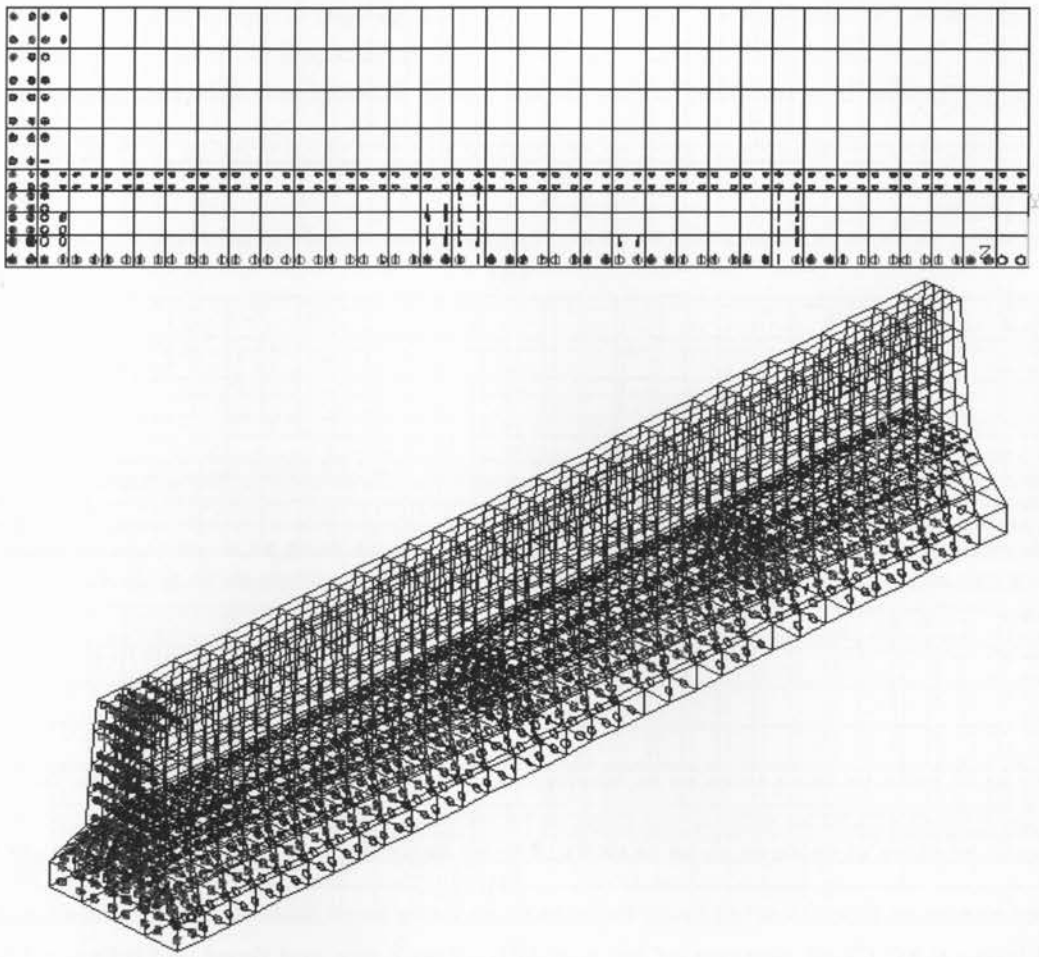

Figure 6.20: Crack patterns of 4m barrier wall with one end fixed and other end free (Time step at 3692 hours)

At 3692 hours, i.e. around 154 days, many second crack formations were found in the bottom elements, in the central region as seen in Figure 6.20. These cracks were transverse cracks and are found in open state.

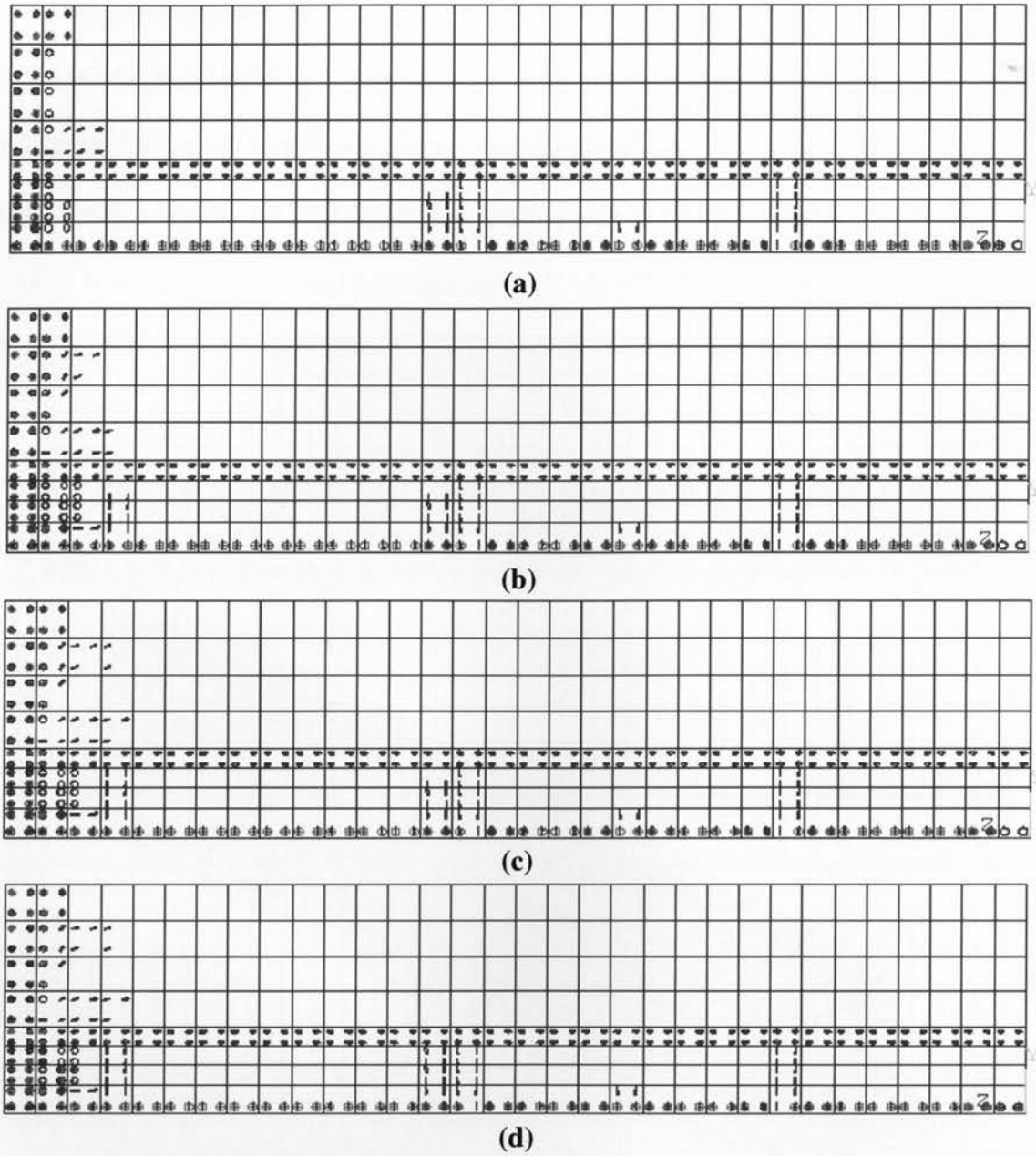

Figure 6.21: Crack patterns of 4m barrier wall with one end fixed and other end free

(Time steps at (a) 4000 hours (b) 5000 hours (c) 6000 hours (d) 8000 hours)

At 4000 hours, i.e around 167 days, diagonal cracks started appearing on the third column layer from the fixed end, above the junction where the barrier wall widens, as seen in Figure 6.21 (a). At 5000 hours, i.e. around 209 days (Figure 6.21(b)), transverse

cracks started coming up in the thicker section of the barrier wall on the elements of the third column layer from the fixed end. At the same time, vertical cracks also started forming in the upward direction from the bottom elements of the fourth column layer from the fixed end. At 6000 hours, i.e. at 250 days (Figure 6.21(c)), diagonal cracks started appearing in the thinner wall section on the fourth column layer elements from the fixed end. At 8000 hours, i.e around 334 days (Figure 6.21(d)), almost completing one year duration, vertical cracks at 1.75 m length from the fixed end started to extend upward. Few open state transverse cracks in the second and third column layer from fixed end are now found to be in the closed position.

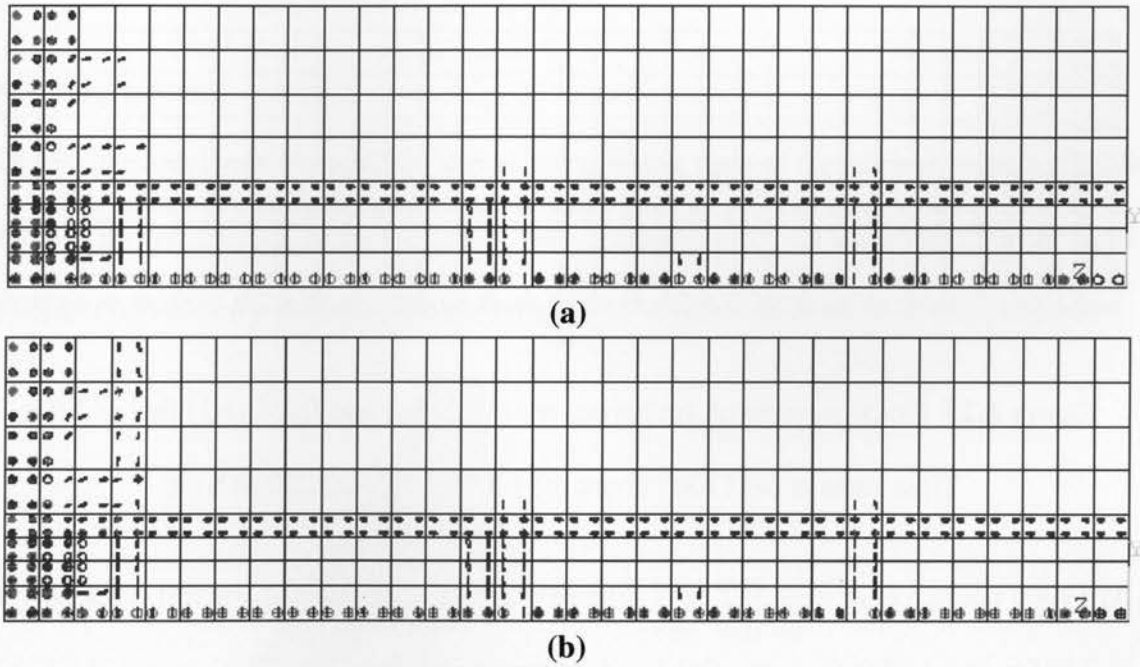

Figure 6.22: Crack patterns of 4m barrier wall with one end fixed and other end free (Time steps at (a) 9000 hours (b) 11000 hours)

At 9000 hours, i.e. at 375 days, vertical cracks at 1.875m and 3.125m from the fixed end started to propagate upwards (Figure 6.22(a)). At 11000 hours, the vertical cracks at 0.5m from the fixed end extended throughout the barrier wall height (Figure 6.22(b)).

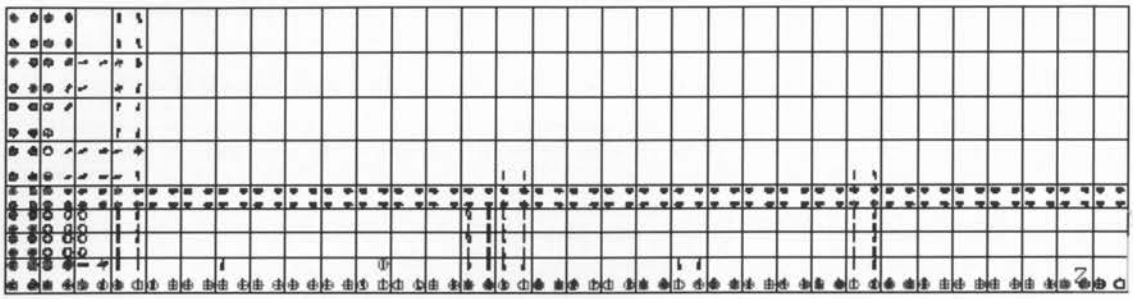

(a)

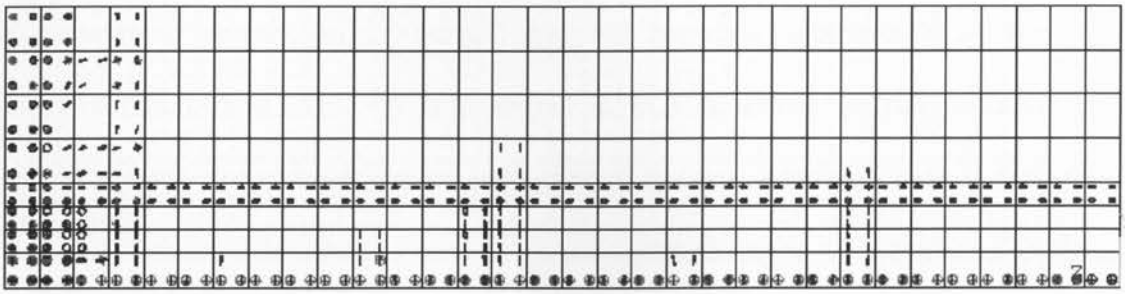

(b)

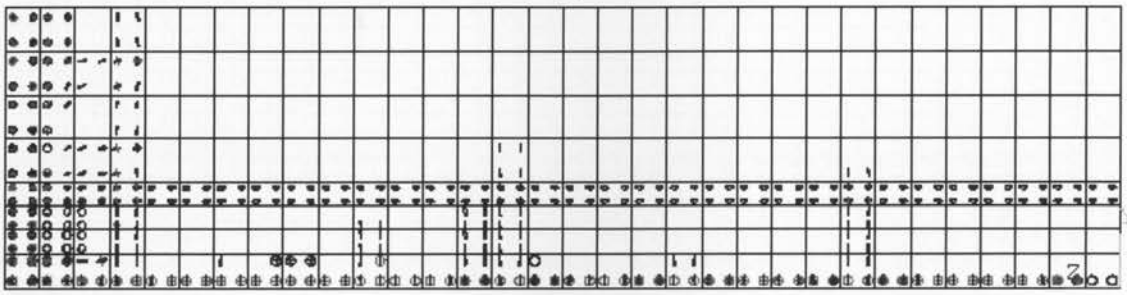

(c)

Figure 6.23: Crack patterns of 4m barrier wall with one end fixed and other end free

Time steps at (a) 13000 hours (b) 17000 hours (c) 22000 hours

At 13000 hours, i.e. around 542 days (Figure 6.23(a)), formation of vertical cracks began at 0.875m and 1.25m from the fixed end, commencing from bottom elements. At 17000 hours, i.e. around 709 days (Figure 6.23(b)), vertical cracks at 1.25m from the fixed end were extended further upward. Closed state transverse cracks were seen at the bottom elements, during the time step of 22000 hours, i.e. around 917 days as seen in Figure 6.23(c). Horizontal cracks at the junction elements were in the open state during this time step.

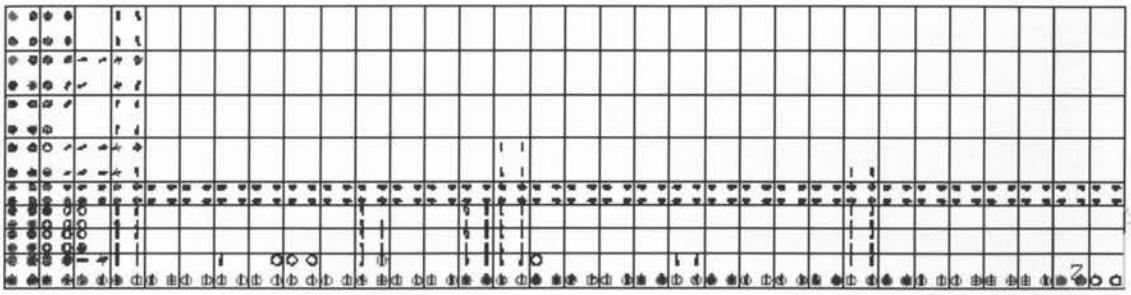

Figure 6.24: Crack patterns of 4m barrier wall with one end fixed and other end free (Time step at 26350 hours)

At the end of 3 years (Figure 6.24), horizontal cracks at the junction elements remain in the closed state, but transverse cracks at the bottom elements were found in open state. The vertical cracks at 1.25m propagated from the bottom to the junction.

6.6 Deformation

Deformation diagram Figure 6.25 shows the warping state of barrier wall with both ends fixed. The deformation of this nature is very devastating for plain concrete barrier walls. Hence it is necessary to reduce the restraint action at the ends to the minimum if possible.

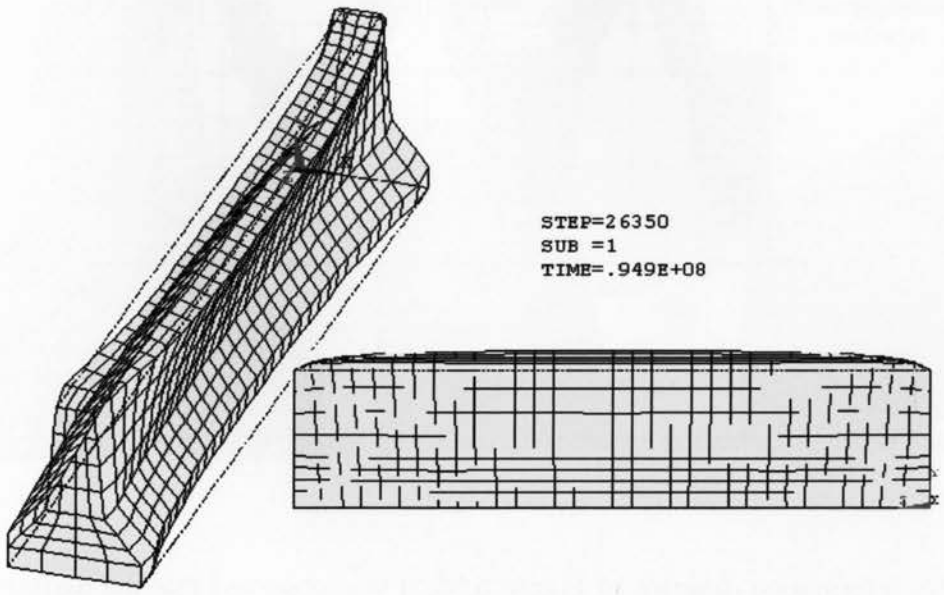

Figure 6.25: Deformation of 4m barrier wall with both ends fixed

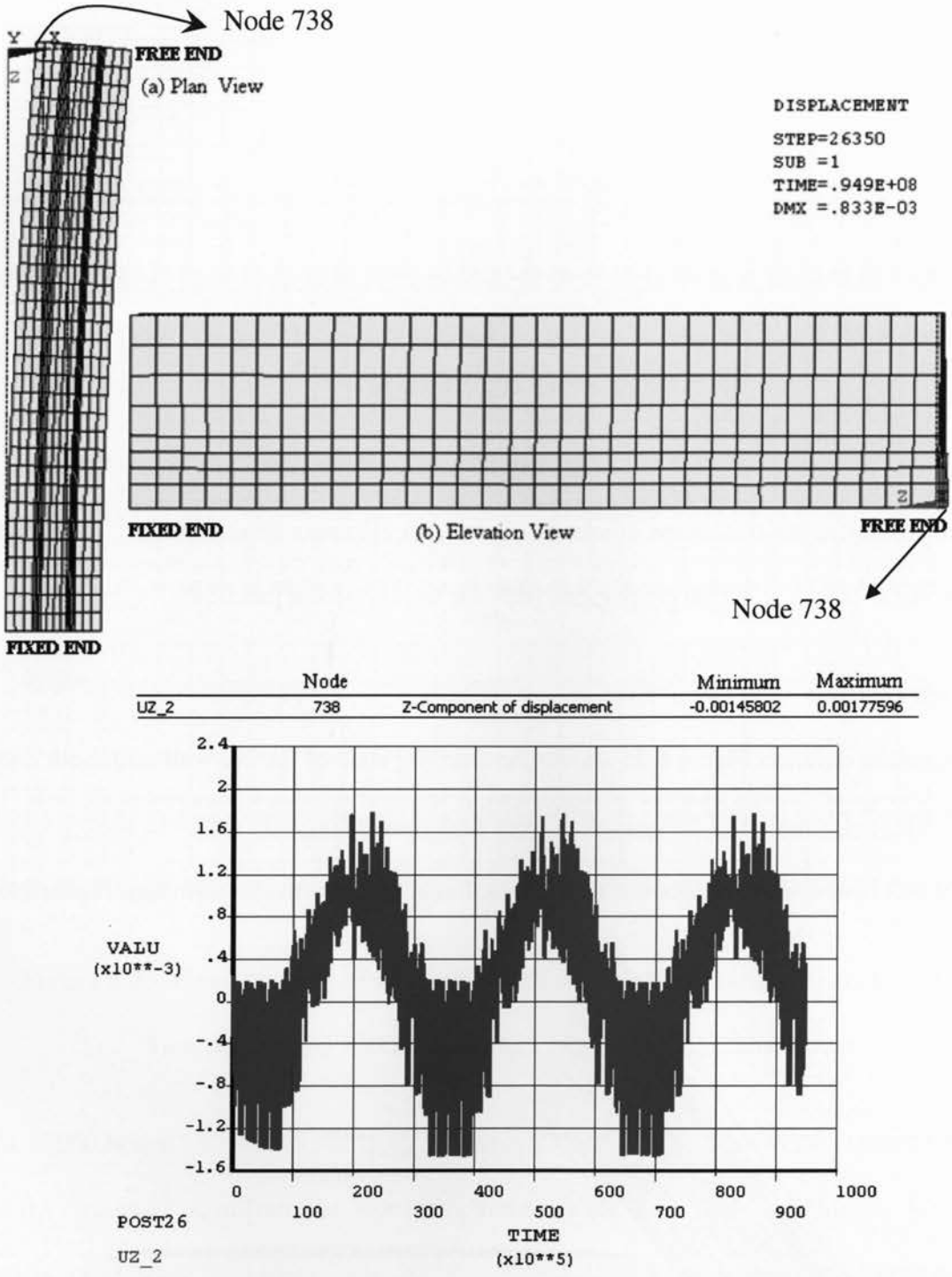

Figure 6.26: Deformation and displacement diagram of 4m barrier wall: free-fixed

From the deformation diagram of Figure 6.26, it was observed that the barrier wall has expanded on the free end side. The maximum change in length was occurred at the

bottom node at origin (node 738 as marked in Figure 6.26), which is 1.45802e-03 meters, i.e. 1.458mm, at the end of three years. In the first year, the change in length was 1.38546e-03 meters, i.e 1.386mm. In the second year, it was 1.45676e-03 meters. i.e. 1.457mm. Maximum change in length at the bottom node indicates that the crack initiates from the bottom of the barrier wall. The length change rate of the bottom node seems to be very low as the time increases. This may be due to the cracks form in between the barrier length.

6.7 Evaluation of Principal stresses at various locations in a 4m barrier wall

Figure 6.27 shows the finite element model with element and node numbers for the discussion of stress development.

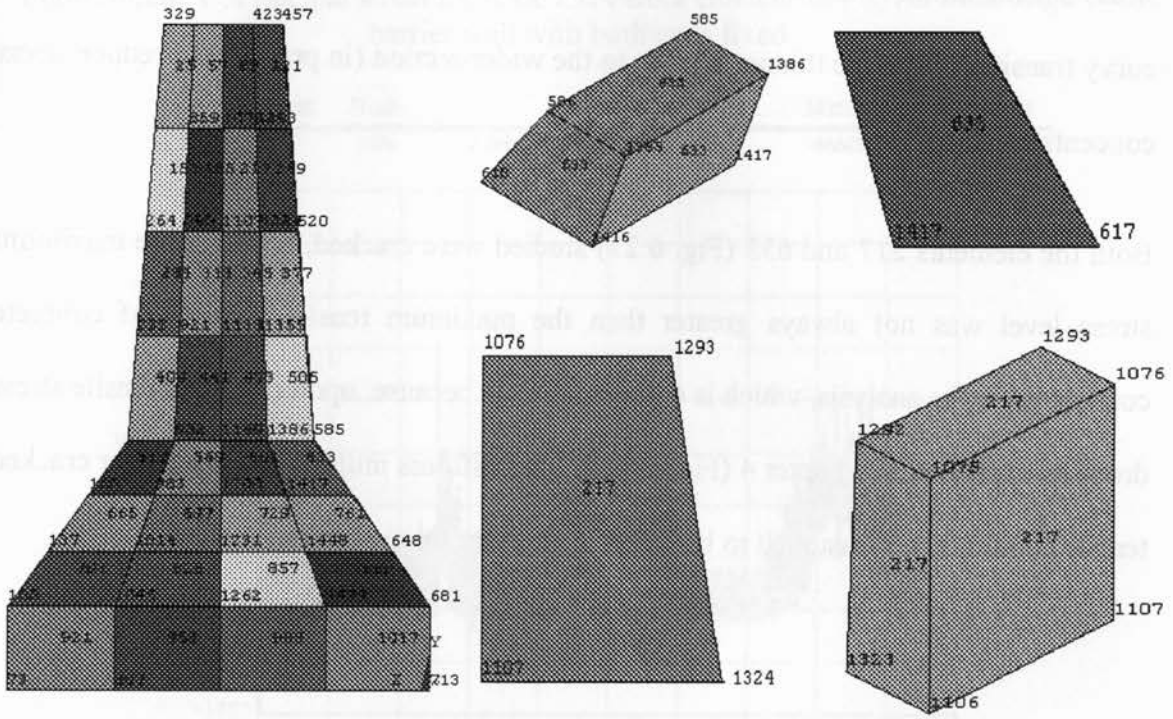

Figure 6.27: Elements and node numbers at 1m length from the origin

Using the crack patterns of 4m barrier wall with both boundary conditions, the stress (Figures 6.28 to 6.33) occurring at 1m from the origin was analyzed for comparison with respect to time. As the barrier wall with free end showed cracks only at the wider section in the 1m range, only elements from the wider section was studied. The stress levels were low for the barrier wall with one end free when compared to the barrier wall with both end restrained. Hence, it is necessary to reduce the restraint action in barrier walls to minimize the occurrence of cracks.

The stress level at the junction node 585 in element 633 from Figure 6.32 was found to increase with time in both boundary conditions. This may be due to the attributes of the finite element model where the junction was treated as a sharp corner. At corners, the stress accumulation is high. It is important to make sure that the junction has a smooth curvy transition from the thinner section to the wider section (in practice) to reduce stress concentration.

Both the elements 217 and 633 (Fig. 6.27) studied were cracked, however the maximum stress level was not always greater than the maximum tensile strength of concrete considered in the analysis, which is 4.5MPa. This is because, upon cracking, tensile stress drops as explained in Chapter 4 (Figure 4.3). The stiffness multiplier constant for cracked tensile condition was assumed to be 0.6 in the current finite element analysis.

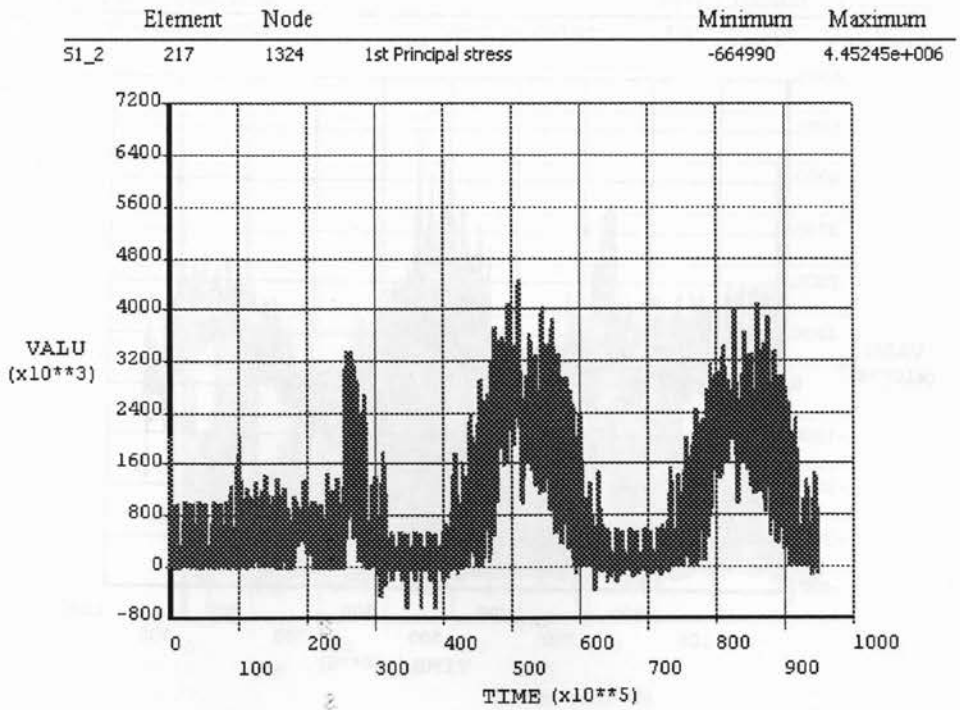

Figure 6.28: 1st Principal stress for node 1324 from element 217 @1m from origin, 4m barrier wall with both ends fixed.

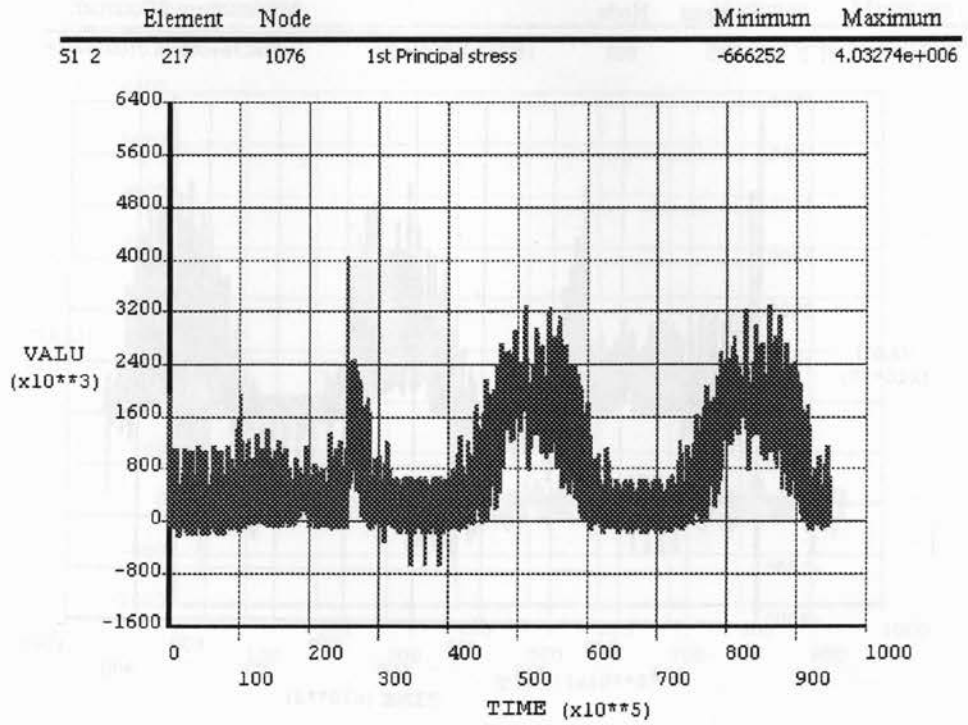

Figure 6.29: 1st Principal stress for node 1076 from element 217 @1m from origin, 4m barrier wall with both ends fixed.

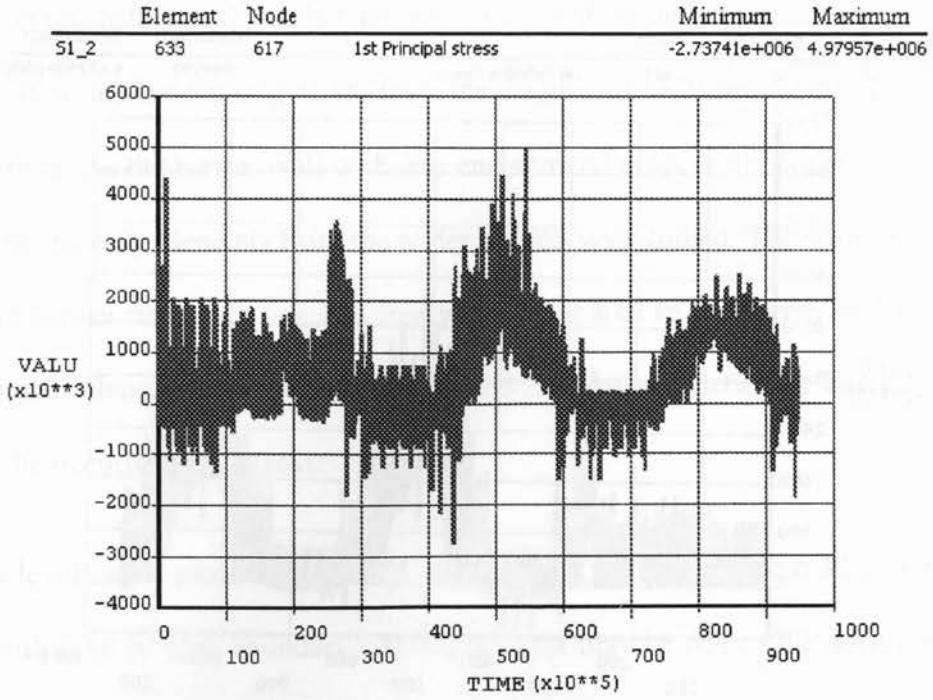

Figure 6.30: 1st Principal stress for node 617 from element 633 @1m from origin, 4m barrier wall with both ends fixed

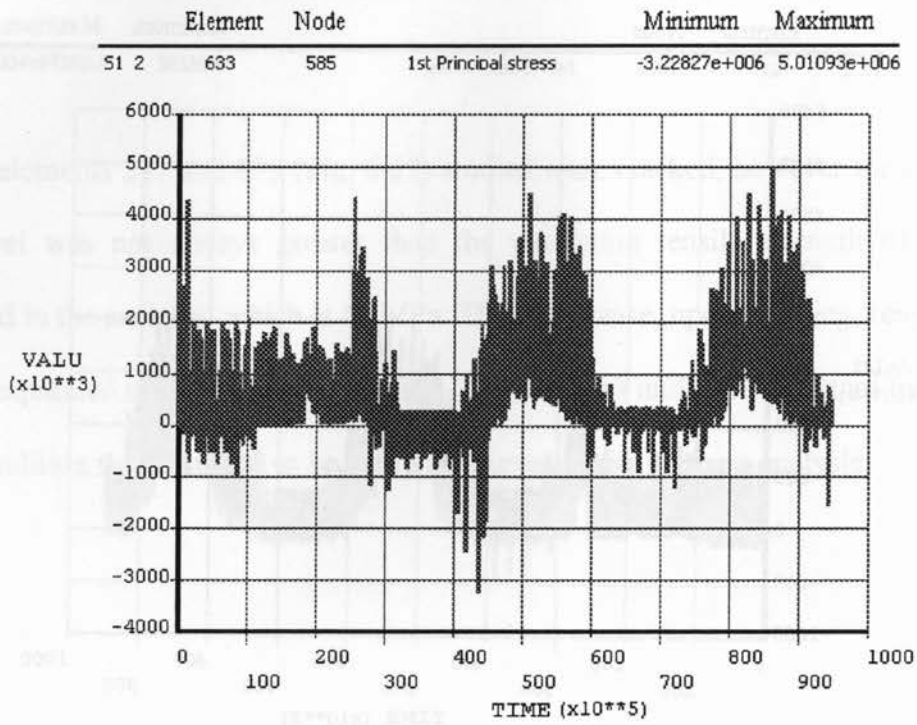

Figure 6.31: 1st Principal stress for node 585 from element 633 @1m from origin, 4m barrier wall with both ends fixed

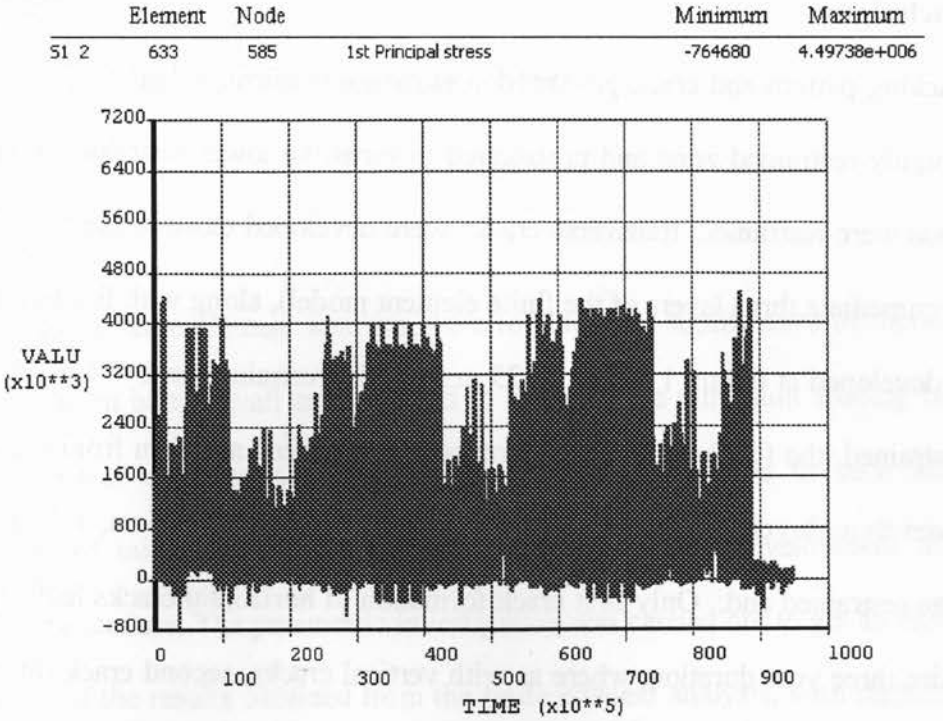

Figure 6.32: 1st Principal stress for node 585 from element 633 @1m from origin, 4m barrier wall with origin end free and other end fixed.

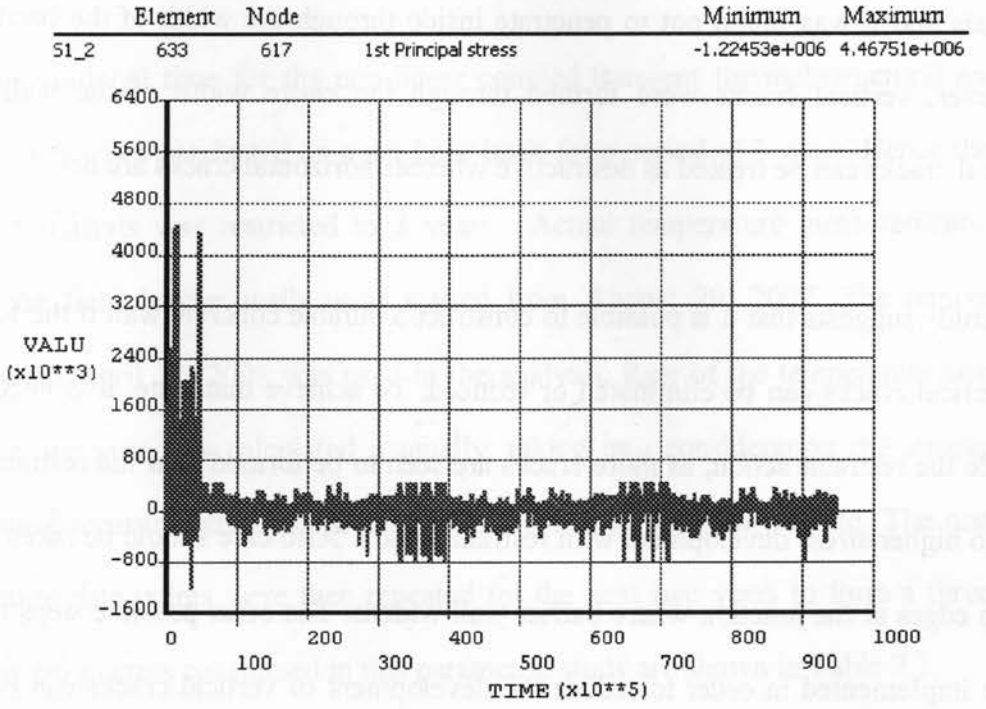

Figure 6.33: 1st Principal stress for node 617 from element 633 @1m from origin, 4m barrier wall with origin end free and other end fixed

6.8 Conclusions

The cracking pattern and crack propagation sequence confirmed that the cracks initiated at the highly restrained zone and propagated towards the lower restrained zones. When both ends were restrained, transverse cracks were developed close to the restrained ends (in the immediate three layers of the finite element model), along with full height vertical cracks developed at 0.5 m, 1 m and 1.125 m from the restrained end. When only one end was restrained, the full height vertical cracks was observed at 0.5 m from the restrained end, even though vertical cracks were developed half way, at 1.25 m, 1.75 m and 3 m from the restrained end. Only first crack formation of horizontal cracks had happened in the entire three year duration, where as with vertical cracks, second crack formation and sometimes even third crack formations had happened depending on the restrained effect or action. Horizontal cracks were observed only on the surface elements in the three year analysis and it was found not to penetrate inside through the width of the barrier wall. However, vertical cracks were formed through the entire width of the wall. Hence vertical cracks can be treated as destructive whereas horizontal cracks are not.

The study suggests that it is possible to construct a durable concrete wall if the formation of vertical cracks can be eliminated or reduced. To achieve that state, it is necessary to reduce the restraint action, as more cracks are seen to be formed near the restrained ends due to higher stress development with restraint action. Also care should be taken to avoid sharp edges at the junction where barrier wall widens. The other possible steps that need to be implemented in order to reduce the development of vertical cracks can be known only if a parametric study is conducted on barrier walls.

Chapter 7

Parametric Study

7.1 Introduction

The objectives of finite element analysis were to study the significance of thermal and shrinkage loads on barrier wall cracking and to establish the minimum spacing between full-length vertical cracking developed in barrier walls subjected to such loadings. Establishment of minimum crack spacing is essential for the development of crack management procedure. The parametric investigation was carried out to get an idea about the sensitivity of the results obtained from the finite element analysis, with respect to the reality. Based on the results of this study, design recommendations are made to reduce the occurrence of cracks in concrete barrier walls.

The computational time for the non-linear coupled transient thermal/structural analysis was too long when conducted on a per hour basis for a period of 3 years. Hence the time frame of analysis was restricted to 3 years. Actual temperature measurements from sensors on field barrier walls were started from August 29, 2007. The temperature recorded till April 22, 2008 was used in the analysis. Rest of the temperature points to complete one year was calculated manually, taking into consideration the atmospheric temperature measurements posted at the Environmental Canada website. The one year temperature data points were then repeated for the next two years to form a three year data. The parameters considered in this parametric study are shown in Table 7.1.

Table 7.1: Range of Variables in Parametric Study

Variables	Range
Length of barrier wall in the analysis	1m to 4m
Age of concrete	Beginning to 3 years
Boundary Conditions	1. Both end restrained against displacement in X, Y and Z directions (fix-fix) 2. One end is restrained against displacement in X, Y and Z direction and the other end free (fix-free)

7.2 Comparison of Expansion Length

From Table 7.2, the rate of increase in maximum barrier displacement is found to decrease with the increase of age. The graphical representation of the displacement occurred at the node for each barrier wall, where the maximum displacement has been recorded, is provided in Figure 7.1, 7.2 and 7.3, as well as, a comparison study is done as shown in Figure 7.4 and Table 7.3.

Table 7.2: Comparison of maximum barrier displacement.(expansion)

Wall Length in meters	Maximum displacement occurring in a barrier wall (Refer Figure 7.1 to 7.4) within a time span of		
	1 year	2 year	3 year
1m	0.4478mm	0.4791mm	0.4782mm
2m	0.7801mm	0.8286mm	0.8306mm
3m	1.0955mm	1.1637mm	1.1780mm
4m	1.3855mm	1.4568mm	1.4580mm

1 m barrier wall

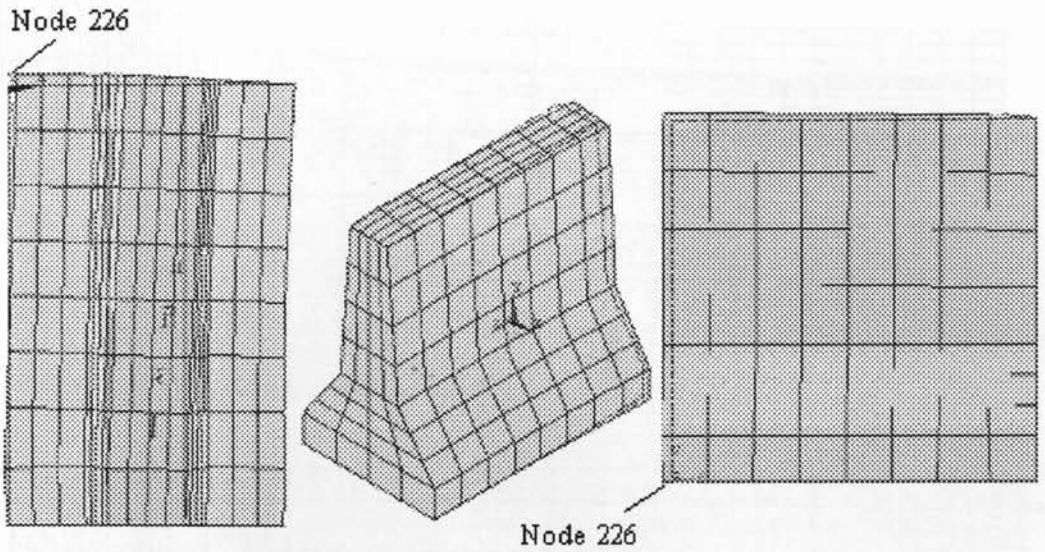

Name	Node	Result	Minimum	Maximum
UZ_2	226	Z-Component of displacement	-0.000479065	0.000440177

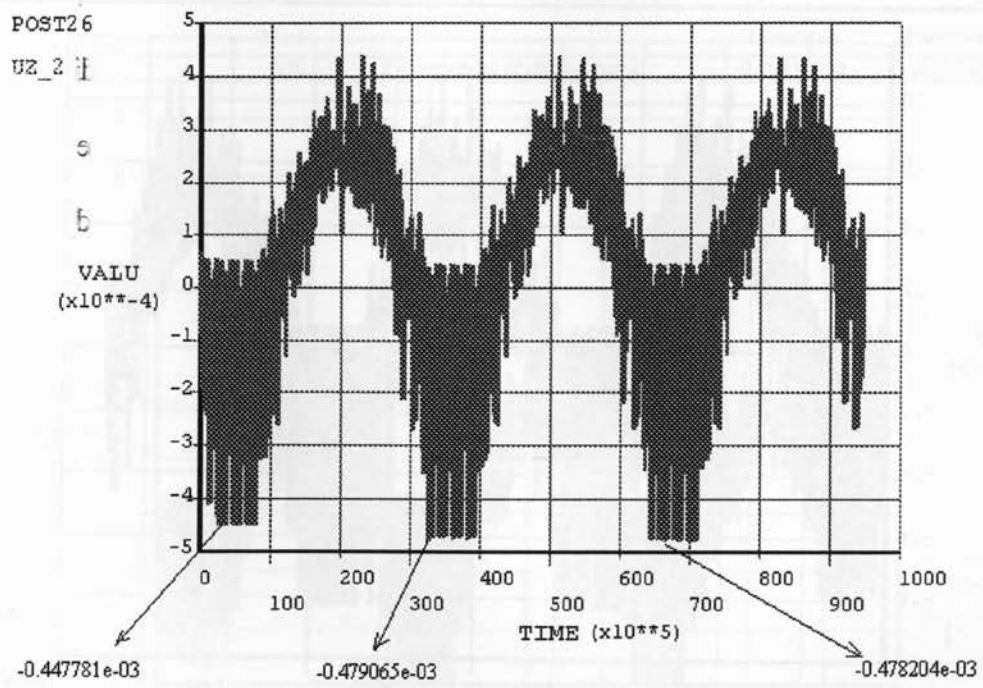

Figure 7.1 : Z component of displacement graph of node 226 of 1m fix-free barrier wall for a time period of 3 years

2 m barrier wall

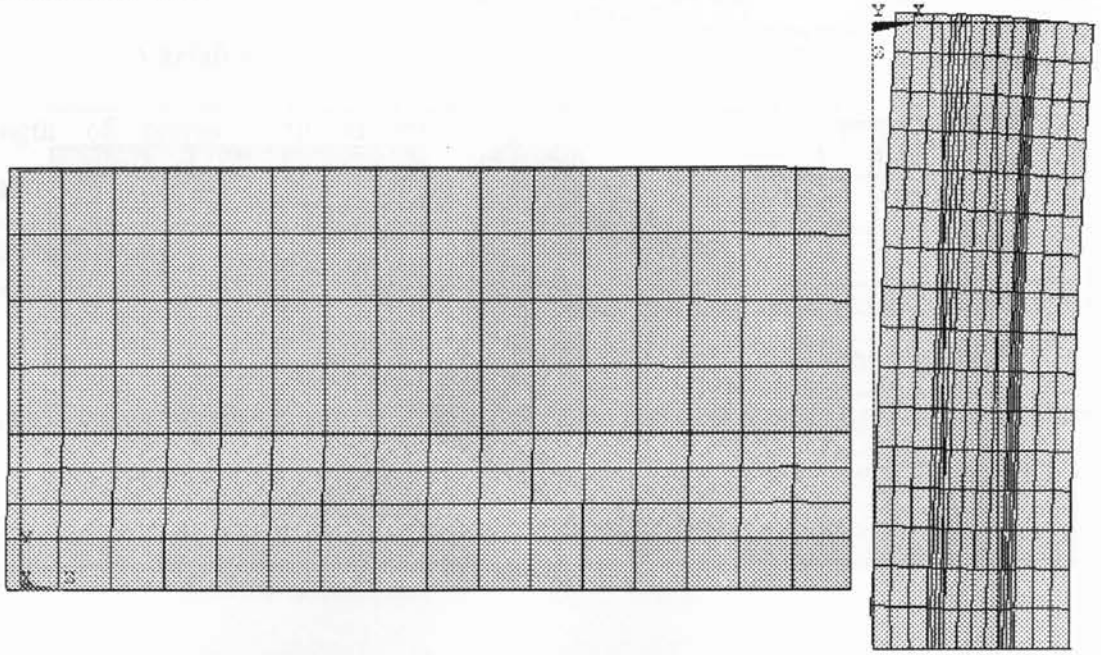

	Node		Minimum	Maximum
UZ_2	402	Z-Component of displacement	-0.000830614	0.000875751

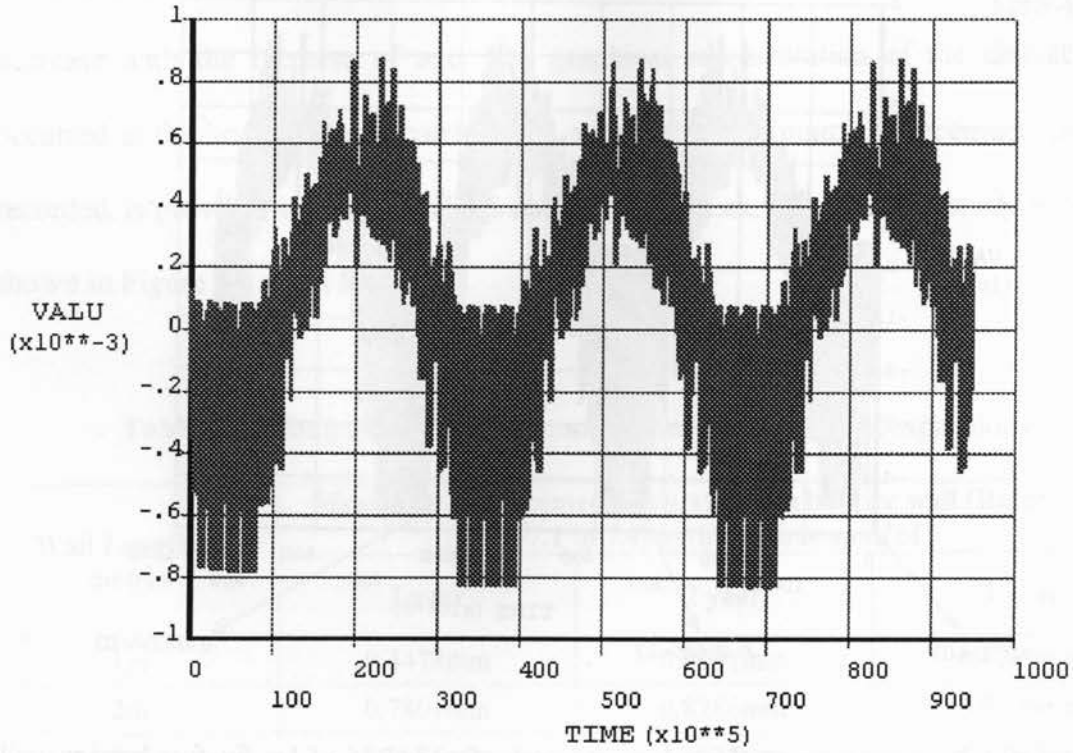

Figure 7.2: Z component of displacement graph of node 402 of 2m fix-free barrier wall for a time period of 3 years

3 m barrier wall

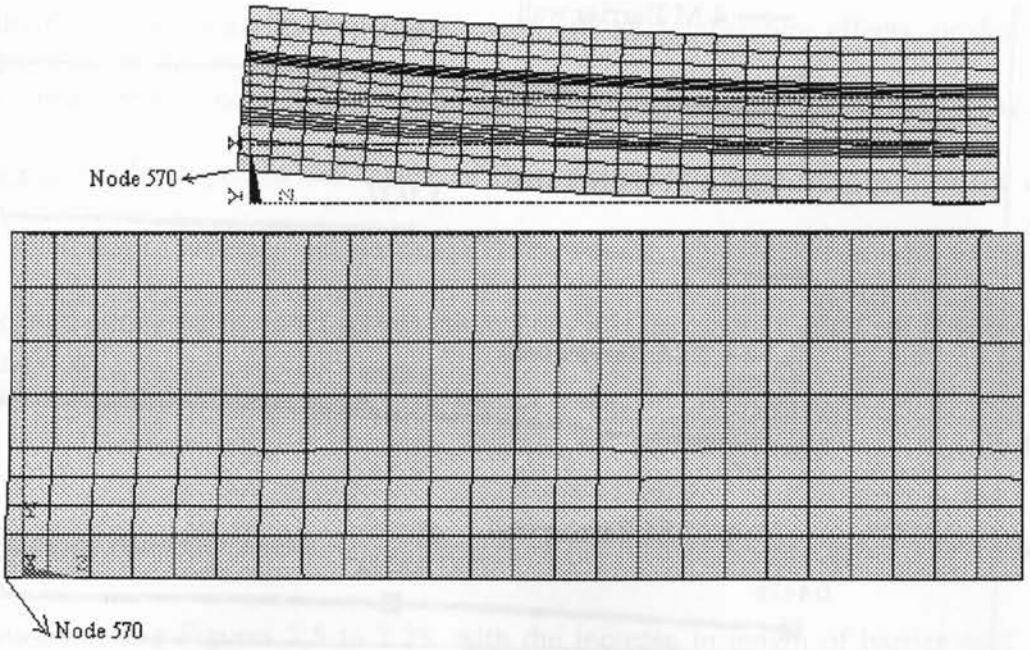

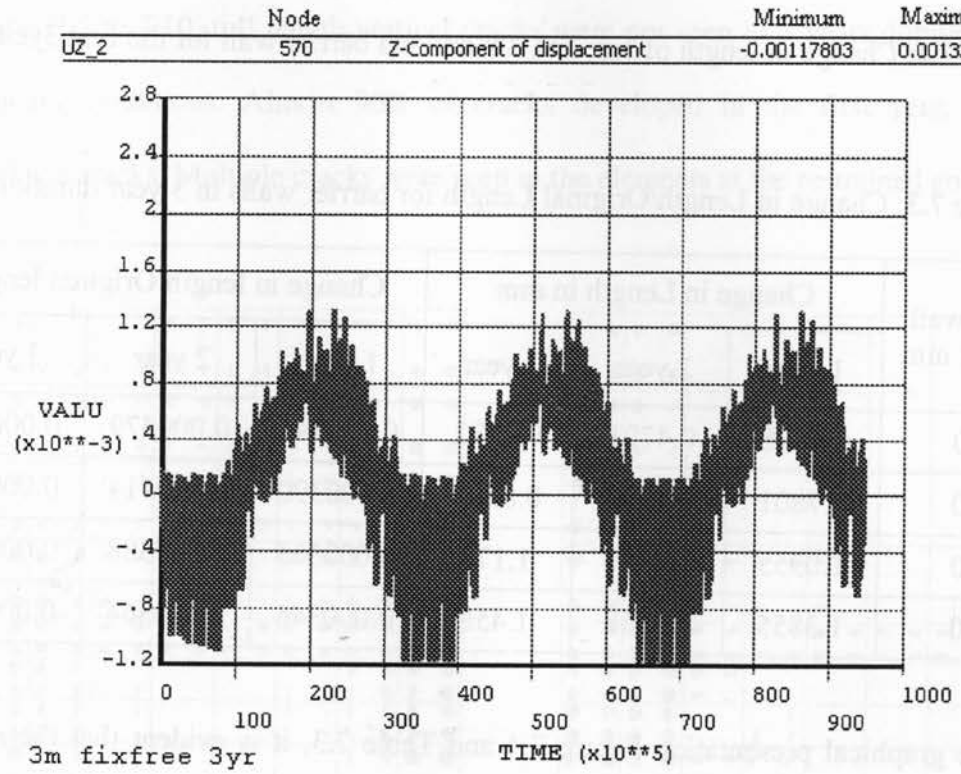

Figure 7.3: Z component of displacement graph of node 570 in a 3m fix-free barrier wall for a time period of 3 years

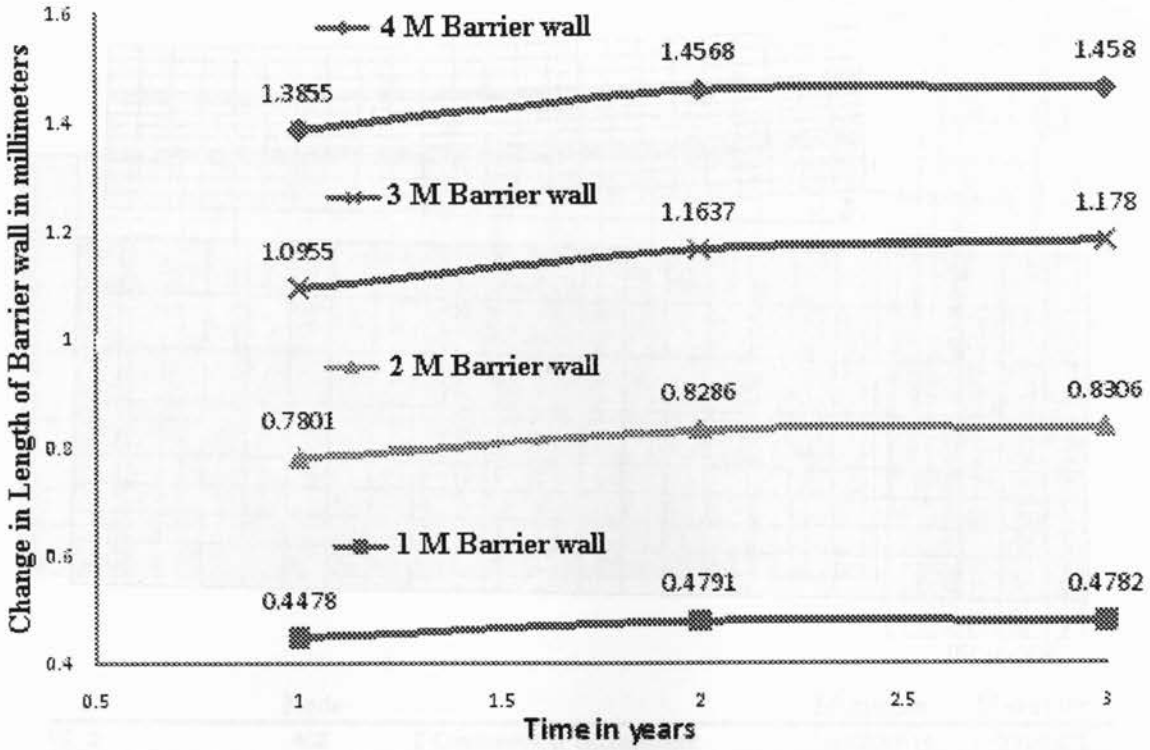

Figure 7.4: Change in length of 1m, 2m, 3m and 4m barrier wall for the first 3years

Table 7.3: Change in Length/Original Length for barrier walls in 3 year duration

Barrier wall length in mm	Change in Length in mm			Change in length/Original length		
	1 year	2 year	3 year	1 year	2 year	3 year
1000	0.4478	0.4791	0.4782	0.000448	0.000479	0.000478
2000	0.7801	0.8286	0.8306	0.000390	0.000414	0.000415
3000	1.0955	1.1637	1.178	0.000365	0.000388	0.000393
4000	1.3855	1.4568	1.458	0.000346	0.000364	0.000365

From the graphical presentation Figure 7.4 and Table 7.3, it is evident that the rate of change in length is negligible after 2 years, for all barrier wall lengths. Hence the major possibility of crack formation due to expansion of concrete can happen within the first

three years only. The cracks that occur in the barrier wall in the long run should be due to other reasons, such as freezing and thawing effects, temperature effects, or due to the combined effect of both on the weaker areas of concrete wall. The weaker areas of the wall can be developed in due course of time because of many reasons, like the cracks generated due to restraint and shrinkage effects, or the cracks generated due to the flaws happened during barrier wall construction. Thus it is necessary to find out how the crack patterns develop with time on concrete barrier walls.

7.3 Comparison of Cracks

While observing Figures 7.5 to 7.28, with the increase in length of barrier wall, more vertical cracks were formed at the barrier surface. For 1 m length barrier wall from Figures 7.5 to 7.10, full length vertical cracks were not seen in 3 years duration, in both boundary conditions. Almost 90% of cracks developed in the first year, indicating shrinkage cracks. Multiple cracks were seen in the elements at the restrained ends.

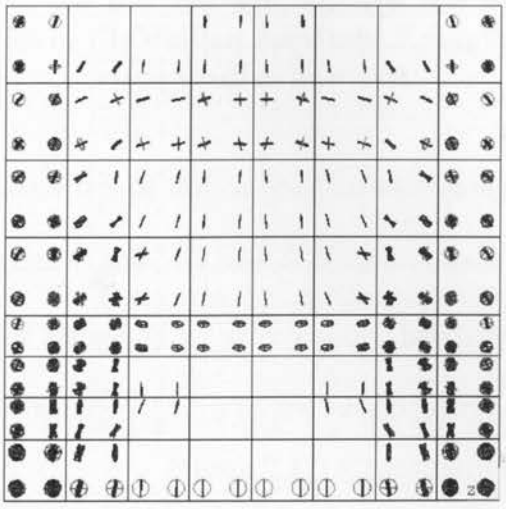

Figure 7.5: Crack pattern of 1 m fix-fix wall in one year

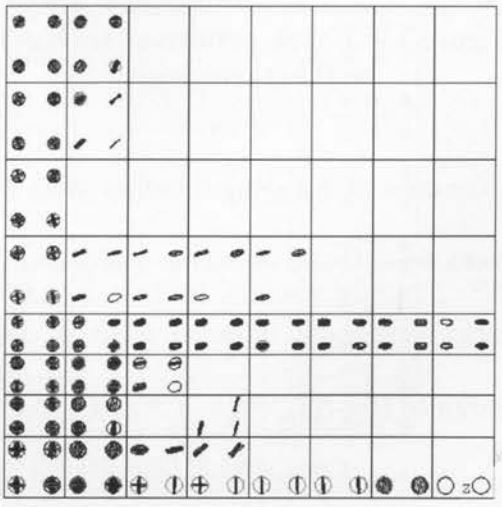

Figure 7.6:Crack pattern of 1 m fix-free wall in one year

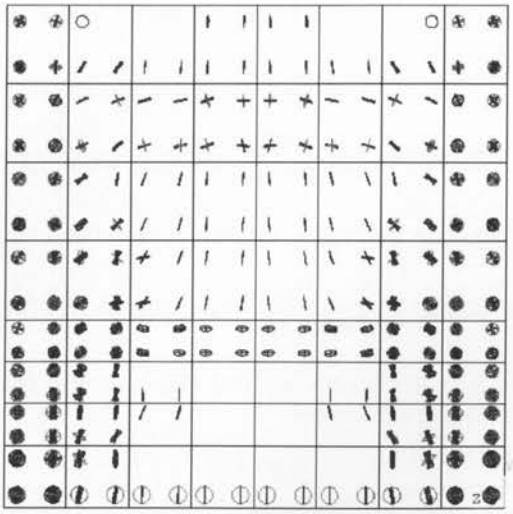

Figure 7.7: Crack pattern of 1 m fix-fix wall in two years

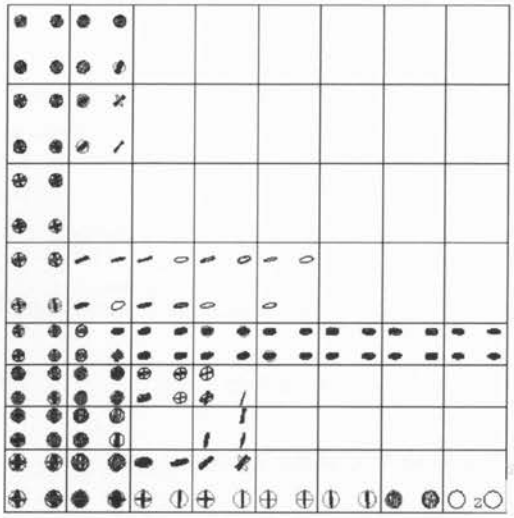

Figure 7.8: Crack pattern of 1 m fix-free wall in two years

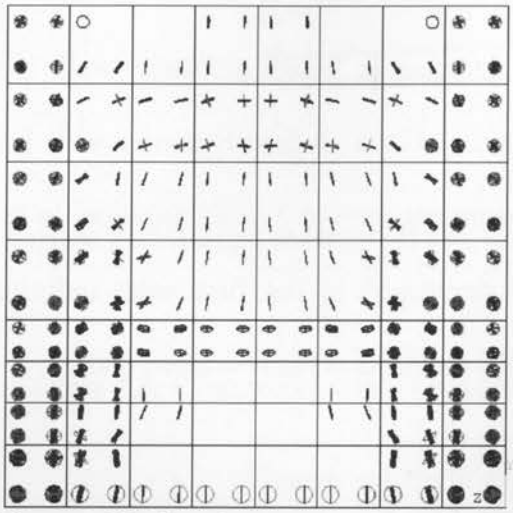

Figure 7.9: Crack pattern of 1m fix-fix wall in three years

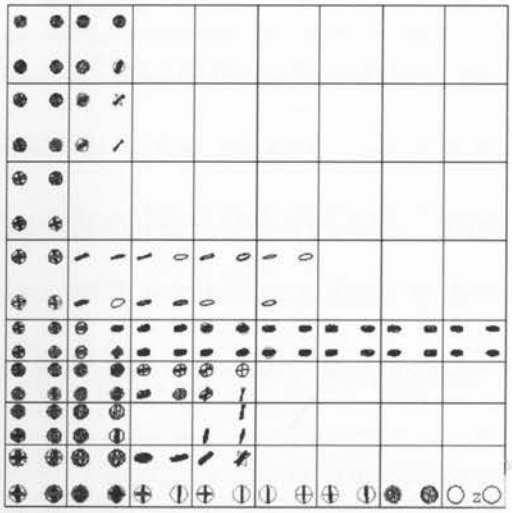

Figure 7.10: Crack pattern of 1 m fix-free wall in three years

In the case of 2 m length barrier wall, from Figures 7.11 to 7.16, no full length vertical cracks were found in barrier walls with only one end fixed, in 3 year duration. Multiple cracks were found in the elements at the restrained end. However, when both ends were restrained (fix-fix), even in the first year itself, vertical cracks were formed, commencing from the bottom elements near the mid span and progressing upwards.

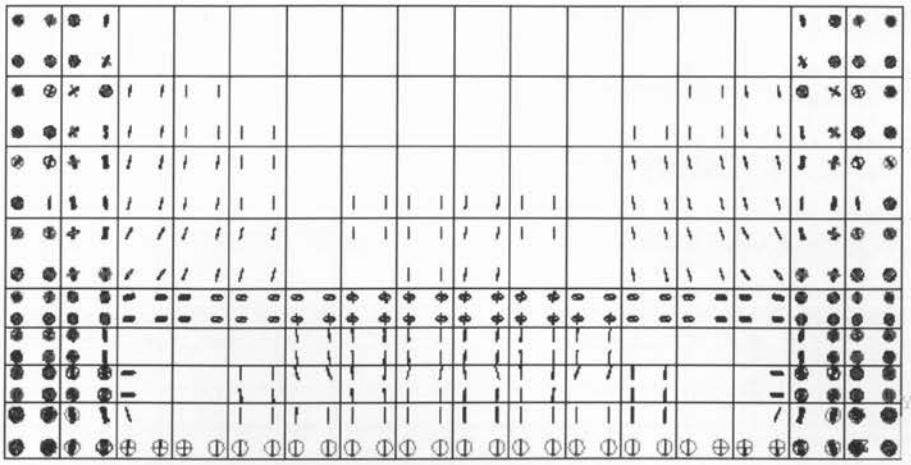

Figure 7.11: Crack pattern of 2m fix-fix wall in one year

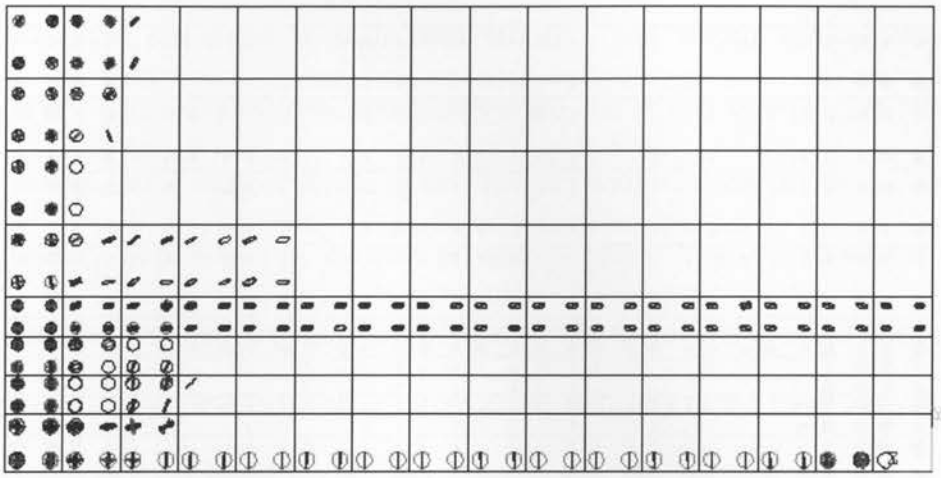

Figure 7.12: Crack pattern of 2m fix-free wall in one year

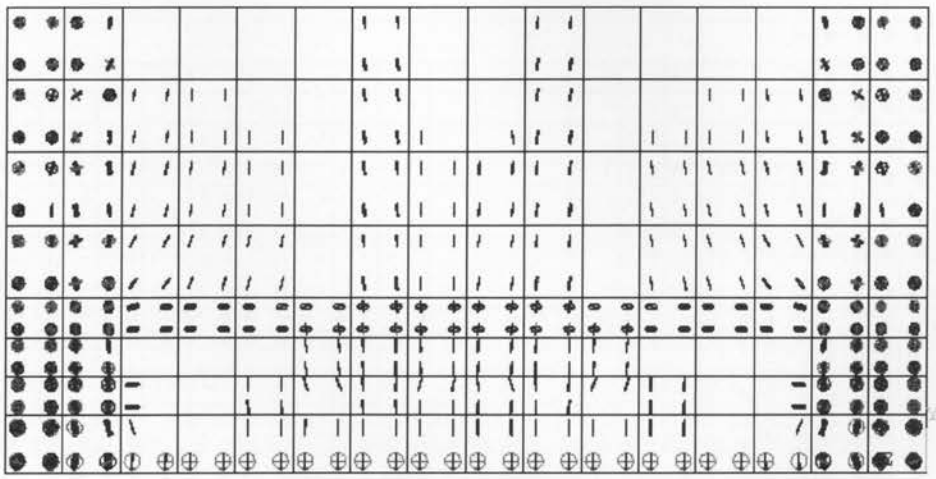

Figure 7.13: Crack pattern of 2m fix-fix wall in two years

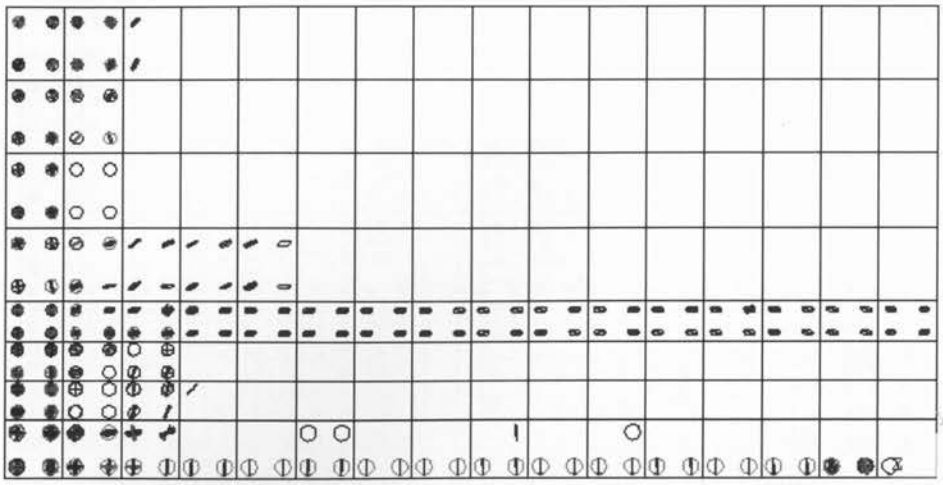

Figure 7.14: Crack pattern of 2m fix-free wall in two years

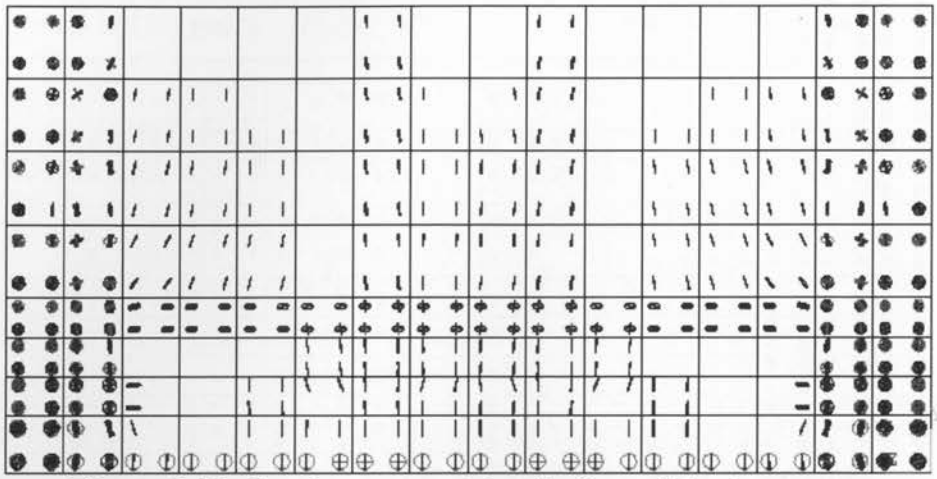

Figure 7.15: Crack pattern of 2m fix-fix wall in three years

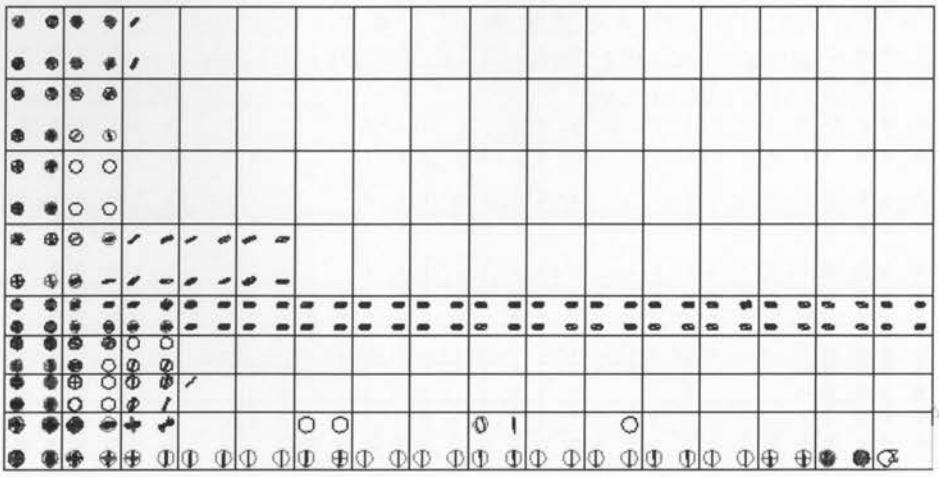

Figure 7.16: Crack pattern of 2m fix-free wall in three years

In the case of 2 m barrier wall with both ends fixed, vertical cracks at 0.875m from both fixed ends were developed fully throughout the barrier height in two years (Figure 7.13). In three years (Figure 7.15), vertical cracks found at the elements in the central region were seen progressing upward, which might end up as fully developed cracks in 4-5 years. Multiple cracks were found in the immediate two column layer elements from the fixed end.

In the case of 3 m barrier wall (Figures 7.17 to 7.22) at the end of first year, when the barrier wall was restrained at both ends (fix-fix), full length vertical cracks were developed at 1m distance from the fixed ends at the end of first year (Figure 7.17). Many vertical cracks, some almost reaching full height, were formed in the nearby layers. Multiple cracks were found in the two immediate layers from the fixed end. Vertical cracks were also seen developing in the bottom at mid span. At the end of third year, few multiple cracks were developed at 1m from fixed ends and at the third immediate layer from the fixed ends (Figure 7.21).

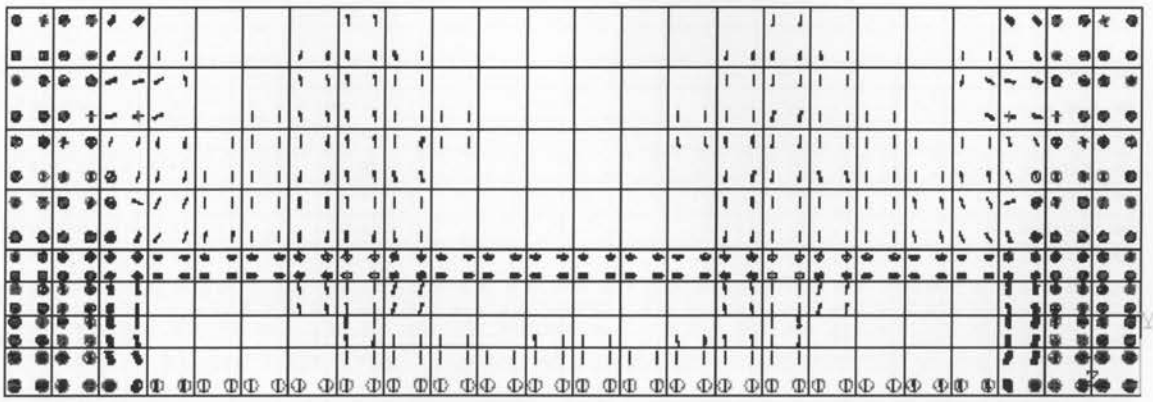

Figure 7.17: Crack pattern of 3m fix-fix wall in one year

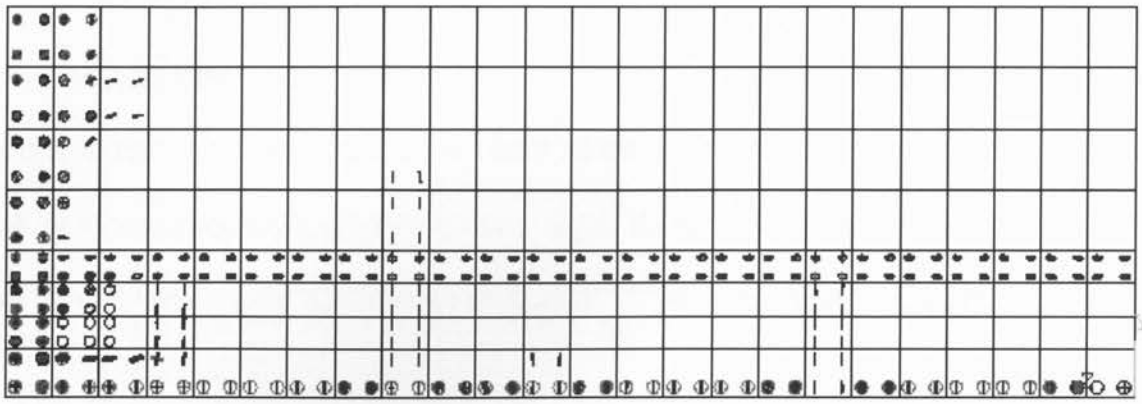

Figure 7.18: Crack pattern of 3 m fix-free wall in one year

When the boundary condition was different, i.e. when only one end was restrained and the other end was kept free (fix-free), multiple cracks were seen only on the first immediate column layer elements at the fixed end. Vertical cracks started to develop in the thicker wall area at 0.5 m, 1.125 m, 1.5 m and 2.25 m from the fixed end, at the end of one year (Figure 7.18). In two years, vertical cracks at 1.125 m from the fixed end progressed upward. Many vertical cracks were formed in the thinner wall area within 1.125 m from fixed end (Figure 7.20). By the end of three years, vertical crack at 2.25 m progressed to the thinner wall area (Figure 7.22)

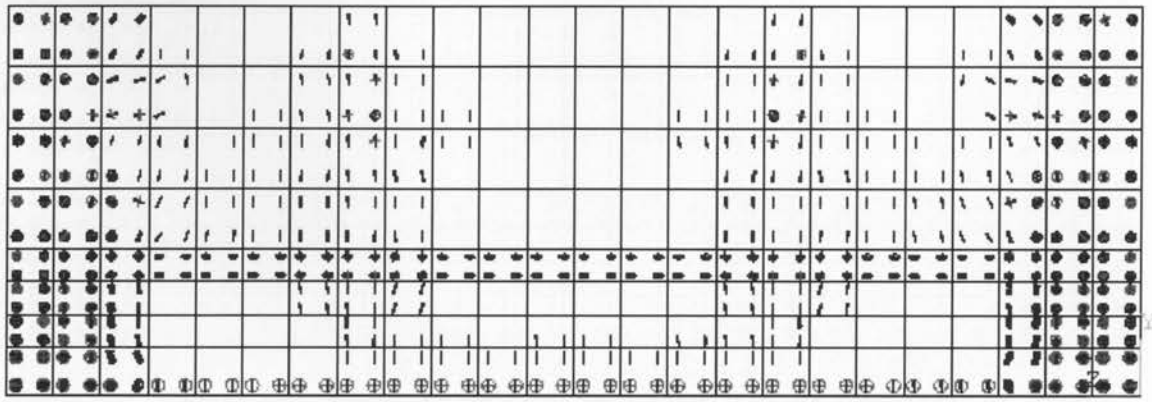

Figure 7.19: Crack pattern of 3 m fix-fix wall in two years

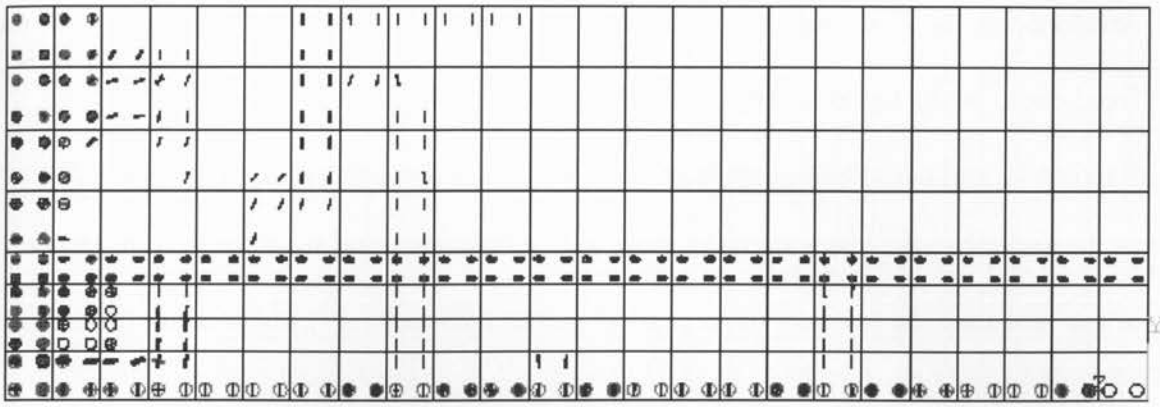

Figure 7.20: Crack pattern of 3 m fix-free wall in two years

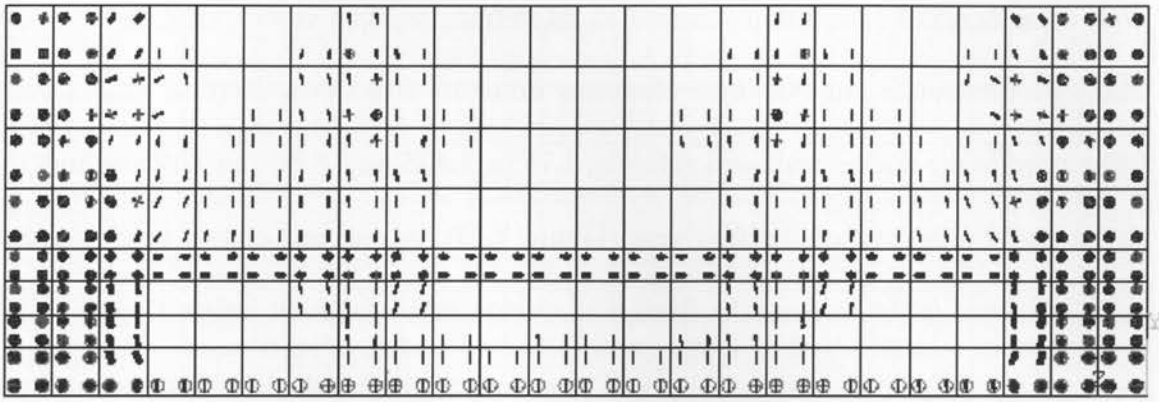

Figure 7.21: Crack pattern of 3 m fix-fix wall in three years

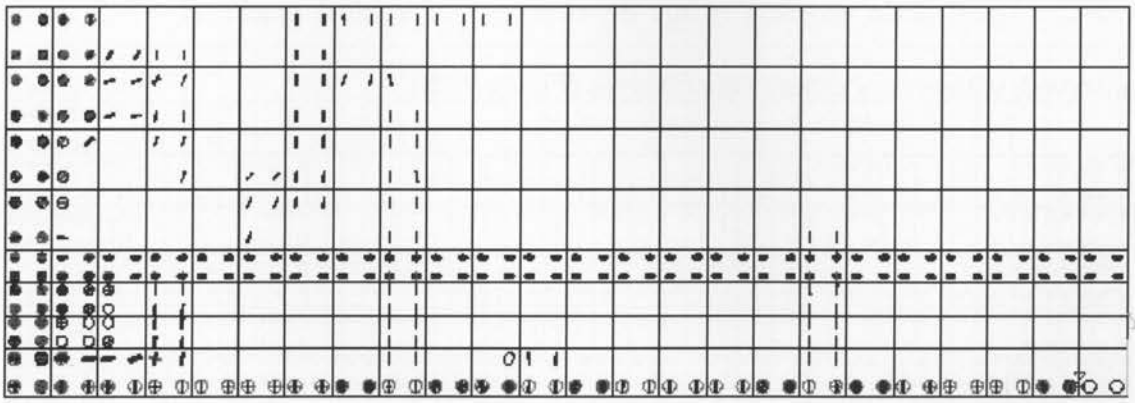

Figure 7.22: Crack pattern of 3 m fix-free wall in three years

In 4 m wall, with both ends restrained (fix-fix), at the end of first year, full length vertical cracks were found at 1.0 m from the fixed ends (Figure 7.23). Multiple cracks were

developed at the immediate layer elements from the fixed end. At 1 m length from the fixed ends, in the top element, multiple cracks were found. At 1.125 m length from the fixed ends, vertical cracks were developed in most of the column layer elements, but not in the entire height. Vertical cracks were also seen developing from the bottom elements at the mid span. In two and three years (Figures 7.25 and 7.27), the number of multiple cracks developed at 1 m from the fixed ends, increased from top to mid height.

When the boundary condition changed to fixed-free, multiple cracks were seen only in the first immediate column layer elements from the fixed end. Vertical cracks were developed in the thicker wall area at 0.5 m, 1.75 m, 1.875 m, 2.5 m, and 3.125 m from the fixed end, by the end of the first year (Figure 7.24). At the end of two years, vertical cracks formed at 0.5 m from the fixed end, developed to full wall height (Figure 7.26). Vertical crack at 1.875 m also progressed upward in a small scale. New vertical cracks at 1.375 m from the fixed end were also developed during this time. By the end of three years, a small scale progress in the development of vertical cracks at 1.375 m was observed, without any other major changes (Figure 7.28)

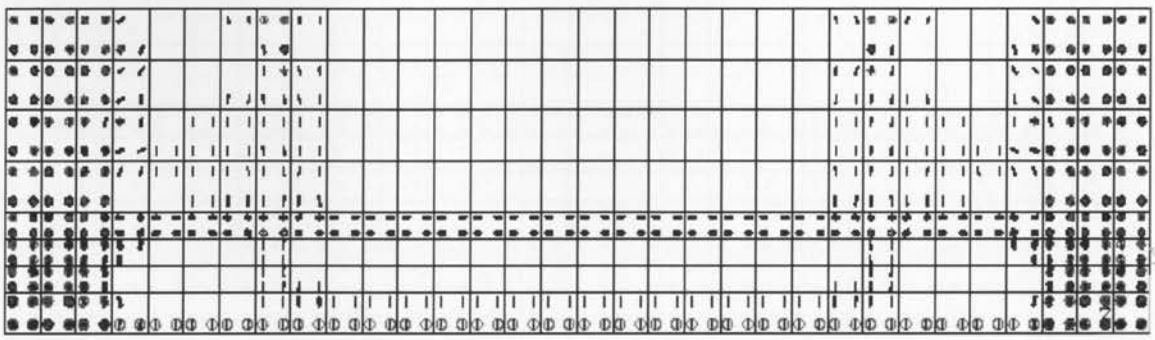

Figure 7.23: Crack pattern of 4 m fix-fix wall in one year

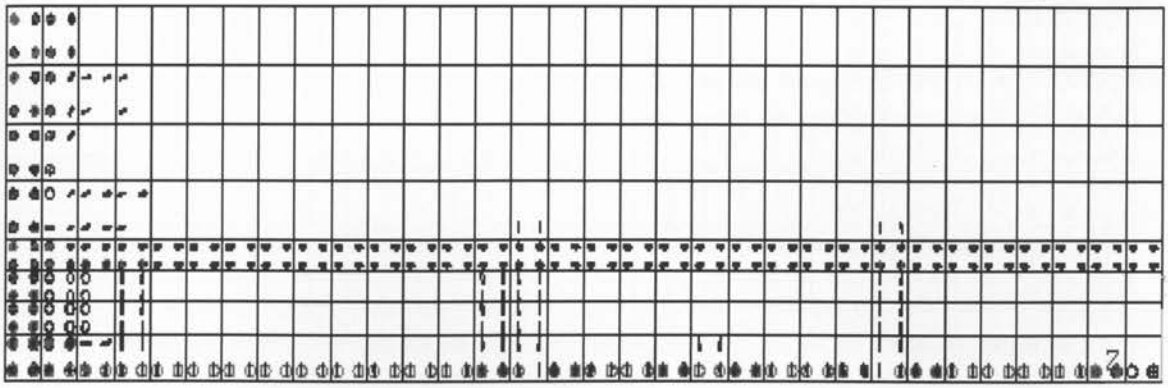

Figure 7.24: Crack pattern of 4 m fix-free wall in one year

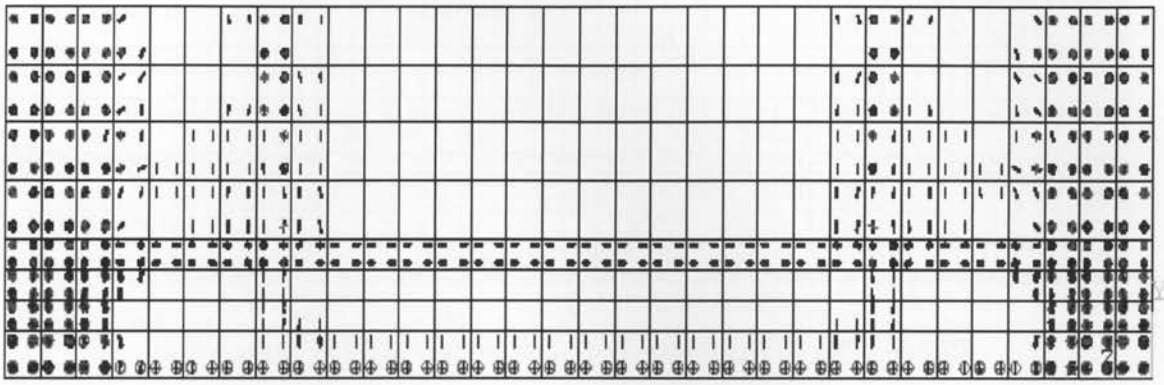

Figure 7.25: Crack pattern of 4 m fix-fix wall in two years

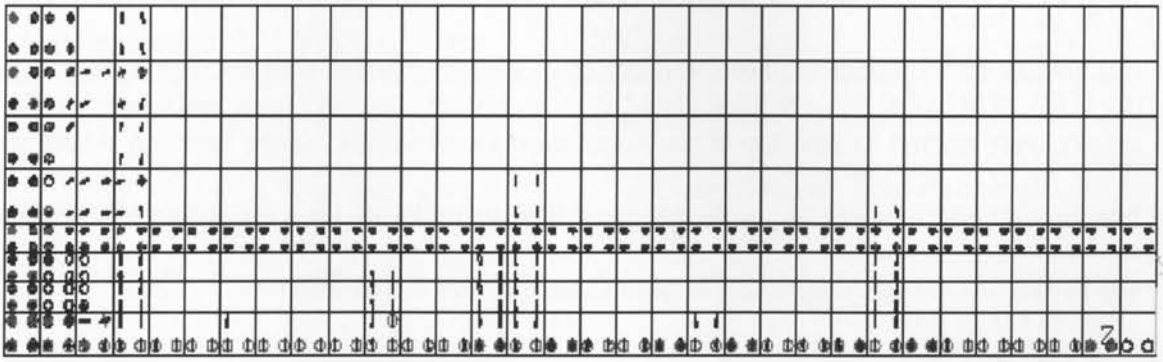

Figure 7.26: Crack pattern of 4 m fix-free wall in two years

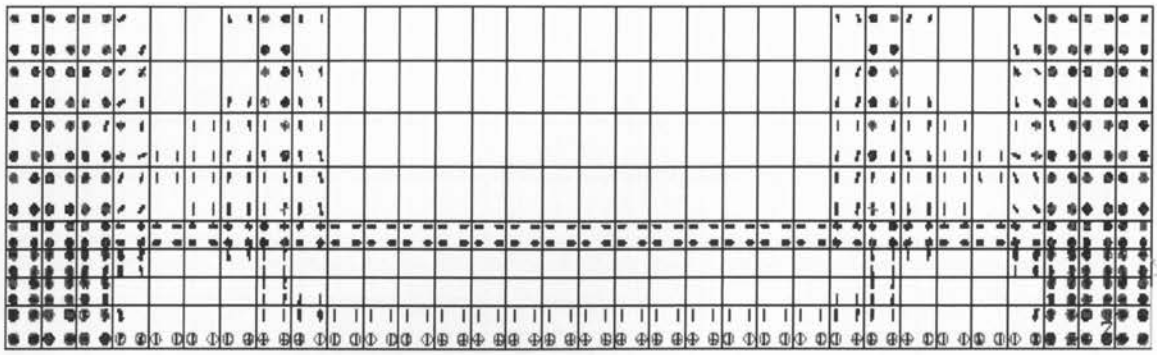

Figure 7.27: Crack pattern of 4 m fix-fix wall in three years

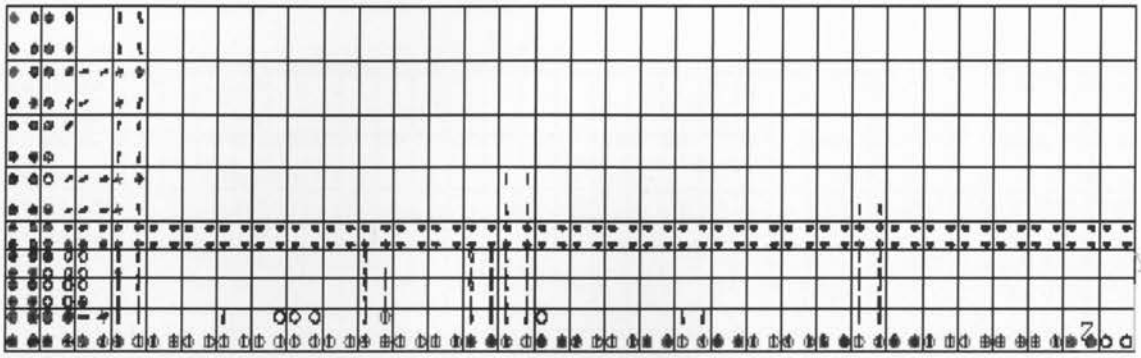

Figure 7.28: Crack pattern of 4 m fix-free wall in three years

From Tables 7.2 and 7.3, the rate of increase in the ratio of change in length per original length of 4 m barrier wall is found to be less than that of 3 m barrier wall. This may be due to the development of more vertical cracks in the barrier wall segment. Horizontal cracks were started to develop at the south west face initially, at the junction where the barrier wall width increases, in all the cases. These cracks are then progressed throughout the barrier length and progressed to both sides (Figures 7.5 to 7.28)

7.4 Sequence of Evolution of Cracks

The sequence of crack evolution for all barrier lengths, (1 m, 2 m and 3 m), with both boundary conditions are shown in Appendix (Figures A.1 to A.37). A comprehensive

comparison study on the vertical crack formation in barrier walls of different lengths from Appendix is made in Table 7.4. It is evident that as the length of the wall increases, the number of crack formations also increases.

Table 7.4: Comparison of vertical crack formation in barrier walls of different length

Vertical cracks	1 m barrier wall		Crack distance from fixed end	
	fix-fix	fix-free	fix-fix (repeat)	fix-free
Full height	No	No		
Thicker section	No	Partial		0.5 m
Thinner section	Yes	No	0.5 m	

Vertical cracks	2 m barrier wall		Crack distance from fixed end	
	fix-fix	fix-free	fix-fix (repeat)	fix-free
Full height	Yes	No	0.875 m	
Thicker section	Yes	Partial	0.625 m to 1 m	1.125 m
Thinner section	Yes	No	0.375 m to 0.625 m, 0.875 m to 1 m	

Vertical cracks	3 m barrier wall		Crack distance from fixed end	
	fix-fix	fix-free	fix-fix (repeat)	fix-free
Full height	Yes	No	1 m	
Thicker section	Yes	yes	0.875 m to 1.5 m	0.5 m, 1.125 m, 1.5 m, 2.25 m
Thinner section	Yes	Partial	0.5 m to 1.25 m	0.875 m to 1.375 m

Vertical cracks	4 m barrier wall		Crack distance from fixed end	
	fix-fix	fix-free	fix-fix (repeat)	fix-free
Full height	Yes	Yes	1 m	0.5 m
Thicker section	Yes	Yes	0.875 m to 2 m	0.5 m, 0.875 m, 1.375 m, 1.75 m, 1.875 m, 2.5 m, 3.125 m
Thinner section	Yes	Yes	0.625 m to 0.875 m	0.5 m, 1.875 m, 3.125 m

7.5 Stress-time graphs of Barrier Wall Elements

A crack plane is formed when concrete reaches its ultimate tensile strength. This crack plane, whether it is closed or open, will be orthogonal to the maximum principal tensile stress, which existed just prior to cracking. The presence of an open crack plane should have caused a complete loss of material stiffness in its orthogonal direction, but not here, since we have assumed shear retention factor for open cracks as 0.3. Thus 30% shear transfer takes place, as per our assumptions.

Usually when open cracks form, a discontinuity is introduced into the hitherto continuous material, thus relieving the high tensile stress or strain concentrations orthogonal to the crack. Therefore stress redistribution takes place, i.e., the tensile stresses that existed before the formation of the crack is transformed into equivalent residual forces and thus redistributed to the adjacent concrete zones. However, as a result of this stress redistribution, new zones of high tensile stress and strain concentrations are created near the crack tips. This crack can be either stable or unstable, depending on the amount of stress redistribution. Let us examine the stress-time graphs taken for concrete barrier wall with different lengths and boundary conditions.

7.5.1 Stress-time graphs of few elements of 1 m Barrier Wall.

The stress-time graphs of few critical elements of 1 m barrier wall with both boundary conditions are shown below. A comparison is made between both boundary conditions to identify the effect of restraints on crack development, and a summary is given in Table 7.3.

Case 1: One meter barrier wall with nodes restrained against displacement in X, Y and Z directions, at both ends

The crack sequences presented in Appendix (Figures A.7 to A.11) explain that the major stress concentrations were formed near the restrained ends. Figure 7.29 shows the element and node numbers at the barrier wall section at 1m from the origin. From the analysis of elements 25, 49, 113 and 249, at the restrained end, it was observed that the cracks had formed within the first four months from the beginning (Figures 7.30 to 7.33).

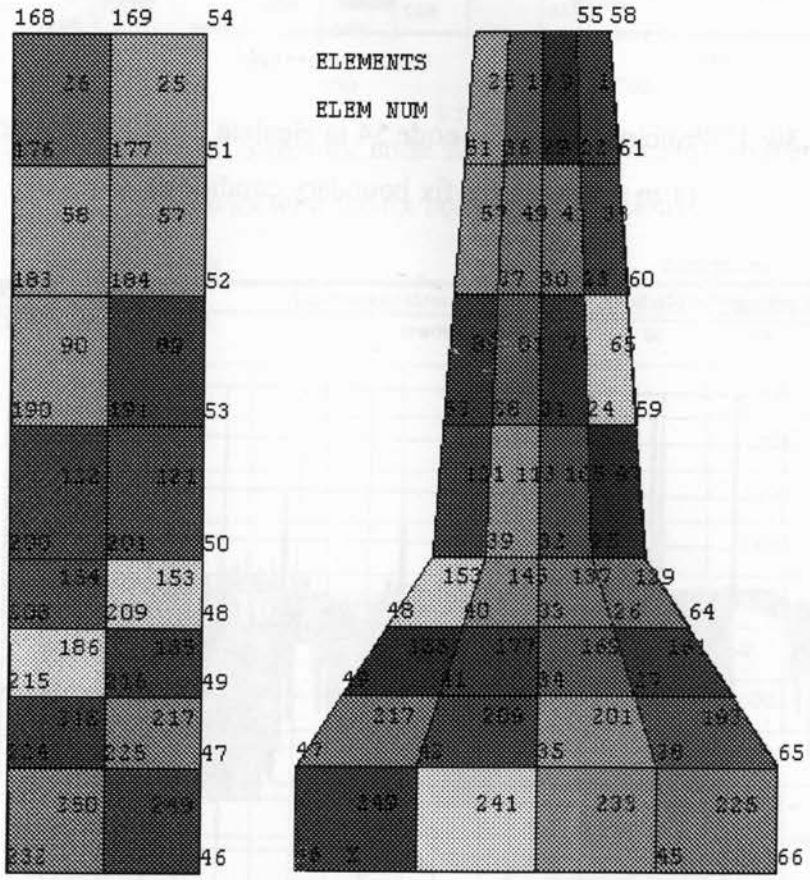

Figure 7.29: Element and node numbers of 1 m barrier wall at 1m from origin.

	Element	Node		Minimum	Maximum
S1_2	25	54	1st Principal stress	-9.4751e+006	4.35186e+006

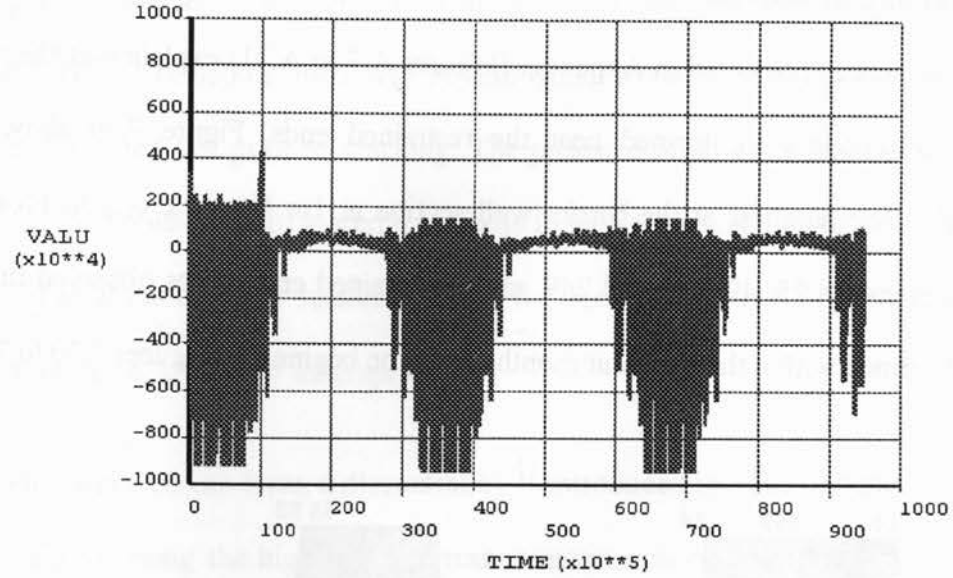

Figure 7.30: 1st Principal Stress for node 54 in element 25@ 1 m from origin.
(1 m wall with fix-fix boundary condition)

	Element	Node		Minimum	Maximum
S1_2	49	30	1st Principal stress	-3.23996e+006	4.48723e+006

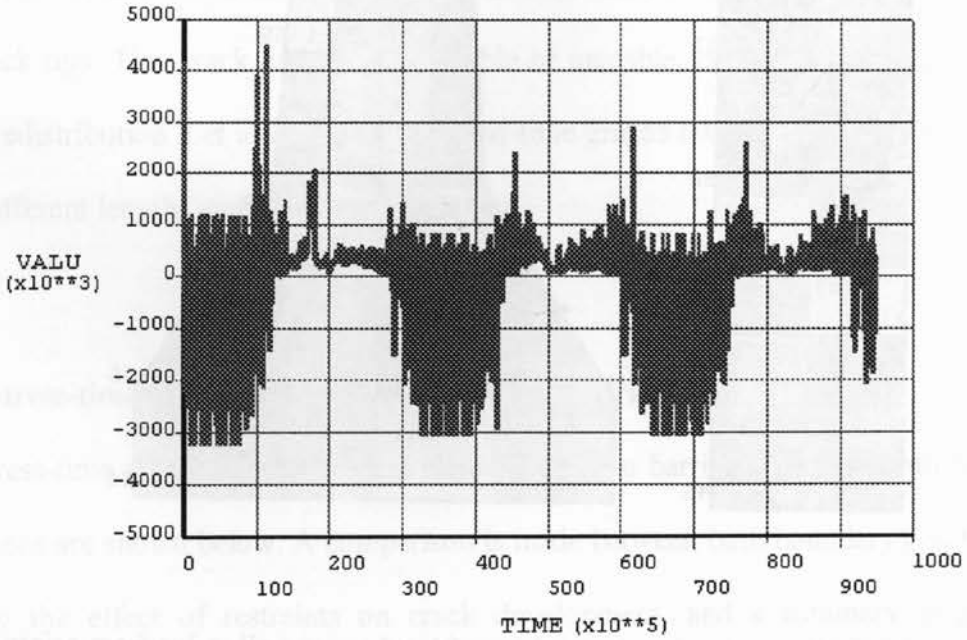

Figure 7.31: 1st Principal Stress for node 30 in element 49 @1 m from origin.
(1 m wall with fix-fix boundary condition)

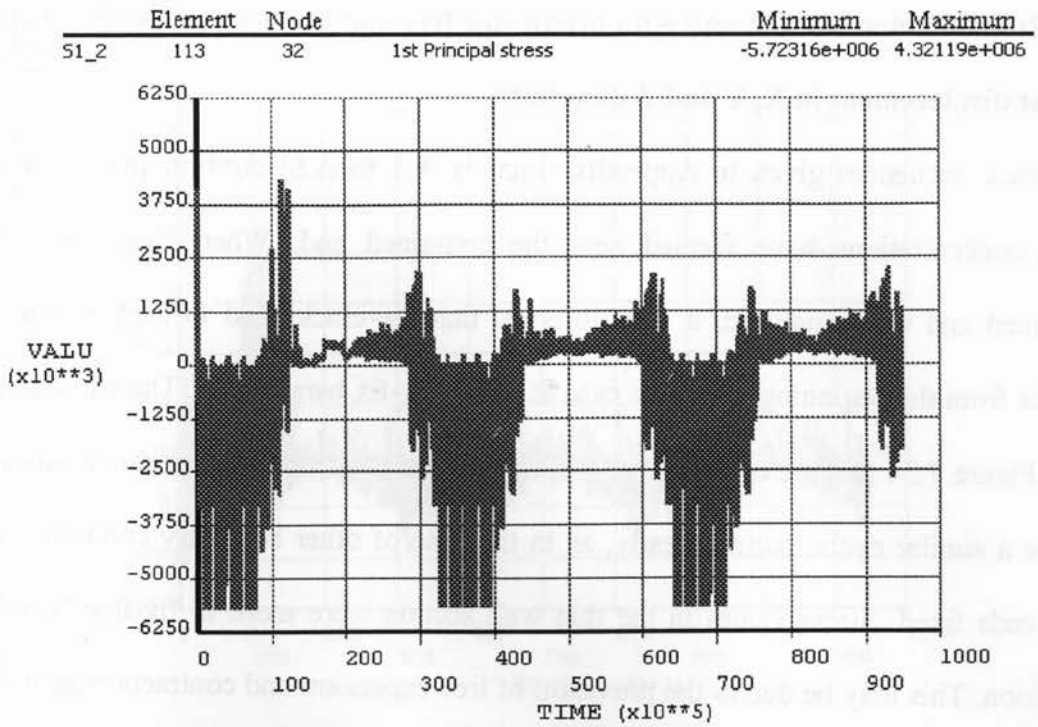

Figure 7.32: 1st Principal Stress for node 32 in element 113 @1 m from origin.

(1 m wall with fix-fix boundary condition)

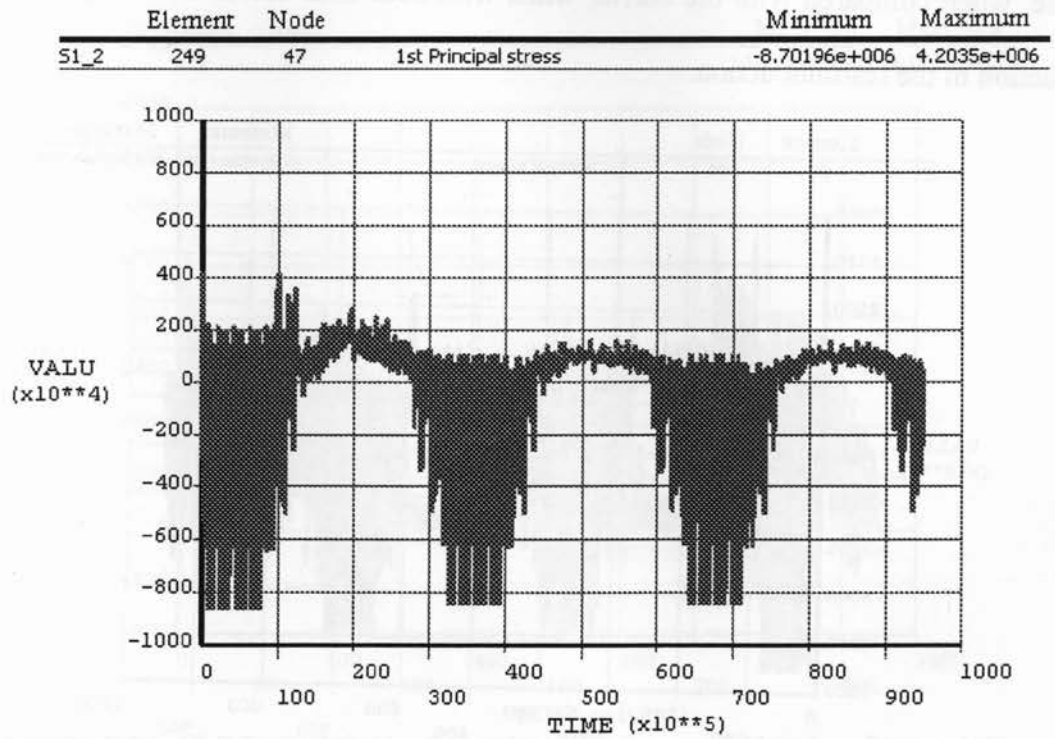

Figure 7.33: 1st Principal Stress for node 47 in element 249 @1 m from origin.

(1 m wall with fix-fix boundary condition)

Case 2: One meter barrier wall with origin end free and other end nodes restrained against displacement in X, Y and Z directions

The crack sequences given in Appendix (Figures A.1 to A.6) confirm that the major stress concentrations have formed near the restrained end. When elements of the restrained end were analyzed, it was observed that the cracks had formed within four months from the beginning, the same case as of 1m fix-fix barrier wall. The stress graphs from Figure 7.34 to Figure 7.39 prove that the compressive stress development does not follow a similar cyclic pattern yearly, as in the case of other boundary condition, with both ends fixed. Stress values in the thin wall section were more in fix-free boundary condition. This may be due to the provision of free expansion and contraction at one end of the wall. However, the stresses at the wider part of the wall were found to be of lesser value, when compared with the barrier walls with both ends fixed. This may be due to reduction in the restraint action.

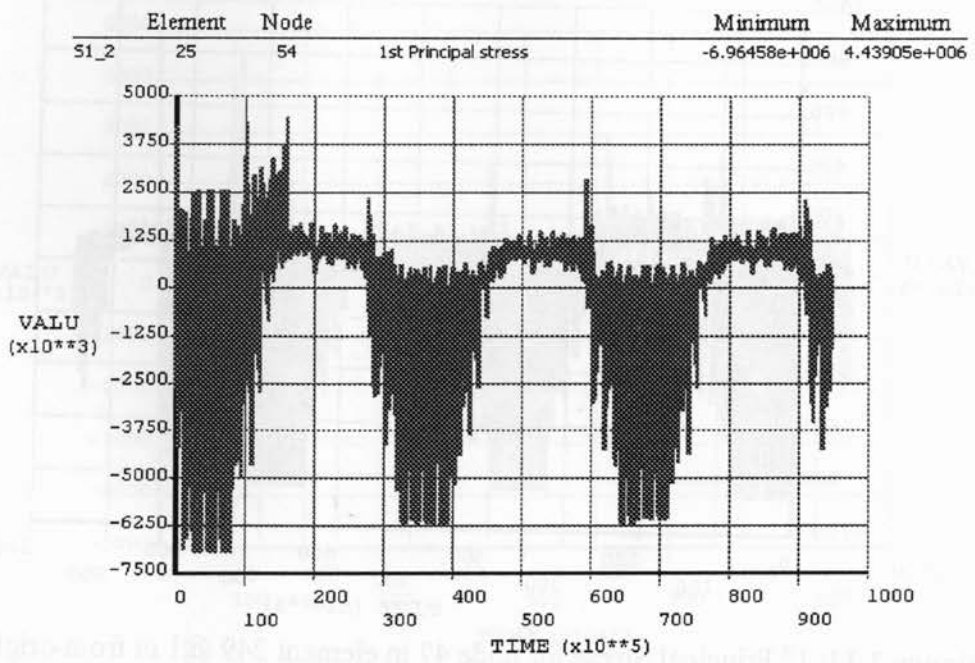

Figure 7.34: 1st Principal Stress for node 54 in element 25@ 1 m from origin (1 m wall with fix-free boundary condition)

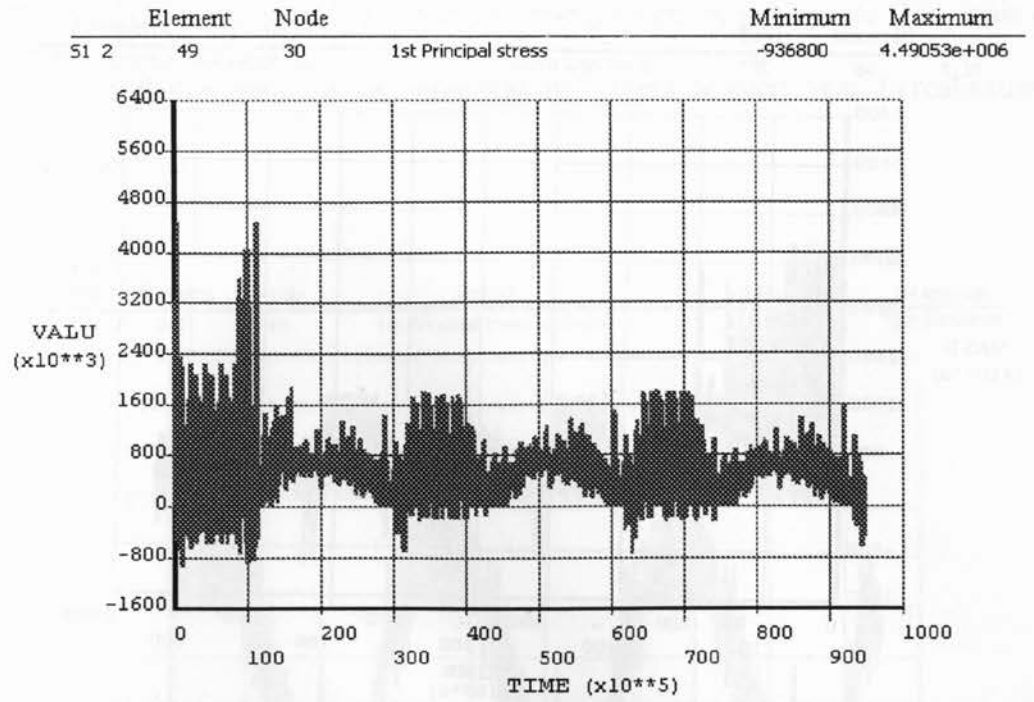

Figure 7.35: 1st Principal Stress for node 30 in element 49 @1 m from origin.

(1 m wall with fix-free boundary condition)

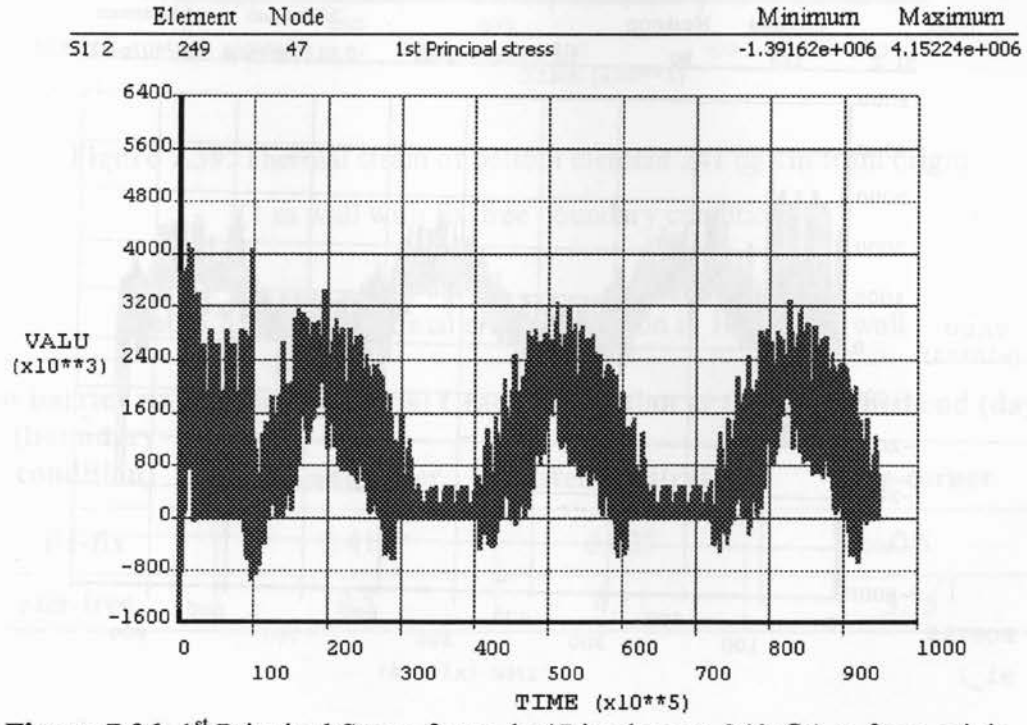

Figure 7.36: 1st Principal Stress for node 47 in element 249 @1 m from origin.

(1 m wall with fix-free boundary condition)

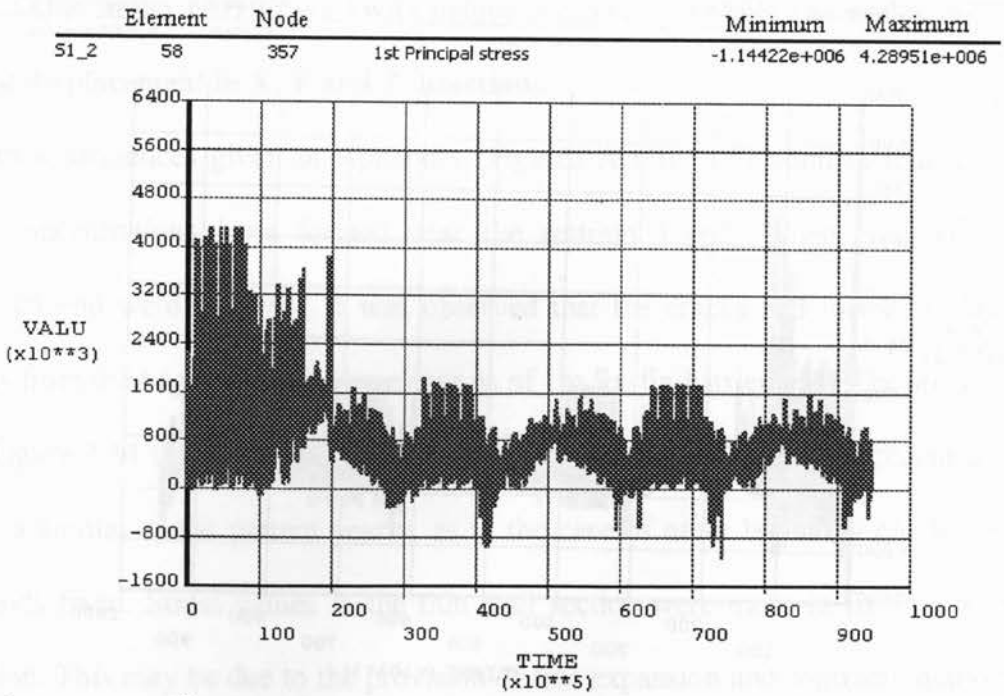

Figure 7.37: 1st Principal stress of the element 58 node 357@ 1 m from origin, (1 m wall with fix-free boundary condition)

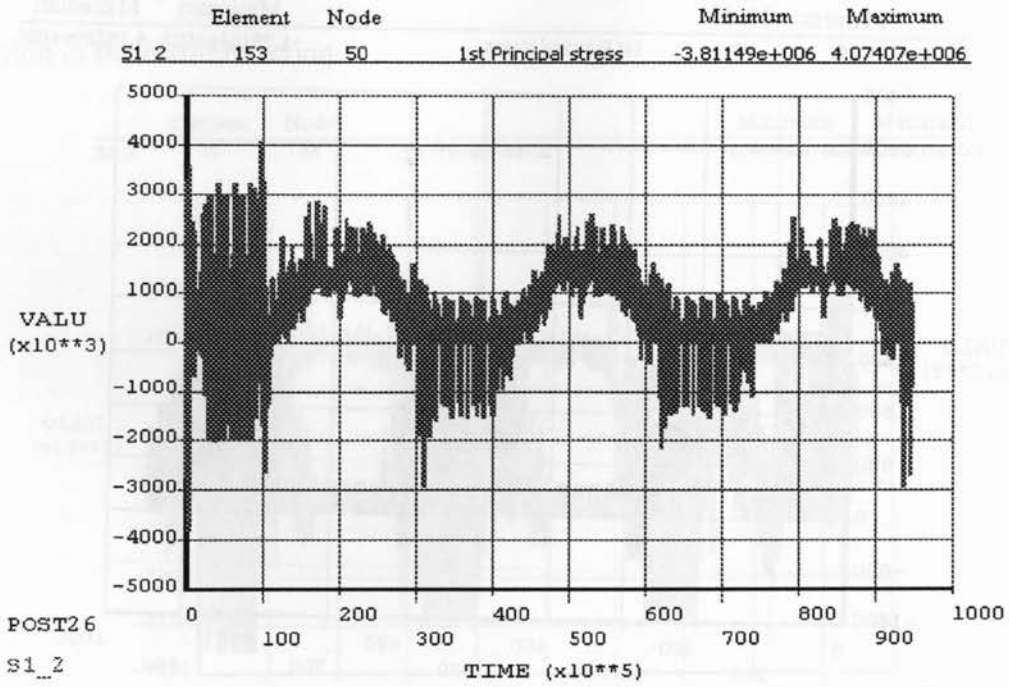

Figure 7.38 : 1st Principal stress on the junction element 153 node 50 @1 m from origin (1 m wall with fix-free boundary condition)

Figure 7.39 shows the thermal strain value of bottom element for 3 years. The strain data is repetitive, as the temperature data input was also repetitive every year. In real situation, the results vary.

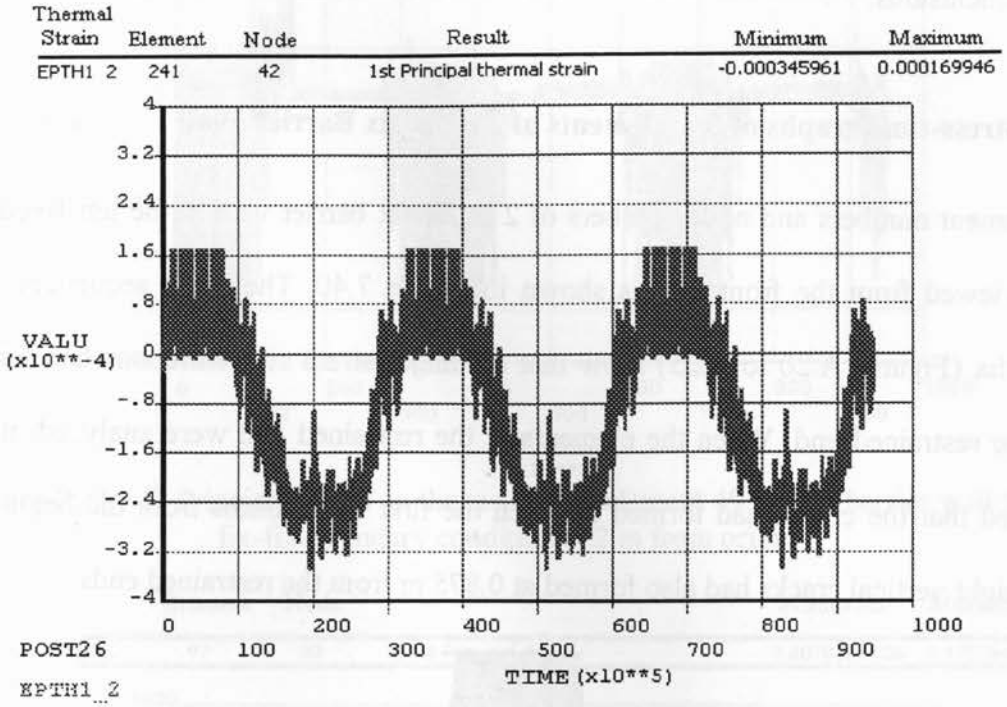

Figure 7.39: Thermal strain of bottom element 241 @ 1m from origin (1 m wall with fix-free boundary condition)

Table 7.5: Time of initial crack formation in 1m barrier wall

1m barrier wall (boundary condition)	Time of Initial Crack Formation at the restrained end (days)		
	Stem-corner	Stem-central	Base-corner
fix-fix	0.417	0.625	0.5
fix-free	0.5	4.17	3.75

The stress graphs from Figures 7.29 to 7.38 indicate that the stress developments drastically changes with restraint conditions. From Table 7.5, the cracks form quicker in

proportional to the restraint effect. However, the findings are not sufficient enough to come to a conclusion. The stress variation with respect to the barrier length also has to be studied. Hence stress analysis on barrier walls with various lengths was done for arriving at the conclusions.

7.5.2 Stress-time graphs of few elements of 2 m fix-fix Barrier Wall

The element numbers and node numbers of 2 m fix-fix barrier wall at the left fixed end when viewed from the front face is shown in Figure 7.40. The crack sequences from Appendix (Figures A.20 to A.25) show that the major stress concentrations had formed near the restrained end. When the elements at the restrained end were analyzed, it was observed that the cracks had formed between the first five months from the beginning. Full height vertical cracks had also formed at 0.875 m from the restrained ends.

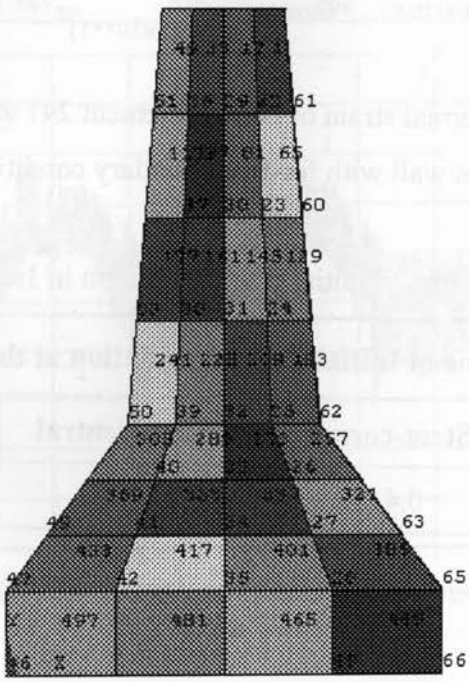

Figure 7.40: Element and node numbers of 2 m barrier wall with fix-fix boundary condition @2 m from origin

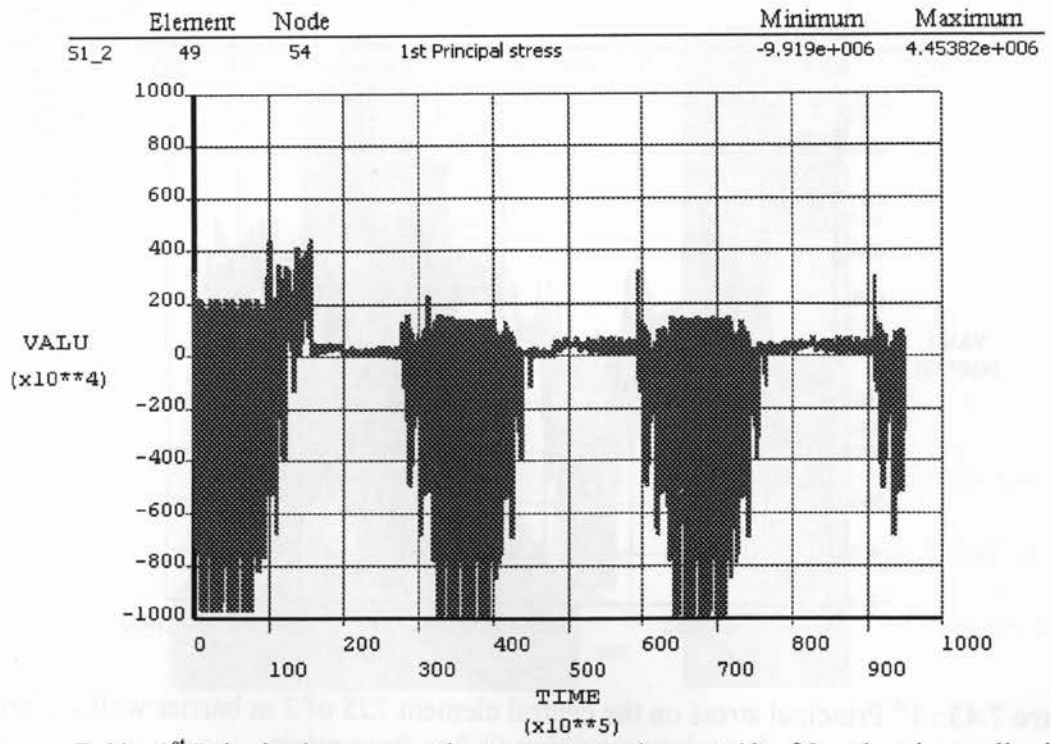

Figure 7.41 : 1st Principal stress on the top corner element 49 of 2 m barrier wall with fix-fix boundary condition @2 m from origin

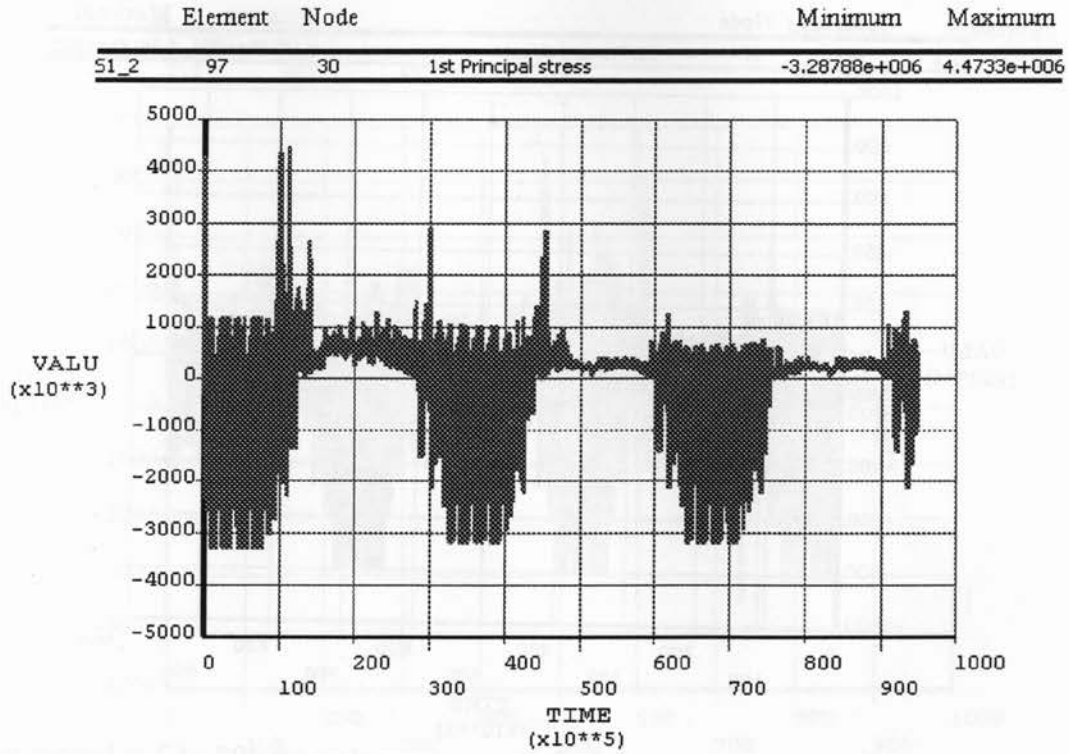

Figure 7.42 : 1st Principal stress on the top central element 97 of 2 m barrier wall with fix-fix boundary condition @2 m from origin

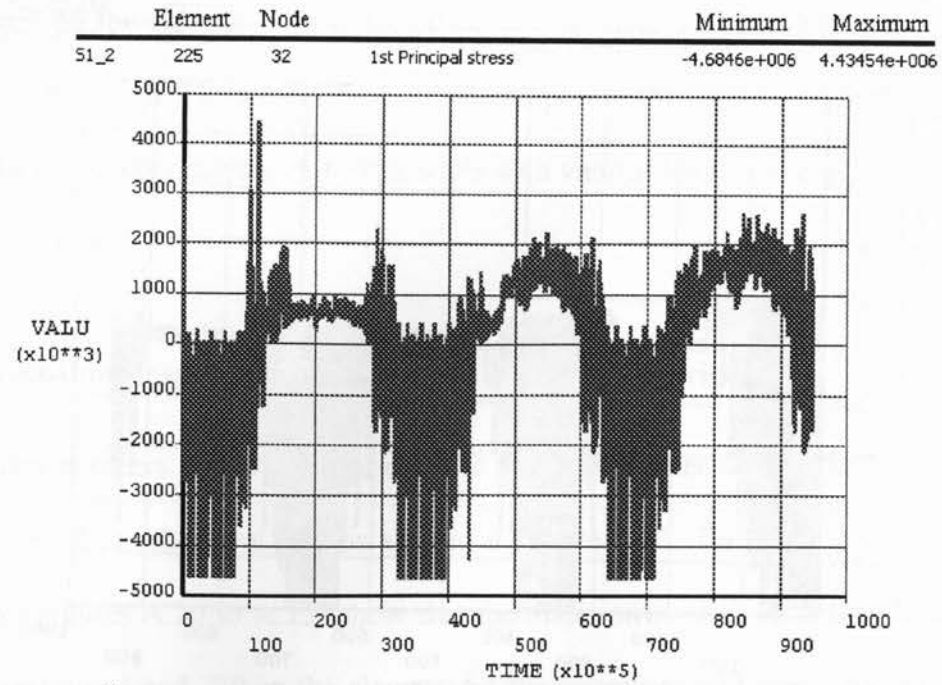

Figure 7.43 : 1st Principal stress on the central element 225 of 2 m barrier wall with fix-fix boundary condition @ 2 m from origin

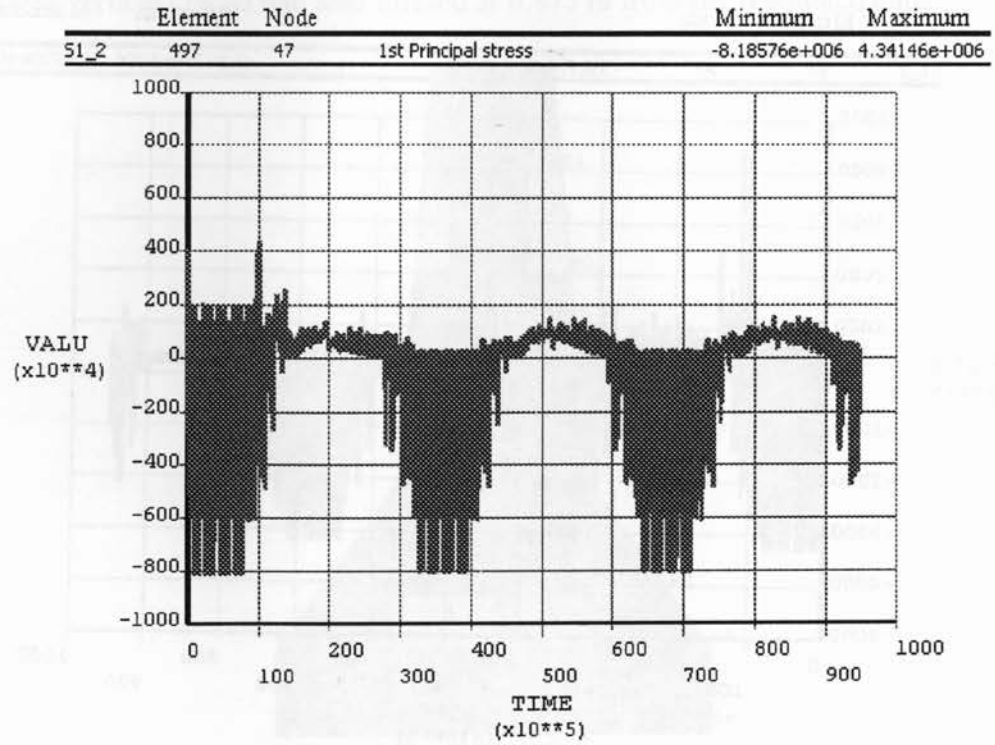

Figure 7.44 : 1st Principal stress on the bottom corner element 497 of 2 m barrier wall with fix-fix boundary condition @2 m from origin

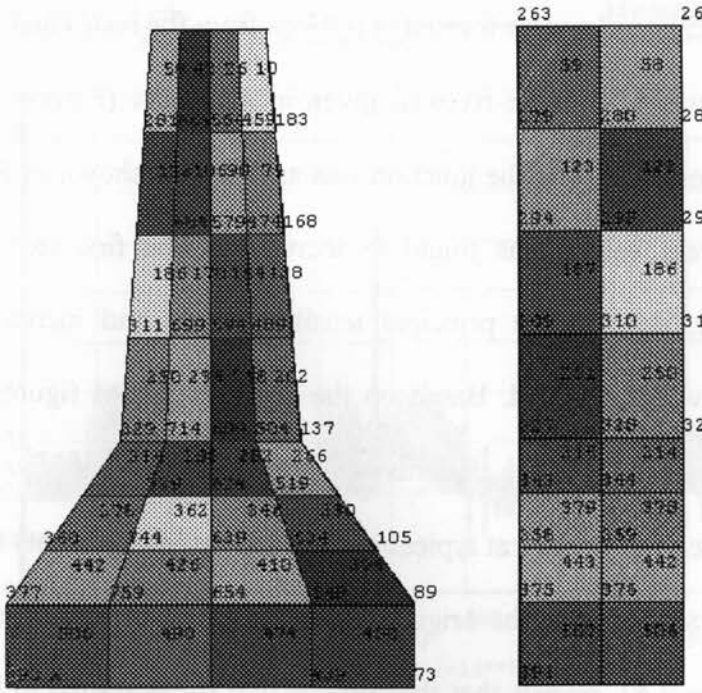

Figure 7.45: Element and node numbers of 2 m barrier wall with fix-fix boundary condition @0.875 m from origin

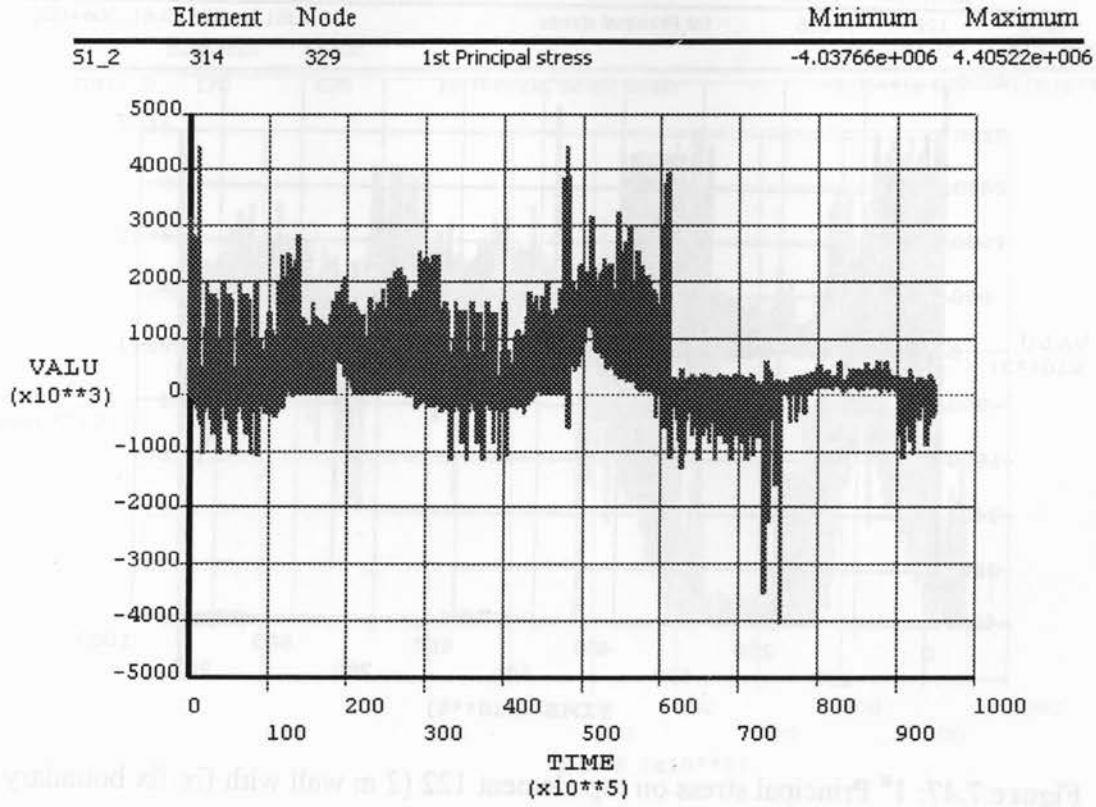

Figure 7.46: 1st Principal stress on the junction element 314 of 2 m barrier wall with fix-fix boundary condition @0.875 m from origin

The full length vertical cracks were formed at 0.875m from the restrained ends as per the crack evolution figures of 2 m fix-fix wall given in Appendix (Figures A.20 to A25). When the surface element 314 at the junction was analyzed as shown in Figure 7.46, the principal tensile stress values was found to increase in the first two year duration. However, thereafter, drop in the principal tensile stresses and increase in principal compressive stress were observed. Based on the crack evolution figures in Appendix, there were no changes in the crack patterns at the junction element after almost 2 years duration. Let us check the stresses at typical surface and middle elements found in the top middle region at 0.875 m from the origin. The stress graph of the top surface element 122, given in Figure 7.47, reveals that the compressive stress started to build up after 2 years time.

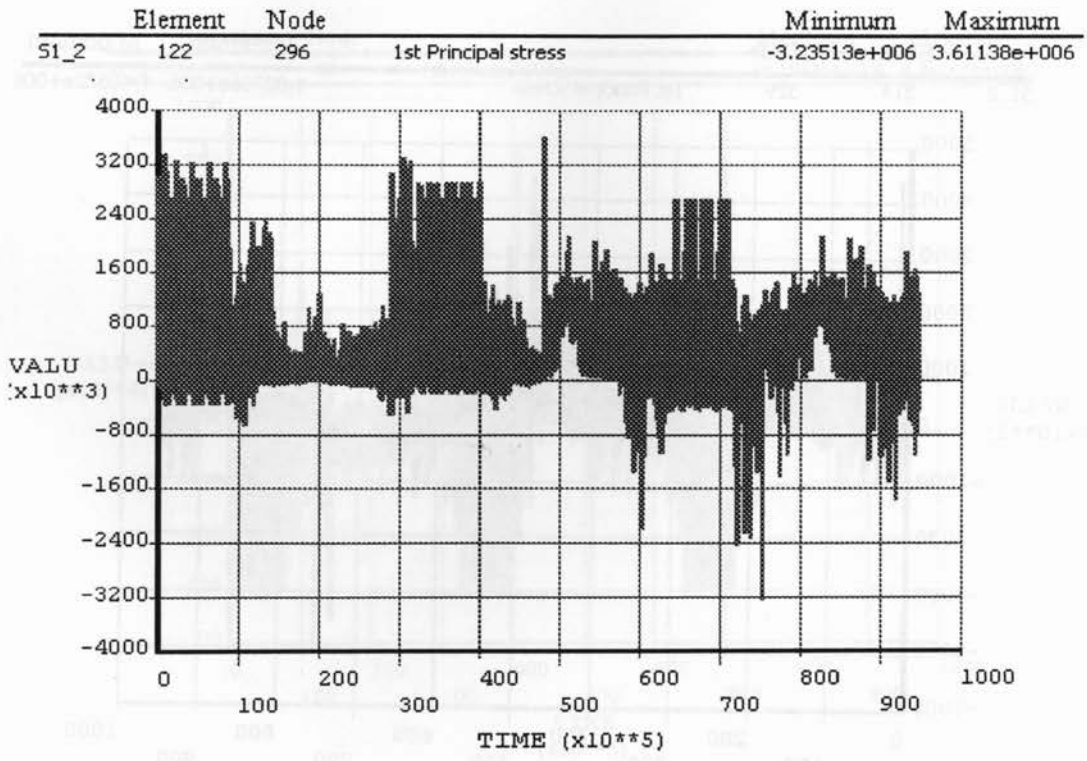

Figure 7.47: 1st Principal stress on top element 122 (2 m wall with fix-fix boundary condition) @0.875 m from origin

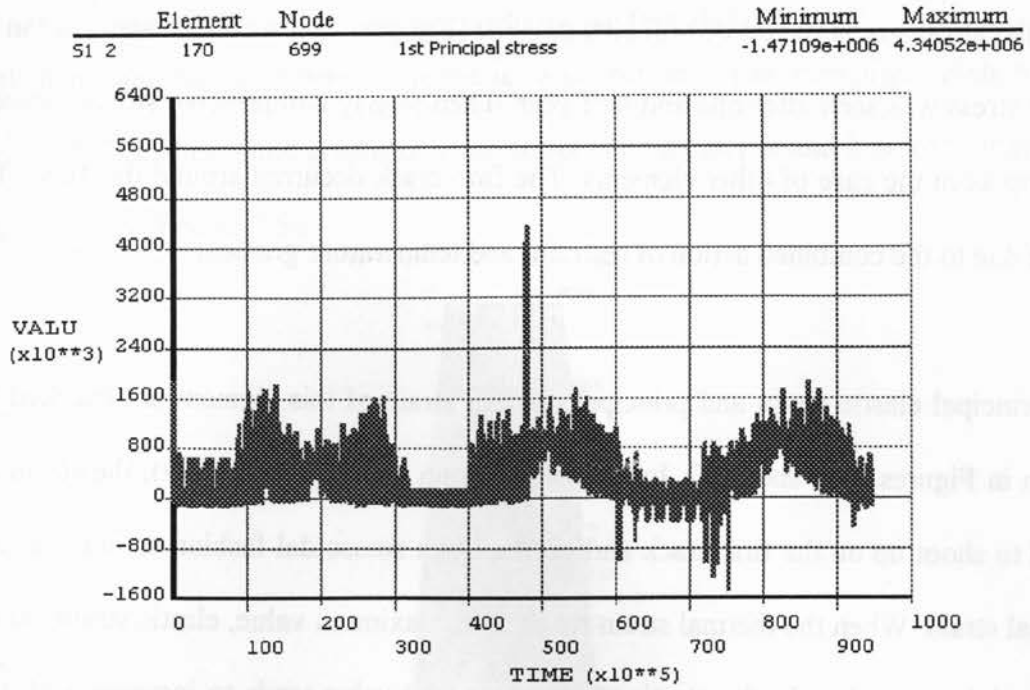

Figure 7.48: 1st Principal stress on top central element 170 (2 m barrier wall with fix-fix boundary condition) @0.875 m from origin

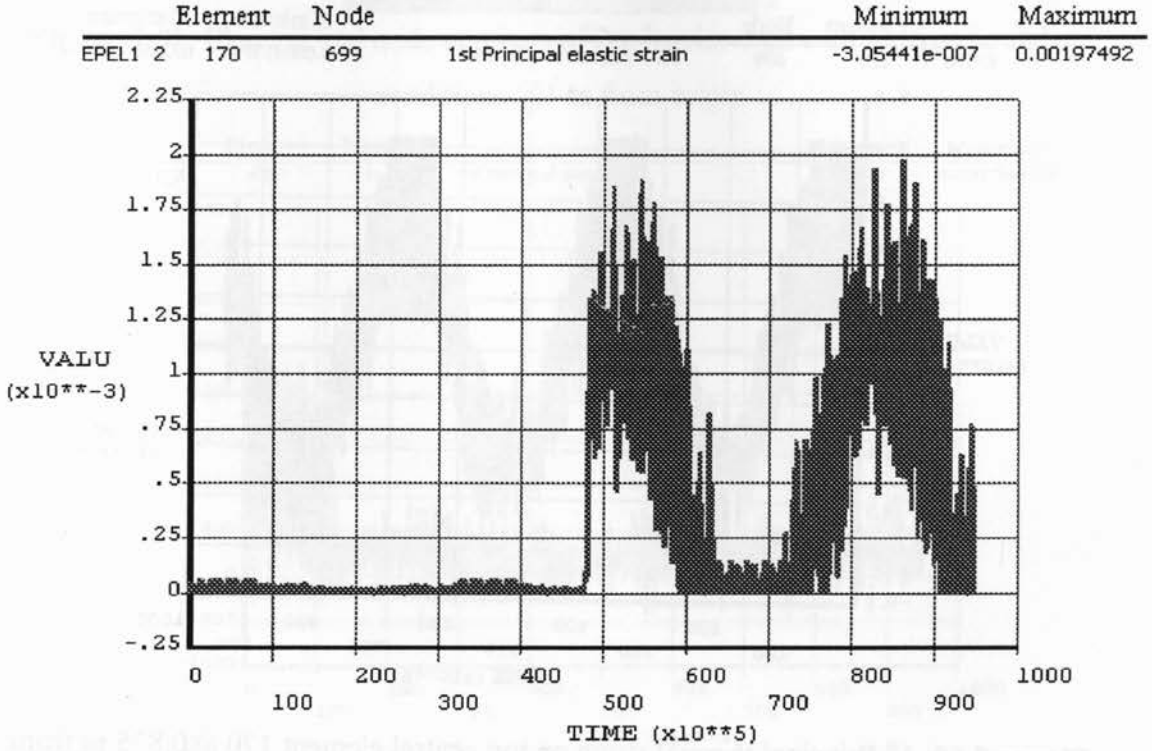

Figure 7.49: 1st Principal elastic strain on top central element 170 @0.875 m from origin

From the stress graph of top central element 170 (Figure 7.48), a sudden shoot up in the tensile stress was seen after one and half year. Then slowly compressive stress started to build up as in the case of other elements. The first crack occurred around this time. This can be due to the combined action of restraint and temperature gradient.

The principal elastic strain and principal thermal strain of this element are checked and shown in Figures 7.49 and 7.50. In the elastic strain graph (Figure 7.49), the strain was found to shoot up on the first crack and proceed in a sinusoidal fashion as in the case of thermal strain. When the thermal strain reached its maximum value, elastic strain reduced to its minimum value. In the elastic strain graph, the value tends to increase with time, maintaining its inverse relationship with thermal strain value.

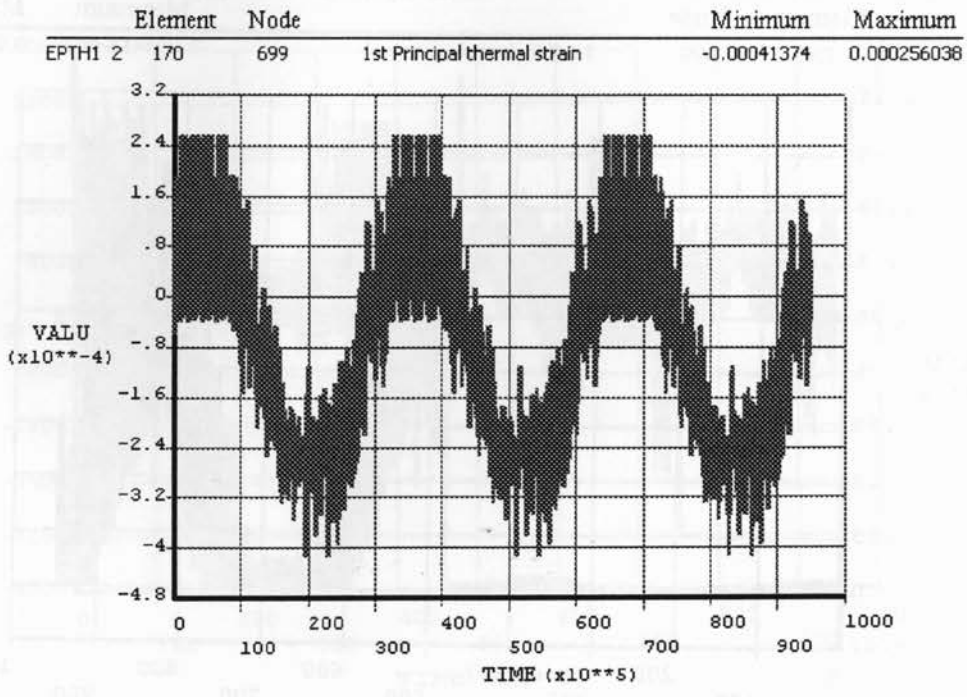

Figure 7.50: 1st Principal thermal strain on top central element 170 @0.875 m from origin

7.5.3 Stress-time graphs of few elements of 2 m fix-free Barrier Wall

The elements and node numbers of the barrier wall section at 1 m from origin is shown in Figure 7.51. The stress-time graphs of some selected nodes at 1 m and 2 m from origin is given in Figures 7.52 to 7.56.

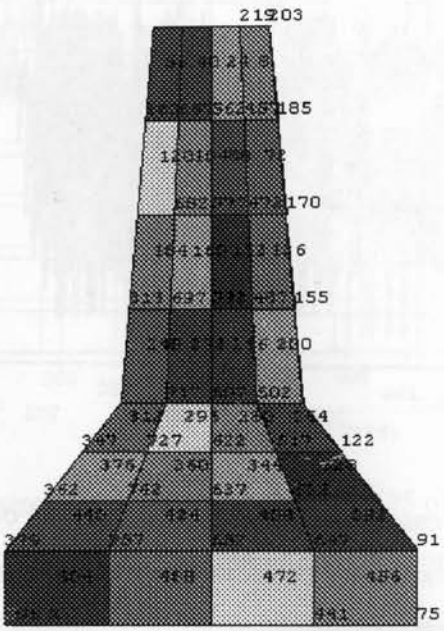

Figure 7.51: Element and node numbers of 2m barrier wall with fix-free boundary conditions @1 m from origin

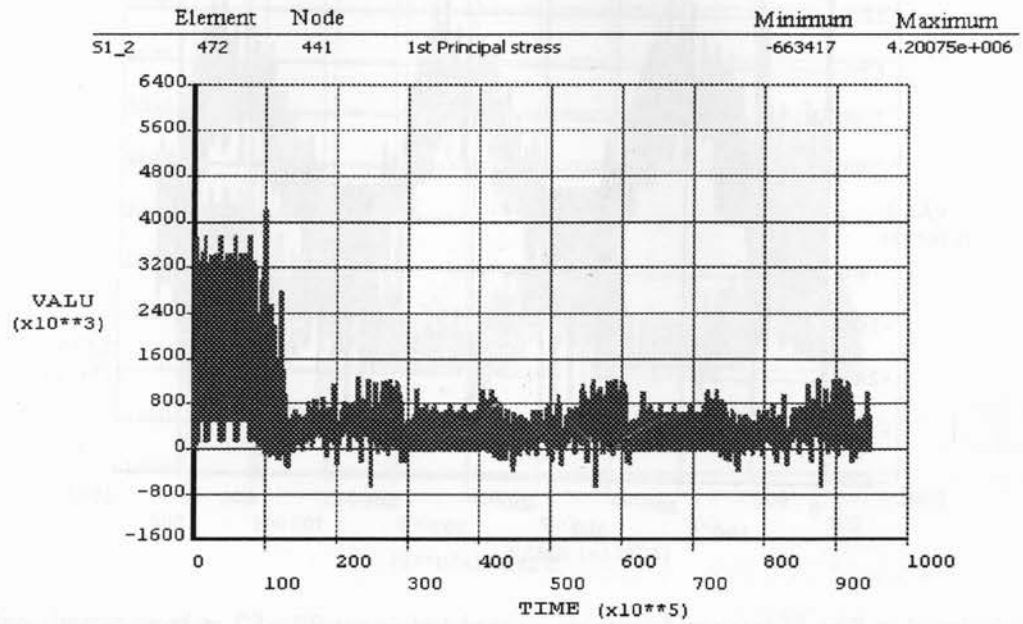

Figure 7.52: 1st Principal stress on the bottom element 472 of 2 m barrier wall with fix-free boundary condition @1 m from origin

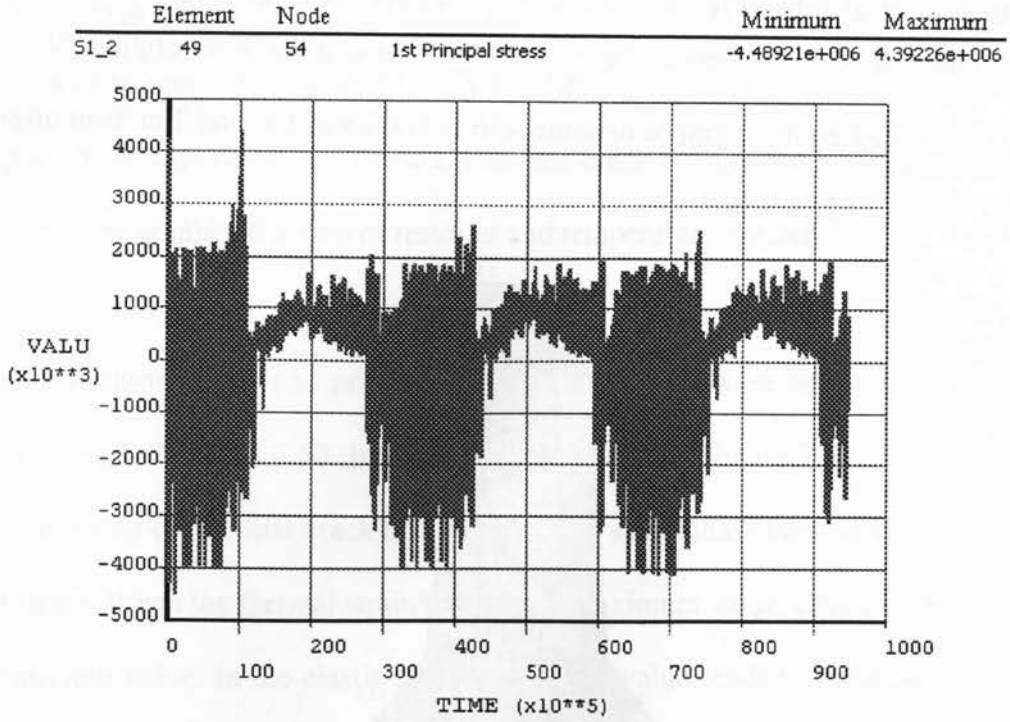

Figure 7.53: 1st Principal stress on the top corner element 49 of 2 m barrier wall with fix-free boundary condition@2 m from origin

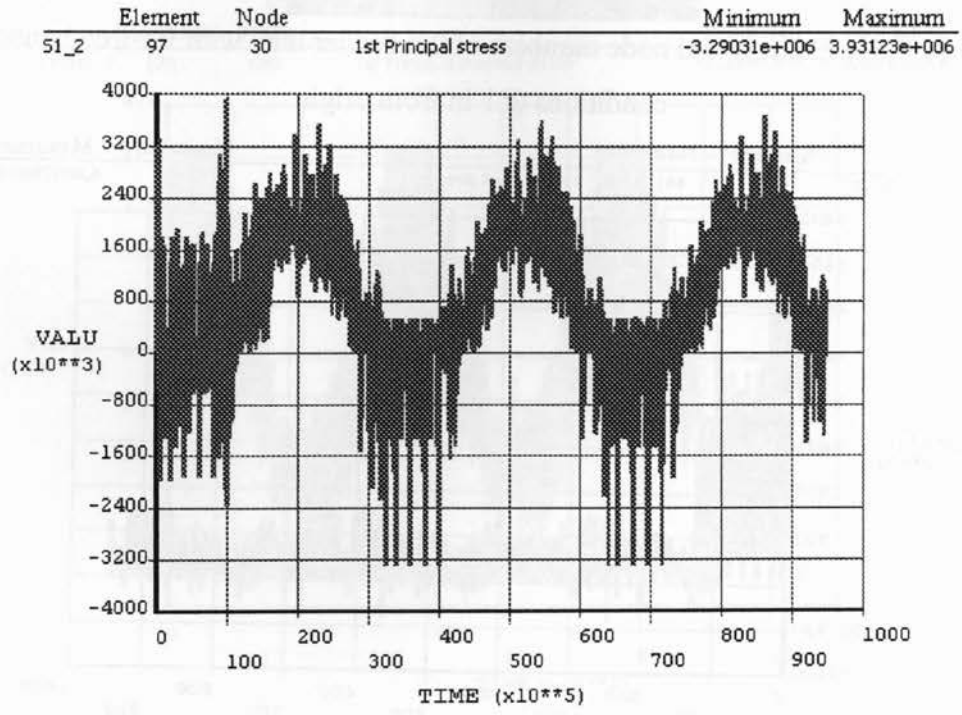

Figure 7.54: 1st Principal stress on the top central element 97 of 2 m barrier wall with fix-free boundary condition @2 m from origin

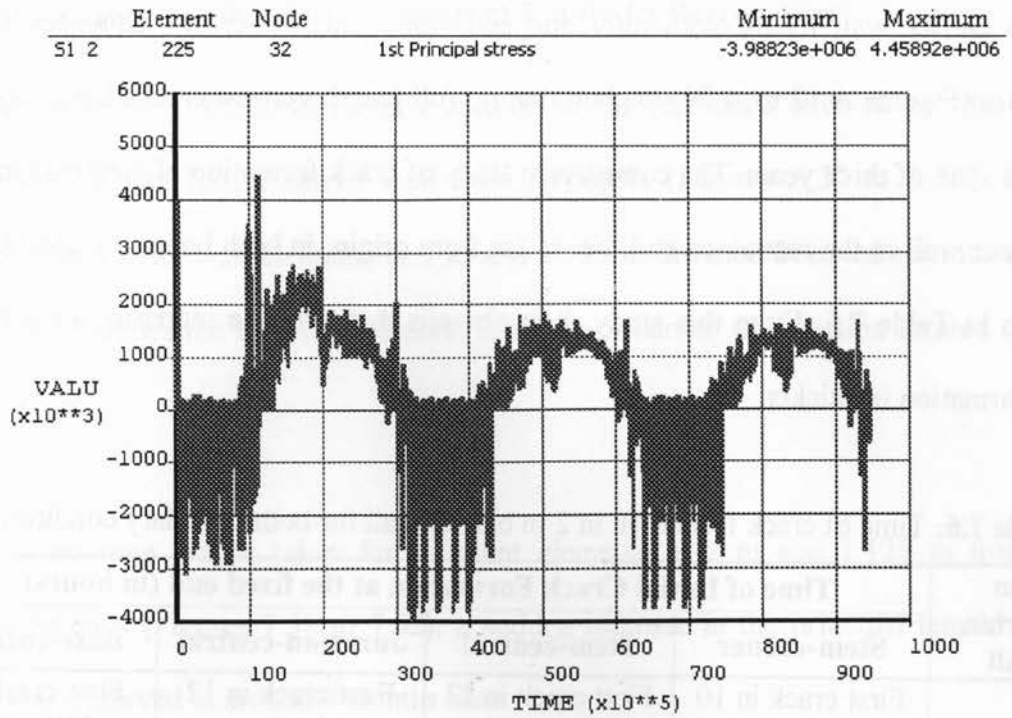

Figure 7.55: 1st Principal stress on the central element 225 of 2 m barrier wall with fix-free boundary condition @2 m from origin

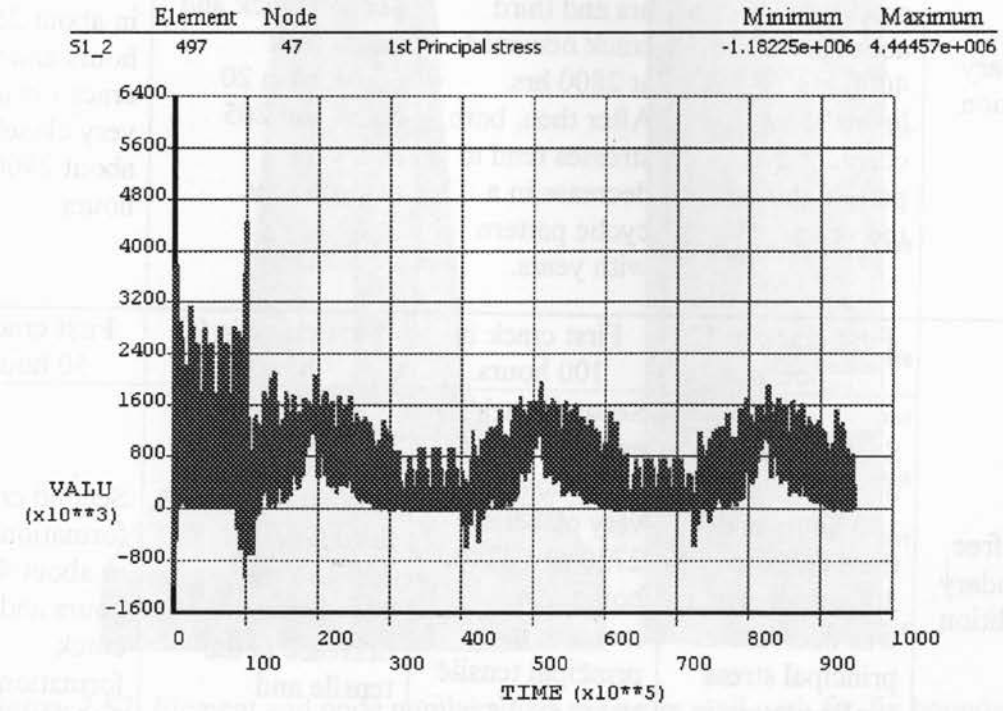

Figure 7.56: 1st Principal stress on the bottom corner element 497 of 2 m barrier wall with fix-free boundary condition @2 m from origin

For 2m barrier wall length with only one end restrained, the crack sequences from Appendix (Figures A.12 to A.20) explain that no full length vertical cracks have formed within a span of three years. The comparison study of crack formation of elements in the 2m barrier wall at the restrained end, i.e. at 2m from origin, in both boundary conditions is given in Table 7.6. From this study, it is obvious that with the increase in restraint, crack formation is quicker.

Table 7.6: Time of crack formation in 2 m barrier wall for both boundary conditions.

2 m barrier wall	**Time of Initial Crack Formation at the fixed end (in hours)**			
	Stem-corner	**Stem-central**	**Junction-central**	**Base-corner**
fix-fix boundary condition	First crack in 10 hours	First crack in 12 hours	First crack in 12 hours	First crack in 14 hours
	Second and third crack occurred in about 2800 and 4000 hrs. Stress levels showed constant cyclic pattern during the years.	Second crack occurred at 14 hrs and third crack occurred at 2800 hrs. After then, both stresses tend to decrease in a cyclic pattern with years.	Second crack and third crack occurred in 20 hours and 205 hours respectively.	Second crack in about 2500 hours and third crack occurred very closely in about 2900 hours.
fix-free boundary condition	First crack in 12 hours	First crack in 100 hours.	First crack in 90 hours	First crack in 50 hours.
	Second crack occurred in about 100 hours and third crack in 300 hours. There was decrease in principal stress cyclic pattern in the following years.	Second crack and third crack formation was very closely in 2720 and 2740 hours. An increase in principal tensile stress cyclic pattern was observed in the following years.	Second crack occurred in about 2900 hours and third crack in 3200 hours. Thereafter, decrease in the tensile and compressive stress cyclic pattern in years.	Second crack formation was in about 400 hours and third crack formation in 2850 hours.

7.5.4 Stress-time graphs of few elements of 3 m fix-fix Barrier Wall

The major stress concentrations have formed in the restrained ends as per the crack sequences of 3 m fix-fix barrier wall from Appendix (Figures A.32 to A.37). Let us analyze few barrier wall elements at 1 m and 1.125 m distance from the restrained end. Figure 7.57 shows the element and node numbers of barrier wall section located at 1 m from origin.

From stress-time graphs taken for different elements at 1 m and 1.125 m from the restrained ends (Figures 7.58 to 7.62), a sudden increase in the principal tensile stress value was observed in around 9 months time.

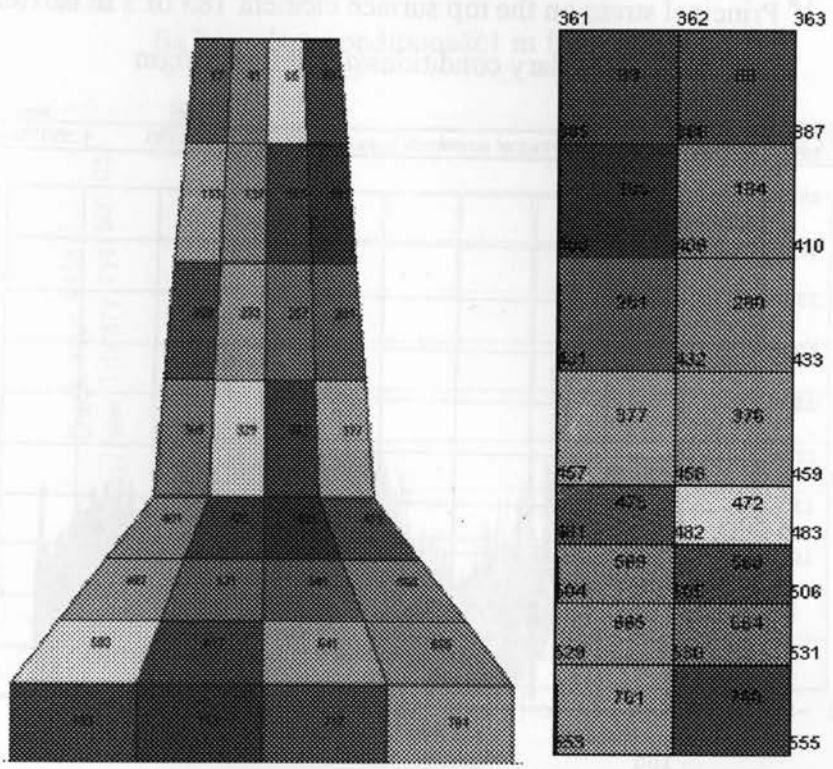

Figure 7.57: Element and node numbers of 3 m barrier wall with fix-fix boundary conditions @1 m from origin

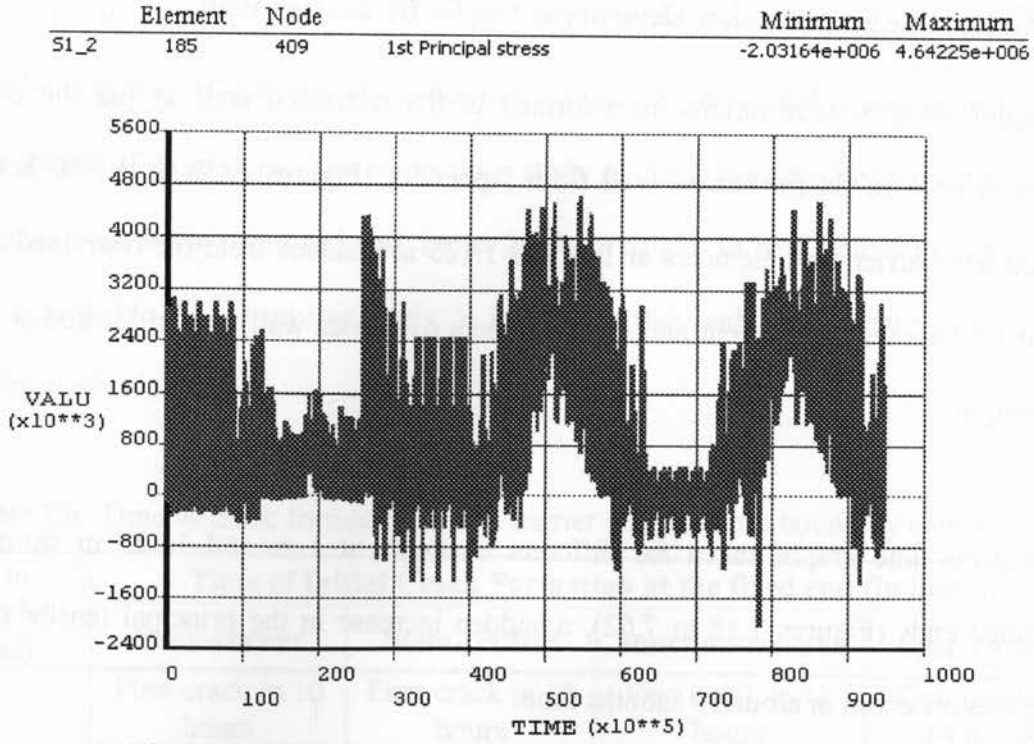

Figure 7.58: 1st Principal stress on the top surface element 185 of 3 m barrier wall with fix-fix boundary conditions@1 m from origin

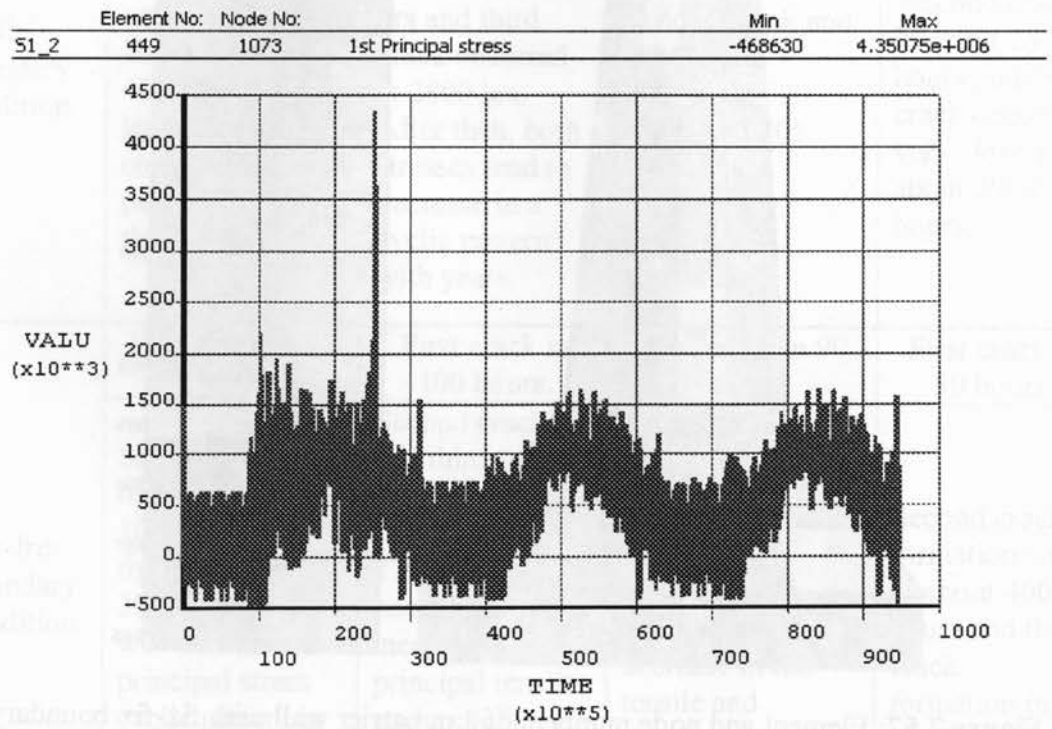

Figure 7.59: 1st Principal stress on the inner junction element 449 of 3 m barrier wall with fix-fix boundary conditions@1 m from origin

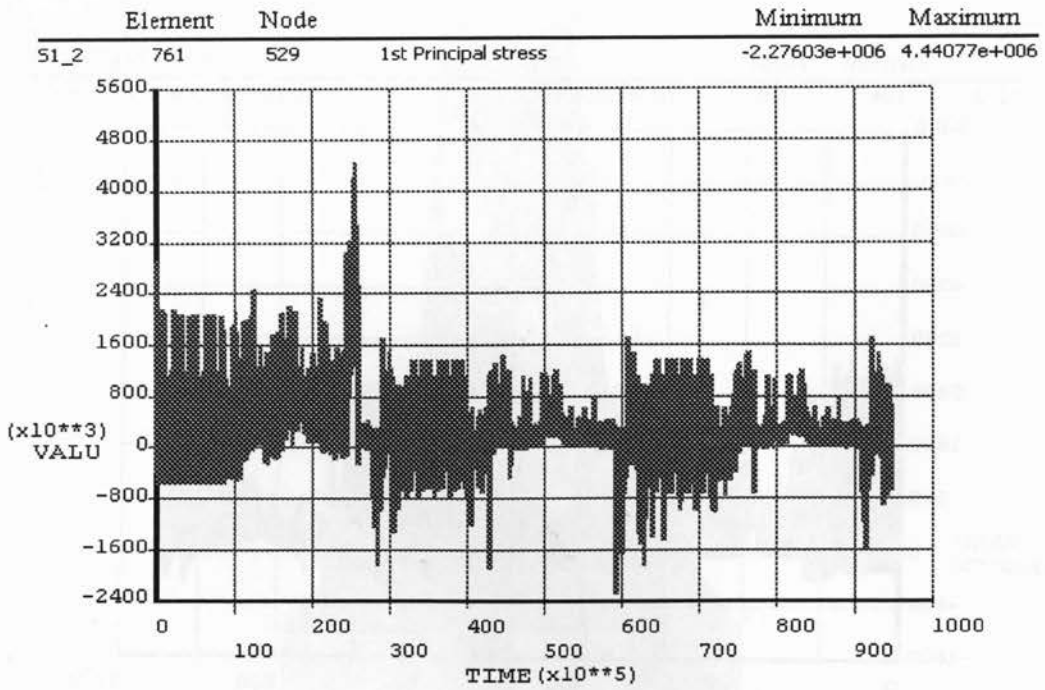

Figure 7.60: 1st Principal stress on the bottom element 761 of 3 m barrier wall with fix-fix boundary conditions@1 m from origin

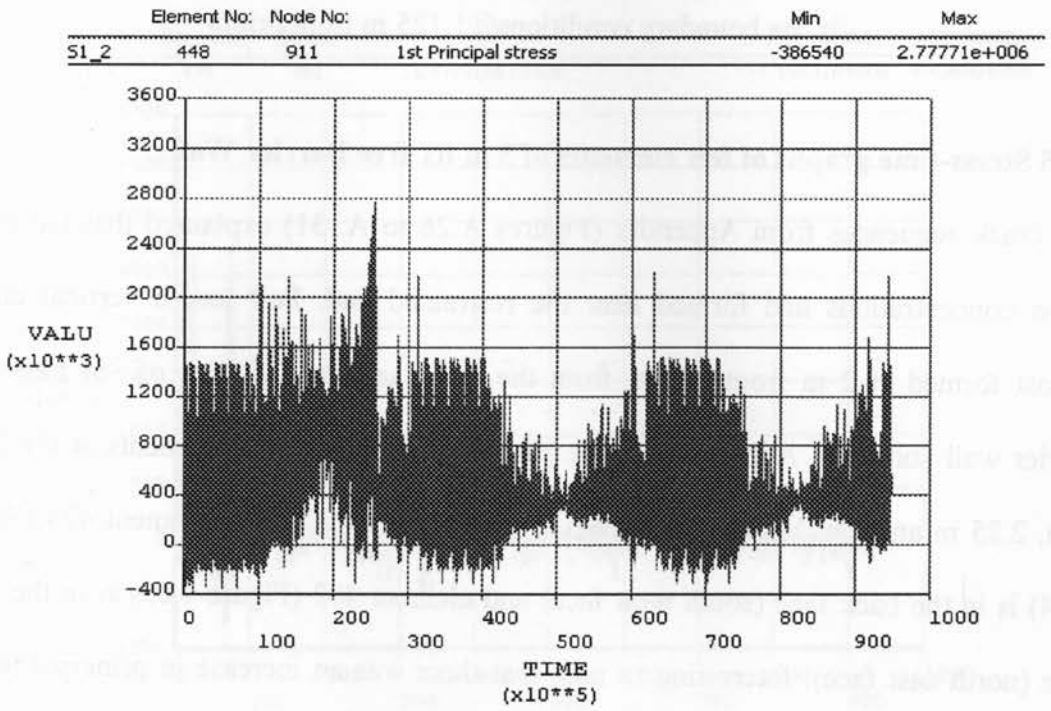

Figure 7.61: 1st Principal stress on the inner junction element 448 of 3 m barrier wall with fix-fix boundary conditions@1.125 m from origin

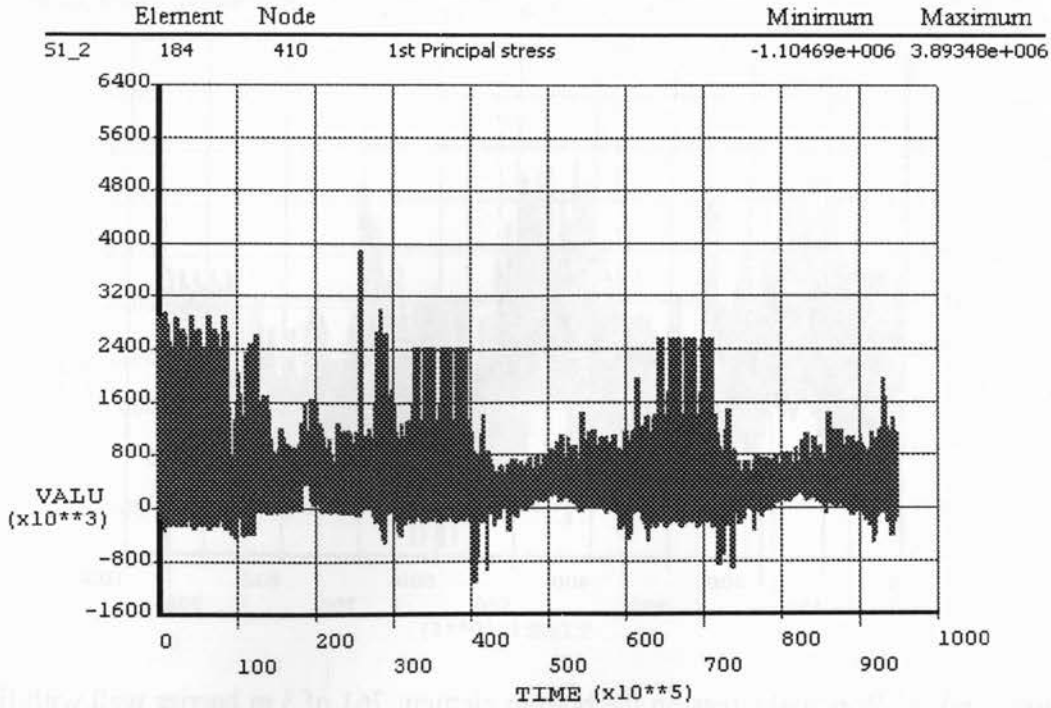

Figure 7.62: 1st Principal stress on the top surface element 184 of 3 m barrier wall with fix-fix boundary conditions@1.125 m from origin

7.5.5 Stress-time graphs of few elements of 3 m fix-free Barrier Wall

The crack sequences from Appendix (Figures A.26 to A. 31) explained that the major stress concentrations had formed near the restrained end. Full length vertical cracks almost formed at 2 m from origin, from the crack sequence figures of 3m free-fixed barrier wall shown in Appendix. Let us analyze few barrier wall elements at 0.875 m, 2 m, 2.25 m and 2.625 m distance from the free end. At 0.875 m, element 474 (Figure 7.64) is in the back face (south west face) and element 402 (Figure 7.65) is in the front face (north east face). Interesting to note that there was an increase in principal tensile stress development in the front face (north east face) and decreasing principal tensile stress developments in the back face (south west face).

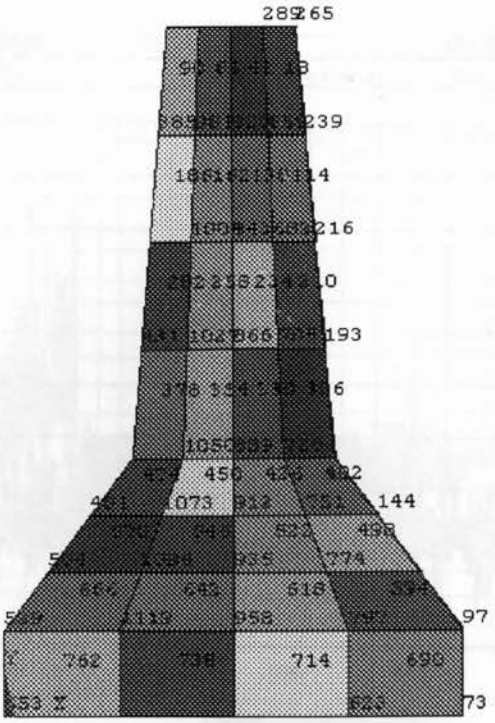

Figure 7.63: Element numbers of 3 m barrier wall with fix-free boundary conditions@0.875 m from origin

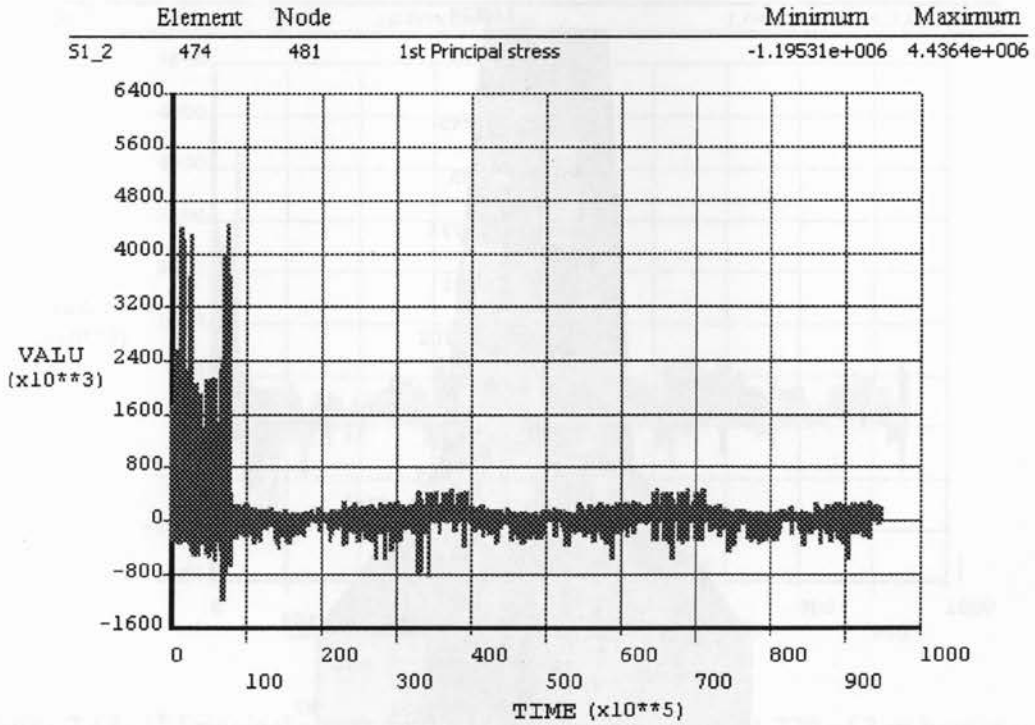

Figure 7.64: 1st Principal stress on surface junction element 474 of 3 m barrier wall with fix-free boundary conditions@0.875 m from origin

	Element	Node		Minimum	Maximum
S1_2	402	144	1st Principal stress	-985549	4.38652e+006

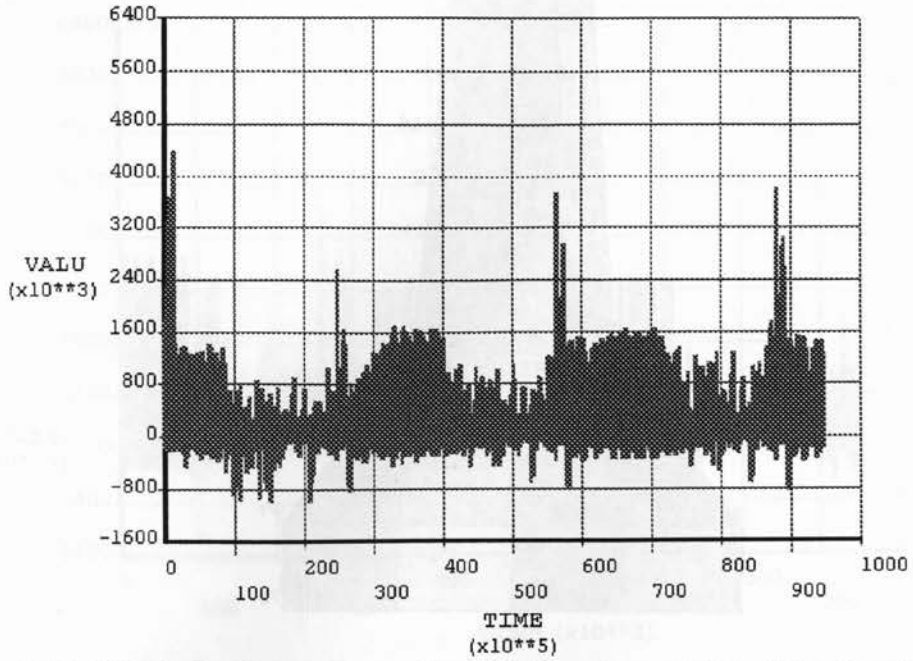

Figure 7.65: 1st Principal stress on surface junction element 402 of 3 m barrier wall with fix-free boundary conditions@0.875 m from origin

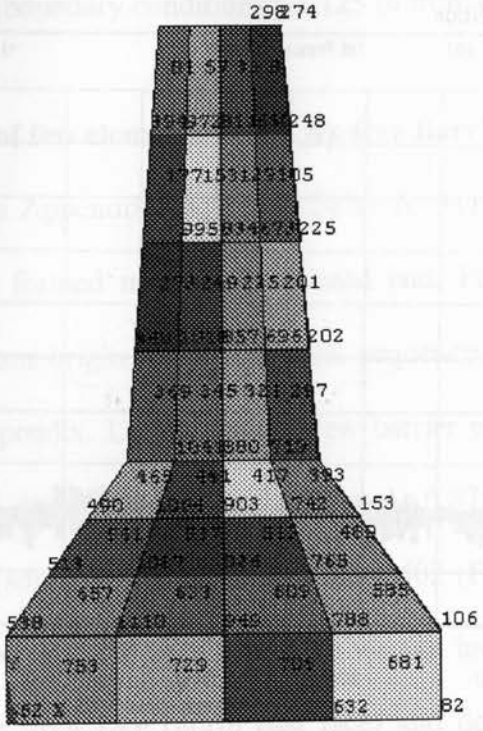

Figure 7.66: Element and node numbers of 3 m barrier wall with fix-free boundary conditions @2 m from origin

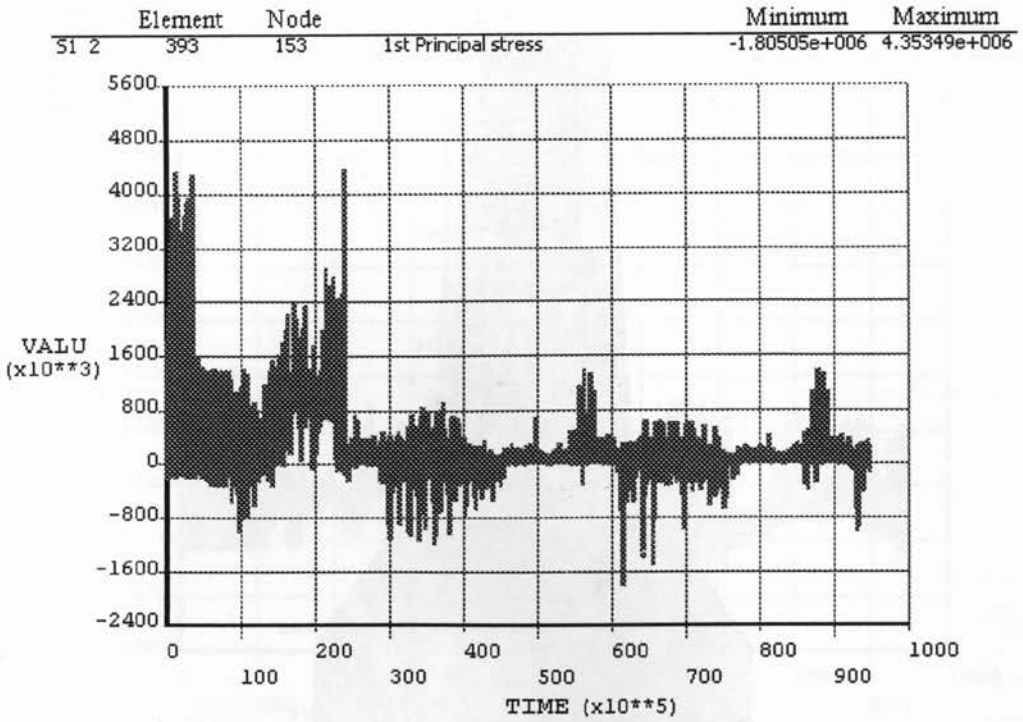

Figure 7.67: 1st Principal stress on the surface junction element 393 of 3 m barrier wall with fix-free boundary conditions@2 m from origin

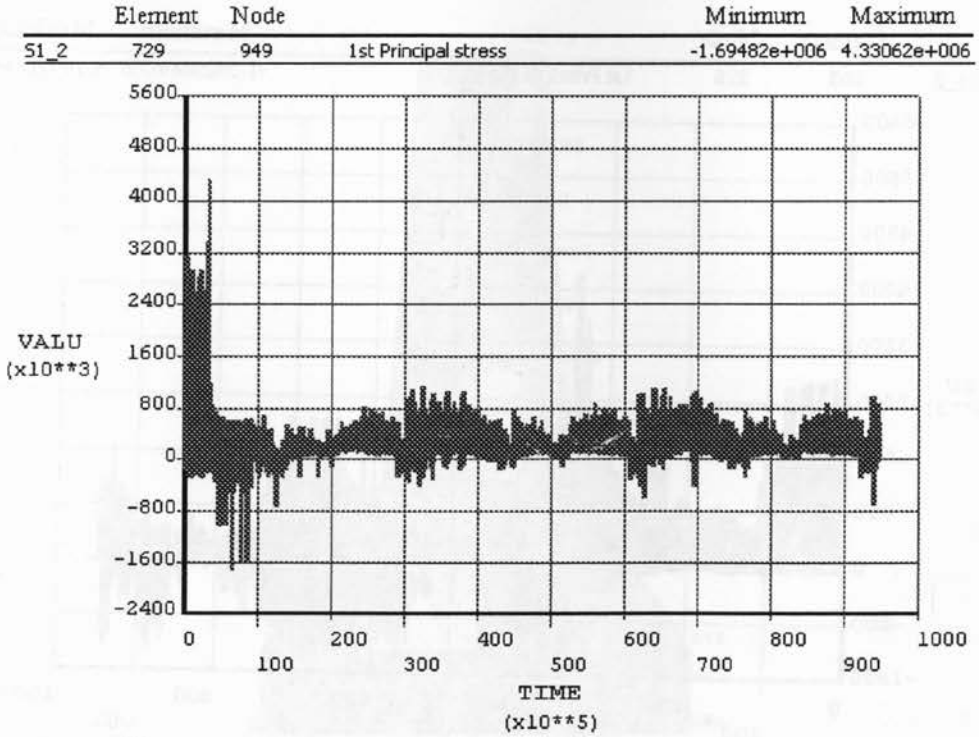

Figure 7.68: 1st Principal stress on the bottom middle element 729 of 3 m barrier wall with fix-free boundary conditions@2 m from origin

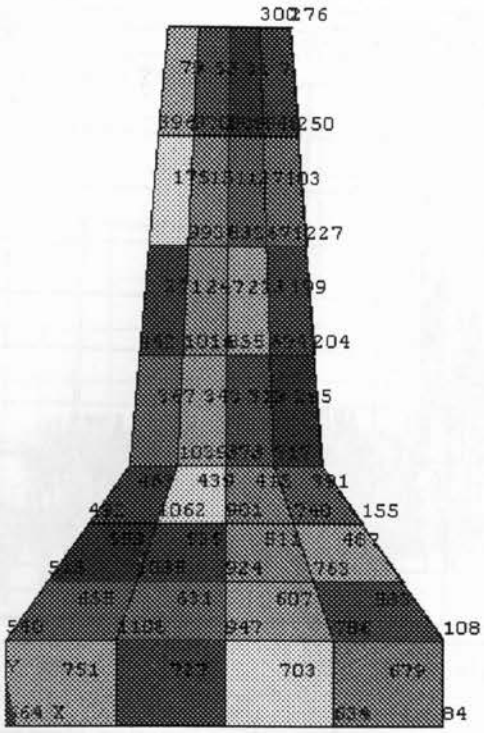

Figure 7.69: Element & node numbers of 3 m barrier wall with fix-free boundary conditions @2.25 m from origin

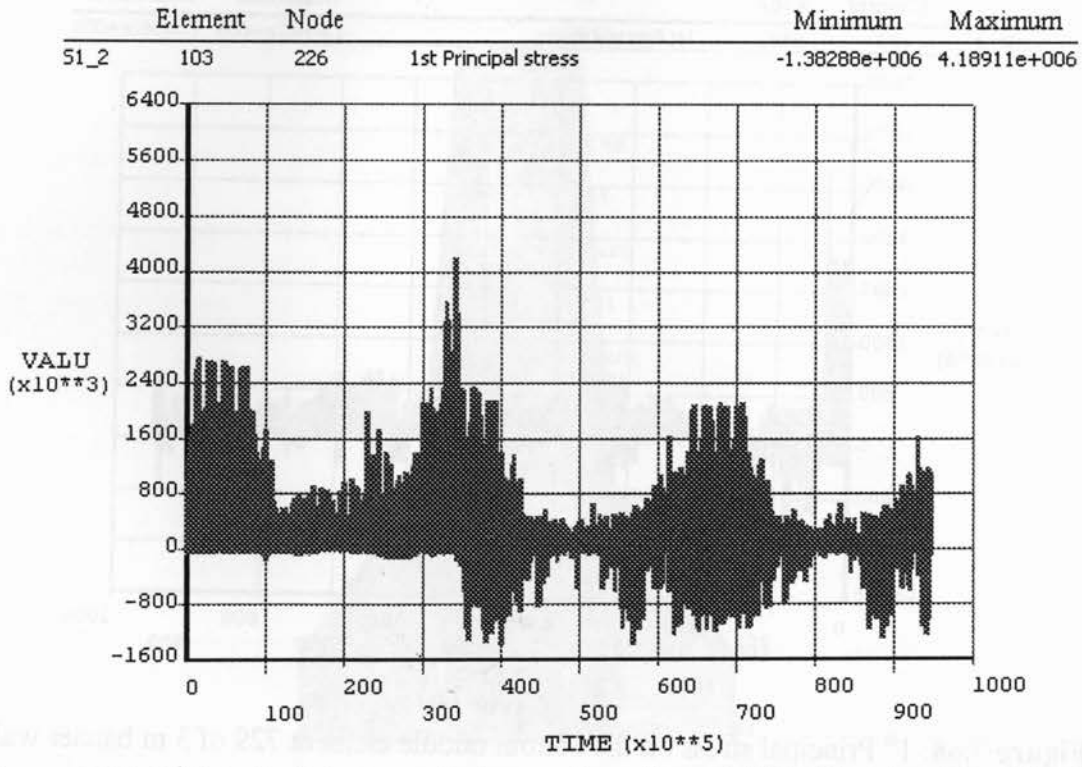

Figure 7.70: 1st Principal stress on the top surface element 103 of 3 m barrier wall with fix-free boundary conditions@2.25 m from origin

	Element	Node		Minimum	Maximum
S1_2	271	993	1st Principal stress	-657603	3.89329e+006

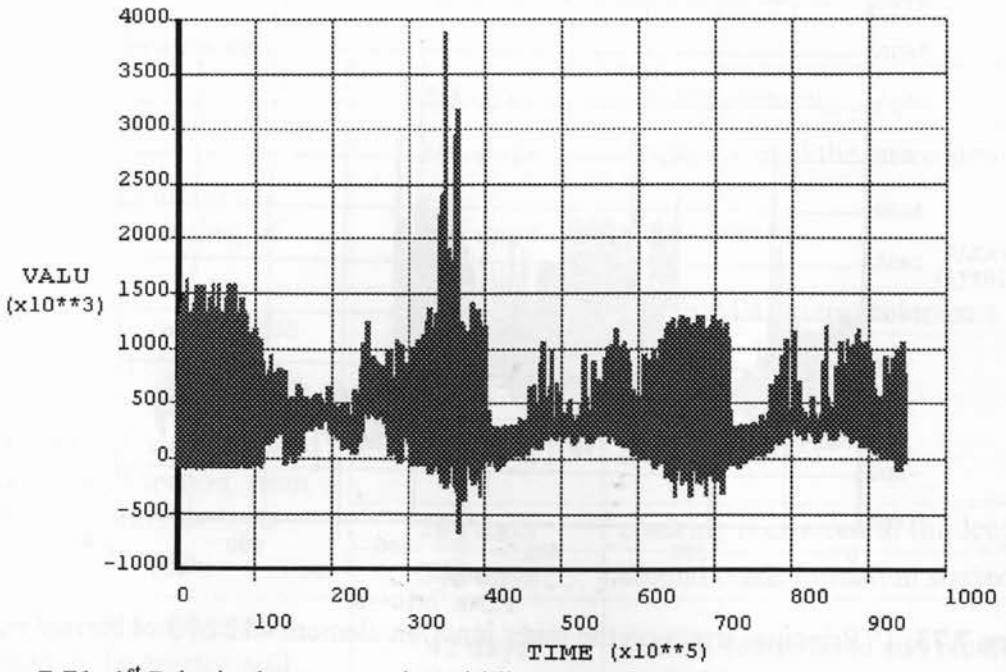

Figure 7.71: 1st Principal stress on the middle top surface element 271 of 3 m barrier wall with fix-free boundary conditions@2.25 m from origin

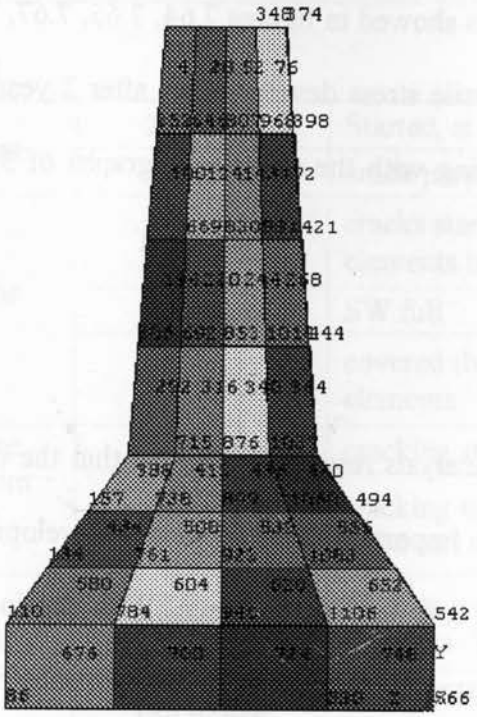

Figure 7.72: Element and node numbers of 3 m barrier wall with fix-free boundary conditions@2.625 m from origin

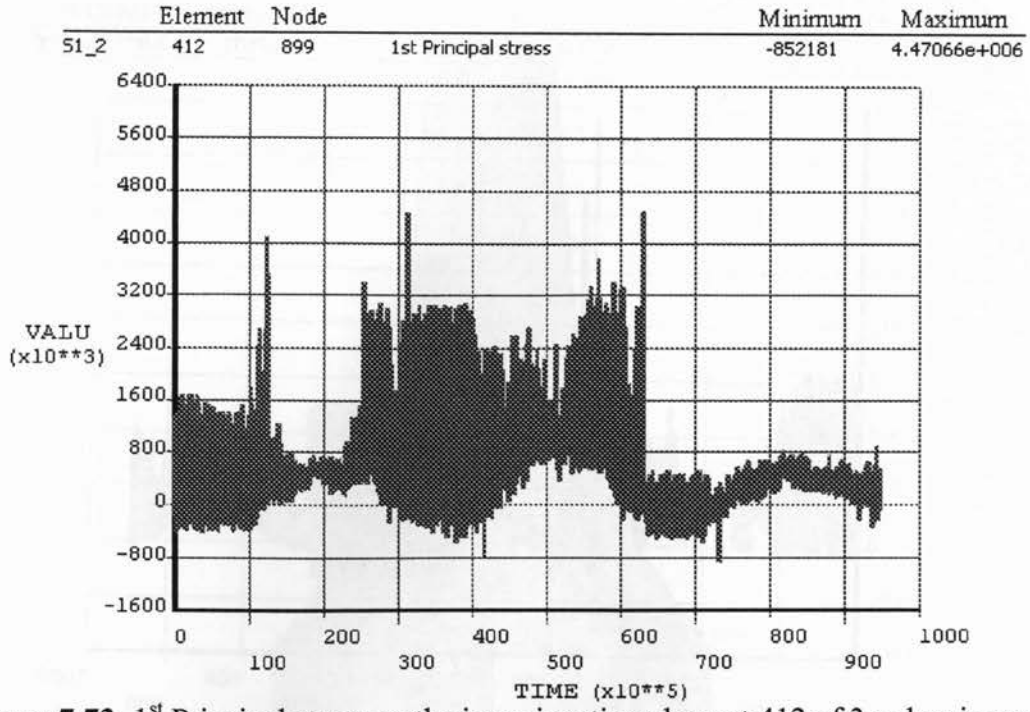

Figure 7.73: 1st Principal stress on the inner junction element 412 of 3 m barrier wall with fix-free boundary conditions@2.625 m from origin

From the stress-time graphs showed in figures 7.64, 7.65, 7.67, 7.68, 7.70, 7.71 and 7.73, the progression rate of tensile stress developments after 2 year duration was found in a slower pace, after comparing with the stress-time graphs of 3 m barrier wall in fix-fix boundary condition.

7.6 Discussion

From the finite element analysis results, it is found that the degree of restraint and the barrier wall length play an important role in the crack development and propagation with respect to time, in plain concrete barrier walls. With the increase in wall length and restraint, vertical cracks start to form at multiple locations along the wall length. The initiating time of the cracks in barrier walls with different boundary conditions is given in Tables 7.7 to 7.10.

Table 7.7: Starting and finishing time of cracks in 1 m fix-fix and 1 m free-fix barrier wall

1m fix-fix barrier wall

Vertical cracks at 0.5 m	**8.5 days**	SW top element
	346 days	cracks covered the entire stem height
Vertical cracks in thinner wall section, spreading of cracks	**346 days**	cracks started
Horizontal cracks at the junction elements	**13 days**	SW middle external elements
	29 days	SW full
Horizontal cracks at the thinner wall section, from top, second row layer elements.	**121 days**	cracking started
	200 days	cracking is covered in full length
	346 days	second crack formation started
Second crack formation initiated in the barrier wall	**42 days**	Bottom centre fixed end elements
Third crack formation initiated in the barrier wall	**104 days**	Thinner wall section, at fixed end elements. SW side

1m fix-free barrier wall

Vertical cracks at 0.5 m	**283 days**	Started, at bottom middle elements
	325 days	crack propagation ceased
Horizontal cracks at the junction elements	**105 hours**	cracks started forming at the junction elements in the free end Middle
	42 days	SW full
	159 days	covered the entire junction periphery elements
Horizontal cracks at the thinner wall section, from top, fourth row layer elements.	**346 days**	cracking started
	271 days	cracking is covered in half length from fixed end
Second crack formation initiated in the barrier wall	**100 hours**	Thinner wall section, at fixed end elements. SW side
Third crack formation initiated in the barrier wall	**180 hours**	Thinner wall section, at fixed end elements. Middle

Table 7.8: Starting and finishing time of cracks in 2 m fix-fix and 2 m free-fix barrier wall

2m fix-fix barrier wall

Vertical cracks at 0.875 m	**283 days**	From bottom, central elements
	334 days	Covered the base height and wall width
	557 days	cracks covered the entire stem height and wall width
Vertical cracks in thinner wall section, spreading of cracks	**348 days**	cracks started
Vertical cracks in thicker wall section, spreading of cracks	**283 days**	cracks started
Horizontal cracks at the junction elements	**13 days**	SW middle external elements
	25 days	SW full
Second crack formation initiated in the barrier wall	**13 hours**	Top corner NE element at the fixed end
Third crack formation initiated in the barrier wall	**13 days**	SW corner junction element at fixed end

2m fix-free barrier wall

Vertical cracks at 1.125 m	**584 days**	From bottom, central elements, just started and no progress
Horizontal cracks at the junction elements	**11 days**	NE corner elements
	120 days	Entire junction periphery
Second crack formation initiated in the barrier wall	**97 hours**	Top two row elements at fixed end, in the middle
Third crack formation initiated in the barrier wall	**99 hours**	Top row elements at fixed end, in the middle

Table 7.9: Starting and finishing time of cracks in 3 m fix-fix & free-fix barrier wall

3 m fix-fix barrier wall

Vertical cracks at 1.00 m	**283 days**	From bottom, central elements
	298 days	Covered the base height and wall width
	300 days	cracks covered the entire stem height and wall width
Vertical cracks in thinner wall section, spreading of cracks	**347 days**	cracks started
Vertical cracks in thicker wall section, spreading of cracks	**283 days**	cracks started
Horizontal cracks at the junction elements	**15.5 days**	SW middle external elements
	29 days	SW full
Second crack formation initiated in the barrier wall	**13 hours**	Top corner NE element at the fixed end
Third crack formation initiated in the barrier wall	**35 hours**	Stem element at fixed end, above junction

3m fix-free barrier wall

Vertical cracks at 0.5 m	**196 days**	From bottom, central elements
	334 days	Covered base height and width
Vertical cracks at 0.875 m	**382 days**	From top, central elements
Vertical cracks at 1.125 m	**38 days**	Started from bottom, central elements
	63 days	Covered base height and width
Vertical cracks at 1.5 m	**155 days**	Started from bottom
Vertical cracks at 2.25 m	**63 days**	Started from bottom, SW elements
	88 days	Covered base height and width
Horizontal cracks at the junction elements	**11 days**	NE corner elements
	82 days	Entire junction periphery
Second crack formation initiated in the barrier wall	**90 hours**	Top second row elements at fixed end, in the middle
Third crack formation initiated in the barrier wall	**95 hours**	Top row elements at fixed end, in the middle

Table 7.10: Starting and finishing time of cracks in 4 m (fix-fix and free-fix) barrier wall

4m fix-fix barrier wall

Vertical cracks at 1 m	**283 days**	From bottom, central elements
	288 days	Covered the base height and wall width
	295 days	cracks covered the entire stem height and wall width
Vertical cracks in thinner wall section, spreading of cracks	**297 days**	cracks started
Vertical cracks in thicker wall section, spreading of cracks	**283 days**	cracks started
Horizontal cracks at the junction elements	**14 days**	SW middle external elements
	29 days	SW full
Second crack formation initiated in the barrier wall	**13 hours**	Top corner NE element at the fixed end
Third crack formation initiated in the barrier wall	**12 days**	bottom NE corner element at fixed end

4m fix-free barrier wall

Vertical cracks at 0.5 m	**186 days**	From bottom, central elements
	248 days	Covered base height and width
	430 days	Covered stem height and width
Vertical cracks at 1.375 m	**646 days**	Started from bottom
Vertical cracks at 1.75 m	**19 days**	Started from bottom, SW elements
	375 days	Covered base height and width
Vertical cracks at 1.875 m	**19 days**	Started from bottom, SW elements
	34 days	Covered base height and width
Vertical cracks at 2.5 m	**167 days**	Started from bottom, full width
Vertical cracks at 3.125 m	**38 days**	Started from bottom, SW elements
	50 days	Covered base height and width
Horizontal cracks at the junction elements	**9 days**	NE corner elements
	17 days	Entire junction periphery
Second crack formation initiated in the barrier wall	**95 hours**	Top row elements at fixed end, SW end
Third crack formation initiated in the barrier wall	**98 hours**	Top row elements at fixed end, in the middle

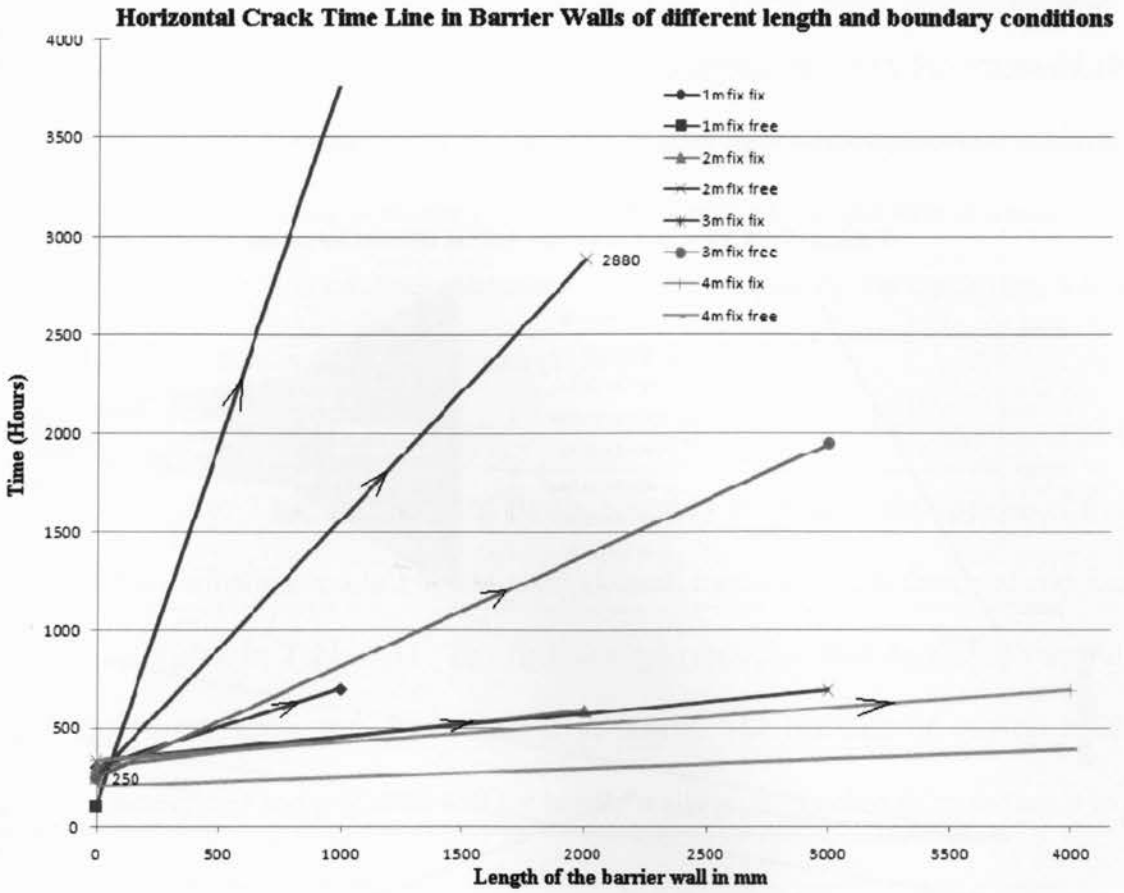

Figure 7.74: Horizontal crack time line in barrier walls of different length and boundary condition

Horizontal crack time lines shown in Figure 7.74 indicate that the horizontal cracks are initiated in the barrier wall almost at the same time, irrespective of the barrier wall length. When both ends are fixed, the speed of horizontal crack progression is faster, in the case of 1 m, 2 m and 3 m barrier walls. However in the case of 4 m barrier wall, the situation is just opposite. As the length of the barrier wall decreases, the speed of horizontal crack progression also decreases. In Figure 7.74, greater slope indicates slower growth of crack progression. From Tables 7.7 to 7.10, when the boundary condition is fix-fix, the horizontal cracks are seen developing in the south west wall face, i.e. the back face. The

situation is same in the actual barrier wall at the site which is considered in this study. Horizontal cracks are seen progressing in the south west face of the barrier wall near the junction where the barrier wall widens, as shown in Figure 3.6(b).

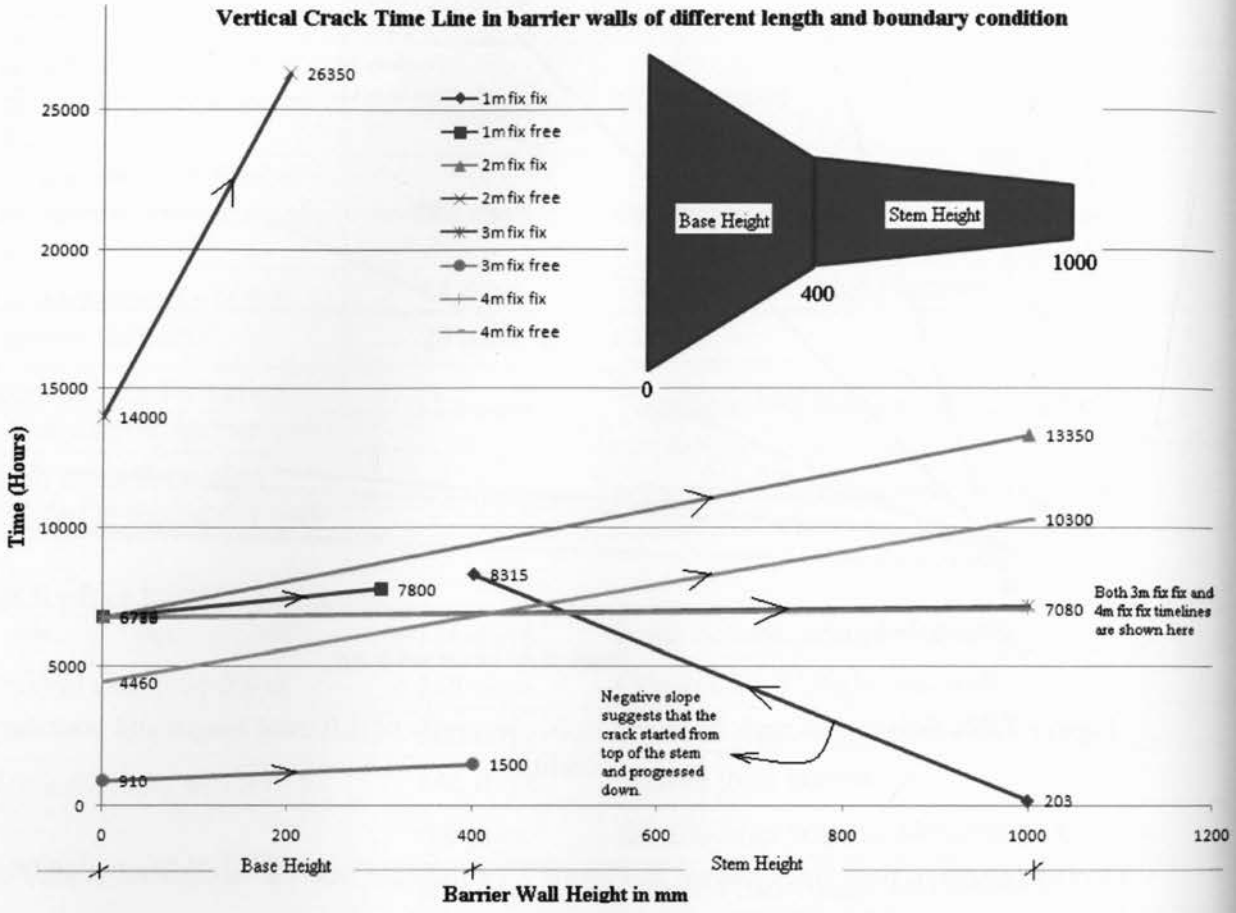

Figure 7.75: Vertical crack time line in barrier walls of different length and boundary condition

Vertical crack time lines shown in Figure 7.75 indicate that in fix-fix boundary conditions, full height vertical cracks are formed when barrier length is more than 1 m. Also, in the case of 3 m and 4 m barrier wall with fix-fix boundary condition, the initiation and completion time (to reach full height) of vertical crack are almost equal. This may suggest that when the length of the barrier wall is more than 3 m, the full height

vertical crack initiation and completion happens almost at the same time, irrespective of the length of the barrier wall. In fix-free boundary condition, when the length of the barrier wall is equal to or greater than 4 m, full height vertical cracks are found. In the case of 2 m fix free barrier wall, the growth of vertical crack progression is found to be very slow. However, second crack formation was observed along the crack line, which may cause an increase in deterioration rate in the coming years.

From Tables 7.7 to 7.10, in the case of fix-fix boundary conditions, the distance of first vertical crack formation and full height vertical crack formation from the fixed end was recorded as shown in Table 7.11. The first vertical crack line had developed into full height for barrier walls with more than 2 m length. The distance of vertical crack formation from fixed end remained 1 m for barrier wall length equal to or more than 3 m.

Table 7.11: Distance of vertical crack formation from fixed ends of fix-fix barrier wall

Fix-fix barrier wall length in m	Distance of first vertical crack formation from fixed end in m	Distance of full height vertical crack formation from fixed end in m
1	0.5	No full height crack formation
2	0.875	0.875
3	1	1
4	1	1

Stress-time graphs of external nodes (presented earlier) showed cracks occurring within 3-4 months after placement of concrete. They were formed mainly due to non uniform concrete shrinkage. Since drying occurs non-uniformly from the concrete surface to its core, shrinkage can create internal tensile stresses near the concrete surface and

compression in the core. With time, even the surface cracks formed due to differential shrinkage will penetrate deeper into the concrete as the inner concrete is subjected to additional shrinkage. This is how a crack grows. In order to curtail this growth, it is necessary to clear the surface cracks by scheduling the first maintenance work on barrier walls within the first four months of construction but definitely before the first winter period, whichever comes first.

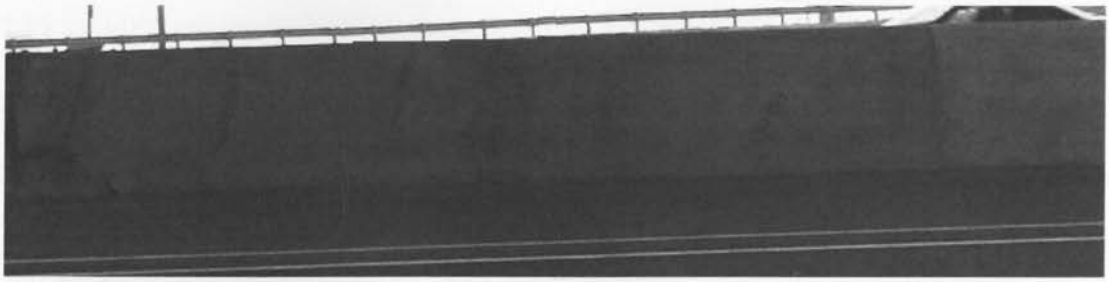

Figure 7.76: Photo of a plain concrete wall of approximately 8-10 years of age with vertical cracks

Figure 7.77: Photo of a plain concrete wall of approximately 3 years of age with vertical cracks

The study of the crack evolution with respect to time and stress-time graphs revealed more information on the behavior of the plain concrete barrier walls. The crack pattern in the Figure 7.76 shows vertical crack formations from the ends at a distance of almost equal to its height. Multiple vertical cracks were also seen between these two full height cracks at the ends. Figure 7.77 showed full height vertical crack formation on a plain concrete barrier wall of approximately 3 years of age. The vertical crack formation happened at a distance of almost equal to the barrier wall height. These field observations can be matched with the results obtained from the finite element study. Thus the results from the finite element analysis (done in this study) can be adapted for deriving recommendations. In finite element models, full height vertical cracks were seen penetrating through the entire width of the barrier wall, whereas horizontal cracks were seen to develop only the surface elements. Therefore, full height vertical cracks should be considered as the most destructive cracks affecting the performance of barrier walls. According to the results of finite element models, vertical cracks are formed at 6778 hours for fix-fix barrier walls of length 2 m to 4 m, i.e. around 9.5 months from the start. Hence, it is highly recommended to have a thorough maintenance check on barrier walls within the nine months of its construction. If the first winter comes before this nine month period, then maintenance should be undertaken before winter starts.

As per the observations from the finite element analysis results done for 3 year duration on barrier walls of 1m height, in a continuous slip form process, it is advisable to provide crack arrester joints at 1m intervals to have barrier walls standing with a pleasing aesthetics. This is because, when control joints are provided at 1 m intervals, it ensures

the initial vertical crack to form at the joint line rather than at random. Once the full height vertical cracks are formed in the crack arrestor joints placed at 1 m intervals, each wall segment between the crack arrestor joints can be considered as an individual barrier wall of 1m length with a reduced restraint at both ends. This will definitely reduce the formation of principal stresses in the concrete, thereby minimizing the crack formations in the barrier wall. The reduction in principal stresses also controls the spreading of vertical cracks near the full height crack observed in barrier walls with fix-fix boundary conditions.

The vertical crack developed at 0.5 m from the ends of 1 m fix-fix barrier wall will not be a concern since this crack was observed only on the back face, i.e. on the south west face of the barrier wall. Figure 7.78 shows the cracks formed at 0.5 m from both ends.

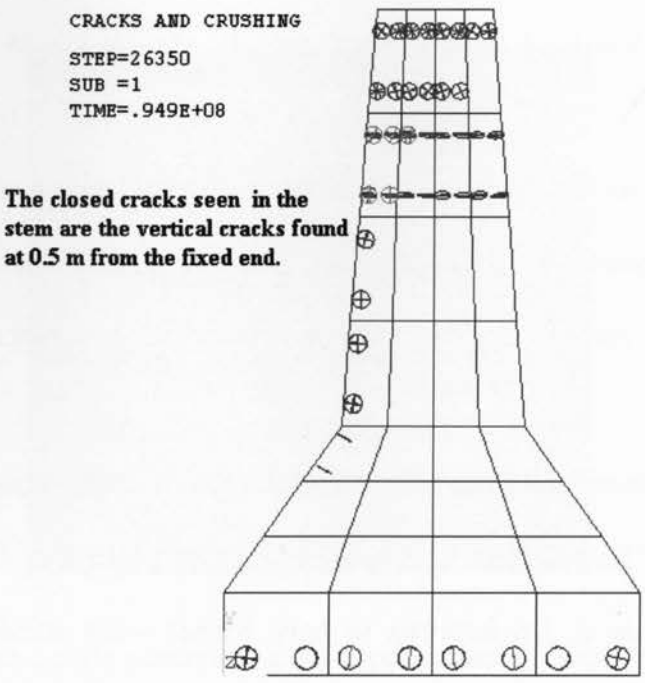

Figure 7.78: Section at 0.5 m from the fixed ends of 1 m fix-fix barrier wall

Chapter 8

Conclusions, Suggestions and Recommendations

8.1 Introduction

This research was mainly conducted to formulate guidelines for minimizing the environmental and age related deterioration mechanism of concrete median barriers. During the life of a properly constructed plain concrete barrier wall, the concrete is exposed to various stresses, such as thermal stresses due to temperature variation, shrinkage stresses depending on the degree of restraint and environmental stresses due to climatic variation such as freezing and thawing as well as wetting and drying conditions. The cracks that develop due to these stresses are all tensile failures. Because concrete is much weaker in tension, the cracking of concrete barrier wall initiates when concrete fail in tension. Tensile stresses developed in concrete are reduced due to stress relaxation with time. However the stress relaxation decreases with concrete age. Hence the cracking tendency of concrete becomes greater with increased time. The effect of shrinkage stresses is a main concern in the early ages of concrete, however thermal and environmental stresses have an ever-lasting action on concrete in long term. The deterioration due to these environmental factors can be minimized or delayed for many years, if proper care is given from the construction phase through the maintenance phase.

The study concentrated on the response of plain concrete barrier walls under time-dependent thermal loads and associated volume changes. The actual surface and core temperature acting on the barrier was collected on an hourly basis from the temperature sensors installed in a

live plain concrete barrier wall. In order to monitor the deviation of significant concrete parameters in varying temperature and environmental conditions, an experimental study was undertaken using ample concrete samples. Based on the results from experimental study and incorporating the temperature data collected from the sensors, a transient thermal and structural analysis was carried out on a three-dimensional model, developed using ANSYS program, for a time period of three years.

8.2 Conclusions

1. According to the experimental study, the tensile strength of concrete is lowest when it is exposed to wet condition with freeze and thaw cycle effect. Therefore, it is necessary not to keep the concrete barrier wall from getting exposed to wet condition continuously for a long time period during winter. Snow ploughs usually try to dump snow from roads to the rear side of the barrier wall, which result in keeping the barrier wall wet for a long duration, at the same time, experiencing freeze and thaw cycles. Hence precautions should be taken for the complete removal of snow around the barrier wall during winter.

2. The outcomes from the analytical study done for 3 year duration on 1 m high barrier wall with variable length of 1 m to 4 m having different boundary conditions are as listed:

    a. The full height vertical cracks are the most destructive of all types of cracks formed in a plain concrete barrier wall, since they are formed in full depth and width of the barrier wall. Full height vertical cracks starts to form at 6778 hours from the beginning (construction) for barrier walls of length 2 m, 3 m and 4 m with both ends in fixed boundary condition. This is approximately 9 months from

the construction. Hence a thorough maintenance check is recommended on barrier walls before 9 months. The distance of the full height vertical crack from the restrained end is 1 m for barrier walls of length equal to or more than 3 m, with both ends in fixed boundary condition.

b. From the finite element analysis results, horizontal cracks initiates in the barrier wall almost at the same time, within the first two weeks of construction, irrespective of the length of the barrier wall. They are formed at the junction where the barrier wall widens, and are only superficial. When the boundary condition is fixed at both ends, horizontal cracks develop at the back face of the barrier wall (the south west face for the case of field barriers). The rate of horizontal crack progression is faster in barrier walls with both ends in fixed boundary condition and also in walls with larger length. When the boundary condition is free on one end, irrespective of barrier wall length, the horizontal crack initiates at the junction surface (base-stem) on the free end and propagates throughout the junction surface on the front and back faces of the wall. Since horizontal cracks forms at the surface only, they are not considered destructive to the barrier wall.

c. Multiple cracks are formed at the fixed end, irrespective of the length of the barrier wall. The cracks normally initiate in the high restraint zone and propagate towards the lower restraint zones.

d. Based on the analysis results, it is recommended to provide control joints at 1m intervals to ensure the initial vertical crack to form at the joint line rather than at random, thus having barrier walls with pleasing aesthetics.

e. It is necessary to clear any surface cracks observed on the wall surface by scheduling the first maintenance work on barrier walls within the first four months of construction, but definitely before the first winter period, whichever comes first. Any minor cracks that are not attended can develop into major problems in future.

f. Stress analysis of element nodes at the junction of base and stem showed increase in stress concentrations, compared to other nodes of the element away from the junction. This is due to the existence of sharp corners in the numerical (finite element) models. Therefore care should be taken to avoid sharp edges at the junction where barrier wall widens.

8.3 Suggestions on Construction Practices

First and the most important step to successfully minimize the deterioration is to implement measures right from the pre-construction stage. Only a properly constructed and maintained barrier wall can withstand the environmental actions and has an increased service life. Some suggestions are given here to accomplish a properly constructed slip form barrier wall.

- One of the major factors that reduce the service life of a concrete structure is due to error in placement and curing. The severity of the effect of these errors on the service life is controlled by exposure conditions. Specifications should be made accommodating these possible errors, by adjusting the factor of safety. Local environmental and material property variations should also be considered to verify concrete performance.

- Slip form construction is now-a-days commonly used in barrier construction, because of its speed in construction. Slip forming needs a stiffer mix, which reduces the workability. Plasticizers are required for improving the workability; hence a well defined mix design should be included in the specifications, mentioning cement content, plasticizer content, pozzolan content, water binder ratio, aggregate gradation etc. Improper consolidation of concrete mix due to lack of vibration, as in the case of slip-formed barriers, results in bleeding of mix water. This causes plastic shrinkage of newly placed constrained concrete, leading to premature cracking. Permanent strength loss, increase in permeability and map cracking can result if moisture supply is insufficient. To prevent this, curing need to be applied immediately after concrete placement, even though specifications allow some time gap for applying curing compound. It is the creative discretion of engineer at site to efficiently perform these types of preventive actions, for the better quality of concrete.
- Care should be taken to achieve a monolithic structure without any cold joints.
- Sawing of control joints should be done as soon as the concrete has hardened sufficiently to prevent uncontrolled cracking, but within 12 hours of casting. The specification for the depth and spacing of control joints provided in Ontario should be considered for a revision. The control joints should be sealed because during winter, concrete will contract and make the joint open. Dust and sediments from the flowing traffic and wind, salt from the road snow removal etc can be accumulated in the opened joint. When the temperature increases due to season change, the concrete expands and closes the joint. The external particles present in the joint, prevent the concrete to close the joint, which may result in spalling.

- Expansion joints should be placed when the barrier wall is constructed adjacent to any rigid structure like bridge pier, lamp post foundations etc. During slip forming, any difficulty in placing expansion joints should be overcome by saw cutting through the plastic concrete, to full depth and width of barrier section.

8.4 Recommendations

1. In this thesis, a uniform coefficient of thermal expansion for concrete, i.e. 11E-06/°C is considered during the finite element analysis. Since the age of concrete is one of the principal factors affecting the coefficient of thermal expansion, it is important to understand how this concrete property changes with time. Hence a thorough investigation on this aspect is highly recommended.
2. In the finite element analysis performed here, only the actual temperature readings from August 2007 to April 2008 have been used. Rest of the three year temperature readings is approximated. Also, only barrier walls of 1m high and up to 4 meter in length have been analyzed. This work should be extended to different barrier wall lengths and heights as well as to more time duration. Time and software limitations did not allow me to carry out this kind of analysis. The strain and temperature data from the sensors should be recorded continuously without any interruption for a longer period, so that any future work done on this area will be highly benefited.
3. A comprehensive field investigation done on barrier wall of 1 m high, with crack arrestors at every 1 m interval will reveal the actual behavior of proposed barrier wall. Such a field study conducted for a longer duration will definitely help in assessing the barrier wall durability in the extreme weather conditions of Canada.

REFERENCES

1. ACI Committee 207 (1995) "Effect of Restraint, Volume Change and Reinforcement on Cracking of Mass Concrete (207.2R-95)," *American Concrete Institute*, Farmington Hill, MI, 26 pp.
2. ACI Committee 517, (1980) "Accelerated Curing of Concrete at Atmospheric Pressure," State-of-the-Art Report, ACI 517.2R-80, *ACI Manual of Concrete Practice*, Part 5, Detroit, MI, pp. 214–219.
3. ACI Committee 305, (1992) "Hot Weather Concreting", ACI 305.R-91, *ACI Manual of Concrete Practice*, Part 2, Detroit, MI, 20 pp.
4. ACI 318-95 Building code requirements for structural concrete, [1996], *ACI Manual of Concrete Practice* Part 3: Use of Concrete in Buildings – Design, Specifications and Related Topics, Detroit, Michigan, pp. 345
5. Aïtcin, P.-C., (1999) "Does Concrete Shrink or Does it Swell," *Concrete International*, Vol 21, No.12, pp. 77–80.
6. Aïtcin, P.-C., Neville, A.M., and Acker, P., (1997) "Integrated View of Shrinkage Deformation," *Concrete International*, Vol 19, No.9, pp. 35–41.
7. Aïtcin, P.-C., (1999) "Demystifying Autogenous Shrinkage," *Concrete International*, Vol 21, No.11, pp. 54–56
8. Aïtcin, P.-C., Lachemi, M., and Tagnit-Hamou, A., (2000) "Long Term Durability of Silica Fume Concretes: A Twenty Year Experience," *Fifth CANMET/ACI International Conference on Durability of Concrete*, Barcelona, Spain, 4–9 June, 11p.

9. Al Rawi, A. and Kheder, G.F., [1990] "Control of Cracking due to Volume Change in Base Restrained Concrete Members", *ACI Structural Journal*, Vol. 87, Issue 4, pp. 397-405.

10. ANSYS Release 9.0 Documentation Manual, ANSYS Inc., Canonsburg, PA 15317.

11. Bazant, Z.P. (1976) "Instability, Ductility and Size Effect in Strain-Softening Concrete," *Journal of Engineering Mechanics*, ASCE, Vol 102, April, pp. 331-344.

12. Bissonnette, B., Pierre, P. and Pigeon, M, [1999], "Influence of Key Parameters on Drying of Cementitious Materials", *Cement and Concrete Research*, Vol. 29, No. 10, pp.1655-1662.

13. Bissonnette, B., Marchand, J., Charron, J.P., Delagrave, A., and Barcelo, L. (2001) "Early Age Behaviour of Cement- Based Materials," *Materials Science of Concrete (VI)*, S. Mindess & J. Skalny, Eds., The American Ceramic Society, pp. 243-326.

14. Bonacina, C., Campanale, M. and Moro, L., [2003] "Analytical and Experimental Investigations on the Heat Transfer Properties of Light Concrete", *International Journal of Thermophysics*, Vol, 24, No. 5, pp. 1407-1414.

15. Byfors, J., (1980) "Plain Concrete at Early Ages," *Swedish Cement and Concrete Institute*, Stockholm, Sweden, 465 pp.

16. Carlson, R.W. and Reading. T. J., (1988) "Model Study of Shrinkage Cracking in Concrete Building Walls," *ACI Structural Journal*, **85**(4), pp. 395–404.

17. Chun-Qing Li and Jian-Jun Zheng [2007] "Closed-Form Solution for Predicting Elastic Modulus of Concrete", *ACI Materials Journal*, Vol.104, No. 5, pp. 539-545.

18. Cusson, D. and Repette, W.L., (2000) "Early-Age Cracking in Reconstructed Concrete Bridge Barrier Walls," *ACI Materials Journal*, Vol.97, No.4, pp. 438–446.

19. Davis, R.E., (1940) "Autogenous Volume Change of Concrete," *Proceedings of the 43rd Annual ASTM Meeting*, Atlantic City, NJ, June, No.40, pp. 1103–1113.

20. Davis, R.E., (1930) "A summary of the Results of Investigations Having to do with Volumetric Changes in Cements, Mortars and Concretes Due to Causes other than Stress," *ACI Journal*, **26**(4), pp. 407–443.

21. Design guide for durable concrete structures - *The Euro-International Committee for Concrete*, 1989, 2nd edn, Lausanne and Thomas Telford, London.

22. Dubouchet, A., (1992) "Développement d'un pôle de calcul: CESAR-LCPC," *Bulletin de Liaison des Laboratoires des Ponts et Chaussées,* March-April, pp. 77–84.

23. Emanuel, J.H., and Hulsey, L., (1977) "Prediction of the Thermal Coefficient of Expansion of Concrete," *ACI Journal*, April, pp. 149–155.

24. FitzGibbon, M.E., [1976] "Large Pours for Reinforced Concrete Structures", *Concrete*, Vol.10, No.3, p.41

25. Fu, X. and Chung, D.D. (1999) "Effect of Admixtures on Thermal and Thermo-mechanical Behavior of Cement Paste," *ACI Materials*, V.96, N0.4, pp. 455-461.

26. Helmuth, R.A. (1961) "Dimensional changes of hardened Portland cement pastes caused by temperature changes," *Highway Research Record*, Vol.40, pp.315-366.

27. Howells, R.W., Lark, R.J. and Barr B.I.G.,[2005], "A study of the influence of environment effects on the behavior of a pre-stressed concrete viaduct", *Structural Concrete*, Volume 6, No 3, pp. 89-100.

28. Inkyu Rhee., (2004) "Cohesive Interfacial Crack Analysis of Concrete Materials and Reinforced Concrete Structures", University of Colorado, Boulder, Colorado.

29. Japanese Concrete Institute Technical Committee (1998) "Report on Autogenous Shrinkage of Concrete," *Autoshrink '98*, Hiroshima, Japan, pp. 5–64.

30. Kachlakev, D.I., Miller, T., Yim, S., Chansawat, K., Potisuk, T., [2001] "Finite Element Modeling of Reinforced Concrete Structures Strenghtened with FRP Laminates", California Polytechnic State University, San Luis Obispo, CA and Oregon State University, Corvallis, OR for Oregon Department of Transportation.

31. Kada, H., Lachemi, M., Petrov, N., Bonneau, O., and Aïtcin, P.-C., (2002) "Determination of the Coefficient of Thermal Expansion of High Performance Concrete from Initial Setting," *Materials and Structures*, Vol 35, No. 245, pp. 35–42.

32. Kim, J.K. and Lee. C.S., (1998) "Prediction of Differential Drying Shrinkage in Concrete", *Cement and Concrete Research*, Vol.28, Issue 7, pp.985-994.

33. Klieger, P and Lamond, J.F., (1994) "Significance of Tests and Properties of Concrete and Concrete-making Materials", *ASTM special technical publication 169C*, 4th edition, Chapter 23, pp 223.

34. Kristensen, L. and Hansen, T.C., (1994) "Cracks in Concrete Core due to Fire or Thermal Heating Shock", *ACI Materials Journal*, Vol. 91, No. 5, pp 453-459.

35. Lachemi, M., Li, G., Tagnit-Hamou, A., Aïtcin, P.-C. (1998) "Long-Term Performance of Silica Fume Concretes," *Concrete International (ACI)*, Vol.20, No.1, pp. 59–65.

36. Lachemi, M., and Aïtcin, P.-C. (1997) "Influence of Ambient and Fresh Concrete Temperatures on the Maximum Temperature and Thermal Gradient in a High Performance Concrete Structure," *ACI Materials Journal*, Vol.94, No.2, pp. 102–110.

37. Lachemi, M., Sculthorpe, R., and Wright, B. (2001) "Placing Concrete in Insulated Forms Under Very Low Temperatures," Proceeding of the *Third International Conference on Concrete Under Severe Conditions: CONSEC'01,* Vol. I, Vancouver, BC, 18–20 June, pp. 301–308.

38. Lachemi, M., Mesbah, H.A., Petrov, N., and Aïtcin, P.-C., (2001) "Parameters Affecting Autogenous Shrinkage in High Performance Concrete Structures," *Creep, Shrinkage & Durability Mechanics of Concrete and other Quasi-Brittle Materials: CONCREEP-6@MIT,* Cambridge, MA, 20–22 August, pp. 319–324.

39. Lydon, F. D., and Balendran, R. V., (1986) "Some Observations on Elastic Properties of Plain Concrete," *Cement and Concrete Research*, Vol.16, No.3, pp. 314–423.

40. Mehta, P.K., and Monteiro, P.J.M., (1993) "Concrete: Structure, Properties and Materials," Prentice Hall Inc., Englewwod Cliffs, NJ, 548 p.

41. Mesbah, M.A., Lachemi, M., and Aïtcin, P.-C., (2002) "Determination of Elastic Properties of High Performance Concrete at Early Ages," *ACI Materials Journal*, Vol.99, No.1, pp. 37–41.

42. Morin, R., Haddad, G., and Aïtcin, P.-C.,(2002) "Crack-Free High-Performance Concrete Structures," *Concrete international*, Vol.24, No.9, pp. 42–48.

43. Michigan DOT Center of Excellence, (2004) "Causes and Cures for Cracking of Concrete Barriers" Centre of Structural Stability, Wayne State University, Michigan, 222 p.

44. Mindess, S. and Young, J.F., (1981) "Concrete", Prentice-Hall, Inc., Englewood Cliffs, NJ.

45. Neville, A.M., [1997] "Properties of Concrete", 4th edition, Prentice Hall.

46. Oluokun, F. A., Burdette, E. G., and Deatherage, J. H., (1991) "Elastic Modulus, Poisson's Ratio, and Compressive Strength Relationships at Early Ages," *ACI Materials Journal*, Vol. 88, No. 1, pp. 3–10.

47. Popovics.S., [1973], "A Numerical Approach to the complete Stress-Strain Curve of Concrete", *Cement and Concrete Research*, Vol. 3, pp.583-599.

48. Regourd, M. and Gauthier, E., (1982) "Comportement des ciments au durcissement accéléré," *Annales de l'institut technique du bâtiment et des travaux publics*, No 387, Série Béton, pp. 83-96.

49. RILEM-42-CEA, [1981] "Properties of Set Concrete at Early Ages – State of the Art Report", *Materiaux et Constructions*, Vol. 14, No.84, pp.399-450.

50. Saucier, F., Claireaux, F., Cusson, D., Pigeon, M. (1997) "The Challenge of Numerical Modeling of Strains and Stresses in Concrete Repairs," *Cement and Concrete Research*, V.27, No.8, pp. 1261-1270.

51. Schoppel, K., Plannerer, M. and Springenschmid, R., [1994] "Determination of Restraint Stress and of Materials Properties during Hydration of Concrete with the Temperature-stress Testing Machine", 25th Proceedings of the International RILEM Symposium, Munich, Germany, pp. 154-160.

52. Tazawa, E., and Miyazawa, S., (1996) "Influence of Autogenous Shrinkage on Cracking in High-Strength Concrete," *4th International Symposium on the Utilisation of High Strength and High Performance Concrete*, Paris, France, pp. 321–330.

53. Willam, K.J. and Warnke, E.D., [1975], "Constitutive Model for the Triaxial Behavior of Concrete" Proceedings, *International Association for Bridge and Structural Engineering*, Vol.19, ISMES, Bergamo, Italy, p. 174.

54. Wolanski, A.J., [2004] "Flexural Behaviour of Reinforce and Prestressed Concrete Beams Using Finite Element Analysis", Marquette University, Milwaukee, Wisconsin.

55. Yang, S., Kim, J., Jeon, S., Kim, K. (2003) "An experimental study on thermal conductivity of concrete," *Cement and Concrete Research*, V.33, No.3, pp. 363-371.

56. Yang, S., Kim, J., Kim, N., Park, J. (2003) "Experimental Measurement of Concrete Thermal Expansion," *Journal of the Eastern Asia Society for Transportation Studies*, Vol.5, October 2003.

57. Zhenhua, W., [2006], "Behavior of High-Strength Concrete members under Pure flexure and Axial-Flexural loadings", PhD dissertation, North Carolina State University, NC 27695.

APPENDIX

A.1 Sequence of crack evolution in a 1m barrier wall with fix-free boundary condition

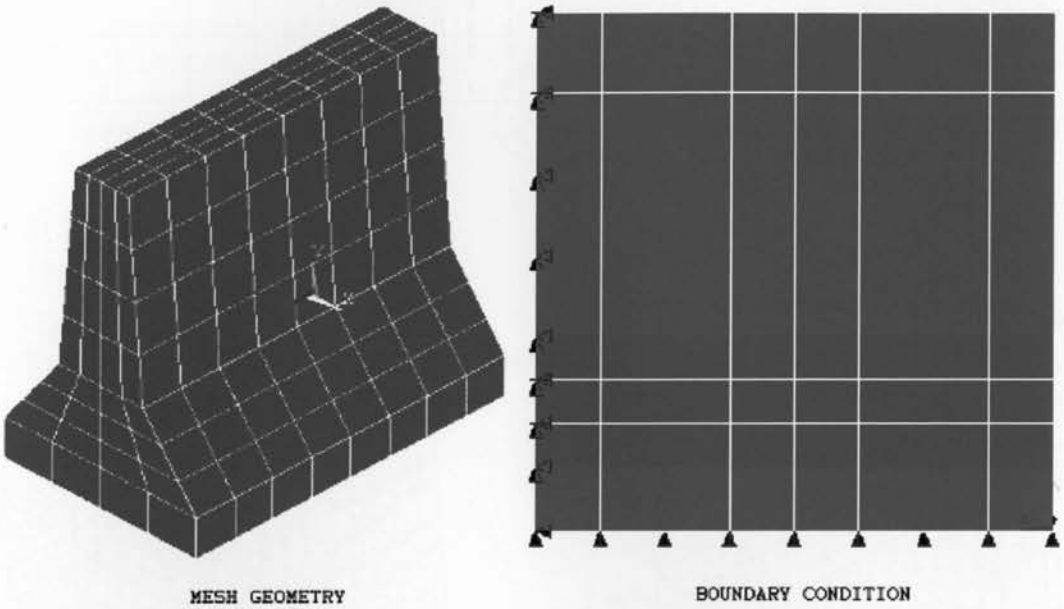

Figure A.1: Mesh Geometry and Boundary Condition of 1m barrier wall with one end free and the other end fixed

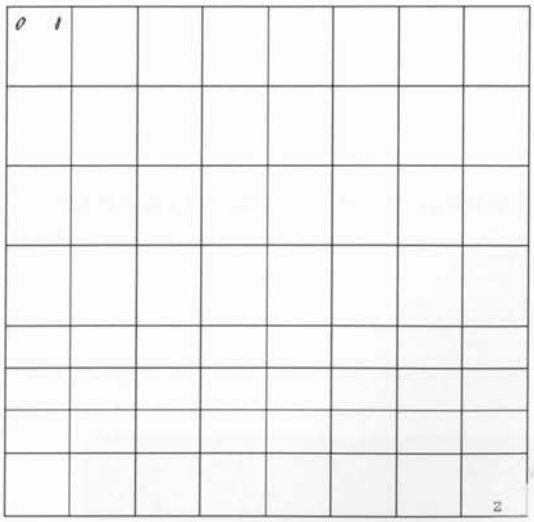

Time Step : 10 hours

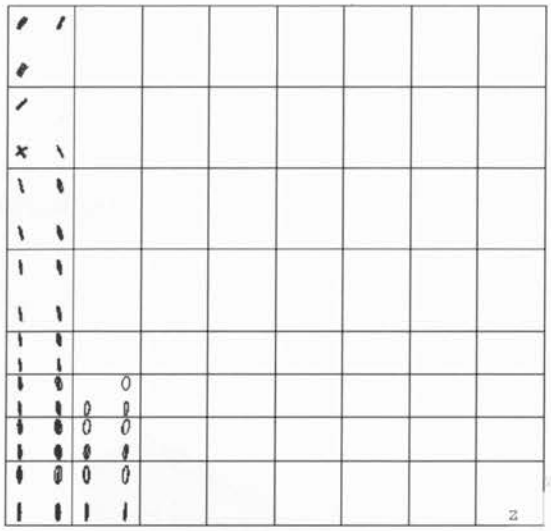

Time Step : 100 hours

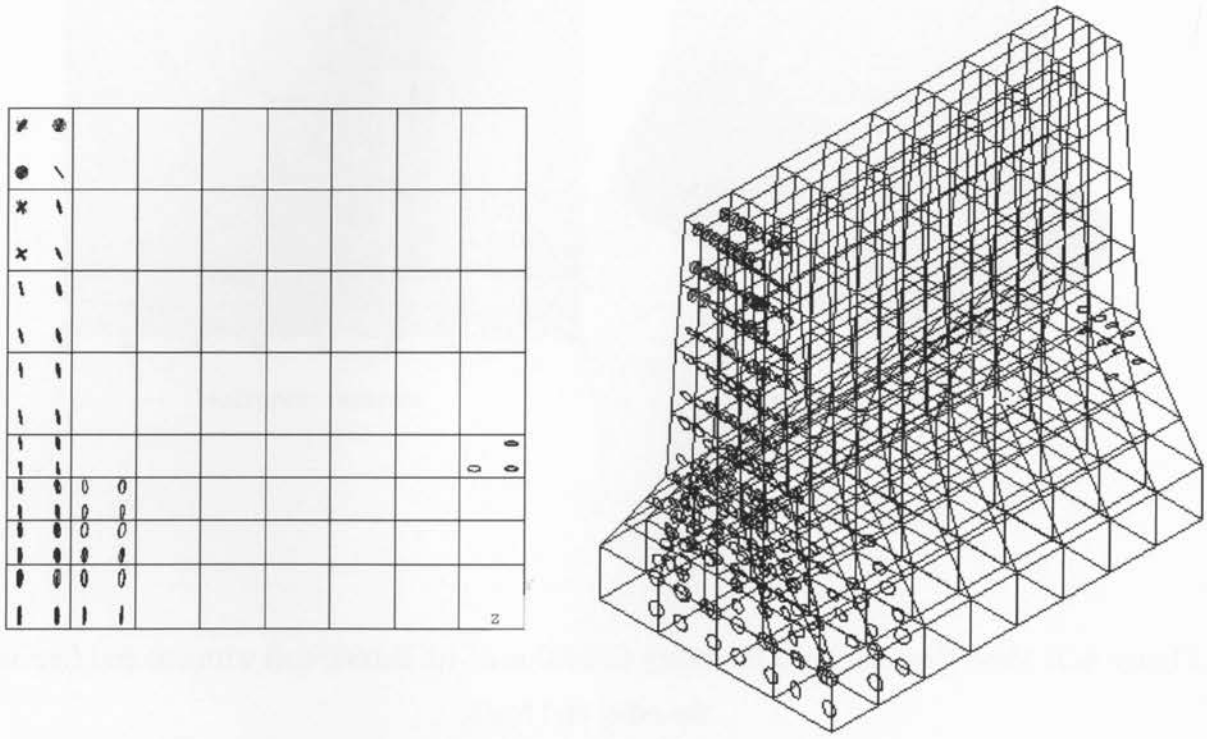

Time Step : 200 hours

Figure A.2 : Cracks in 1m barrier wall with fix-free ends, @10, 100 and 200 hours

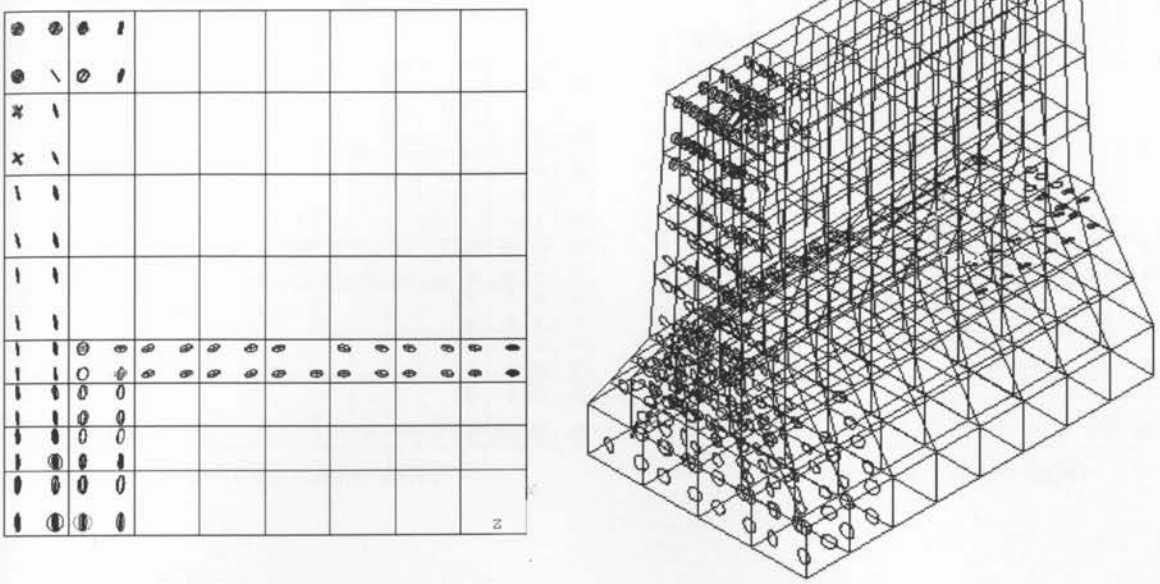

Time Step : 350 hours

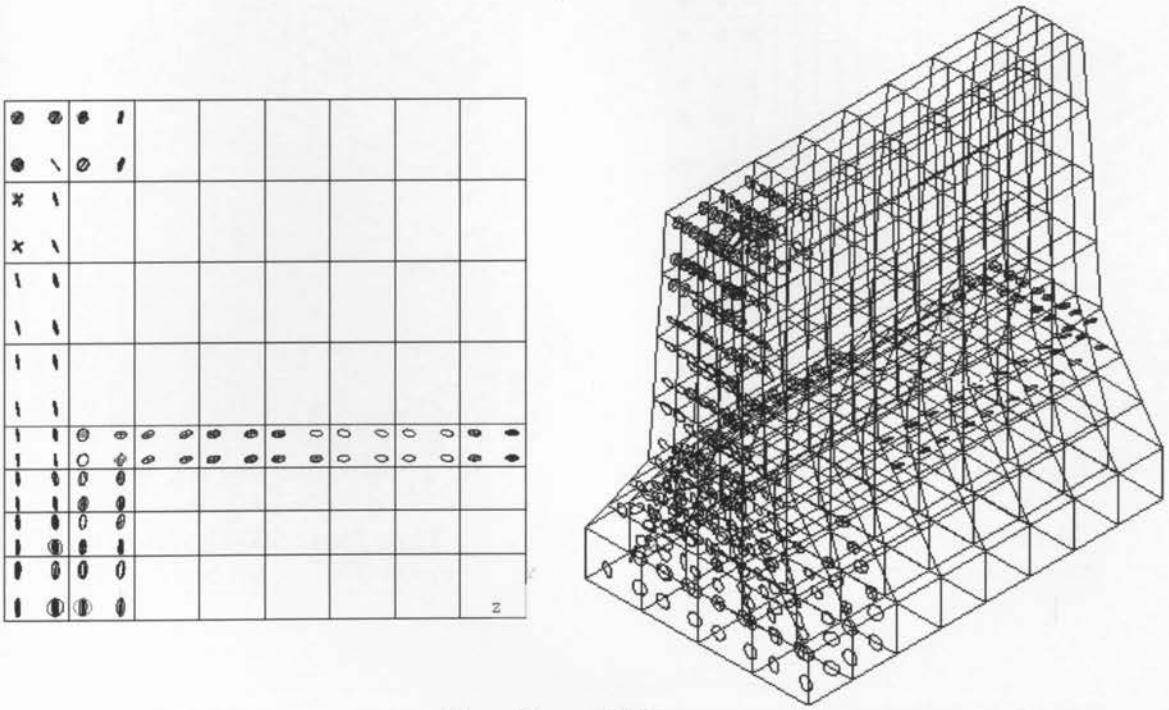

Time Step : 500 hours

Figure A.3 : Cracks in 1m barrier wall with fix-free ends, @350 and 500 hours

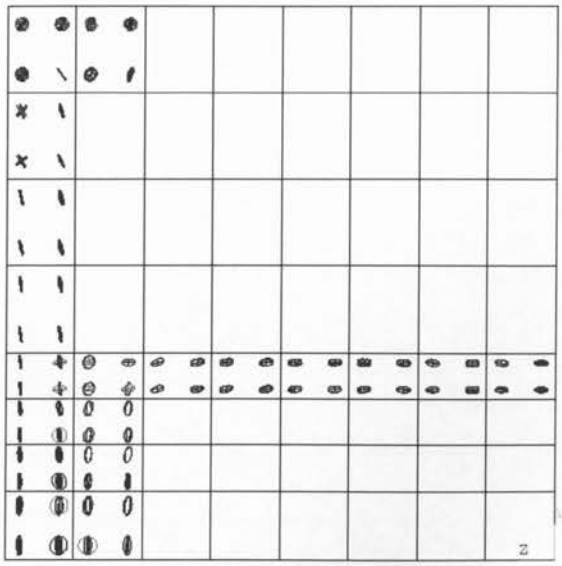

Time Step : 1000 hours

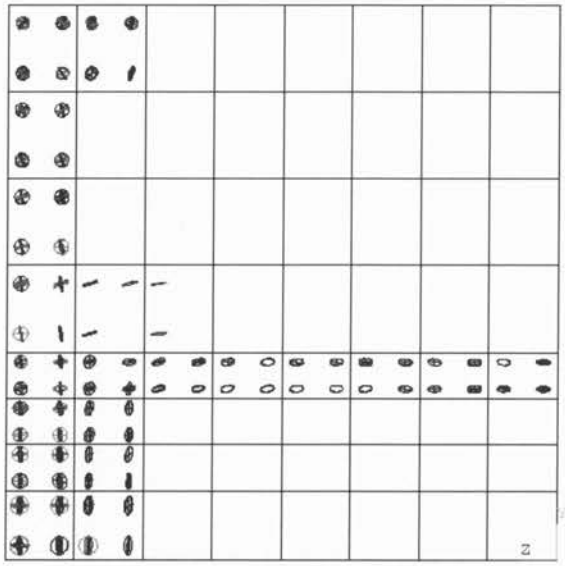

Time Step : 3000 hours

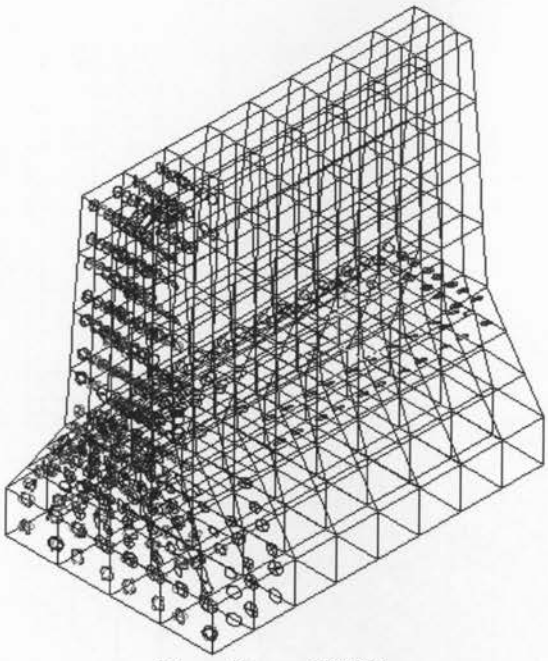

Time Step : 3000 hours

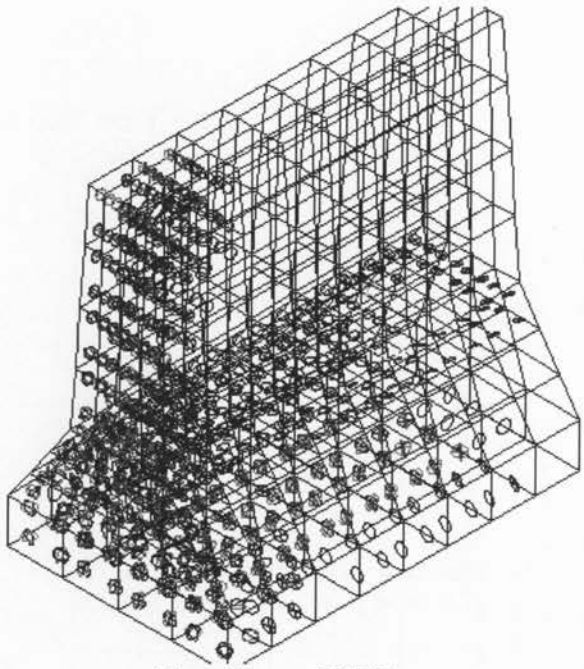

Time Step : 5000 hours

Figure A.4 : Cracks in 1m barrier wall with fix-free ends, @1000, 3000 and 5000 hours

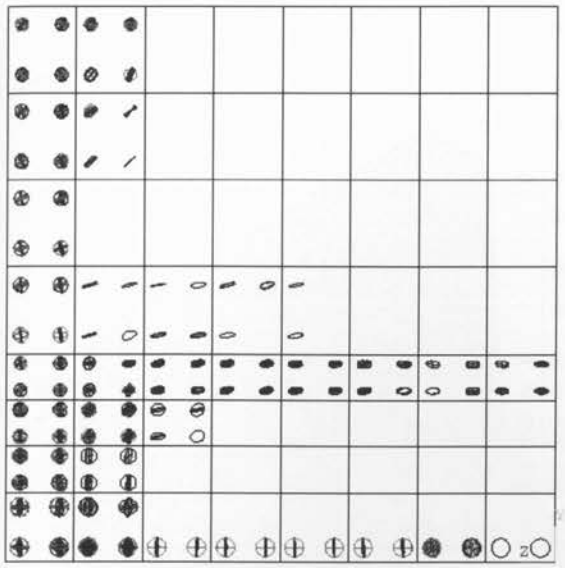

Time Step : 5000 hours

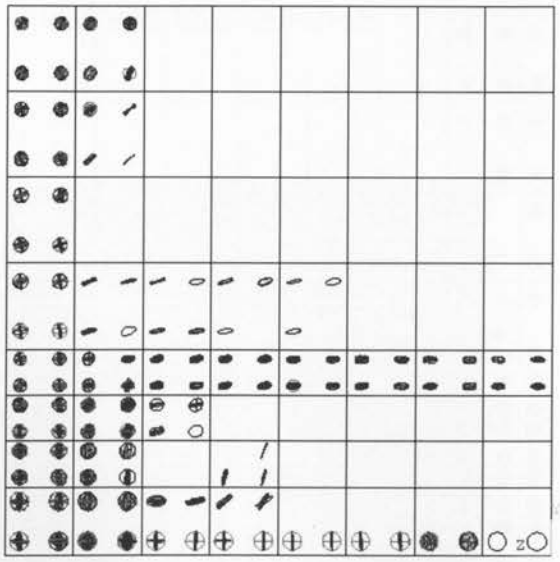

Time Step : 7500 hours

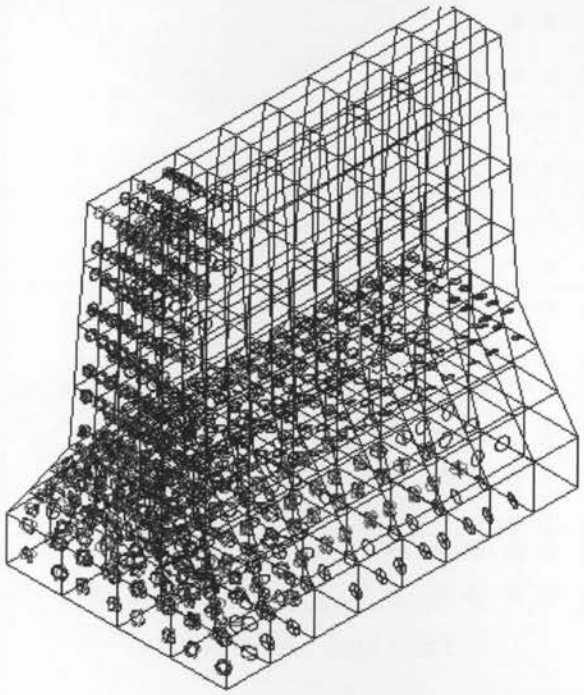

Time Step : 7500 hours

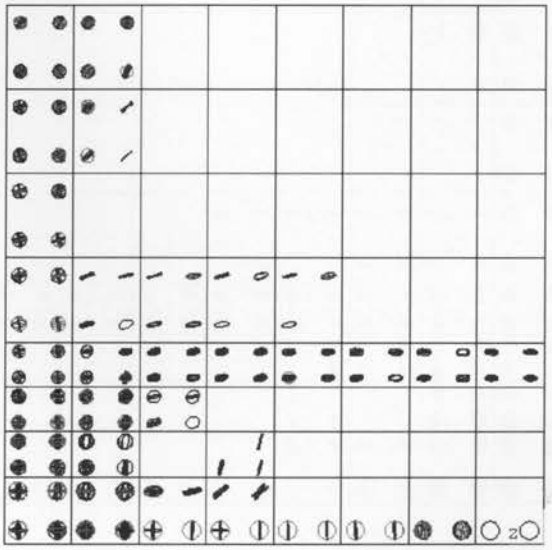

Time Step : 10000 hours

Figure A.5 : Cracks in 1m barrier wall with fix-free ends, @5000, 7500 and 10000 hours

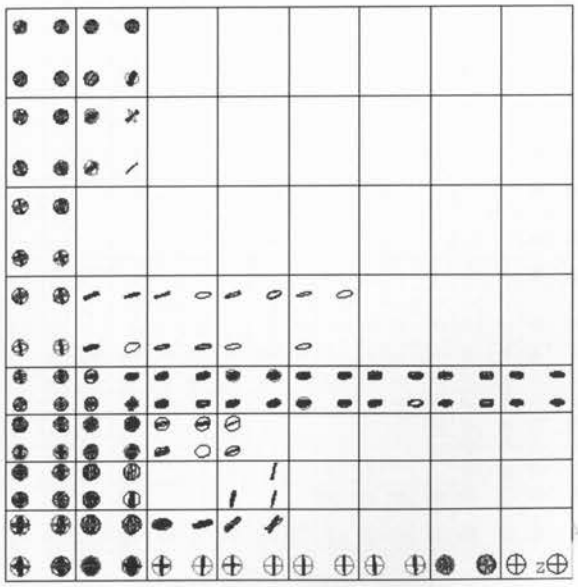

Time Step : 15000 hours

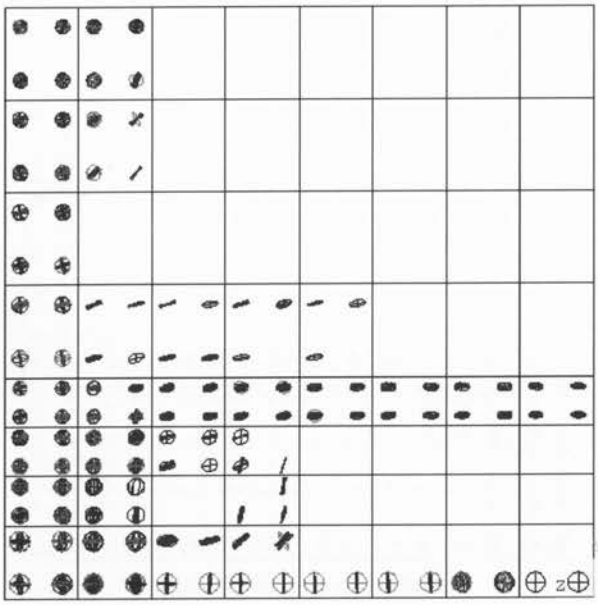

Time Step : 20000 hours

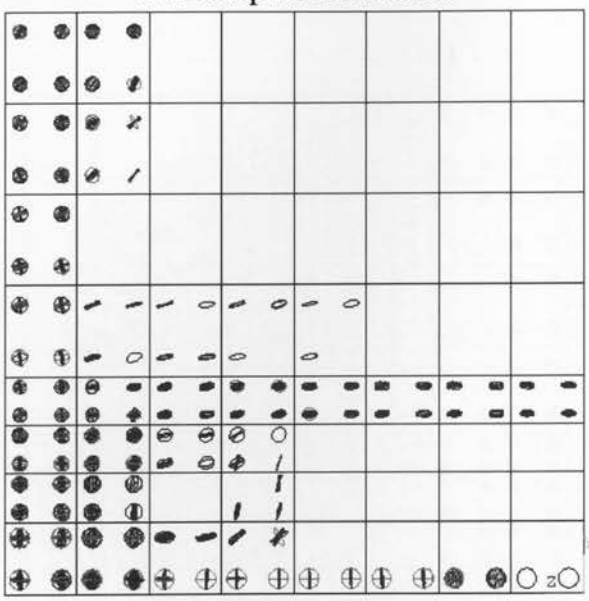

Time Step : 24000 hours

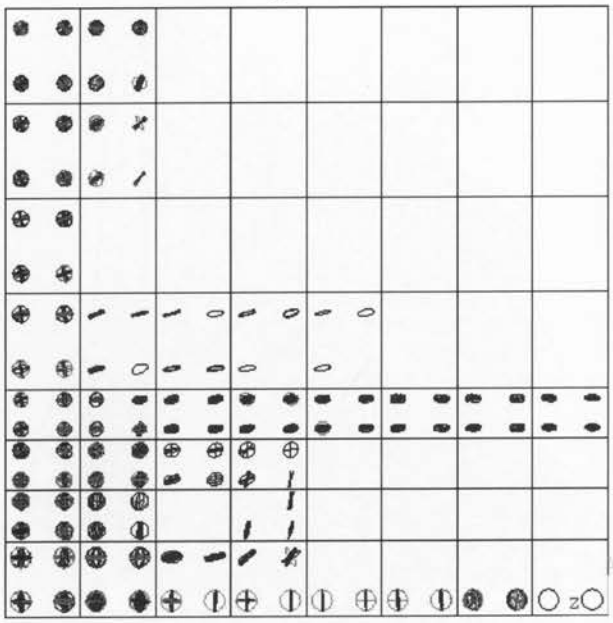

Time Step : 26350 hours

Figure A.6 : Cracks in 1m barrier wall with fix-free ends, @15000, 20000, 24000 and 26350 hours

A.2 Sequence of crack evolution in a 1m barrier wall with both ends fixed

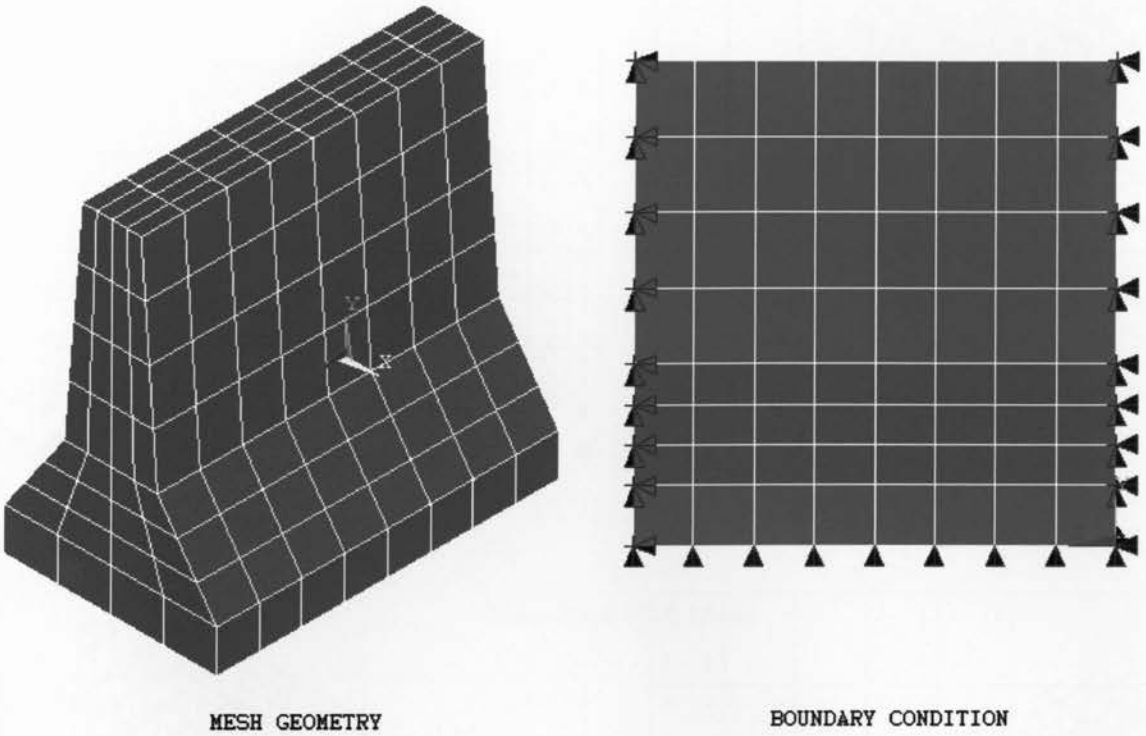

Figure A.7: Mesh Geometry and Boundary Condition of 1m barrier wall with both end nodes fixed

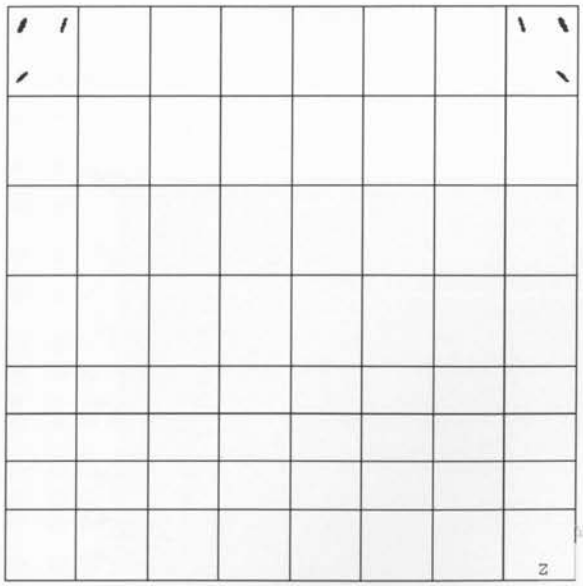

Time Step: 10 hours

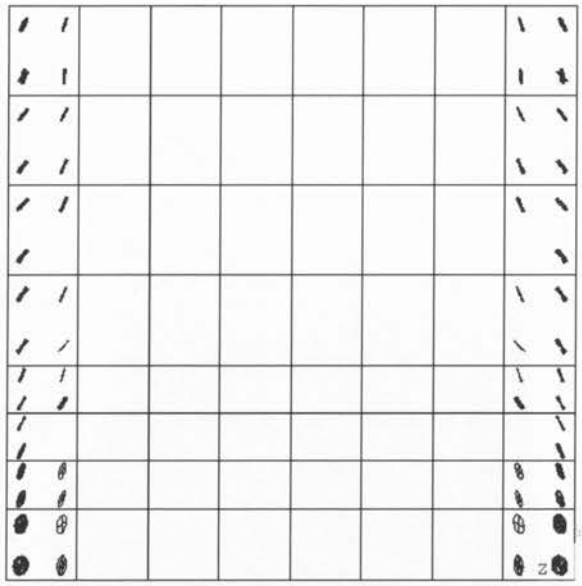

Time Step: 100 hours

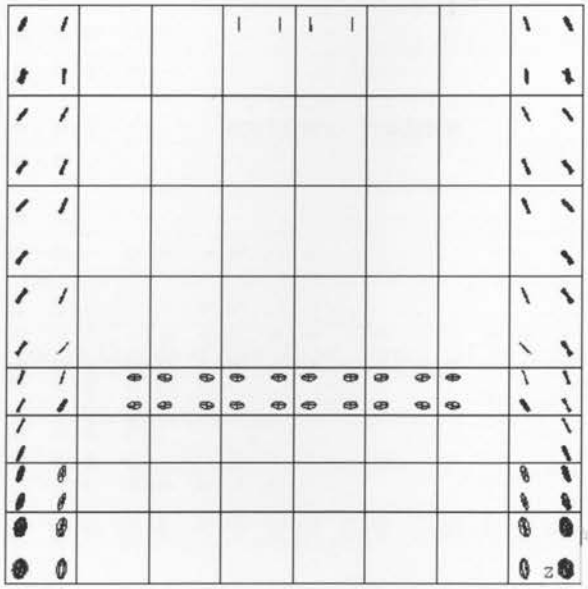

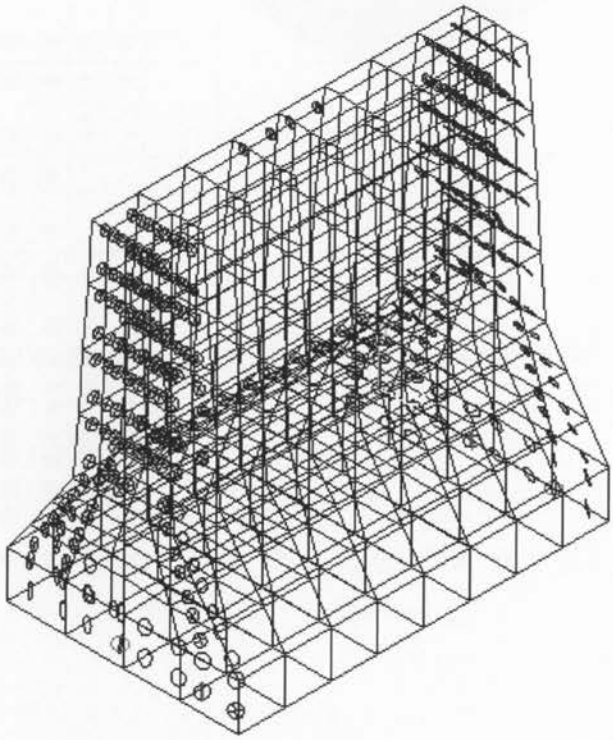

Time Step: 500 hours

Figure A.8 : Cracks in 1m barrier wall with fix-fix ends, @10, 100 and 500 hours

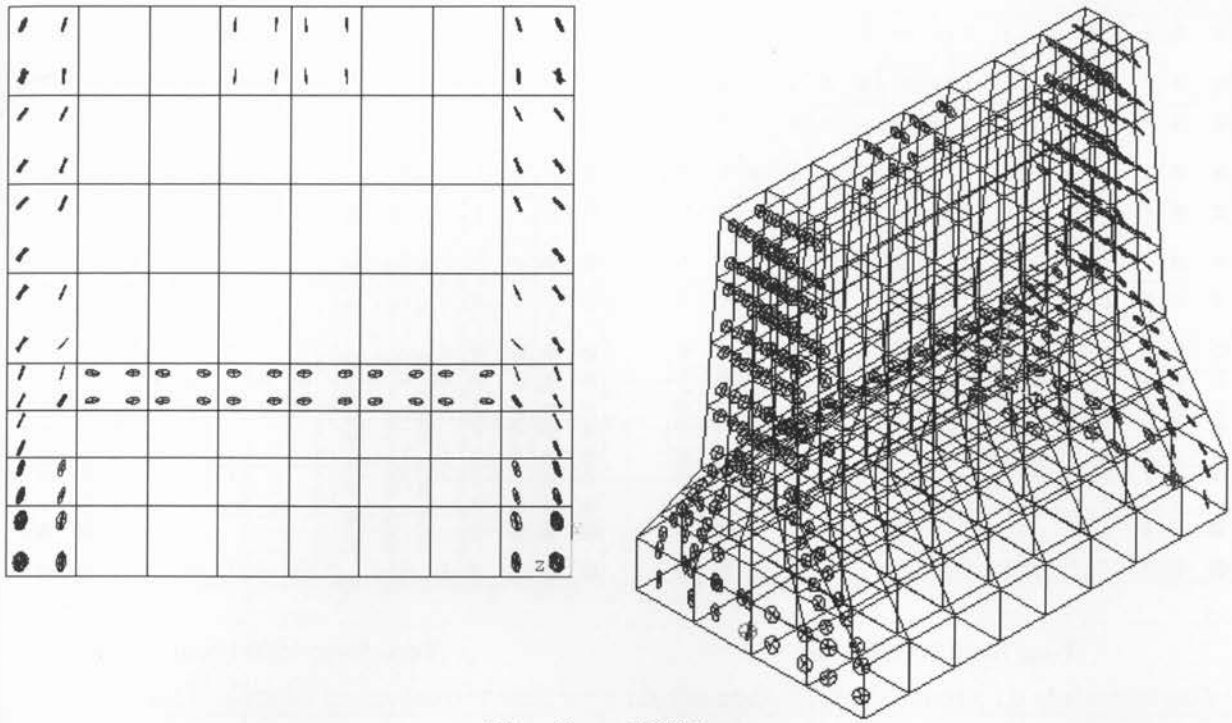

Time Step: 1000 hours

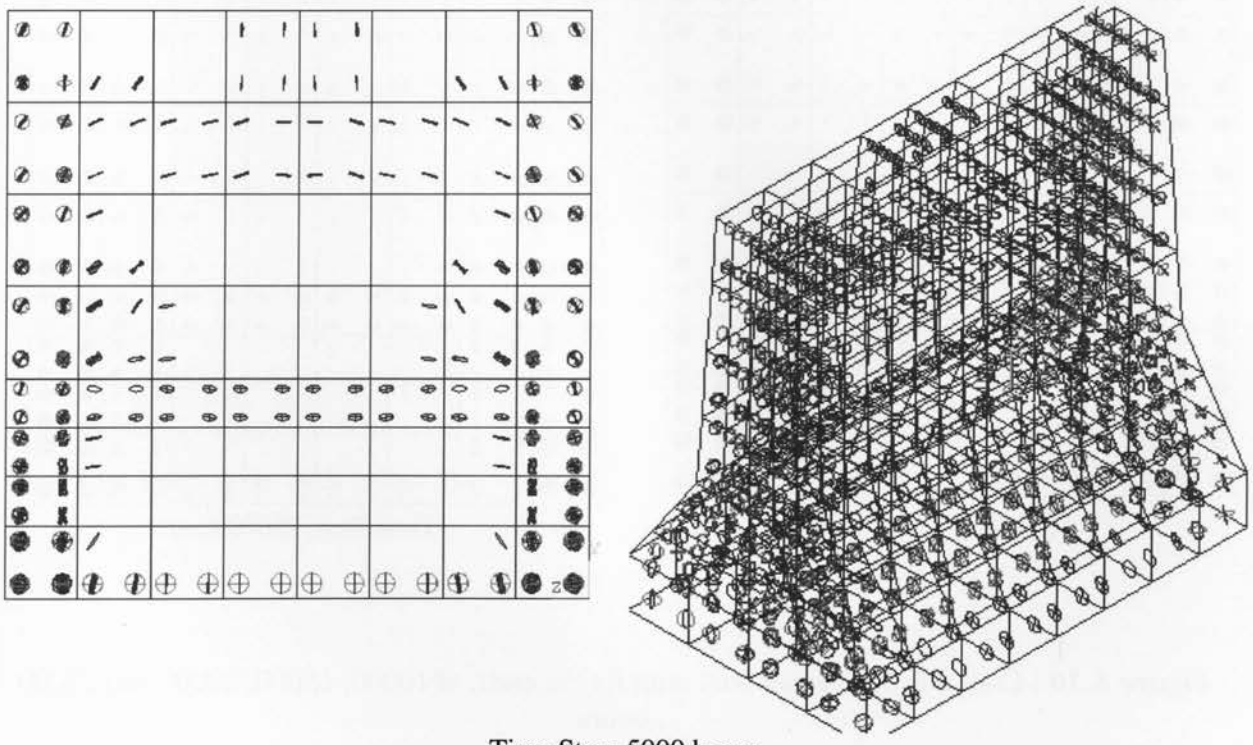

Time Step: 5000 hours

Figure A.9 : Cracks in 1m barrier wall with fix-fix ends, @1000 and 5000 hours

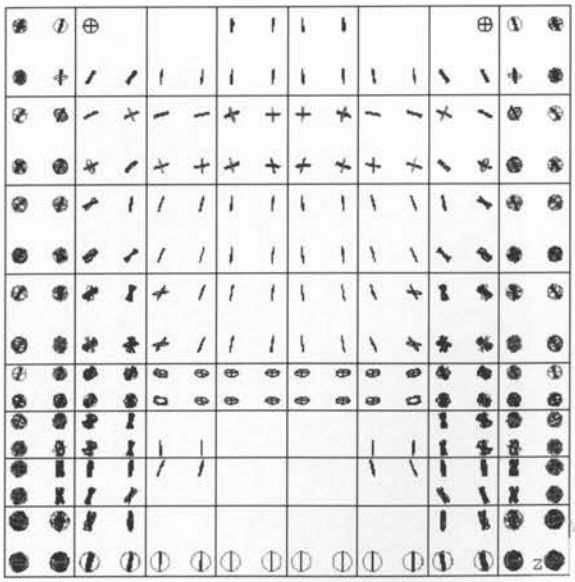

Time Step: 10000 hours

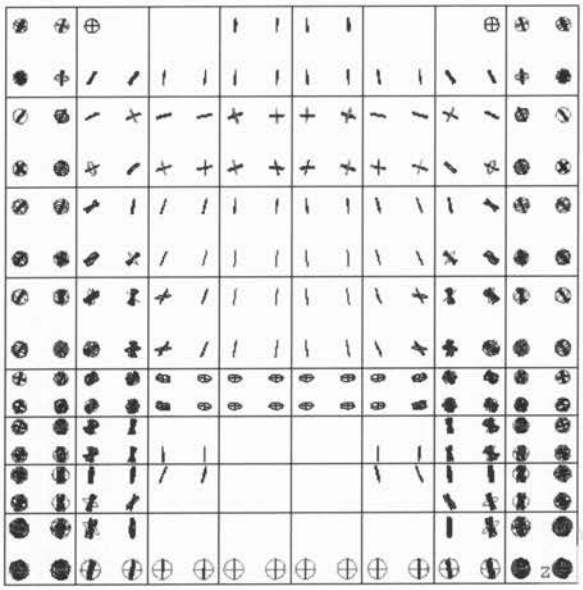

Time Step: 15000 hours

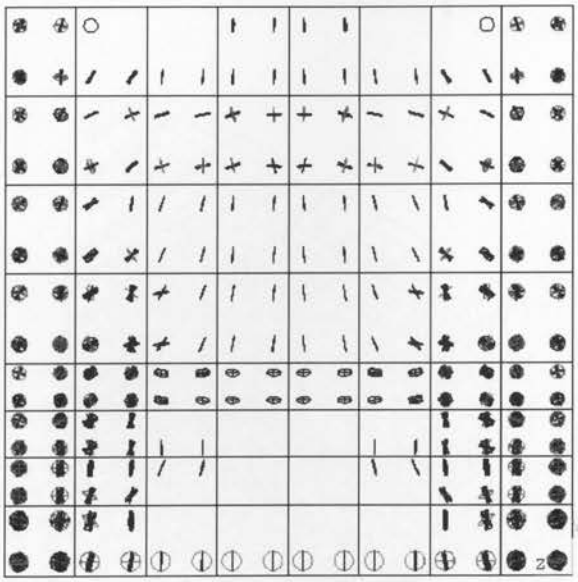

Time Step: 20000 hours

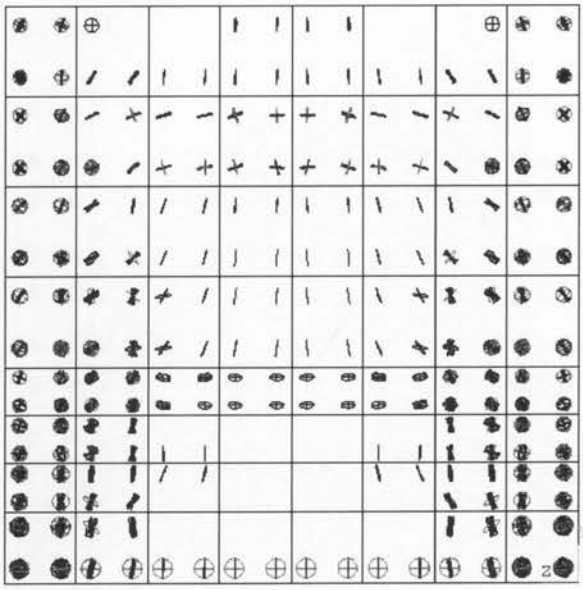

Time Step: 25000 hours

Figure A.10 : Cracks in 1m barrier wall with fix-fix ends, @10000, 15000, 20000 and 25000 hours

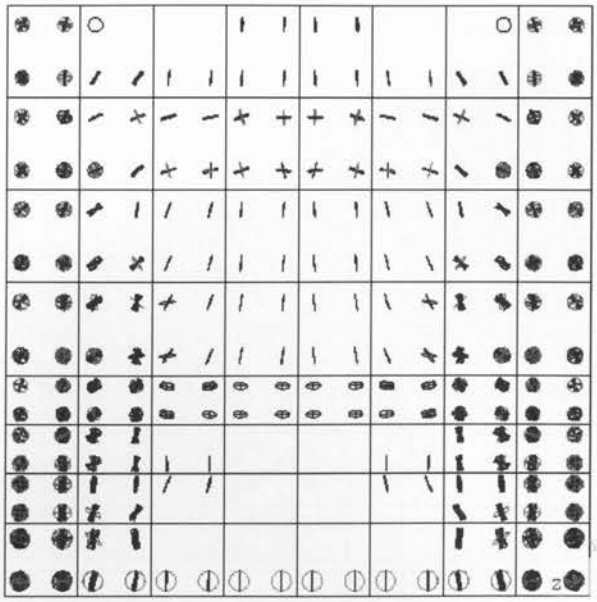

Figure A.11 : Cracks in 1m barrier wall with fix-fix ends, @26350 hours, i.e at the end of 3 years

7.2.3 Sequence of crack evolution in a 2m barrier wall with origin end free and other end fixed

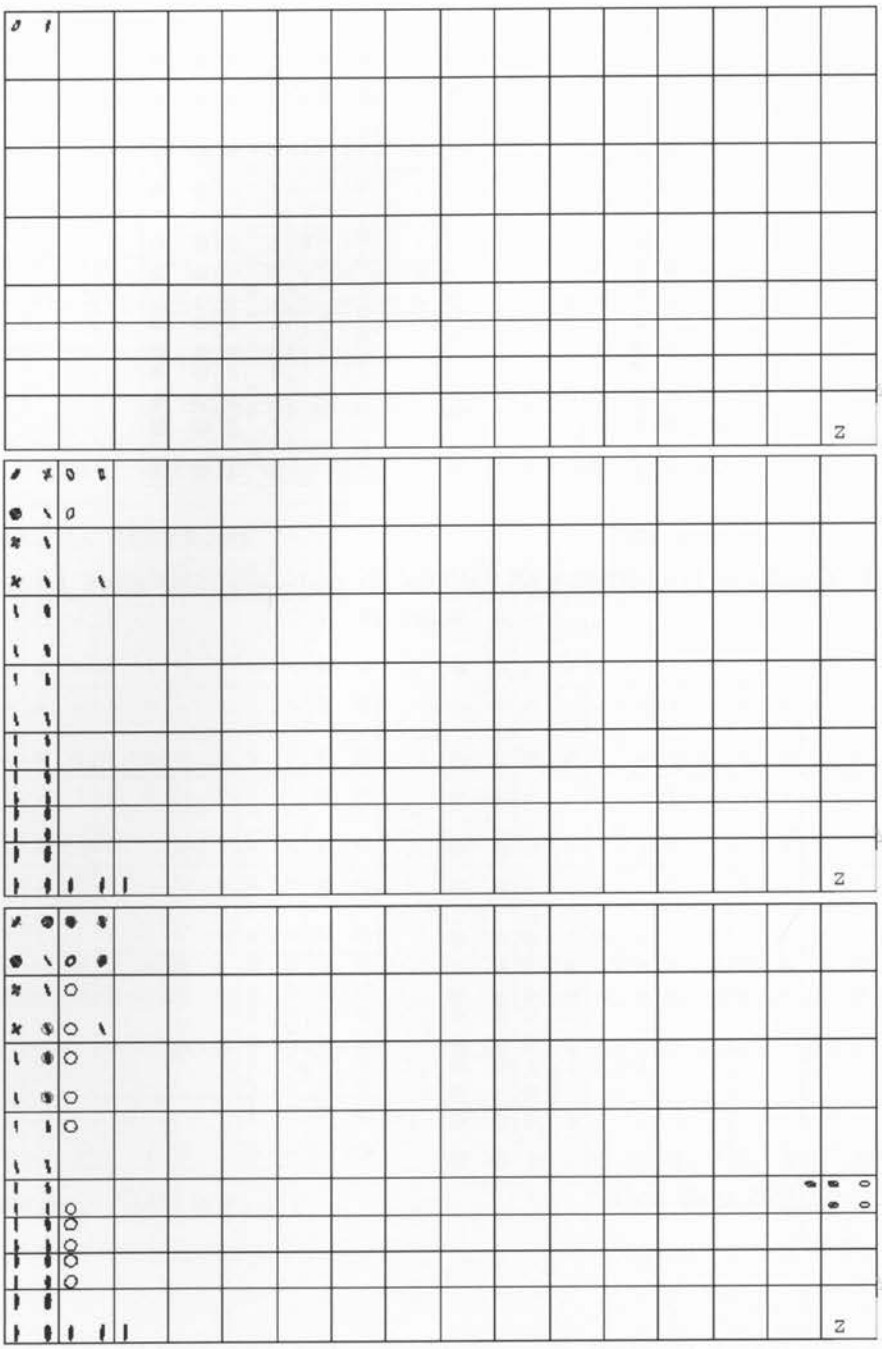

Figure A.12: Crack patterns of 2 m barrier wall (fix – free) @ 10, 100 & 300 hours

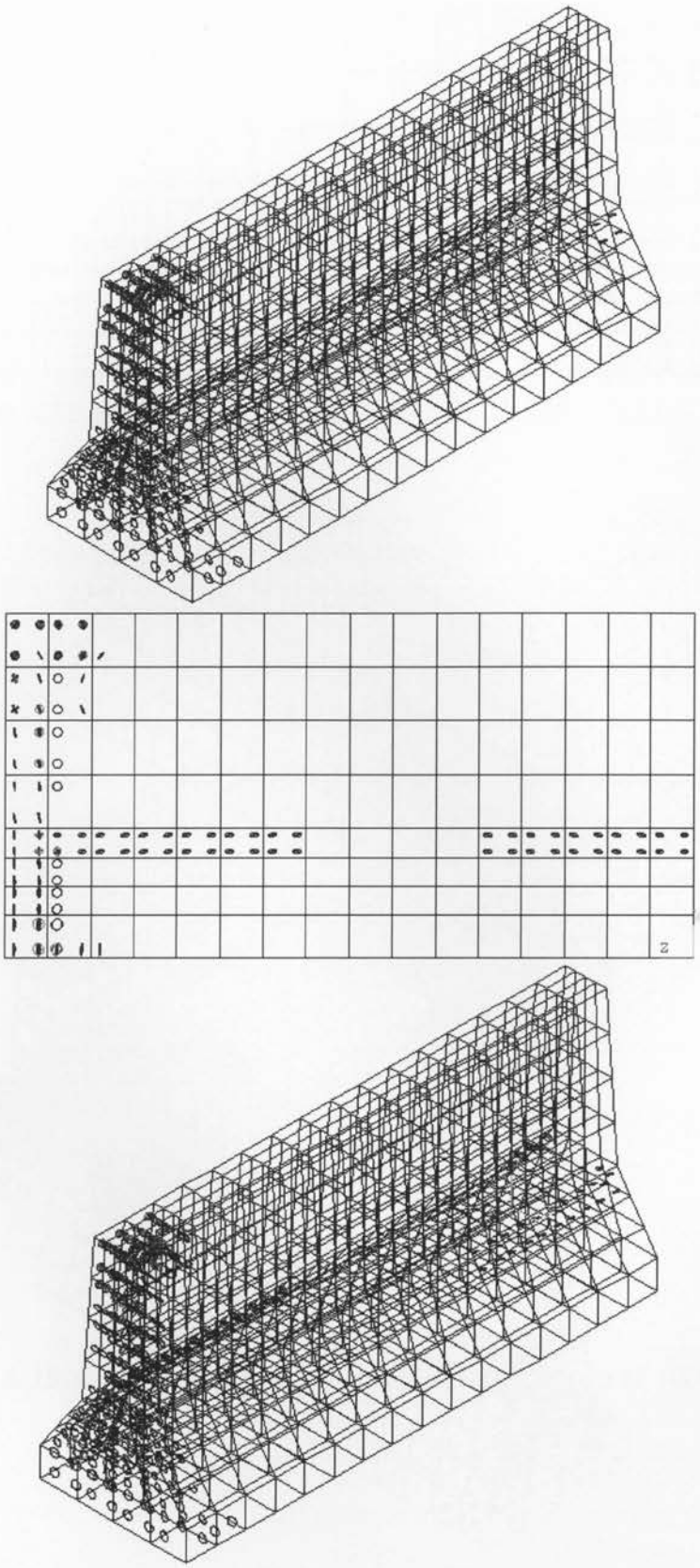

Figure A.13 : Crack patterns of 2 m barrier wall (fix – free) @ 300 & 400 hours

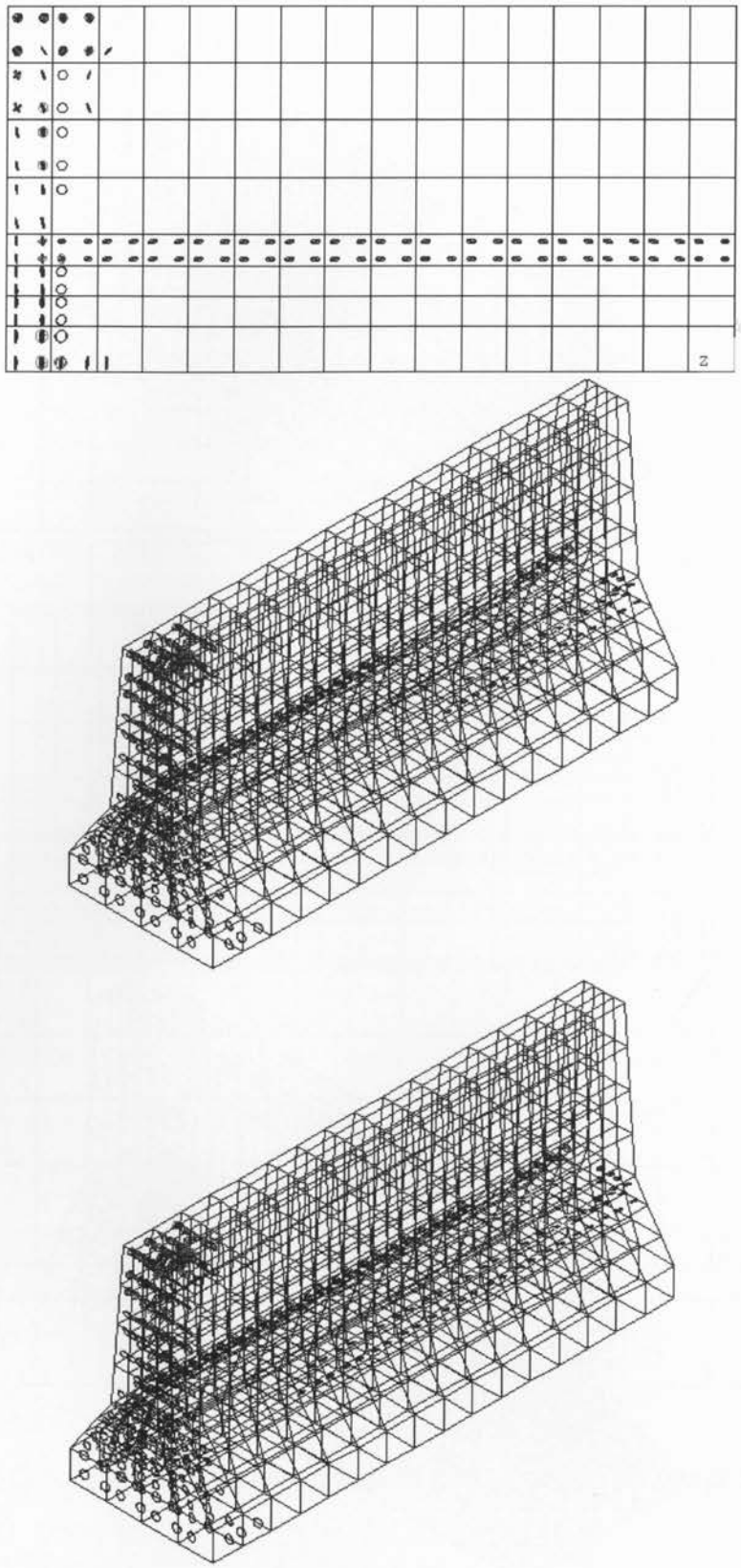

Figure A.14: Crack patterns of 2 m barrier wall (fix – free) @ 500 and 800 hours

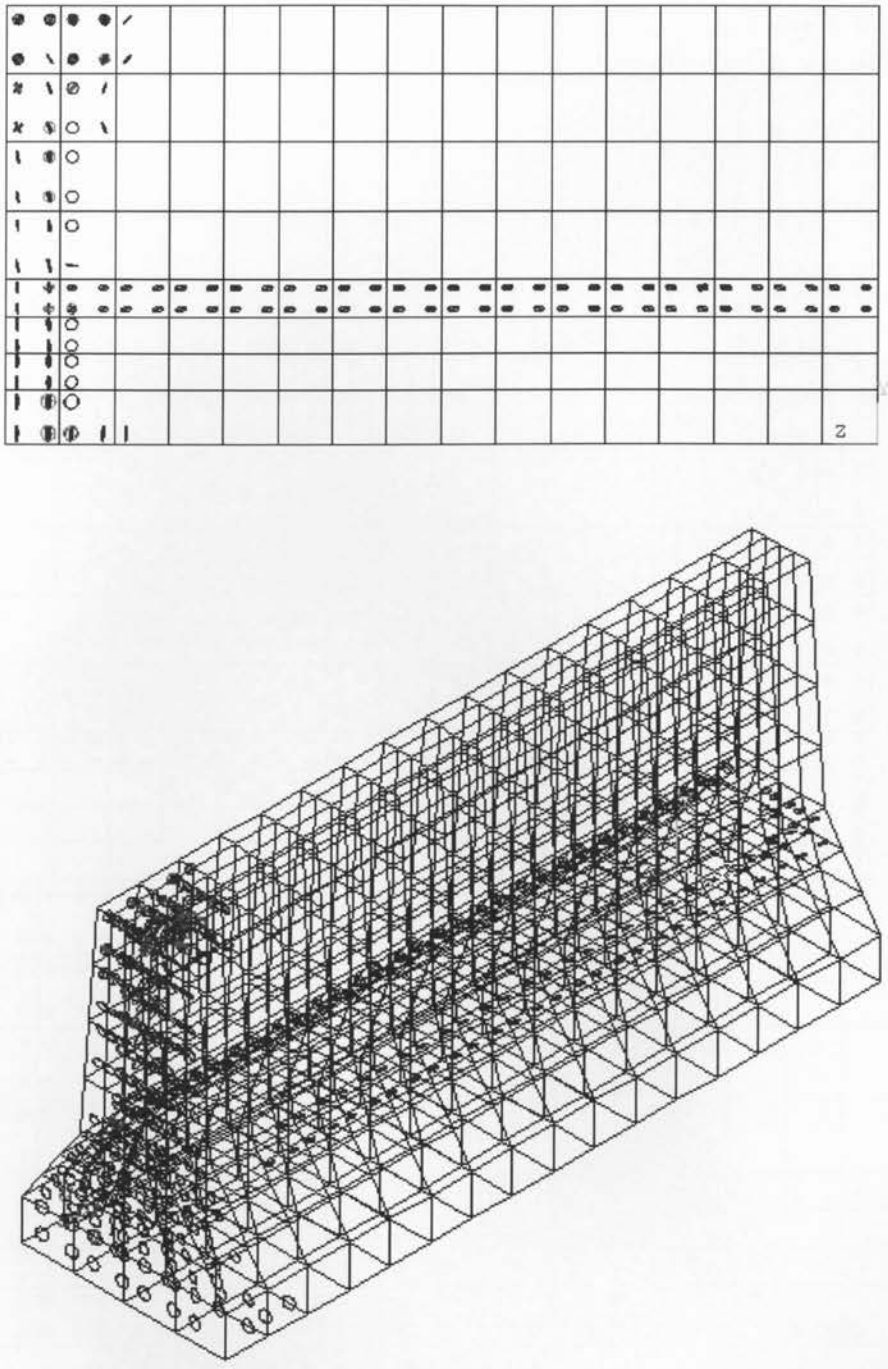

Figure A.15: Crack patterns of 2m barrier wall (fix – free) @ 1000 hours

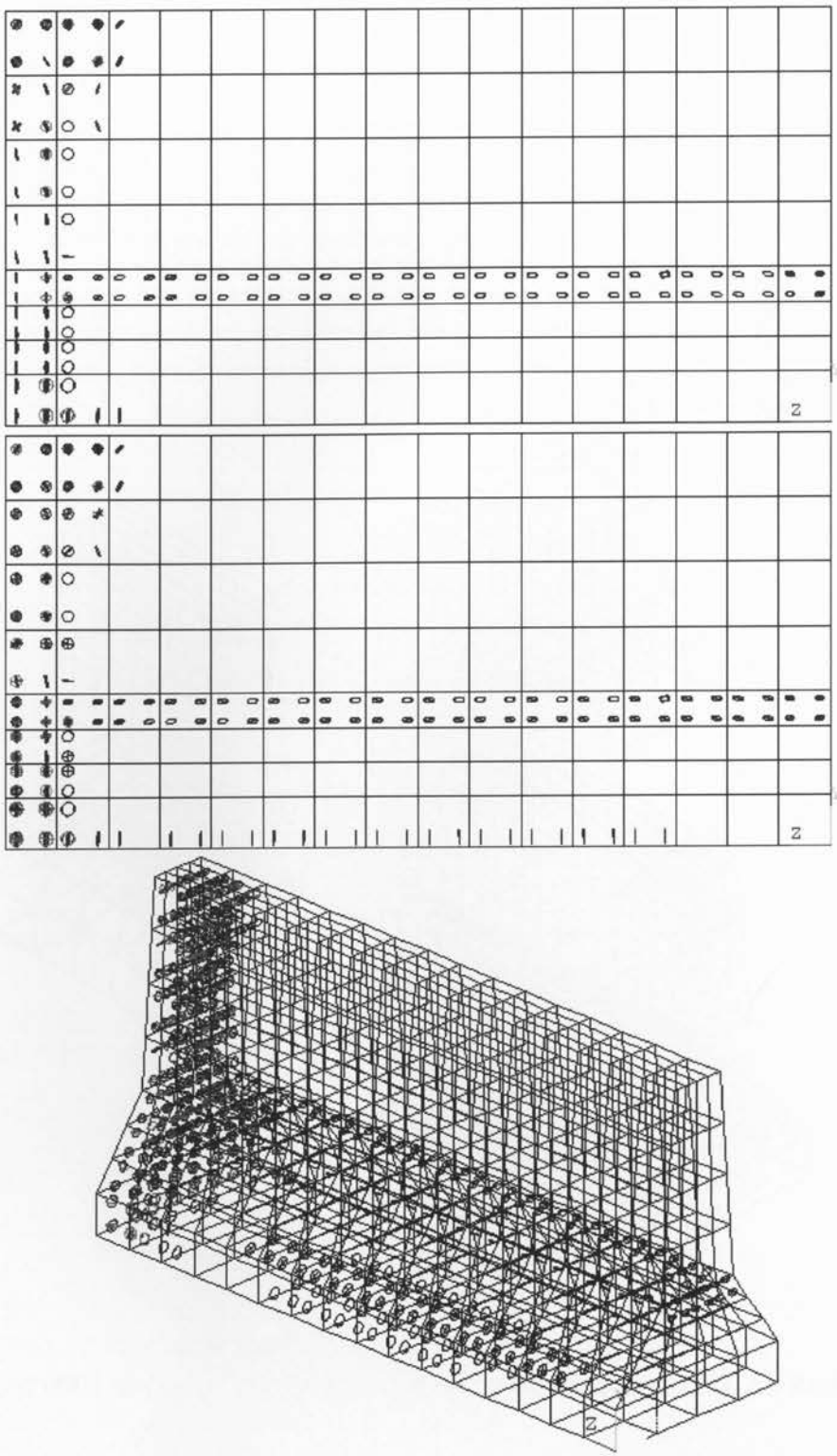

Figure A.16 : Crack patterns of 2m barrier wall (fix – free) @ 2000 & 3000 hours

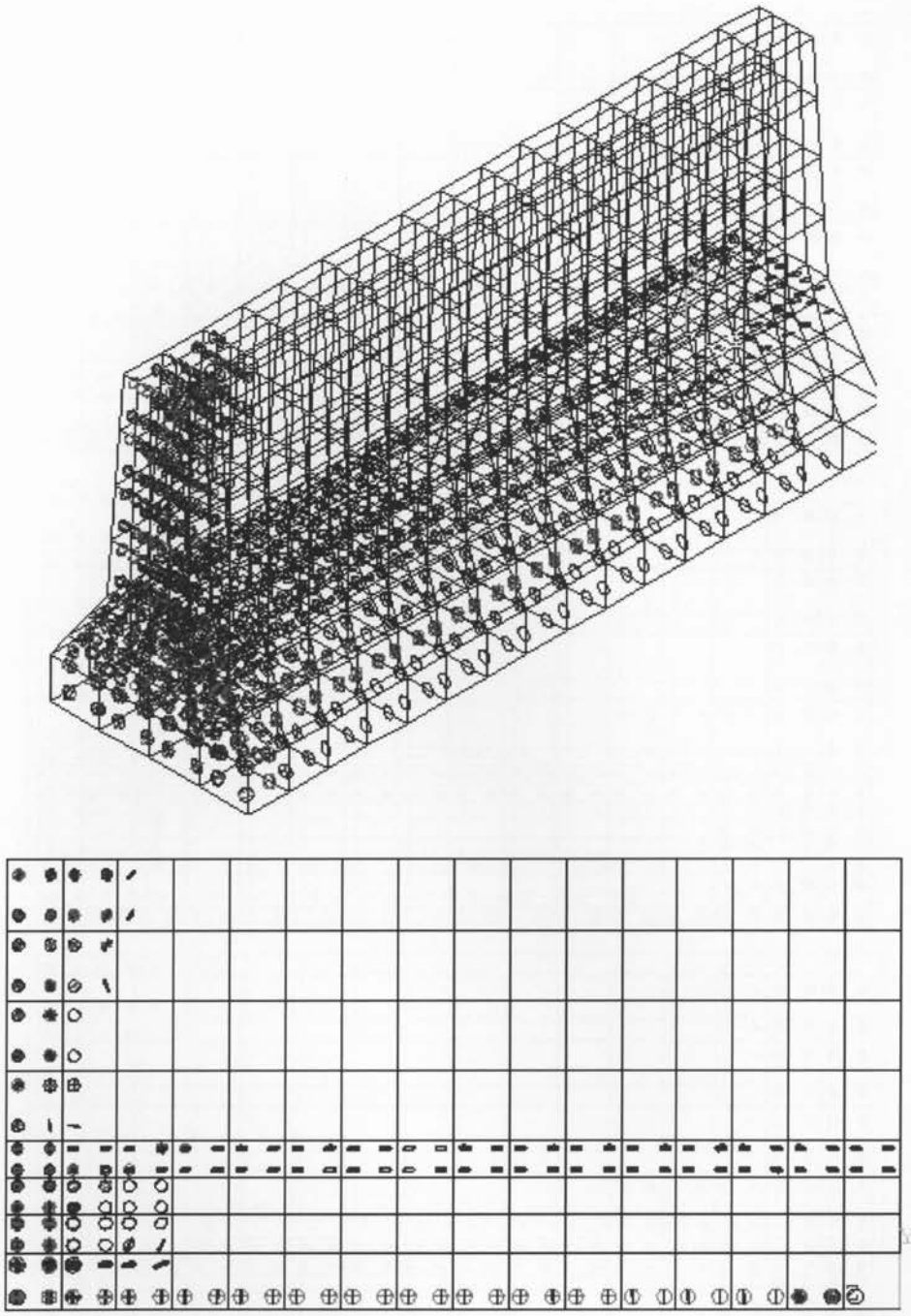

Figure A.17 : Crack patterns of 2m barrier wall (fix – free) @ 5000 hours

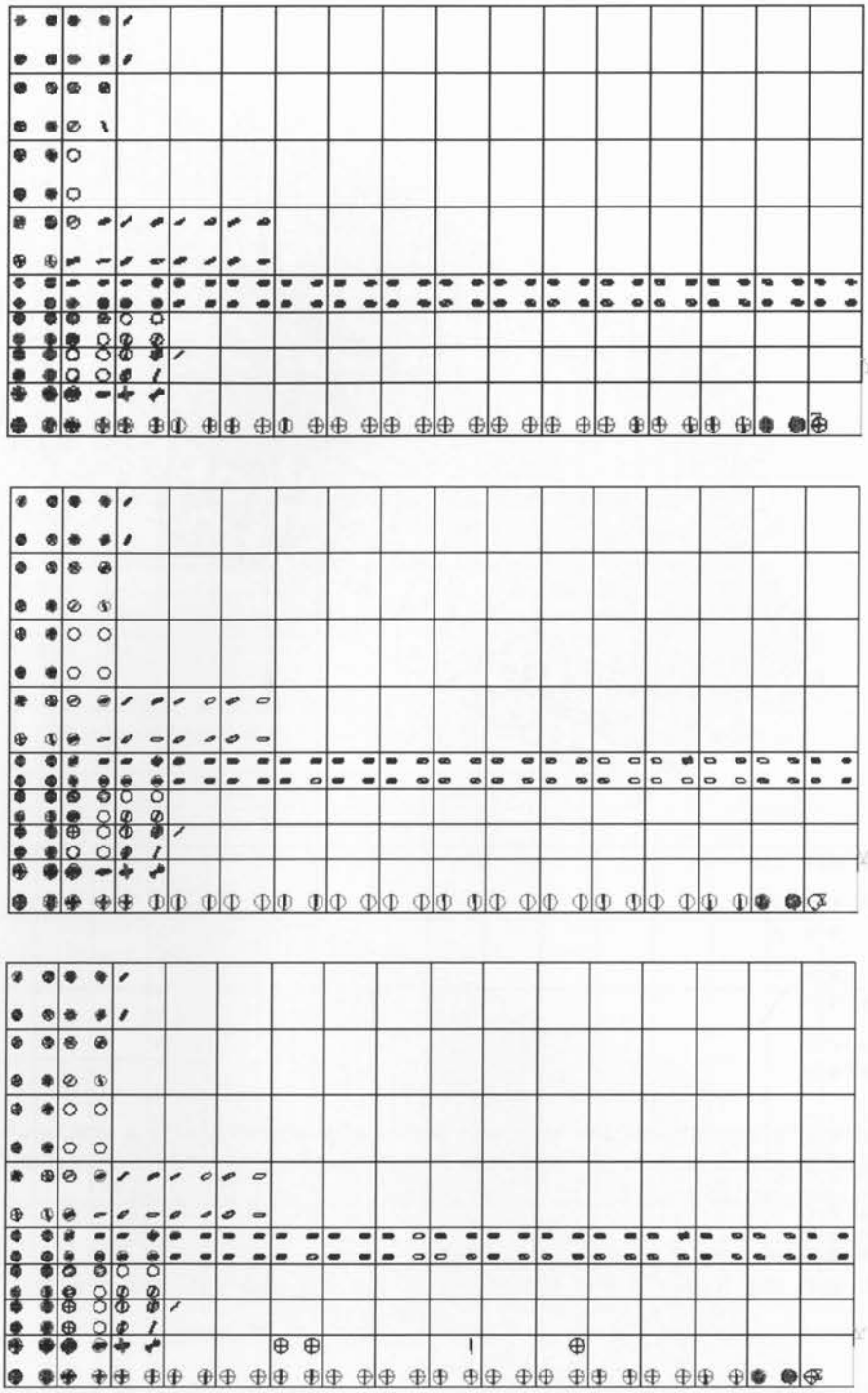

Figure A.18 : Crack patterns of 2m barrier wall (fix – free) @ 8000, 10000 & 15000 hours

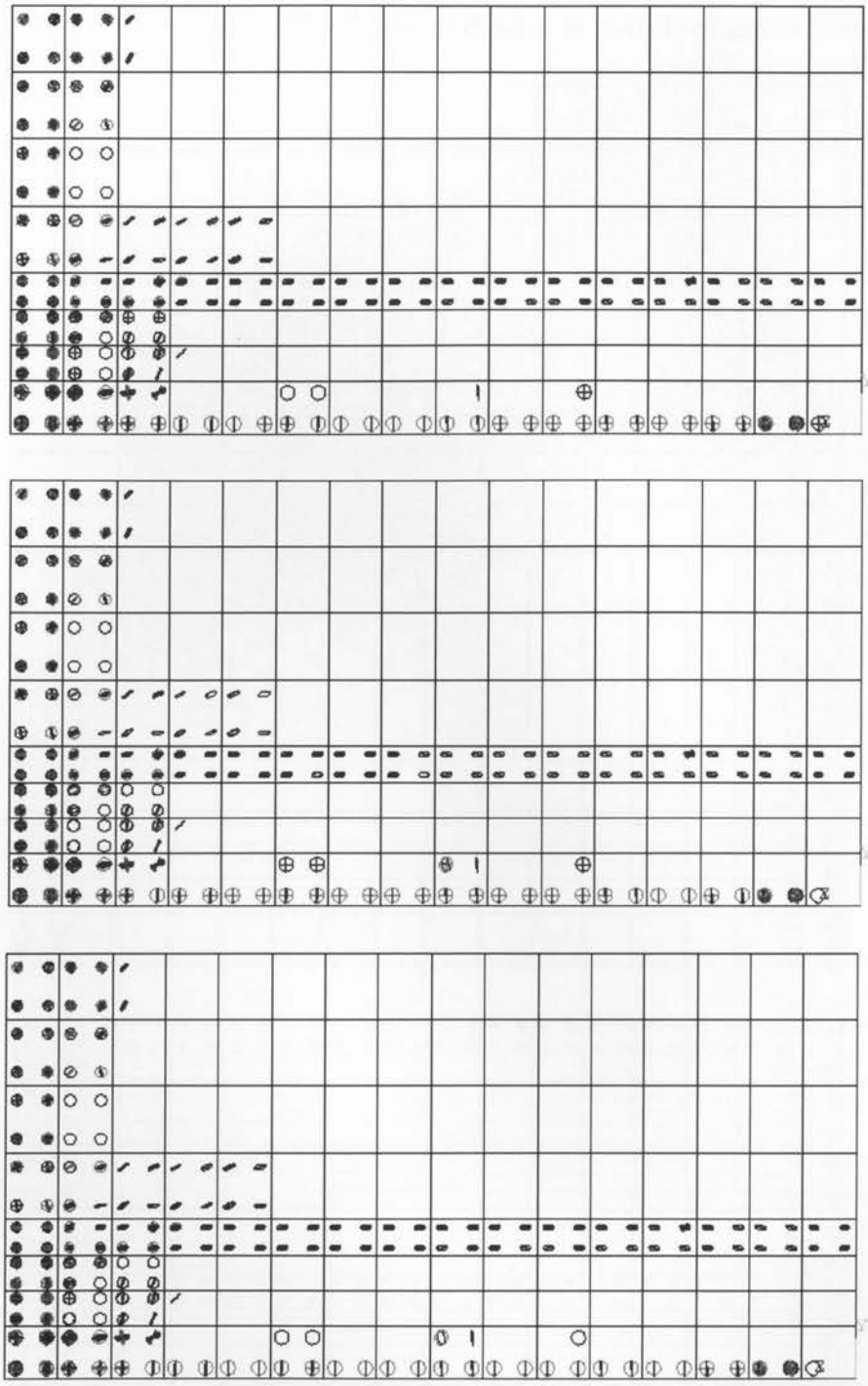

Figure A.19: Crack patterns of 2m barrier wall (fix – free) @ 20000, 25000 & 26350 hours

7.2.4 Sequence of crack evolution in a 2m barrier wall with both ends fixed

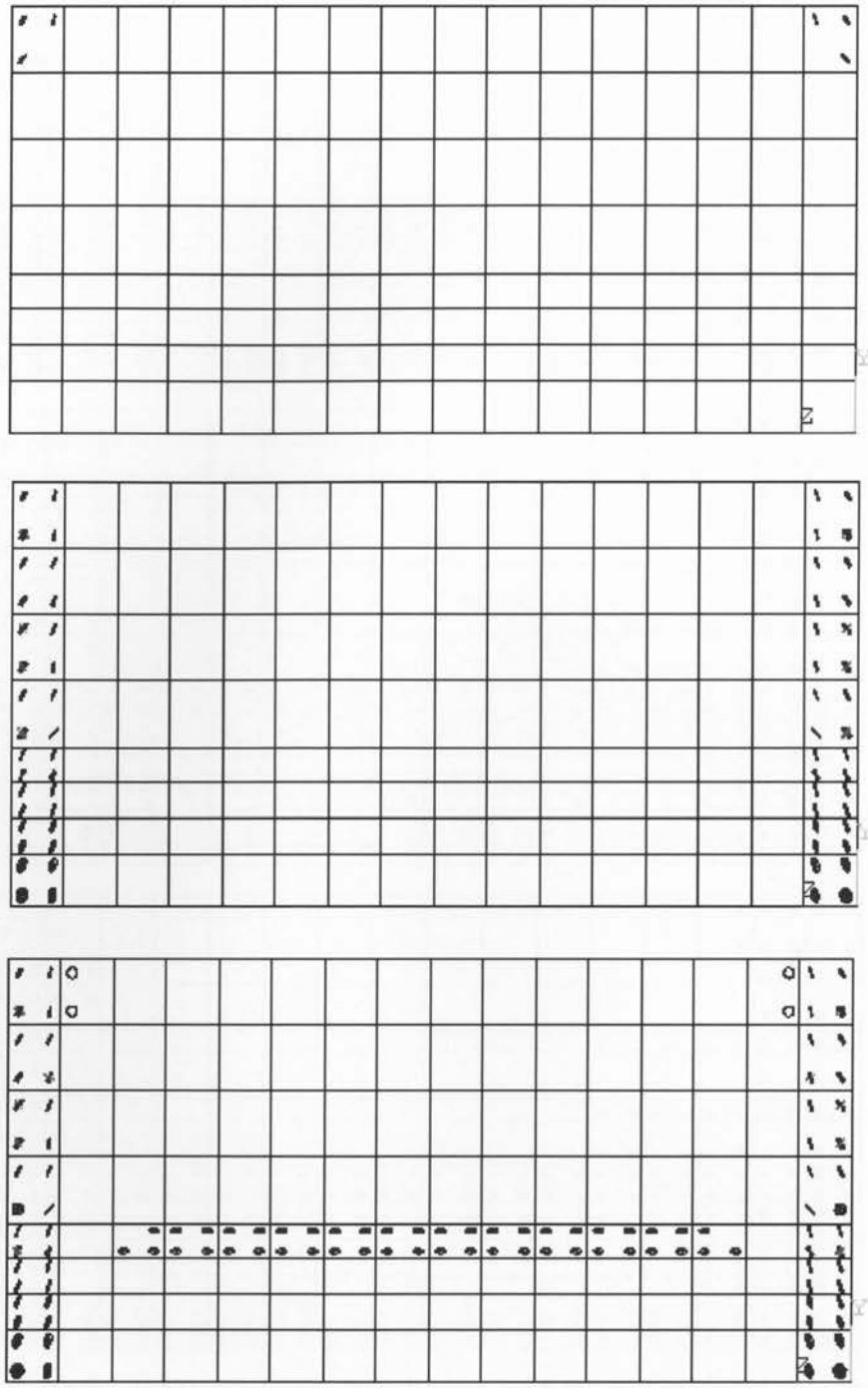

Figure A.20: Crack patterns of 2m barrier wall (fix – fix) @ 10, 100 & 500 hours

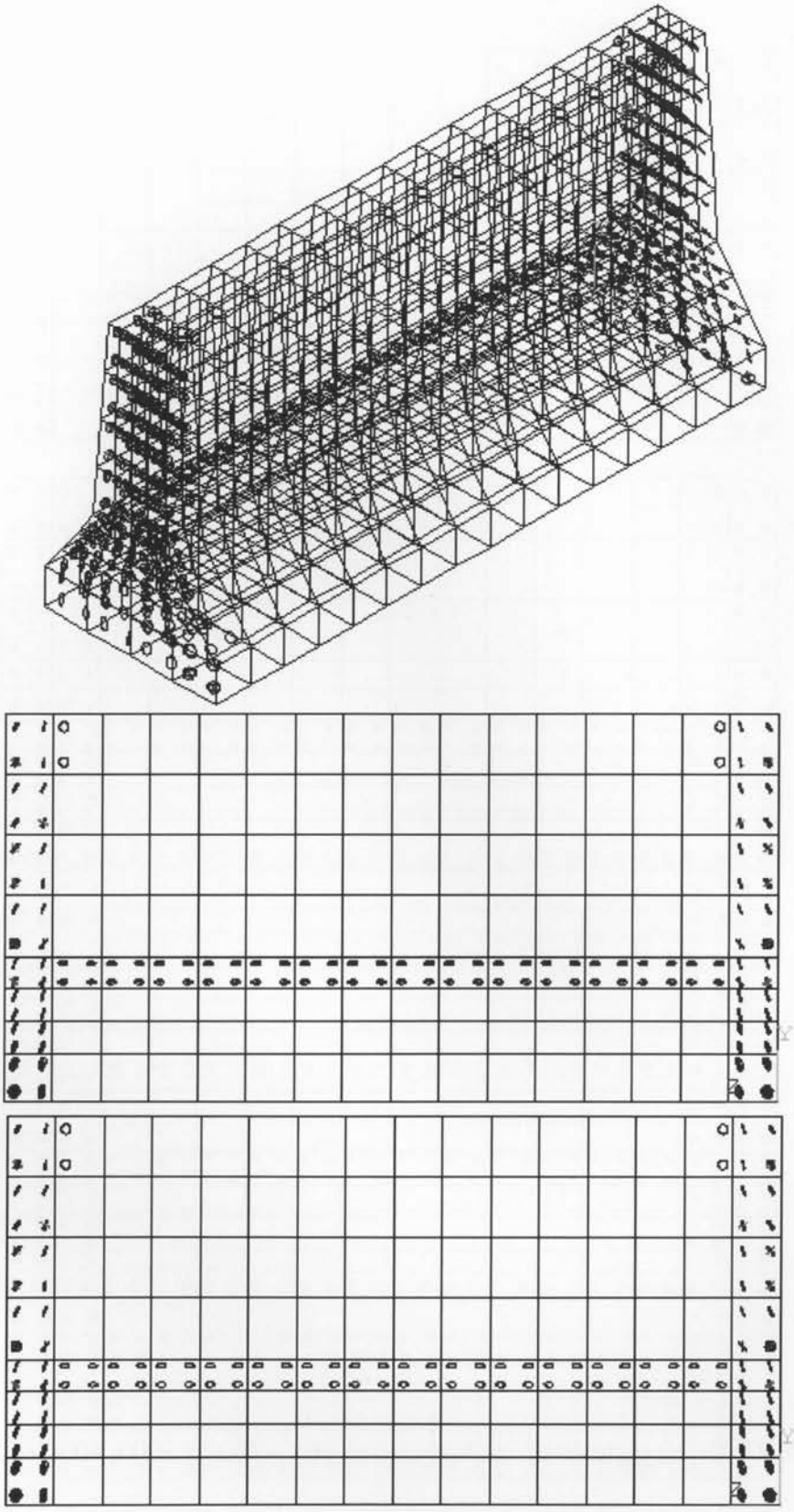

Figure A.21: Crack patterns of 2m barrier wall (fix – fix) @ 500, 1000 & 2000 hours

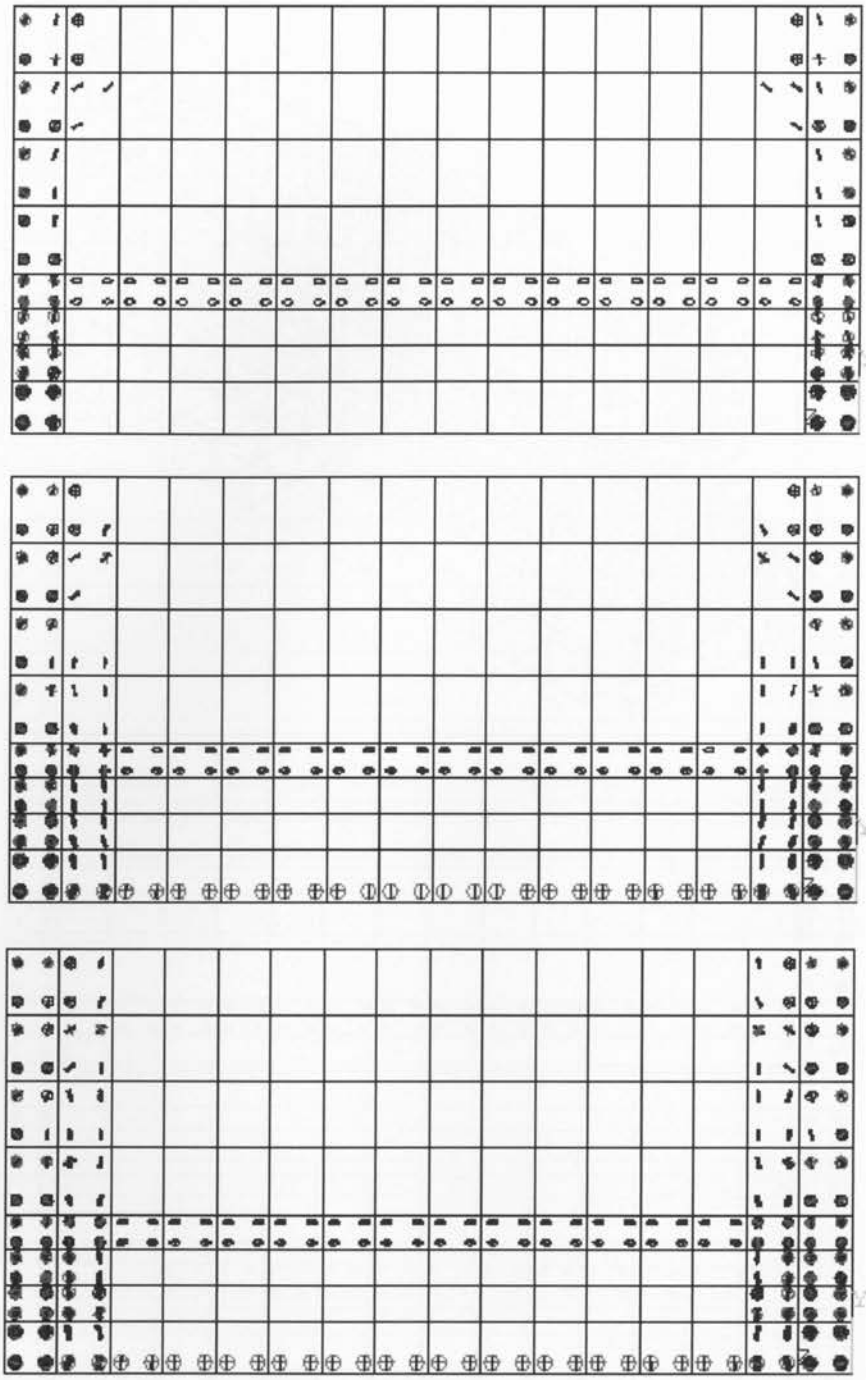

Figure A.22: Crack patterns of 2m barrier wall (fix – fix) @ 3000, 4000 & 5000 hours

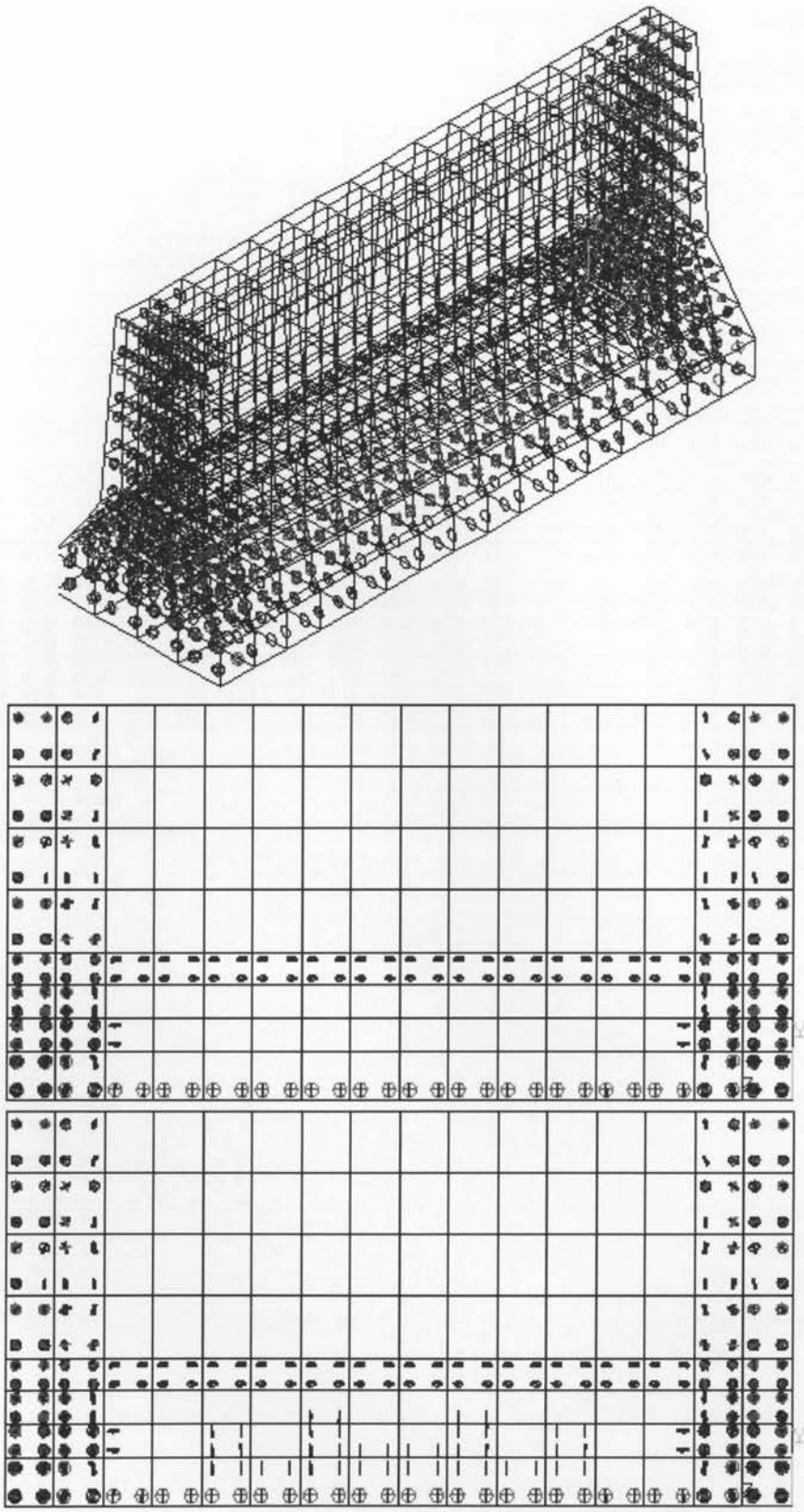

Figure A.23: Crack patterns of 2m barrier wall (fix – fix) @ 5000, 6500 & 7000 hours

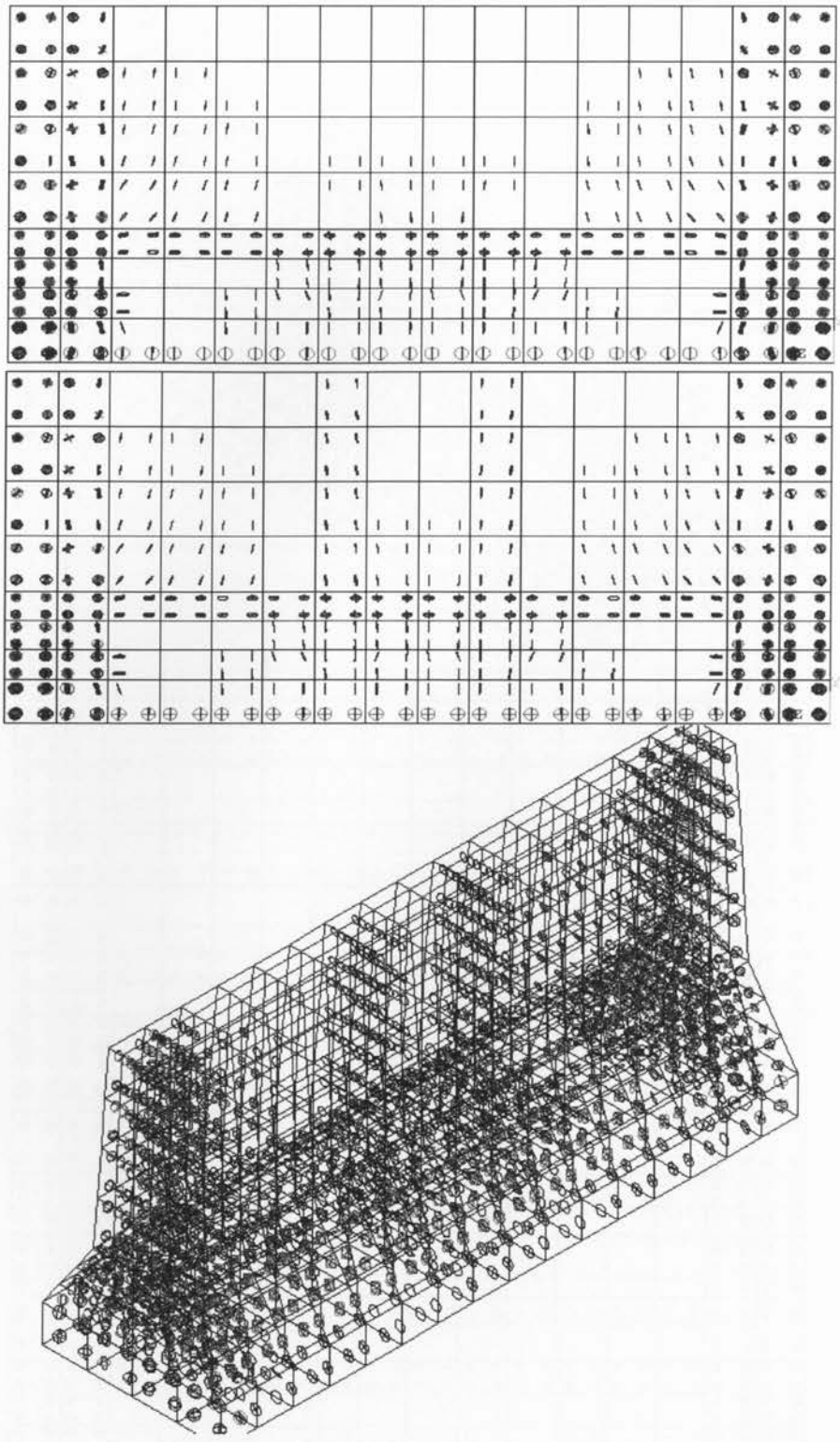

Figure A.24: Crack patterns of 2m barrier wall (fix – fix) @ 10000 & 15000 hours

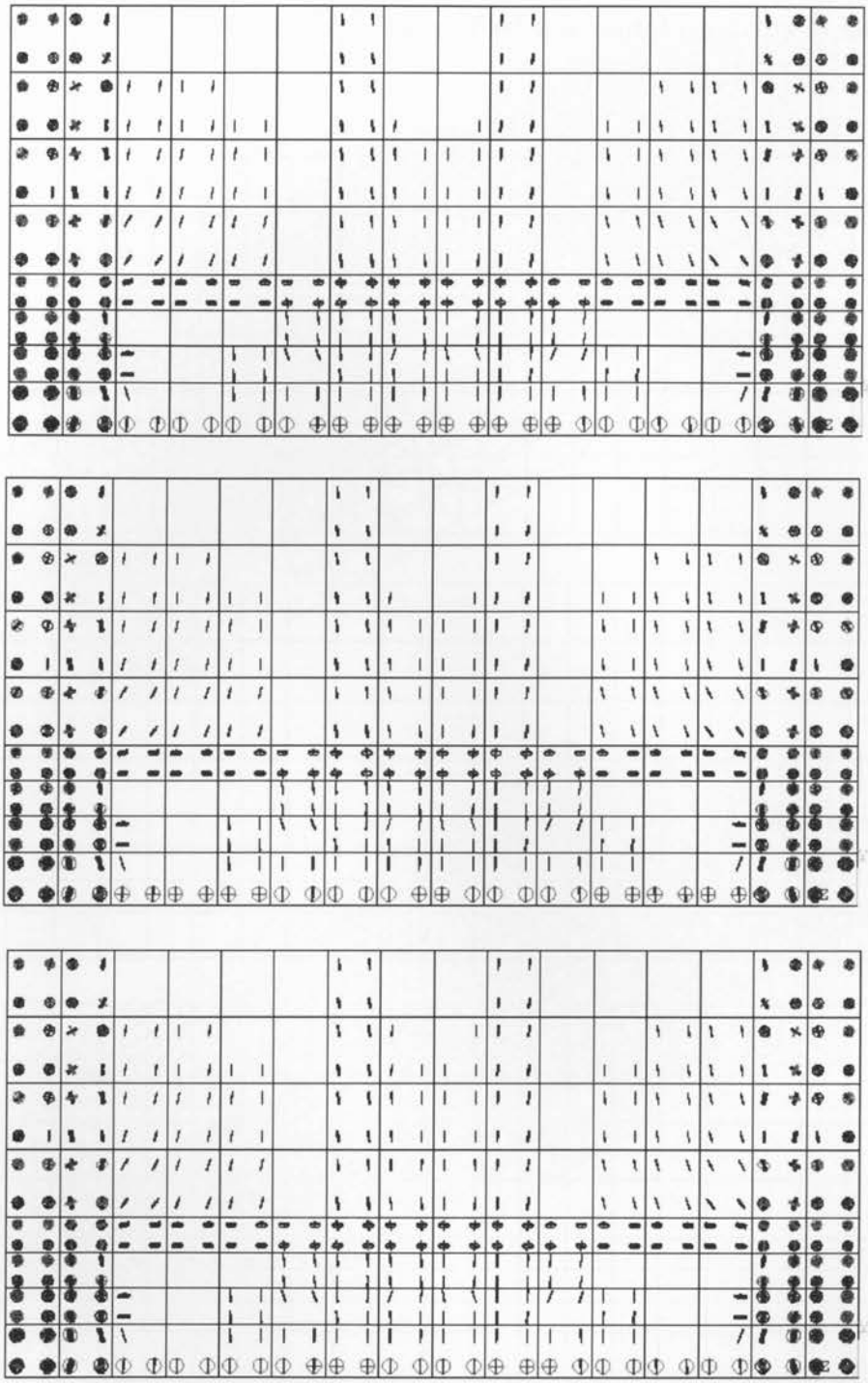

Figure A.25: Crack patterns of 2m barrier wall (fix – fix) @ 20000, 25000 & 26350 hours

7.2.5 Sequence of crack evolution in a 3m barrier wall with origin end free and other end fixed

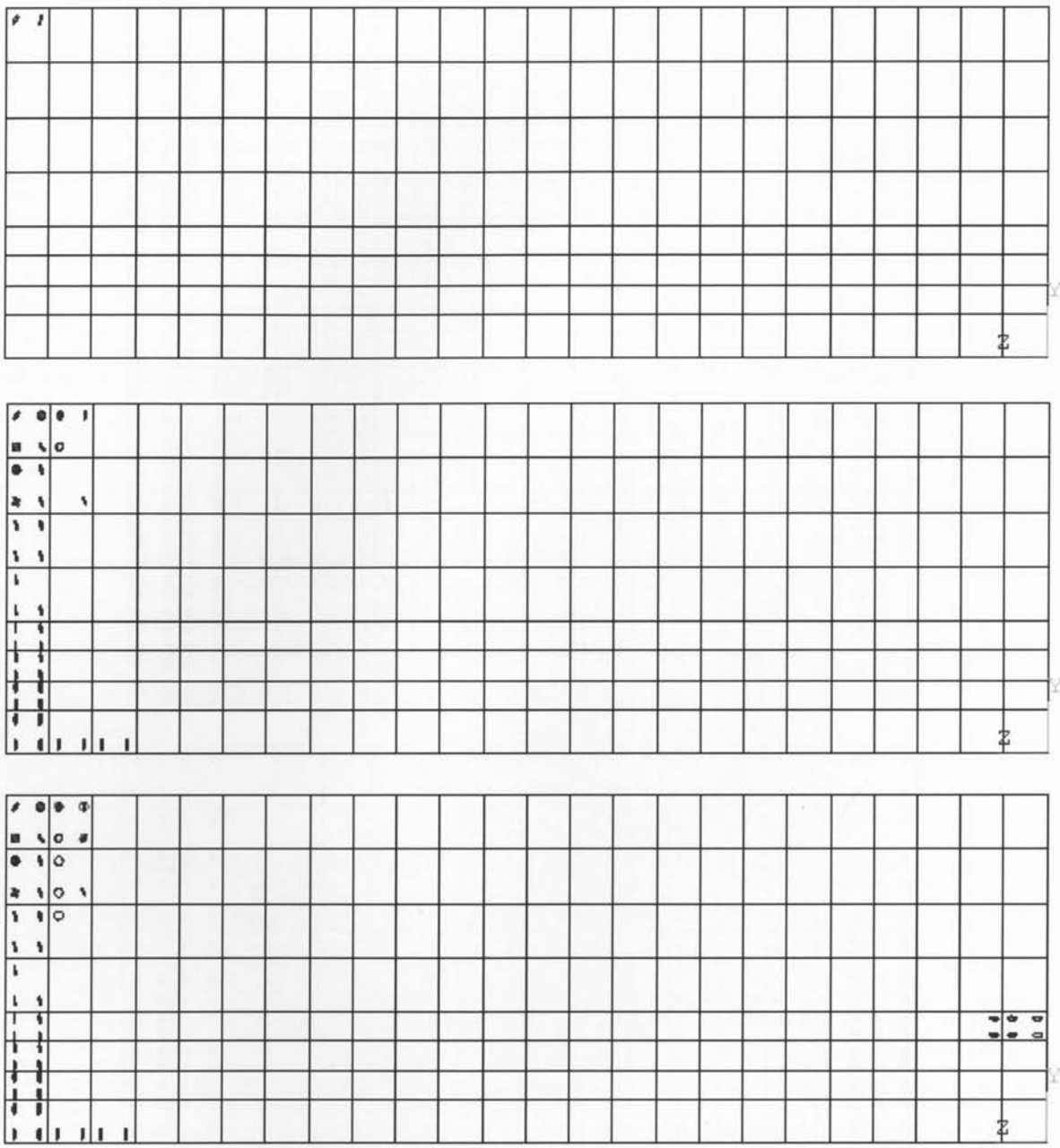

Figure A.26: Crack patterns of 3m barrier wall (fix – free) @ 10, 100 & 300 hours

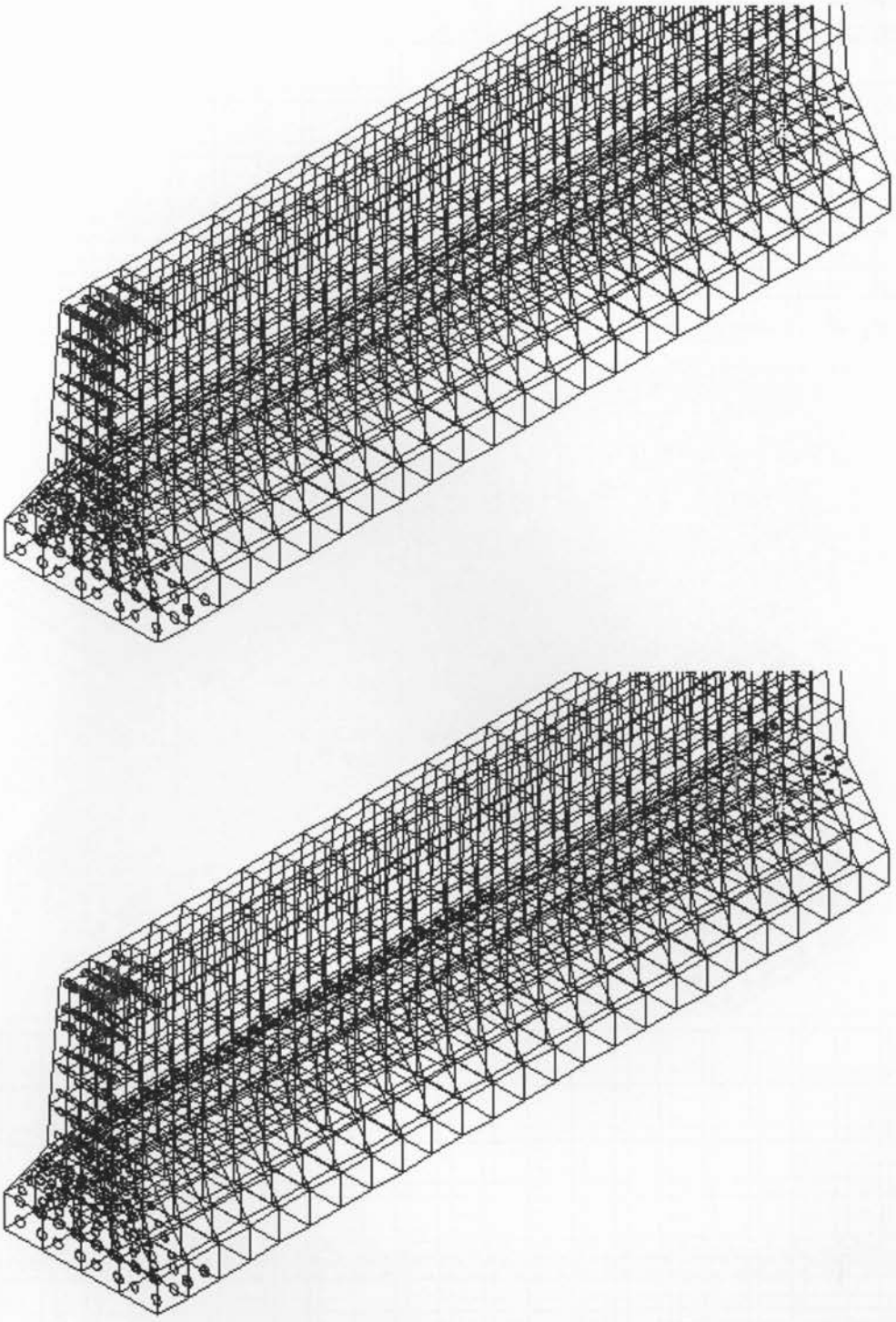

Figure A.27: Crack patterns of 3m barrier wall (fix – free) @ 300 & 400 hours

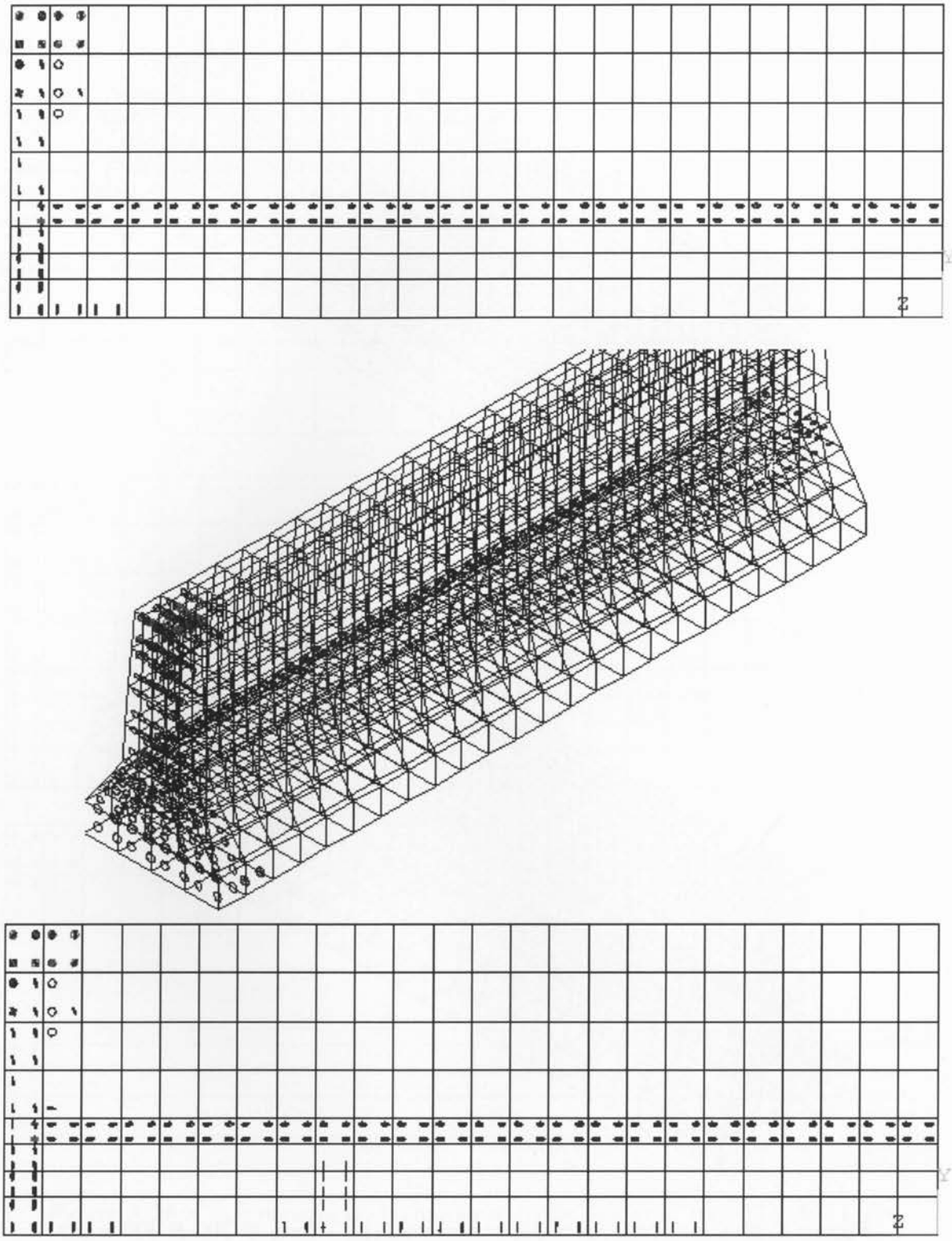

Figure A.28: Crack patterns of 3m barrier wall (fix – free) @ 500, 800 & 1000 hours

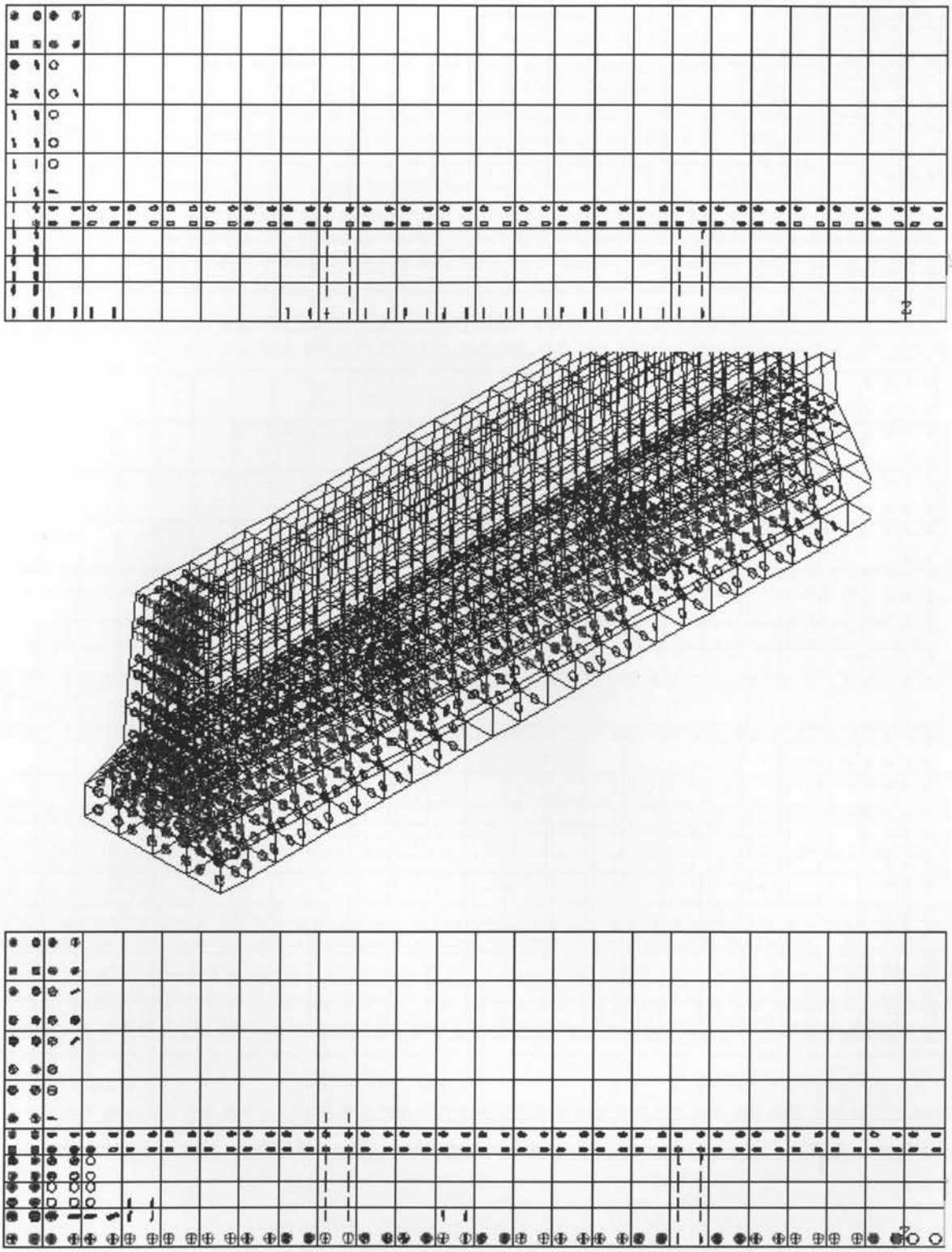

Figure A.29: Crack patterns of 3m barrier wall (fix – free) @2000, 3000 & 5000 hours

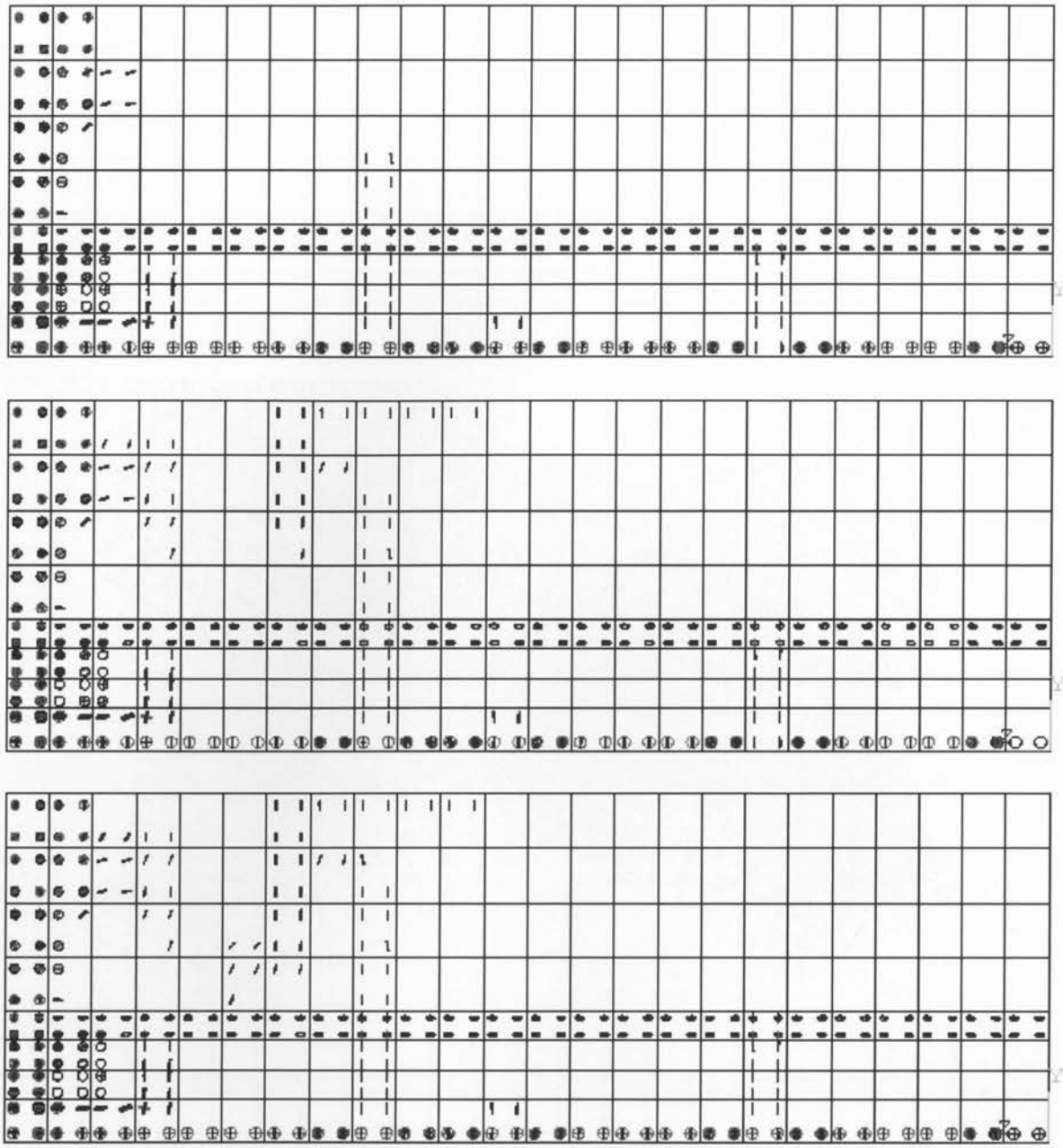

Figure A.30: Crack patterns of 3m barrier wall (fix – free) @ 8000, 10000 & 15000 hours

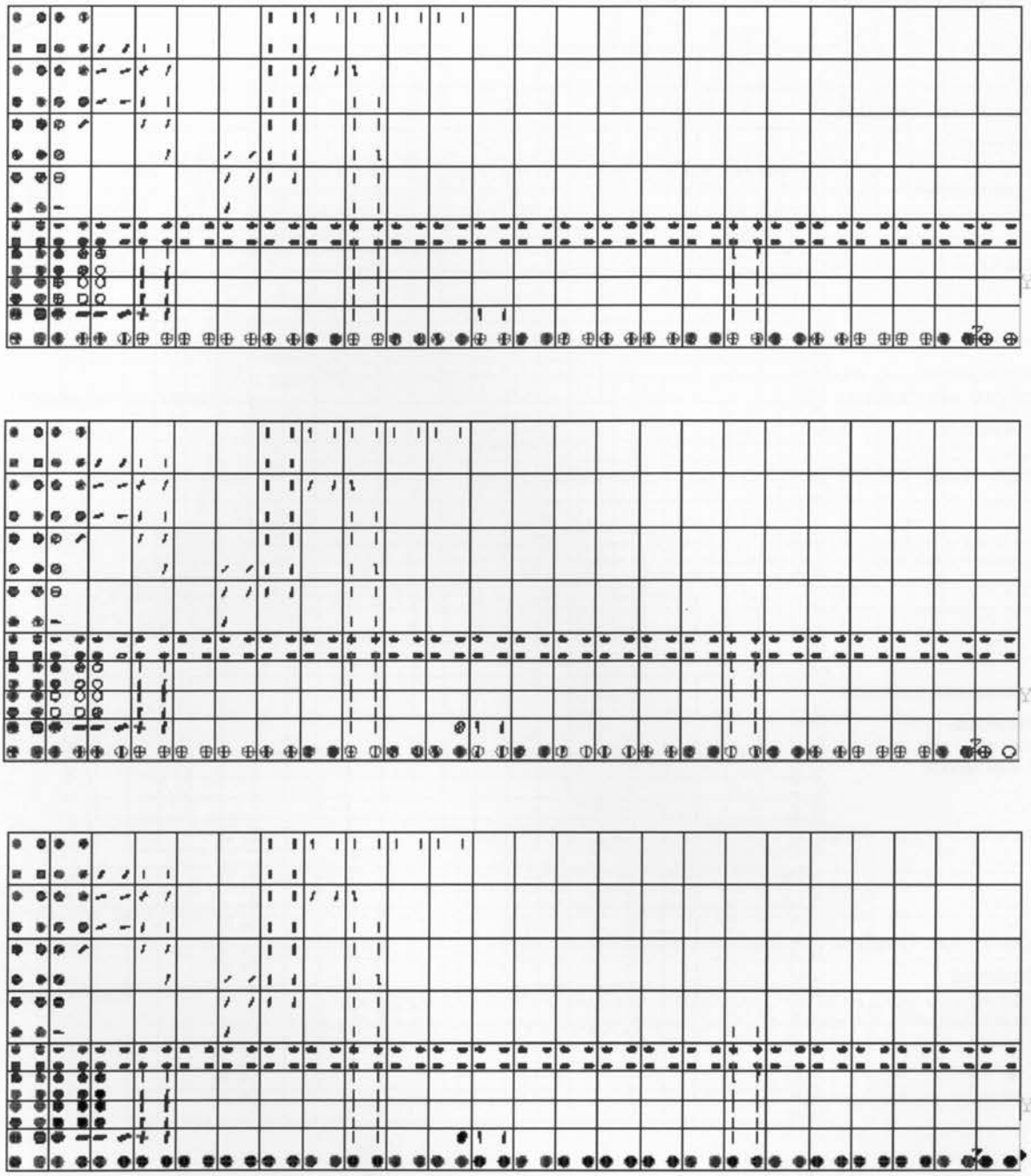

Figure A.31: Crack patterns of 3m barrier wall (fix – free) @ 20000, 25000 & 26350 hours

7.2.6 Sequence of crack evolution in a 3m barrier wall with both ends fixed

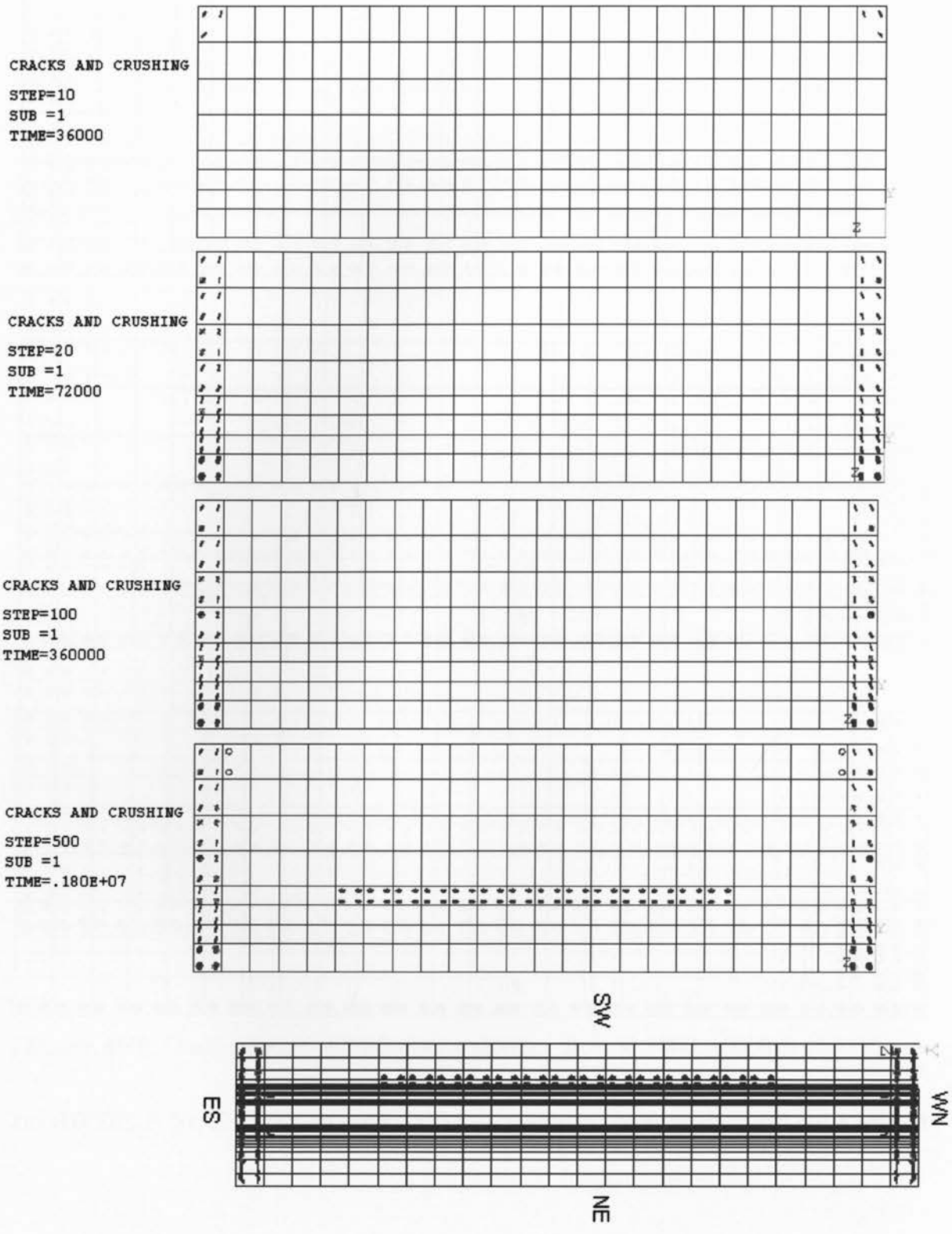

Figure A.32: Crack patterns of 3m barrier wall (fix – fix) @ 10, 20, 100 & 500 hours

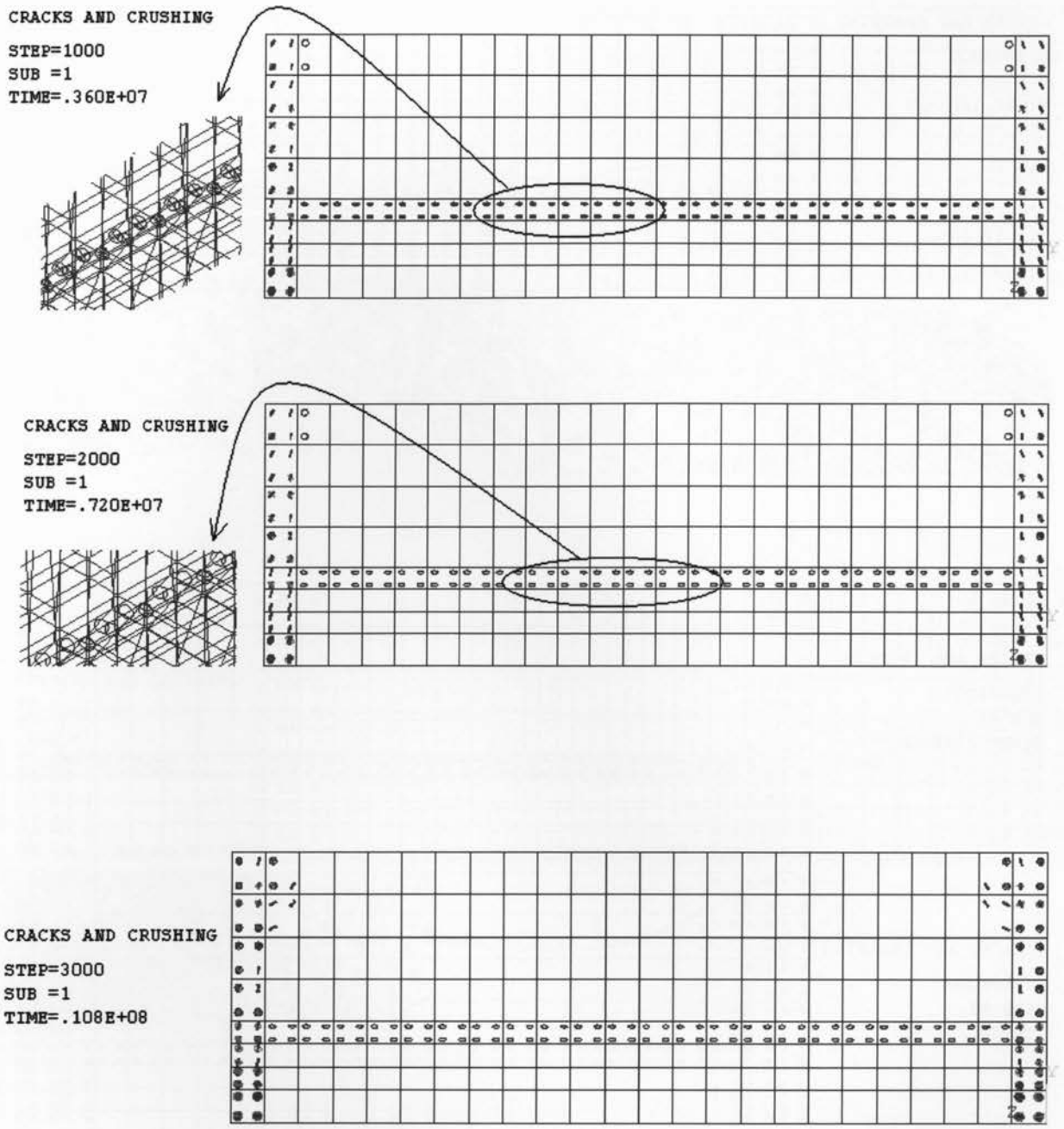

Figure A.33: Crack patterns of 3m barrier wall (fix – fix) @ 1000, 2000 & 3000 hours

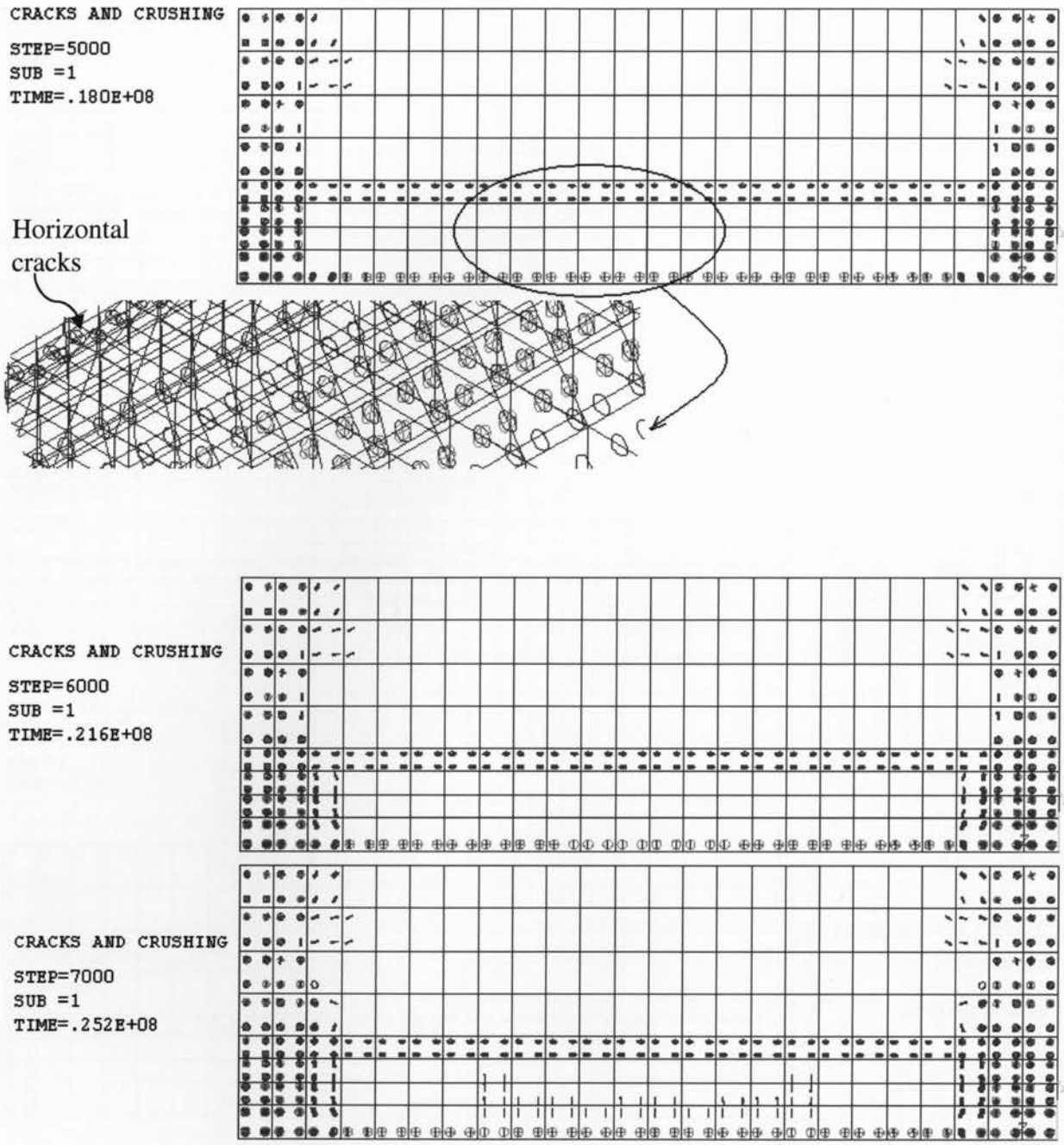

Figure A.34: Crack patterns of 3m barrier wall (fix – fix) @ 5000, 6000 & 7000 hours

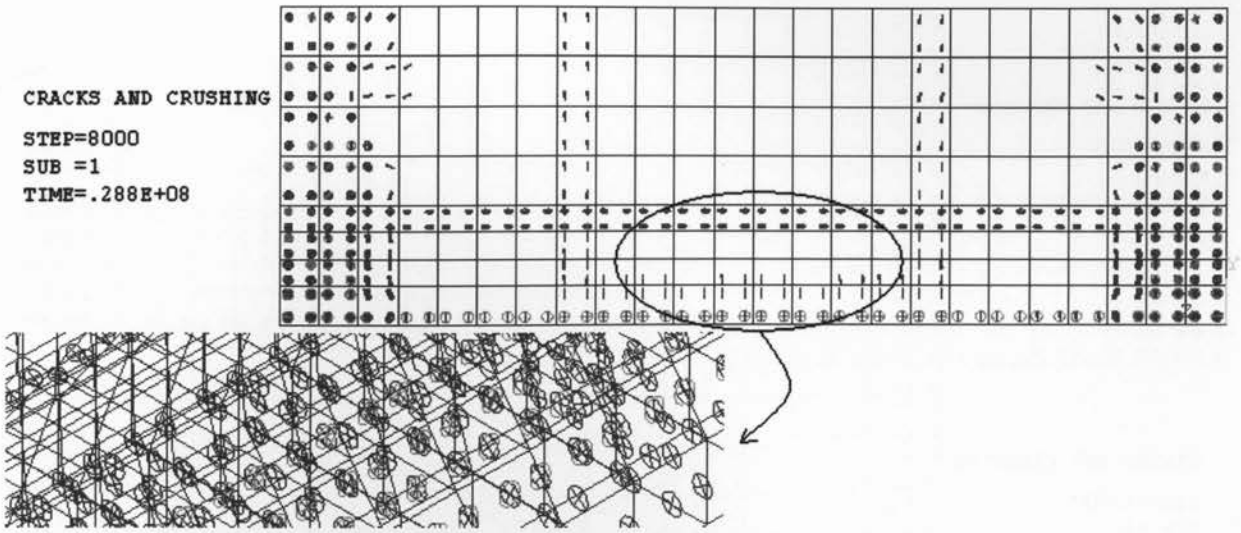

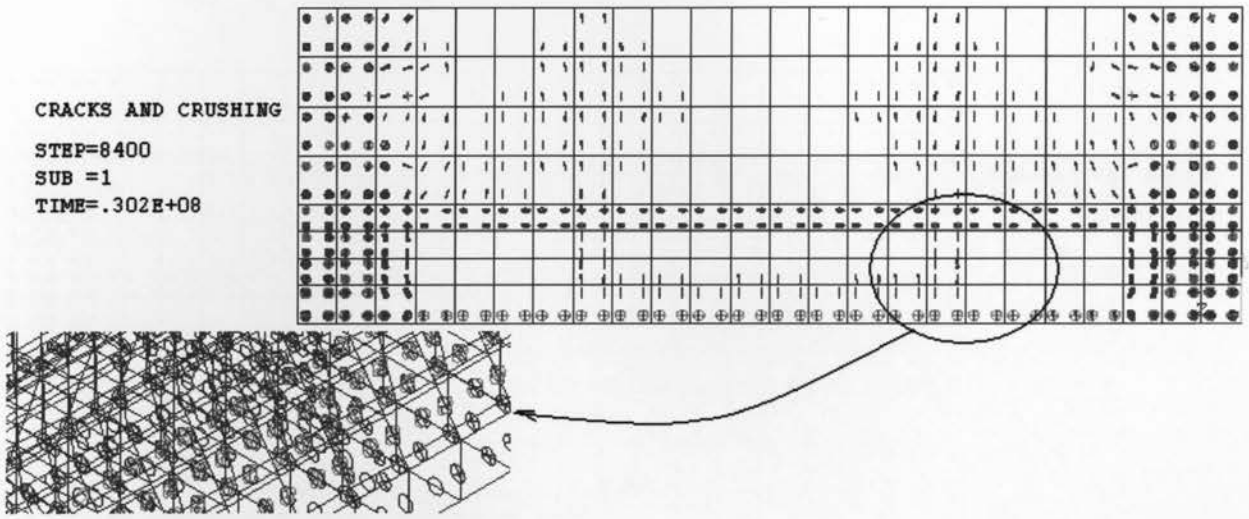

Figure A.35: Crack patterns of 3m barrier wall (fix – fix) @ 8000 & 8400 hours

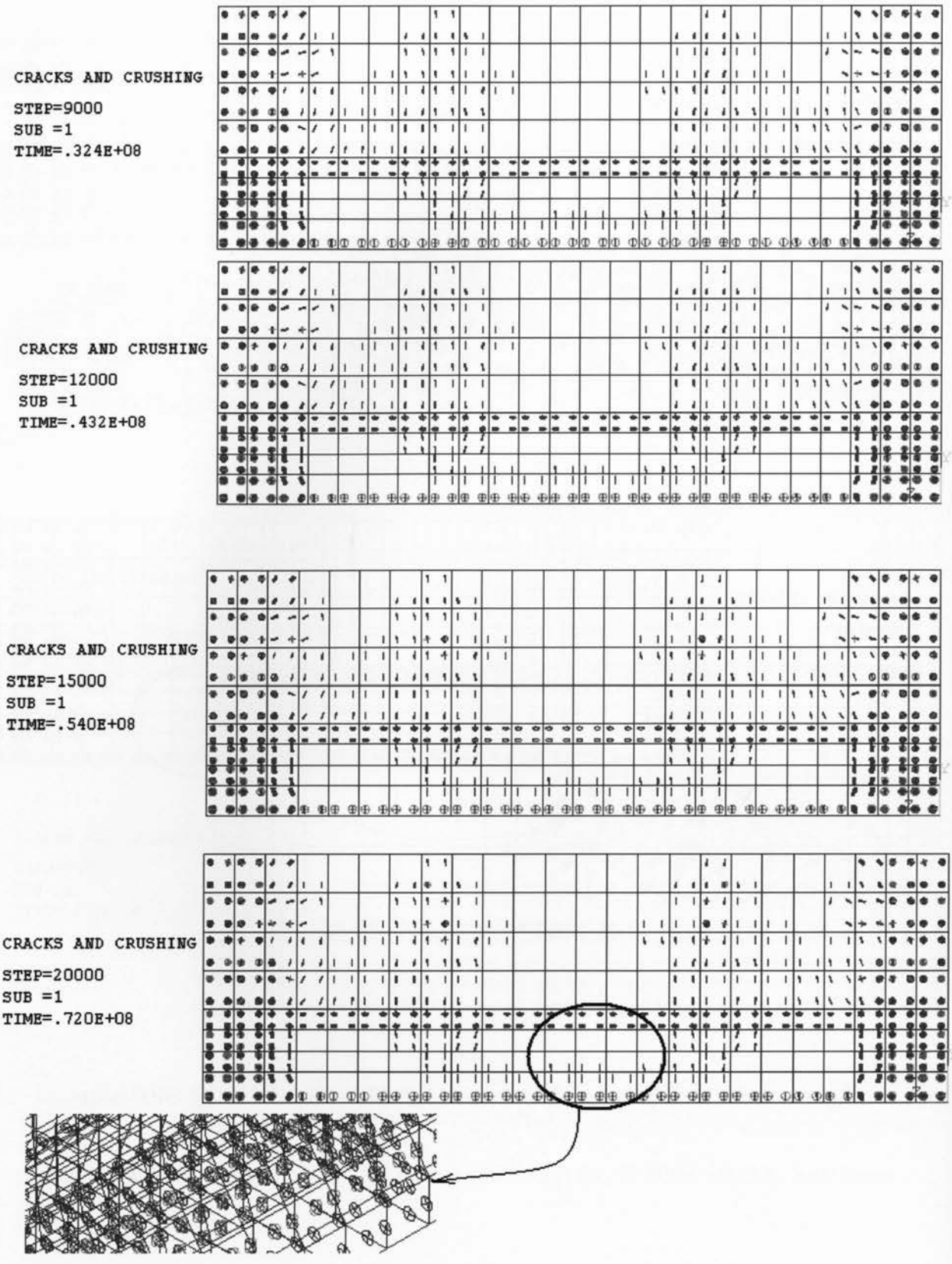

Figure A.36: Crack patterns of 3m barrier wall (fix – fix) @ 9000, 12000, 15000 & 20000 hours

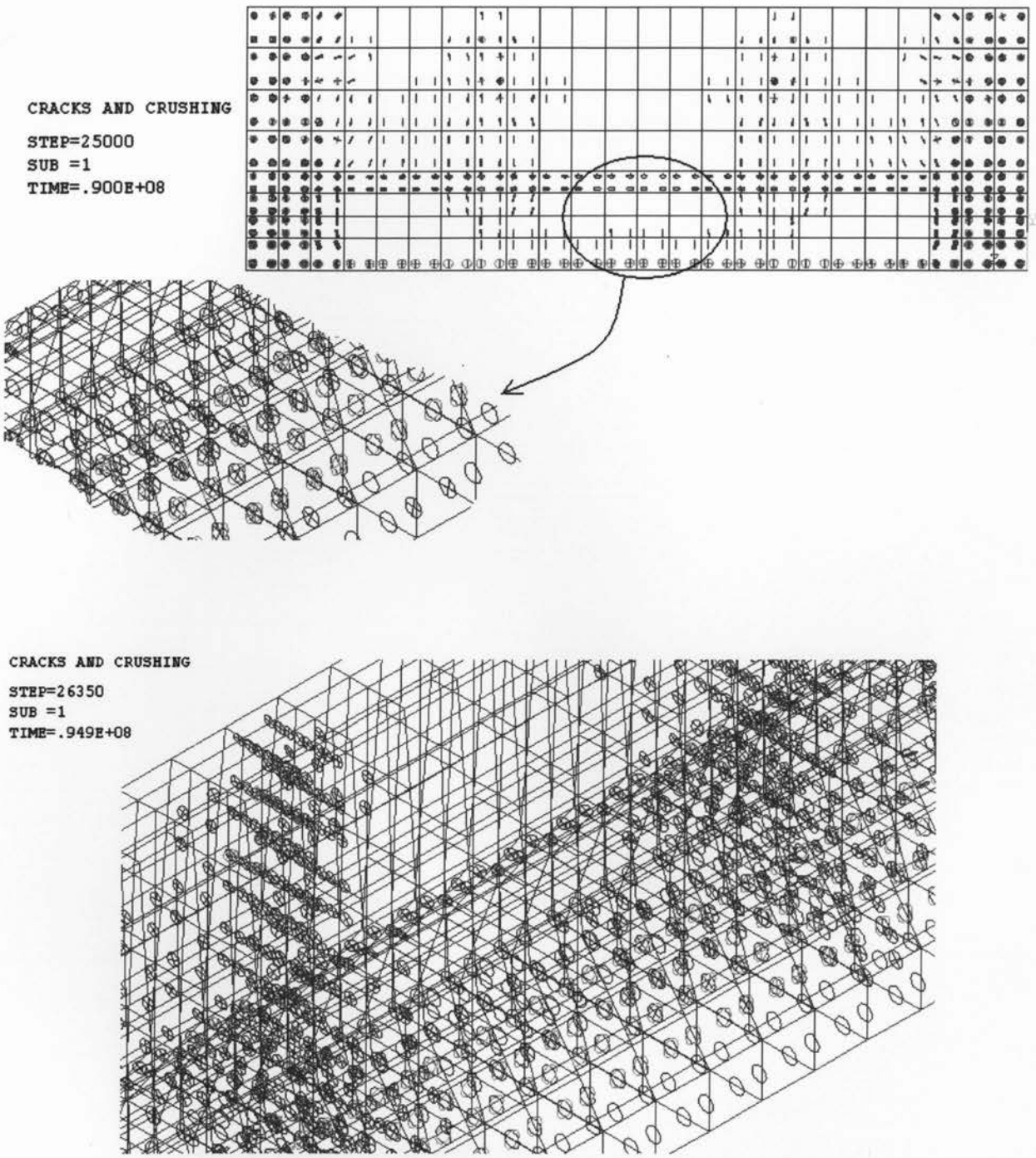

Figure A.37: Crack patterns of 3m barrier wall (fix – fix) @ 25000 & 26350 hours